REMOVING OF FORMATION DAMAGE AND ENHANCEMENT OF

FORMATION PRODUCTIVITY USING ENVIRONMENTALLY FRIENDLY

CHEMICALS

A Dissertation

by

MOHAMED AHMED NASR ELDIN MAHMOUD

Submitted to the Office of Graduate Studies of
Texas A&M University
in partial fulfillment of the requirements for the degree of

DOCTOR OF PHILOSOPHY

May 2011

Major Subject: Petroleum Engineering

REMOVING OF FORMATION DAMAGE AND ENHANCEMENT OF

FORMATION PRODUCTIVITY USING ENVIRONMENTALLY FRIENDLY

CHEMICALS

A Dissertation

by

MOHAMED AHMED NASR ELDIN MAHMOUD

Submitted to the Office of Graduate Studies of
Texas A&M University
in partial fulfillment of the requirements for the degree of

DOCTOR OF PHILOSOPHY

Approved by:

Chair of Committee,	Hisham A. Nasr-El-Din
Committee Members,	A. Daniel Hill
	Jerome Schubert
	Mahmoud El-Halwagi
Head of Department,	Stephen A. Holditch

May 2011

Major Subject: Petroleum Engineering

ABSTRACT

Removing of Formation Damage and Enhancement of Formation Productivity Using
Environmentally Friendly Chemicals. (May 2011)

Mohamed Ahmed Nasr Eldin Mahmoud, B.S.; M.S., Suez Canal University

Chair of Advisory Committee: Dr. Hisham A. Nasr-El-Din

Matrix acidizing is used in carbonate formations to create wormholes that connect the formation to the wellbore. Hydrochloric acid, organic acids, or mixtures of these acids are typically used in matrix acidizing treatments of carbonate reservoirs. However, the use of these acids in deep wells has some major drawbacks including high and uncontrolled reaction rate and corrosion to well tubulars, especially those made of chrome-based tubulars (Cr-13 and duplex steel), and these problems become severe at high temperatures. Hydrochloric acid (HCl) and its based fluids have a major drawback in stimulating shallow (low fracture gradient) formations as they may cause face dissolution (formation surface washout) if injected at low rates. The objective of stimulation of sandstone reservoirs is to remove the damage caused to the production zone during drilling or completion operations. Many problems may occur during sandstone acidizing with Hydrochloric/Hydrofluoric acids (HCl/HF) mud acid. Among those problems: decomposition of clays in HCl acids, precipitation of fluosilicates, the presence of carbonate can cause the precipitation of calcium fluorides, silica-gel filming, colloidal silica-gel precipitation, and mixing between various stages of the treatment. To overcome problems associated with strong acids, chelating agents were introduced and used in the field. However, major concerns with most of these chemicals are their limited dissolving power and negative environmental impact.

Glutamic acid diacetic acid (GLDA) a newly developed environmentally friendly chelate was examined as stand-alone stimulation fluid in deep oil and gas wells. In this study we used GLDA to stimulate carbonate cores (calcite and dolomite). GLDA was also used to stimulate and remove the damage from different sandstone cores containing different compositions of clay minerals. Carbonate cores (calcite and dolomite) of 6 and 20 in. length and 1.5 in. diameter were used in the coreflood experiments. Coreflood experiments were run at temperatures ranging from 180 to 300°F. Ethylene diamine tetra acetic acid (EDTA), hydroxyl ethylethylene diaminetriacetic acid (HEDTA), and GLDA were used to stimulate and remove the damage from different sandstone cores at high temperatures. X-ray Computed Topography (CT) scans were used to determine the effectiveness of these fluids in stimulation calcite and dolomite cores and

removing the damage from sandstone cores. The sandstone cores used in this study contain from 1 to 18 wt% illite (swellable and migratable clay mineral).

GLDA was found to be highly effective in creating wormholes over a wide range of pH (1.7-13) in calcite cores. Increasing temperature enhanced the reaction rate, more calcite was dissolved, and larger wormholes were formed for different pH with smaller volumes of GLDA solutions. GLDA has a prolonged activity and leads to a decreased surface spending resulting in face dissolution and therefore acts deeper in the formation. In addition, GLDA was very effective in creating wormholes in the dolomite core as it is a good chelate for magnesium. Coreflood experiments showed that at high pH values (pH =11) GLDA, HEDTA, and EDTA were almost the same in increasing the permeability of both Berea and Bandera sandstone cores. GLDA, HEDTA, and EDTA were compatible with Bandera sandstone cores which contains 10 wt% Illite. The weight loss from the core was highest in case of HEDTA and lowest in case of GLDA at pH 11. At low pH values (pH =4) 0.6M GLDA performed better than 0.6M HEDTA in the coreflood experiments. The permeability ratio (final/initial) for Bandera sandstone cores was 2 in the case of GLDA and 1.2 in the case of HEDTA at pH of 4 and 300°F. At high pH HEDTA was the best chelating agent to stimulate different sandstone cores, and at low pH GLDA was the best one. For Berea sandstone cores EDTA at high pH of 11 was the best in increasing the permeability of the core at 300°F.

The low pH GLDA based fluid has been especially designed for high temperature oil well stimulation in carbonate and sandstone rock. Extensive studies have proved that GLDA effectively created wormholes in carbonate cores, is gentle to most types of casing including Cr-based tubular, has a high thermal stability and gives no unwanted interactions with carbonate or sandstone formations. These unique properties ensure that it can be safely used under extreme conditions for which the current technologies do not give optimal results. Furthermore, this stimulation fluid contributes to a sustainable future as it based on readily biodegradable GLDA that is made from natural and renewable raw material.

DEDICATION

TO MY PARENTS, MY WIFE, AND MY KIDS

ACKNOWLEDGEMENTS

NOMENCLATURE

a	constant based on core type, dimensionless
A	cross section area of the core, cm^2
$[Ca^{2+}]$	calcium concentration, ppm
CE_{50}	half maximal effective concentration, is a measure of drug's potency
C_{HCl}	HCl concentration, $kmole/m^3$
C_o	initial GLDA concentration, M
CT_a	CT number of air
CT_{ar}	CT number of core saturated with air
C_{tip}	GLDA concentration at the tip, M
CT_w	CT number of water
CT_{wr}	CT number of core saturated with water
$D(H^+)$	diffusion of hydrogen ions, cm^2/s
d_{core}	core diameter, in.
De	effective diffusion coefficient for reactants and products, cm^2/s
D_f	formation depth, ft
d_p	pore diameter, μm
d_{wh}	wormhole diameter, in.
E_f	reaction rate constant, kmole HCl/[m^2.s(kmole HCl/m_3 acid soln)$^\alpha$]
E_f^0	reaction rate constant, cm^{3m-3}/(mole m^{-1}.s)
F_{PI}	productivity improvement factor, dimensionless
g_{fr}	formation fracture gradient, psi/ft
h	reservoir thickness, ft
J_a	productivity index after the treatment, bbl/day/psi
J_{a0}	productivity index before the treatment, bbl/day/psi
k	rock permeability, md
K_{Cp}	mass transfer coefficient for products, cm/s
K_{cR}	mass transfer coefficient for reactants, cm/s
k_d	permeability of damaged zone, md
K_{eq}	reaction equilibrium constant, dimensionless
k_{final}	final permeability after the treatment, md
$k_{initial}$	initial permeability before the treatment, md
K_s	surface reaction rate constant, cm/s
k_t	Permeability of treated zone, md

L_{core}	core length, in.
L_{GLDA}	GLDA invasion length, in.
L_{D50}	median lethal dose
Log P_{wo}	it is a measure of portioning coefficient (log of the ratio solute with octanol and solute with water)
$LogK_{Ca-GLDA}$	stability constant of GLDA with calcium and it equals 5.9
$LogK_{Mg-GLDA}$	stability constant of GLDA with magnesium and it equals 5.2
l_p	pore length, cm
L_{radial}	length of radial core, cm
L_{wh}	wormhole length, cm
m	reaction order, dimensionless
M	factor depends on the sandstone core type, = 3
$[Mg^{2+}]$	magnesium concentration, ppm
MW_{CaCO3}	molecular weight of calcite, lbmole
MW_{GLDA}	molecular weight of GLDA, lbmole
n	factor depends on the sandstone core type, = 1
N_{AC}	acid capacity number
$N_{ac, GLDA}$	acid capacity number for the GLDA, dimensionless
N_{Da}	Damköhler number, dimensionless
$N_{Da(mt)}$	Damköhler number based on mass transfer, dimensionless
$N_{Da(opt)}$	optimum Damköhler number, dimensionless, dimensionless
$N_{Da(rxn)}$	Damköhler number based on reaction rate, i.e., reaction rate limited, dimensionless
NOAEL	the maximum concentration of a substance that is found to have no adverse effects upon the test subject, mg/kg body weight/day
NOEC	no adverse effect concentration
N_{pe}	Peclet number, dimensionless
p_e	initial reservoir pressure, psi
p_r	reservoir pressure, psi
PV	pore volumes of the fluid used
PV_{bt}	pore volume required to create wormholes along the core length, PV
p_{wf}	wellbore flowing pressure, psi
q	flow rate, cm^3/s
Q	injection rate, cm^3/min
q_{core}	optimum injection rate from coreflood, cm^3/min

q_{linear}	flow rate in linear coreflood, cm^3/min
q_o	oil production rate, bbl/day
Q_{opt}	optimum injection rate, cm^3/min
q_{radial}	injection rate required in the field based on radial cores, cm^3/min
q_T	total injection rate, cm^3/min
q_w	injection rate in the field, bbl/min
R	universal gas constant, = 8.314 J/(mole.^{o}K)
r_{core}	core radius, in.
r_D	total dissolution rate, mol/cm^2/s
r_e	reservoir drainage radius, ft
r_{GLDA}	radius of penetration required to penetrated by GLDA, ft
r_H	dissolution rate due to hydrogen ion attack, mol/cm^2/s
r_{HCl}	reaction rate of HCl with dolomite, kmole dolomite/m^2.s
r_{HmY}	dissolution rate due to chelation, mol/cm^2/s
R_{linear}	linear coreflood radius, cm
r_{max}	maximum pore radius, cm
r_t	treated radius, ft
r_w	radius of the wellbore, ft
S	skin damage, dimensionless
T	Temperature, ^{o}C
T_r	reaction temperature, ^{o}K
U_{max}	maximum injection flux that can be used for acidizing, cm/s
U_{opt}	optimum flux, cm/s
V_{CaCO3}	volume of calcite dissolved by the GLDA, ft^3
V_{GLDA}	volume of GLDA required to create wormholes, ft^3
v_i	interstitial velocity, cm/min
$v_{i,opt}$	optimum interstitial velocity, cm/min
$v_{i,tip}$	interstitial velocity at the wormhole tip, cm/min
v_{wh}	wormholing rate, cm/min
X	volumetric dissolving power, ft^3 CaCO$_3$/ft^3 acid
ΔE	activation energy, J/mole
$\Delta E/R$	constant = 11.32 x 103 ^{o}K for the reaction of HCl with dolomite
Δp	pressure drop across the core, psi
$\Delta p_{initial}$	initial pressure drop across the core during injecting water, psi
Δp_{max}	maximum pressure drop across the core, psi

Δp_{GLDA}	pressure drop due to flowing GLDA inside the core, psi
Δp_w	pressure drop due to flowing water inside the core, psi
Δp_{wh}	pressure drop across the wormhole, psi
$\Delta \phi_{max}$	maximum change in core porosity after treatment by GLDA, = 0.08
α	reaction order
α_{CaCO3}	stoichiometric coefficient of $CaCO_3$
α_{GLDA}	stoichiometric coefficient of GLDA
β	gravimetric dissolving power, lbmole $CaCO_3$/lbmole acid
β_o	oil formation volume factor, bbl/stb
ϕ	core porosity, fraction
ϕ_f	core porosity after the treatment, fraction
ϕ_i	core porosity before the treatment, fraction
κ	overall dissolution rate, cm/s
μ	fluid viscosity, cP
μ_{GLDA}	GLDA solution viscosity, cP
ν	stoichiometric molar ratio of products to reactants
ρ_{CaCO3}	calcite density, g/cm^3
ρ_{GLDA}	GLDA density, g/cm^3
ρ_{rock}	rock density, g/cm^3

TABLE OF CONTENTS

LIST OF FIGURES

LIST OF TABLES

CHAPTER I

INTRODUCTION: THE IMPORTANCE OF RESEARCH

Carbonate Matrix Acidizing

Formation damage may be defined as any impairment of well productivity or injectivity due to plugging within the wellbore, in perforation, in formation pores adjacent to the wellbore or fractures communicating with the wellbore. Almost all wells are damaged, the problem is to determine the degree of damage, location, probable causes of damage and approaches to alleviate any serious damage.

Formation damage may be indicated by well tests, pressure build up and draw down tests, comparison with offset well, careful analysis of production history.

If multiple zones are open in a single completion, PLT (Production logging Techniques) runs in a flowing well will often show some permeable zones to be contributing little or nothing to the production. A reservoir study may be required to differentiate between:

- Production decline due to gradual formation damage
- Decline due to loss in reservoir pressure, comparison with offset well may not be sufficient to detect gradual damage because all of wells may be subjected to the same damaging mechanisms.

In a relatively high permeability well with skin damage, reservoir pressure may be measured in the well, and it may stabilize within few hours. If reservoir the permeability is low, days or weeks may be required to stabilize the reservoir pressure. Under these conditions, it may be difficult to determine 'skin' damage. Skin damage calculation using pressure build up and draw down analysis are carried out in many areas prior to planning well stimulation.

Once mechanical pseudo skin effects are identified, positive skin effects can be attributed to formation damage. Formation damage is typically categorized by the mechanism of its creation as either natural or induced. Natural damages are those that occur primarily as a result of producing the reservoir fluid. Induced damages are the result of an external operation that was performed on the well such as a drilling, well completion, workover, stimulation treatment or injection operation. In addition, some completion operations, induced damages or design problems may trigger the natural damaging mechanisms.

This dissertation follows the style of *SPE Journal*.

Natural damages include:

- Fines migration
- Swelling clays
- Water-formed scales
- Organic deposits such as paraffins or asphaltenes
- Mixed organic/inorganic deposits
- Emulsions.

Induced Damages Include:

- Plugging by entrained particles such as solids or polymers in injected fluids
- Wettability changes caused by the injected fluids.

Carbonate Matrix Acidizing has been carried out for several years using hydrochloric acid-based stimulation fluids in various concentrations. At high temperatures HCl does not produce acceptable stimulation results because of its fast reaction in the near wellbore area, low acid penetration, and surface dissolution (Huang et al. 2003).

Williams et al. (1979) recommended that carbonate acidizing treatments should be carried out at the highest possible injection rate without fracturing the reservoir rock ($q_{i,max}$). Wang et al. (1993) discovered an optimum acid injection rate to obtain breakthrough during acid treatments for carbonate cores in linear coreflood using a minimum acid volume. The optimum acid injection rate was found to be a function of the rock composition and reaction temperature as well as the pore size distribution of the reservoir rock. A problem occurs if the required optimum injection rate is greater than the maximum acid injection rate. In this case HCl cannot be used because it will cause face dissolution if used at low injection rates, or will fracture the formation if used at high injection rates. Therefore stimulation fluids other than HCl-based fluids such as chelating agents need to be used to achieve deep and uniform penetration and eliminate face dissolution problems.

Another problem encountered during stimulation using HCl-based fluids is the high corrosion rate of these fluids to the well tubulars. Well tubulars are often made of low-carbon steel and may contain rust. HCl will dissolve the rust and produce a significant amount of iron, which in turn will precipitate and cause formation damage. Corrosion becomes more severe at high temperatures, and special additives are needed to compensate for the loss in corrosion inhibition at higher temperatures. The cost of these additives exceeds 5% of the treatment cost (Fredd 1998). Also the excessive use of corrosion inhibitors may cause other problems, as the corrosion inhibitor may adsorb on the reservoir rock and change its wettability, especially in low permeability reservoirs (Schechter 1992).

Chelating agents have the ability to complex metal ions by surrounding them with one or more ring structures. The process of chelation results in the formation of a metal-chelate complex with high stability. For example, ethylenediaminetetraacetic acid (EDTA) compounds are capable of forming stable chelates with di- and trivalent metals like Fe and Ca (Martell and Calvin 1952).

Fredd and Fogler (1997; 1998a; 1999) investigated the use of EDTA and DTPA to stimulate calcium carbonate cores. They performed linear coreflood experiments using Texas cream chalk and Indiana limestone cores of 1.5 in. diameter and 2.5, 4, or 5 in. length. The porosity range of these cores was between 15 and 20 vol%, and the permeability range was 0.8 to 2 md. They used 0.25M EDTA of pH 4.0, 8.8, and 13.0 with a flow rate of 0.3 cm^3/min. The maximum wormhole obtained was at pH 4 with a minimum pore volume required to breakthrough the core (PV = 4.8), whereas at pH 13, a PV of 12.7 was used to breakthrough the core and form a wormhole. Fredd and Fogler (1999) concluded that, the EDTA can effectively wormhole in limestone, even when injected at moderate or non-acidic pH values (4 to 13) and at low flow rates where HCl is not effective. The dissolution mechanism involves chelation of calcium ions and does not require conventional acid attack. The ability to stimulate under acidic conditions combined with the ability to chelate metal ions provides multiple benefits in using EDTA.

Fredd and Fogler (1998b) studied the influence of transport and reaction on wormhole formation during the reaction of chelating agents with calcium carbonate cores. They studied the effect of the Damköhler number (N_{Da}) on the pore volume consumed by the chelating agent to breakthrough the core. The Damköhler number, N_{Da}, can be defined as the ratio of the net rate of dissolution by acid to the rate of convective transport of acid. When the dissolution is mass transfer limited the Damköhler number in this case will be mass transfer limited Damköhler number ($N_{Da(mt)}$) and can be determined from the following equation:

$$N_{Da(mt)} = \frac{aD_e^{2/3}}{Q} \dots\dots\dots\dots\dots\dots\dots\dots\dots\dots\dots\dots\dots\dots\dots\dots\dots\dots\dots (1)$$

where; D_e is the effective diffusion coefficient, Q is the injection rate, and *a* is a constant and depends on the carbonate core. When the net rate of dissolution is reaction rate limited, the Damköhler number, $N_{Da(rxn)}$, is given by:

$$N_{Da(rxn)} = \frac{aK_s d_p l_p}{Q} \dots\dots\dots\dots\dots\dots\dots\dots\dots\dots\dots\dots\dots\dots\dots\dots\dots\dots (2)$$

where; K_s is the surface reaction rate constant, l_p is the pore length, and d_p is the pore diameter.

Fredd and Fogler (1998c) showed that DTPA (at pH 4.3) and EDTA (at pH 13 and 4) exhibit an optimum Damköhler number where the number of pore volumes to breakthrough the core was minimized.

Fredd and Fogler (1998c) studied the effect of NaCl and KCl on the rate of dissolution of calcite by EDTA. They observed that the rate of dissolution increased as the ionic strength was increased with adding KCl. In contrast the rate with EDTA was observed to decrease as the NaCl concentration was increased from 0 to 0.7M.

Frenier et al. (2001 and 2003) examined chelating agents with a hydroxyl group to determine their acid solubility and ability to complex iron and calcium under oilfield conditions. **Fig. 1** shows the chemical structure of the chelating agents that are used in the oil field industry. Dissolution tests were performed using calcite and gypsum in a slurry reactor for 10-24 hrs. The dissolved calcium ion was determined using ICP. Corrosion tests were run in a high pressure autoclave. The results showed that hydroxyethyliminodiacetic acid (HEIDA) is a very effective complexing agent for Fe^{3+} in HCl acid solutions. It has a high-capacity to dissolve calcite, gypsum, and fines clean-up. The environmental impact of HEIDA is less than that of EDTA, as HEIDA is more biodegradable than EDTA (for HEIDA more than 90% was degraded within two weeks, however in the case of EDTA, less than 5 % was degraded within 28 days) (Frenier et al. 2003).

Huang et al. (2003) tested 10 wt% solutions of acetic acid, Na_4EDTA and long-chained carboxylic acid (LCA) using Indiana limestone cores of 1 in. diameter and 4 in. length. These cores have porosities of nearly 15 vol% and permeabilities of 2 to 3 md. The dissolving power of 10 wt% LCA was measured to be 0.45 lb/gal at room temperature. They performed core flow tests at 250°F at different flow rates to determine the optimum injection rate to breakthrough the core will minimum pore volume. All the three chemicals used formed wormholes in the tested cores.
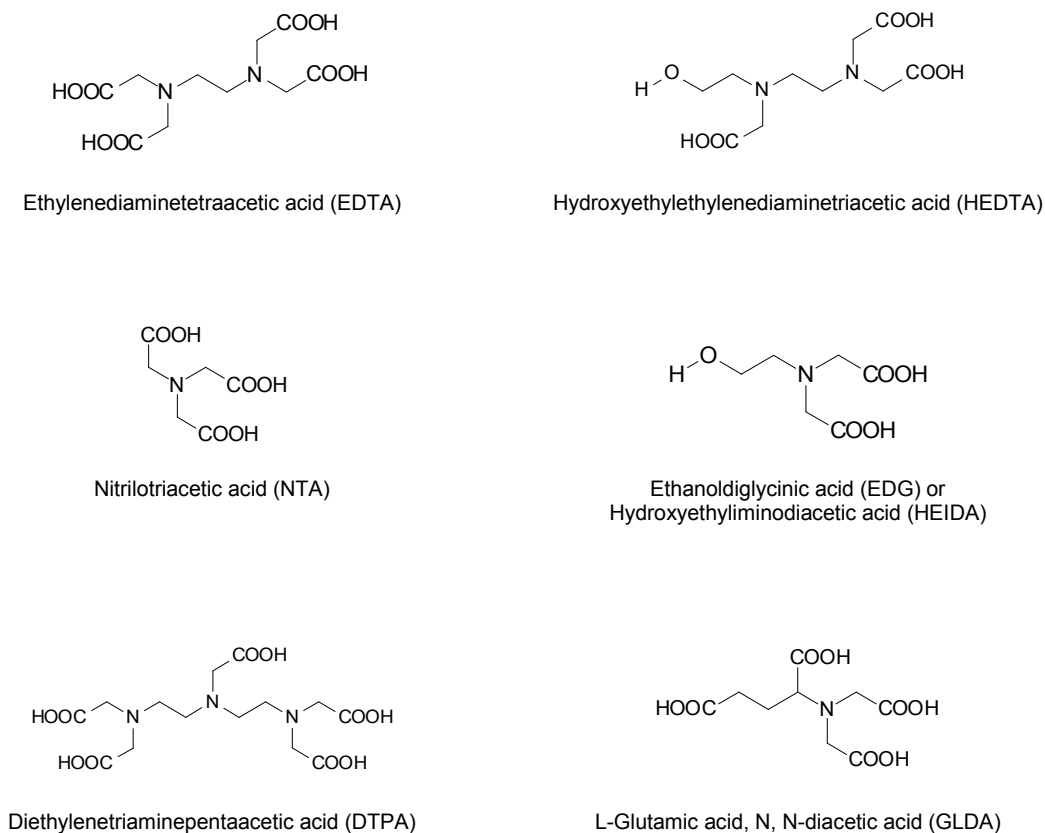
Fig. 1—Structures of chelating agents commonly used in the oil industry. GLDA is the new chelate tested in the present study.

Most of the current chelates have low biodegrability and some of them have very low solubility in 15 wt% HCl solutions. LePage et al. (2010) introduced a new environmentally friendly chelate: L-glutamic acid, N, N-diacetic acid or GLDA, which is manufactured from L-glutamic acid (MSG- Mono-Sodium Glutamate). They compared the new chelate (GLDA) with other chelates, including EDTA, hydroxyethylethylenediaminetriacetic acid (HEDTA), nitrilotriacetic acid (NTA) and ethanoldiglycinic acid (EDG). GLDA was very effective in dissolving calcium carbonate compared to other chelates and organic acids. In their results they showed that one gallon of 20 wt% GLDA dissolved up to 1.5 lb calcium carbonate, whereas one gallon of 15 wt% HCl can dissolve 1.8 lb calcium carbonate. GLDA has better solubility in HCl over a wide pH range, unlike other chelates. Regarding environmental, safety and health issues, GLDA has favorable environmental characteristics as it is readily biodegradable.

Major challenges associated with conventional stimulation fluids include the corrosive nature of these fluids on well tubulars particularly at high temperatures (Wang et al. 2009) and their inability to treat heterogeneous formations without employing diversion techniques. Additionally, highly reactive conventional acids tend to preferentially flow to the higher permeable zones in heterogeneous formations. The diversion and reaction of injected acid into areas of highly permeable zones created increased flow and reaction in these zones. This occurs at the expense of bypassing the low permeable zones leading to inefficient stimulation of the target low permeability or damaged intervals. This is also true for matrix acidizing of long open-hole horizontal wells and extended reach wells. The success of conventional matrix acidizing in carbonate reservoir with HCl is often limited because of the optimal injection rate would exceed the fracture gradient of the formation (Haung et al. 2000).

Different acid systems have been used to reduce the problems associated with HCl such as rapid acid spending and face dissolution at low injection rates. Acid systems based on weak acids, like formic and acetic have a low concentration of H^+ in comparison to HCl and will react with calcium carbonate at a slower rate than HCl (Abrams et al. 1983). Retarded acid systems can also be employed to reduce the reaction rate of HCl with carbonate formations. One such system employed HCl emulsified in an oil phase that reduces acid diffusion to the carbonate surface and allows for deeper penetration of the live acid (Hoefiner and Fogler 1985). Foamed acids have also been employed in a retarded acid system during stimulation of carbonate formation, as the foam will lower the liquid saturation and thus increase the convection rate for the same injection rate. The foam also will lower the liquid permeability and decreases the amount of live acid that leaks-off from the primary channel (Bernadiner et al. 1992). Acetic and formic acids suffer from having a low solubility of calcium salts formed and cannot be used at high acid concentrations (Economides and Kenneth 2000) in addition to corrosion problems at high temperatures (Huang et al. 2002).

Optimum Injection Rate for Different Stimulation Fluids

Several studies investigated the optimum conditions for wormhole formation during carbonate acidizing using hydrochloric acid (HCl). They have shown that the dissolution pattern created can be characterized as being one of the following types (Haung et al. 1997, Fredd 2000a, Robert and Crowe 2000, and Fredd 2000b):

1. compact or face dissolution in which most of the acid is spent near the rock face;
2. conical wormholes;
3. dominant wormholes;
4. ramified wormholes; and
5. uniform dissolution

The transition from dissolution structure 1 to 5 is commonly observed as the injection rate is increased. At low injection rates, the reactant is consumed on the inlet flow face of the core, resulting in face dissolution or complete dissolution of the core starting from the inlet flow face. The face dissolution structure consumed large volumes of reactant and provides negligible depths of live acid penetration. At slightly higher injection rates, the acid or the treating fluid can penetrate into the porous medium and enlarge flow channels. At intermediate injection rates, the acid is transported to the tip of the evolving flow channel, where subsequent consumption propagates the channel and eventually leads to the formation of a dominant wormhole. At high injection rates, the dissolution channels become more highly branched or ramified as the fluid is forced into smaller pores. At very high injection rates, uniform dissolution is observed as the acid is transported to the most pores in the medium.

The type of dissolution structure was found to have a significant effect on the volume of acid required to obtain a given penetration depth of wormhole. This effect was investigated by Fredd and Fogler (1998a, 1999). Fredd and Fogler (1999) studied the dependence of the number of pore volumes to breakthrough, PV_{bt}, on the injection rate for the dissolution of limestone by various stimulation fluids. The fluids that they investigated were: DTPA (Diethylenetriaminepentaacetic acid), EDTA (Ethylenediaminetetraacetic acid), acetic acid, and HCl. All the fluids exhibited an optimum injection rate at which the number of pore volumes required to breakthrough is the minimum and dominant wormhole channels are formed. The number of pore volumes to breakthrough increased to the left and right of the minimum due to the formation of conical wormhole and ramified wormholes, respectively. The optimum injection rate corresponds to conditions at which a minimum volume of fluid is required to achieve a given depth of wormhole penetration. Hence, it represents the most effective and optimum conditions for matrix stimulation. They found these conditions at an optimum Damköhler number of 0.29.

Haung et al. (1997) stated that the optimal acidizing conditions of a given formation can be determined by the following optimum Damköhler number;

$$N_{Da(opt)} = \frac{(\pi/20)^{3/2} r_{max}^2}{k l_p} \quad \text{.. (3)}$$

where; $N_{Da(opt)}$ is the optimum Damköhler number to form wormholes, r_{max} is the maximum pore radius; k is the rock permeability, and l_p is the average pore length.

The optimal Damköhler number is fixed for a given formation and depends on the largest pore size naturally occurring (Huang et al. 2000). Also, we can relate the optimal acid injection rate to the optimal Damköhler number by the following relation:

$$U_{opt} = E_f^0 C_0^{m-1} \exp\left(\frac{\Delta E}{R T_r}\right) / N_{Da(opt)} \quad \text{.. (4)}$$

where; U_{opt} is the optimal flux to form wormholes, E_f^0 is the reaction rate constant, C_0 is the initial acid concentration, m is the reaction order, ΔE is the activation energy, R is the universal gas constant, and T_r is the absolute temperature of the reservoir.

Matrix acidizing under field conditions limits the flow rate to values that cause the bottom hole treating pressure to stay below the fracture initiation pressure and the surface pressure below the maximum allowable surface pressure because of equipments limitations (Glasbern et al. 2009). Therefore, the maximum flux that we can use during the acidizing treatment can be determined using **Eq. 5**:

$$U_{max} = 0.092k\left(g_{fr}D_f - p_r\right) / \left(r_w\mu\left(ln\frac{r_e}{r_w} + S\right)\right) \quad \text{........................... (5)}$$

where; U_{max} is the maximum injection flux that can be used for acidizing (cm/hr), k is the formation permeability (md), g_{fr} is the formation fracture gradient (psi/ft), D is the formation depth (ft), p_r is the reservoir pressure (psi), r_w is the wellbore radius (ft), r_e is the reservoir drainage radius (ft) and S is the skin damage, dimensionless.

Wang et al. (1993) and Fredd and Fogler (1999) identified an optimum injection rate during carbonate acidizing by hydrochloric acid (HCl). This injection rate is the rate at which the minimum amount (minimum pore volume) of acid needed to form uniform wormholes. The optimum rate was found to be a function of rock mineralogy (dolomite or calcite), acid

concentration, and temperature, but the most important factor was rock mineralogy. Temperature was found to have a strong effect on the HCl optimum injection rate and the optimum injection rate increased with increasing the temperature.

Hill et al. (1995) found an optimum injection rate that results in the least amount of acid to breakthrough the core and create wormholes. At injection rates above and below the optimum injection rate, the amount of acid required to break through the core was greater than that at the optimum rate.

Diversion in Stimulation Treatments

Zerhboub et al. (1994) studied the use of foam as a diverting agent in matrix acidizing. Using of foam is a complicated process as it requires mutual solvent to clean the near-wellbore from oil as the oil may destroy the foam. It requires preflush containing surfactant before injecting the foam pill. The well should be shut in after injecting the foam; also, a surfactant should be added to the treating fluid to prevent interaction between acid and foam.

Wang et al. (2009) introduced a nonaggressive fluid to stimulate carbonate reservoirs. The corrosion rate of this fluid is very small compared to HCl and because of its nonreactive nature, it can be used to stimulate heterogeneous reservoirs without using diverting agents. Parallel coreflood experiments showed that the fluid was able to stimulate both high and low permeability cores without using diverting agents.

A good diversion was obtained using the VES-based system in stimulation of carbonate reservoirs. The diversion ability was evidenced by the increase in the down hole pressure during the injection of the diverter and the change in bottom hole injection temperature (Zeiler et al. 2006).

Al-Ghamdi et al. (2009, 2010) did a parallel coreflood on two calcite cores using 15 wt% straight HCl and surfactant-based HCl. Flowing 15 wt% HCl into two different cores with different permeabilities. The acid flowed predominantly into the high permeability core rather than the low permeability core. Surfactant-based acid only worked with low permeability contrast (1.7 permeability ratio) and did not work for high ratios at different rates.

Yu et al. (2009, 2010) studied the retention of surfactant form the surfactant-based acid following the coreflood experiments at different shear rates. More than 60 wt% of the surfactant was retained in the core after the coreflood treatments in all the treatments they did. At low shear rates the surfactant retention reached more than 85 wt% inside the core. To remove the retained surfactant they used mutual solvent (ethylene glycol monobutyl ether). Two pore volumes of mutual solvent were injected at 1.5 cm^3/min and only 21.2 wt% of the retained surfactant was recovered.

Chang et al. (2001) used viscoelastic surfactant (VES) to stimulate calcite cores. They used three cores with different permeabilities to simulate the formation heterogeneity. The VES-based acid only broke through the core with the higher permeability in the three experiments they did, although the permeability contrast between the three cores was not high (2:1:1, 1:3:1, 1:1.5:1).

Taylor et al. (2003) used the Viscoelastic surfactant to stimulate three calcite cores with permeability ratio of 1:3:1.5. The acid only broke through the higher permeability cores and increased the permeabilities of the other cores.

Gomaa et al. (2009) studied the use of in-situ gelled acid based on polymer to acidize calcite cores. They found that the polymer has a very good ability in diversion but the after acidizing they observed a polymer residue around the wormholes. They confirmed the presence of polymer inside the core using a CT scan study. The system they used in the coreflood experiments included breaker and with the presence of the breaker in the system the polymer was trapped inside the core.

Taylor and Nasr-El-Din (2002) used the in-situ gelled acid based on polymer to stimulate calcium carbonate cores. They found that the in-situ gelled acids reduced the permeability of low permeability carbonate rock. Polymer was the source of damage and the cross-linker was retained in the cores during the coreflood treatment.

Nasr-El-Din et al. (2001) used the emulsified acid system to stimulate deep carbonate sour gas reservoirs. Emulsified acid was successfully used to acid fracture eleven vertical wells in deep sour gas reservoirs. No operational problems were encountered during mixing or pumping the emulsified acid. Substantial increases in gas production were obtained from emulsified acid treatments. Temperature stable emulsified acid systems provide incremental conductivity at lengths greater than 150 ft and temperatures in excess of 275°F.

Effect of Reservoir Fluid Type on the Stimulation of Calcite by HCl

Shukla et al. (2003) investigated the effect of injecting nitrogen, decane, and alternate nitrogen/acid injection on the creation of wormholes for Texas Cream Chalk using 15 wt% HCl at room temperature and 50°C. Their experimental results showed that injecting nitrogen inert gas ahead of the acid enhanced the performance of HCl. Injecting nitrogen decreased the amount of acid needed to propagate a wormhole through the 6-in. Texas Cream carbonate core. The volume of acid required to breakthrough the core was decreased by factor of 1.5 to 3 times and the wormholes were narrower and less branched than those created in water saturated cores without gas injection. The injected gas reduced the fluid loss from the wormhole, which in turn resulted from the reduced relative permeability to water in the gas saturated matrix. They found that saturating the cores by decane (oil) gave results similar to the gas. The decane increased

the wormhole propagation efficiency due to the lower relative permeability in matrix to acid solution. Injecting gas alternated with the acid decreased the efficiency of acidizing due to the presence of gas in the wormhole blocked the transport of acid, caused more branching of the wormhole, and more volume was required to create wormholes (Shukla et al. 2006).

Gidley et al. (1996) showed that displacing the crude oil in the formation with CO_2 in the zone to be acidized reduces the interaction between spent acid and oil in the formation. This process eliminated the need to treat the spent acid returns in the produced oil.

Stimulation of Dolomite Reservoirs

Chelating agents have been used as stand-alone stimulation fluids to stimulate calcite formations. Fredd and Fogler (1998a) tested the use of different chelating agents' formulas reaction with calcium carbonate cores and the ability of these chemicals to form wormholes. 0.25M DTPA (pH = 4.3) and 0.25M EDTA (pH = 4 & 13) have been used to create wormholes in calcite cores. The core permeability ratio (final value/original value) reached at least 100 after the test but with different pore volumes for each chemical. The efficiency of the chelating agents at low injection rates is consistent with the dependence of wormhole structure on the Damköhler number and relatively low diffusion coefficients of DTPA and EDTA compared to of HCl.

The dissolution of dolomite by chelating agents has not been thoroughly investigated. Preliminary experiments with EDTA at ambient temperature reveal no significant dolomite dissolution. The dissolution mechanism is probably inhibited by the low stability of the magnesium chelate at that temperature (Fredd 2000a).

The kinetics of dissolution of dolomite by HCl is completely different than that of HCl with calcite. The reaction of HCl with dolomite can be written as follows:

$$4HCl + CaMg\ (CO_3)_2 \rightarrow CaCl_2 + MgCl_2 + 2CO_2 + 2H_2O \ldots\ldots\ldots\ldots\ldots \ (6)$$
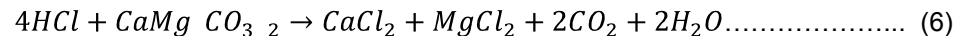
The dissolving power of various acids with both calcite and dolomite are listed in **Table 1** (Schechter 1992). The dissolution power of different acids to dolomite is less than calcite. The dissolution of dolomite by HCl depends on the temperature and the reaction rate equation can be written as follows:

$$r_{HCl} = E_f C_{HCl}^{\propto} \ldots\ldots\ldots\ldots\ldots\ldots\ldots\ldots\ldots\ldots\ldots\ldots\ldots\ldots\ldots\ldots\ldots\ldots\ldots\ldots \ (7)$$

$$E_f = E_f^0 exp\ \left(\frac{\Delta E}{RT_r}\right) \ldots\ldots\ldots\ldots\ldots\ldots\ldots\ldots\ldots\ldots\ldots\ldots\ldots\ldots\ldots\ldots \ (8)$$

C_{HCl} in kmole/m^3, r_{HCl} in kmole dolomite/m^{2}s. The kinetics constants for the reaction models of HCl with both calcite and dolomite are listed in **Table 2** (Schechter 1992).

Hill et al. (1993) stated that the wormhole penetration formed during matrix acidizing by HCl was much less in dolomite formations than calcite formations at the same conditions (Hill et al. 1993). The effect of temperature on the pore volumes required for breakthrough in dolomite cores at different rates is shown in **Fig. 2** (Hill and Schechter 2000). The wormhole radius for the same conditions was much less in dolomite than limestone due to the difference in reaction rate between HCl and both dolomite and calcite.

Table 1—DISSOLVING POWER FOR DOLOMITE AND CALCITE BY DIFFERENT ACIDS			
Acid	**HCl**	**Formic**	**Acetic**
lb dolomite/lb acid	1.27	1.00	0.77
lb calcite/lb acid	1.37	1.09	0.83

Table 2—CONSTANTS IN HCl-MINERAL REACTION KINETICS MODEL			
Mineral	$\underline{\alpha}$	$\dfrac{E_f^0,}{\dfrac{kmoles HCl}{m^2 - - kmoles\,HCl/m^3 acid\,solution)^\alpha}}$	$\dfrac{\Delta}{R}$, °K
Calcite (CaCO$_3$)	0.63	7.314×10^7	7.55×10^3
Dolomite (CaMg(CO$_3$)$_2$)	$\dfrac{6.32 \quad 0^- \; T_r}{1 - 1.92 \quad 0^- \; T_r}$	4.48×10^5	7.9×10^3
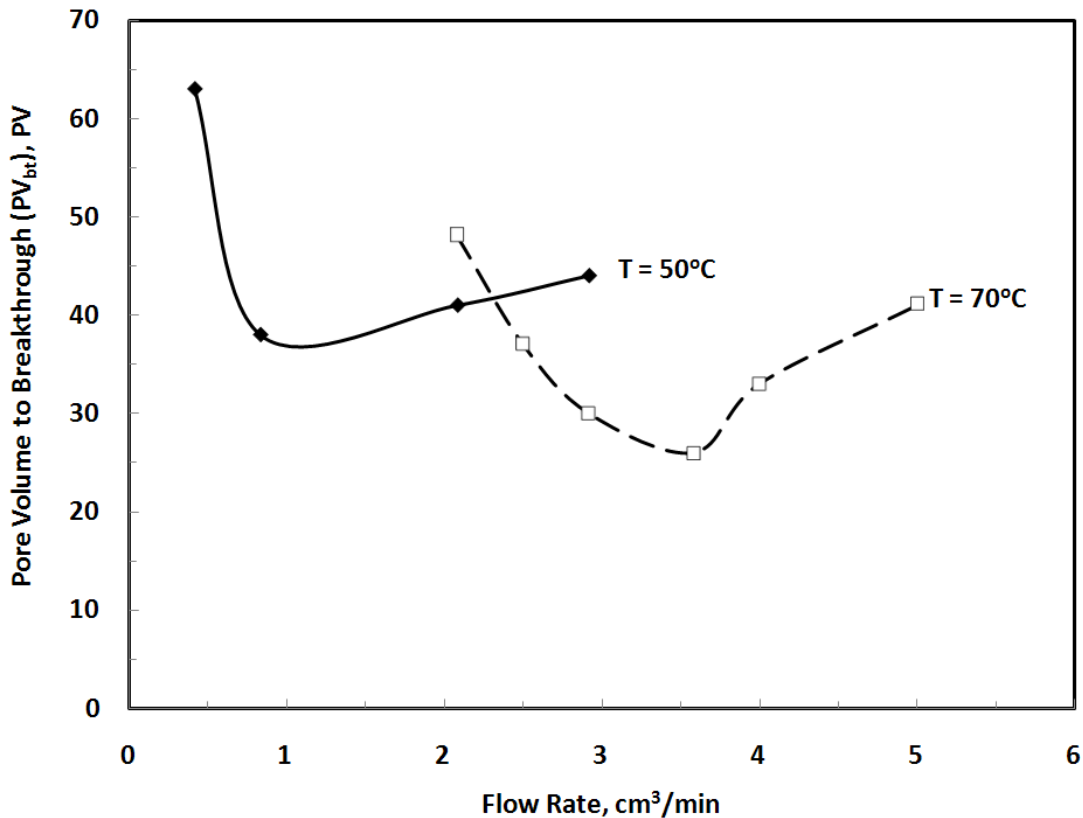
Fig. 2—Effect of temperature on the variation of volumes to breakthrough with the injection rate for dolomite (after Hill and Schechter 2000).

Using rotating disk, different dolomite cores reacted differently with HCl at the same temperature (180°F). Different dolomites may have drastically different kinetics. Five dolomite samples were tested, two of them showed solubility of 80% in HCl and the others showed solubility greater than 90% (Anderson 1991).

Nasr-El-Din et al. (2001) used acid-in-diesel emulsified acid to stimulate deep dolomite reservoirs using core plugs of permeability less than 10 md at 250°F. The acid created deep wormholes which significantly increased the permeability of the treated cores. The reactivity of the average limestone and dolomite are the same at 200°F. At 100°F, the reactivity of an average limestone is about twice that of the average dolomite (Gdanski 2005).

Gdanski (2005) showed that the reactivity of the average limestone and dolomite are the same at 200°F. At 100°F, the reactivity of an average limestone is about twice that of the average dolomite.

Lund et al. (1973 and 1975) studied the dissolution of both calcite and dolomite by HCl using the rotating disk instrument. Their work showed that at 25 °C, the dissolution of calcite is

mass transfer limited even at high disk rotational speeds, while at -15.6 ºC, both mass transfer and surface reaction rates limit the dissolution rate. In contrast, Lund et al. (1975) showed that the dissolution of dolomite was surface reaction rate limited at 25 ºC even at low disk rotational speeds. As the temperature was increased to 100 ºC, the dissolution process approached diffusion limitation even at relatively high rotational speeds.

Taylor et al. (2003) used the rotating disk instrument to measure acid dissolution rates, reaction rates of reservoir rock from a deep Dolomitic gas reservoir. Measurements are made from room temperature up to 85 ºC at rotational speeds of 100 to 1000 rpm and acid concentrations of 0.05 to 5N HCl (0.2 to 17 wt%). The results showed how acid dissolution rates change as the reservoir rock varied from 3 to 100 wt% dolomite. It was found that the reactivity of the rock varied from values expected for pure calcite marble to those expected for pure dolomite marble. At grain densities near 2.72 g/cm^3 (expected for pure calcite), rock dissolution rates varied by more than an order of magnitude due to rock mineralogy. At grain densities near 2.83 g/cm^3 (expected for pure dolomite) rock dissolution rates were higher than that observed with pure dolomitic marble. Reaction rates depended on mineralogy and the presence of trace components such as clays.

The rate of dolomite dissolution is slow compared to marble at 25°C; the dissolution rate for both minerals is rapid at 100°C. The dissolution of marble in HCl is diffusion limited at temperatures above 0°C. The dissolution of dolomite is surface reaction limited at low temperature and mass transfer limited at higher temperatures (Lund et al. 1973). The following rate expressions were found to describe the rate of dissolution of dolomite in HCl:

At 25°C $\quad -r_{HCl} = 2.6 \; x \; 10^{-6} C_{HCl}^{0.44}$ .... (9)

At 50°C $\quad -r_{HCl} = 6.6 \; x \; 10^{-5} C_{HCl}^{0.61}$ .... (10)

At 100°C $\quad -r_{HCl} = 5.4 \; x \; 10^{-3} C_{HCl}^{0.83}$ .... (11)

where: C_{HCl} is the HCl concentration, moles HCl/cm^3, and r_{HCl} is dissolution rate, mole HCl/cm^2/s.

Stimulation of Sandstone Reservoirs

The objective of stimulation of sandstone reservoirs is to remove the damage caused to the production zone during drilling or completion processes. Sandstone acidizing consists of three main stages of sandstone acidizing:

- a preflush, normally of hydrochloric acid,
- a mud-acid stage of hydrochloric and hydrofluoric, and
- an after flush that may be hydrochloric acid

The amount of mud acid required to remove the damage can be determined through the experience within a given area. Oil and gas wells respond differently to the amount of mud used in the treatment. They recommended displacing the oil zone with CO_2 to reduce the interaction between spent acid and oil during the acid treatment process. This process reduces the need to treat spent acid returns and allows the use of large mud-acid treatment for deeper acid penetration (Gidley et al. 1996).

Many problems may occur during sandstone acidizing with HCl/HF mud acid. Among those problems: decomposition of clays in HCl acids, precipitation of fluosilicates, the presence of carbonate can cause the precipitation of calcium fluorides (CaF_2), silica-gel filming, colloidal silica-gel precipitation, and mixing between various stages of the treatment (Gdanski and Shuchart 1998).

Bryant and Buller (1990) noticed during using HCl acid in sandstone acidizing that the migration of amorphous silica (hydrated silica) and mineral fragments occurred. Their study indicates damage normally occurs during the HCl treatment. Aluminum is preferentially leached during the dissolution of kaolinite in HCl. The structure of kaolinite is layered (made up of sheets) in which acid attacks preferentially at the edge. In turn this may cause fines migration and formation damage (Hartman et al. 2006). Magnesium and Aluminum could have been leached from the crystalline lattice during dissolution in 15 wt% HCl (Kline and Fogler 1981).

Quartz reacts relatively slowly with HF, whereas aluminosilicates (clay minerals, feldspar, and mica) reacts relatively rapidly (Li et al 1998). The primary reaction is:

$$SiO_2 + 6HF \rightarrow H_2SiF_6 + 2H_2O \dots\dots\dots\dots\dots\dots\dots\dots\dots\dots\dots\dots\dots (13)$$

$$Aluminosilicates + HF \rightarrow H_2SiF_6 + Fluorides\ of\ Al \dots\dots\dots\dots\dots\dots (14)$$
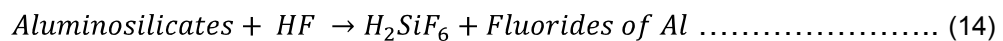
Feldspar dissolution by HF acid:

$$KAlSiO_8 + 13HF \rightarrow K^+ + 2H^+ + AlF^{2+} + 3SiF_6^{2-} + 8H_2O \text{ .... (15)}$$
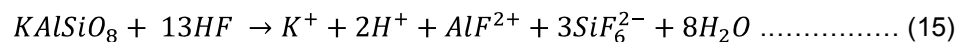
Secondary reaction:

HF with aluminosilicates is the reaction of fluoslilic acid derived from the primary reaction with an aluminosilicates to form hydrated silica gel.

$$SiF_6^{2-} + KAl_3Si_3O_8 + 18H^+ + 10H_2O \rightarrow K^+ + 3AlF^{2+} + 18H_2SiO_3 + H_4SiO_4 \text{.... (16)}$$

and

$$SiF_6^{2-} + 6KAl_3Si_3O_{10}(OH)_2 + 6H^+ + 4H_2O \rightarrow 6K^+ + 6AlF^{2+} + 4H_4SiO_4 \text{ .... (17)}$$
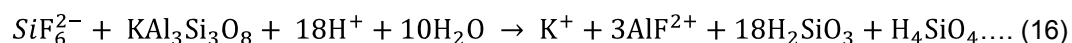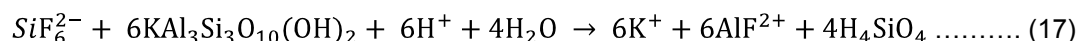
Dissolving the silicon in aluminosilicates results in an amorphous silica gel film. In addition, the silica in SiF_6^{2-} also precipitates as silica gel.

Tertiary reaction:

The tertiary reaction of HF with aluminosilicates involves the further reduction of the F/Al ratio in dissolved aluminum fluoride species. The reaction extracts aluminum out of aluminosilicates and leaves silica gel in the matrix.

The reaction with K-feldspar will be:

$$AlF^{2+} + KAl_3Si_3O_8 + 4H^+ + 4H_2O \rightarrow K^+ + 2AlF^{2+} + 3H_4SiO_2 \text{ ....……….. (18)}$$
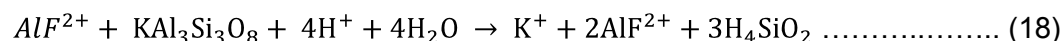
The reaction will continue reducing Al/F ratio in the spent HF until the remaining HCl is consumed.

Mud acid cannot be used in sandstone with high calcite concentration. Calcite reacts very quickly and completely with HCl acid, but in the presence of HF, the reaction proceeds (Martin 2004).

$$CaCO_3 + 2HF \rightarrow CaF_2 + H_2O + CO_2 \text{ ....…………….……………………… (19)}$$
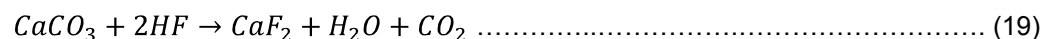
CaF_2 has very low solubility. Preflushing the near-wellbore with HCl minimized this problem.

The reaction products of fluosilicic acid and fluoaluminic acid are readily soluble in water, but their potassium, sodium, and calcium salts are partially insoluble. The salts are formed by the following reaction:

$$SiF_6^{2-} + 2K^+ \rightarrow K_2SiF_6 \dots\dots\dots\dots\dots\dots\dots\dots\dots\dots\dots\dots\dots\dots\dots\dots\dots\dots\dots \text{(20)}$$

$$SiF_6^{2-} + 2Na^+ \rightarrow Na_2SiF_6 \dots\dots\dots\dots\dots\dots\dots\dots\dots\dots\dots\dots\dots\dots\dots\dots\dots\dots \text{(21)}$$

$$SiF_6^{2-} + 2Ca^{2+} \rightarrow CaSiF_6 \dots\dots\dots\dots\dots\dots\dots\dots\dots\dots\dots\dots\dots\dots\dots\dots\dots\dots\dots \text{(22)}$$
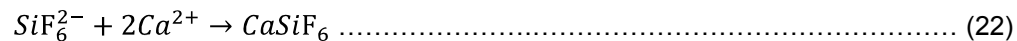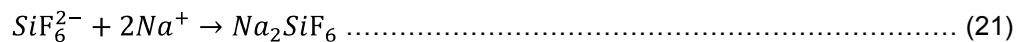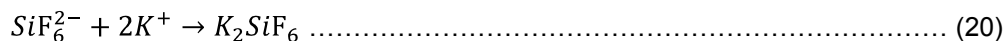
Calcium, potassium, and sodium ions should not be mixed with either spent or unspent HF. Formation water, which contains calcium chloride, potassium chloride, and sodium chloride should be avoided. The only compatible salt solution with HF is ammonium chloride. Ferric hydroxide forms when acid spends and pH rises. Sources of ferric iron include some minerals, such as chlorite, siderite, and hematite, and tubing rust. Problems of stimulating high-temperature sandstone reservoirs with HCl are:

- sand deconsolidation
- clay destabilization
- tubular corrosion

Al-Anazi et al. (2000) used different HF acid formulas to stimulate water injectors. The used retarded HF acid system based on AlCl$_3$. The examined cores contained a large amount of K-feldspar. Therefore, it is not recommended to use retarded HF acid based on fluoboric acid to stimulate water injector in this field. The reservoir cores had high content of iron, therefore, there is a need to add iron control agent to the injected acids. A preflush of 5wt% ammonium chloride solution was effective in enhancing the final permeability after RHF stimulation. It appears that this preflush displaced sodium and potassium from the core and minimized precipitation of fluosilicates. A multi-stage stimulation treatment was designed to remove formation damage to enhance wells injectivity in the new developed field. The recommended treatment was successfully applied in the field.

There are several minerals that may precipitate during an acidizing treatment such as:

i. Fluorides: Calcium fluoride (fluorite), CaF$_2$, has a very low solubility and, consequently, a high potential for precipitation. However, calcium fluoride precipitation can be virtually eliminated if an adequate HCl pre-flush is used to remove carbonates from the near-wellbore region prior to injecting HF. Aluminum

fluoride (fluellite), AlF_3, is another potentially damaging precipitate. Precipitation of AlF_3 occurs at high HF/HCl ratios or when the HF concentration exceeds 4 wt%.

ii. Fluorosilicate and Fluoroaluminate Salts: K_2SiF_6, Na_2SiF_6, N_3AlF_6, and K_3AlF_6 salts are all contingent precipitates. They contended that high HF concentrations favor the precipitation of these minerals, thus, they are more likely to occur during the initial phases of dissolution.

iii. Colloidal Silica: Colloidal silica, $Si(OH)_4$, is perhaps the most important precipitating mineral in sandstone acidizing. Several coreflood experiments have produced evidence of the precipitation of $Si(OH)_4$. In addition, several acidizing models have demonstrated significant colloidal silica precipitation. As reservoir minerals are dissolved, aluminum and silica compete for the available fluorine. Aluminum has the greater affinity for fluorine; thus when the level of free fluorine is reduced, silica precipitates in the form of $Si(OH)_4$.

iv. Iron Compounds: Sandstone reservoirs commonly contain iron bearing minerals such as siderite, ankerite, pyrite, and chlorite. In the presence of HCl, however, iron compounds are unlikely to precipitate. Iron compounds can become a real possibility in carbonates, where there is enough carbonate material present to cause the HCl acid to spend itself completely. This condition is rarely found in sandstones, and, therefore, does not pose much of a problem in sandstone acidization (Quinn et al 2000).

HF can dissolve carbonates, clays, feldspar, micas, and quartz. The primary reason to use HF acid is to remove clays. If carbonates are encountered in sandstone, these should be removed with a preflush of HCl to avoid CaF_2 precipitation. **Table 3** shows the solubility of the different mineral types in mud acid (Allen and Roberts 1993).

Table 3—SOLUBILITY OF DIFFERENT MINERALS IN HCl, AND HCl/HF ACIDS		
Mineral	**Solubility**	
	HCl	**HCl/HF**
Quartz	No solubility	Very low
Feldspars	No solubility	Low to moderate
Kaolinite	No solubility	High
Illite	No solubility	High
Smectite	No solubility	High
Chlorite	Low to moderate	High
Calcite	High	High , CaF_2 is ppt.
Dolomite	High	High , CaF_2 is ppt.

Reaction rate of HF with sand and clays depends on the ratio of the surface area of the rock to volume of acid in sandstone. The fluosilicic acids produced by the reaction of HF on sand and clay will react with Na, K, and Ca producing an insoluble ppt. We should use ammonium chloride solution as a preflush or postflush in HF treatment. Chlorite which contain Fe^{++}, so that HCl can leach Fe^{++} from chlorite leaving an amorphous silica residue.

Productivity Improvement Factor

The success of a given treatment, i.e., the improvement or degradation in well performance, can be measured by the productivity improvement factor (F_{PI}), which is defined as the ratio of post- and pre-stimulation productivity:

$$F_{PI} = \frac{J_a}{J_a^0} = \frac{k_a}{k_a^0}$$ .... (23)

where J_a and J_a^0 are the initial and final productivity indices.

Clay Minerals

Clay minerals are extremely small, platy-shaped materials that may be present in sedimentary rocks as packs of crystals. The maximum dimension of a typical clay particle is less than 0.005 mm. The clay minerals can be classified into three main groups: (1) Kaolinite group, (2) Smectite (or Montmorillonite) group, and (3) Illite group. In addition, there is mixed-layer clay minerals

formed from several of these three basic groups. **Table 4** indicates the chemical structure of the different types of clay minerals (Civan 2000). The interactions of the clay minerals with aqueous solutions are the primary culprit for the damage of petroleum-bearing formations. The rock-fluid interactions in sedimentary formations can be classified in two groups: (1) chemical reactions resulting from the contact of rock minerals with incompatible fluids, and (2) physical processes caused by excessive flow rates and pressure gradients.

Table 4—CHEMICAL STRUCTURE AND SURFACE AREA OF CLAY MINERALS		
Mineral	**Chemical Structure**	**Surface area, m^2/g**
Illite	$K_{1-1.5}Al_4[Si_{7-6.5}Al_{1-1.5}O_{20}](OH)_4$	100
Kaolinite	$Al_4[Si_4O_4](OH)_8$	20
Chlorite	$(Mg, Al, Fe)12[(Si, Al)_8O_{20}](OH)_{16}$	100

Properties and damage processes of the three clay groups can be classified as follows:

i. KAOLINITE has a two-layer structure, K^+ exchange cation, and a small Base Exchange capacity, and is basically non-swelling clay but will easily disperse and move. Kaolinite plates are thought to be some of the more common migratory clays. Damage from fines is located in the near wellbore area within a 3-55 ft radius. Damage also can occur in a gravel pack (silicate and aluminosilicate). Kaolinite can adsorb some water; the adsorbed water is held tightly to the clay surfaces.

ii. Montmorillonite (Smectite) has a three-layer structure, a large Base Exchange capacity of 90 to 150 meq/l00g and will readily adsorb Na^+, all leading to a high degree of swelling and dispersion. Smectite and Smectite mixtures swells by taking water into its structure. It can increase its volume up to 600%, significantly reducing permeability, creating impermeable barrier to flow. The removal of these clays can be accomplished during HF treatment if the depth of penetration was small. If it the depth of penetration was large, the best treatment is to fracture the well to bypass the damage.

iii. Illites are interlayered. Therefore, illites combine the worst characteristics of the dispersible and the swellable clays. The illites are most difficult to stabilize. Also, this type of clay can swell, because it adsorbs water. Osmotic swelling results from concentration imbalances between the ions held at the exchange sites on the clays and the solute content of the contacting fluid, **Fig. 3**.
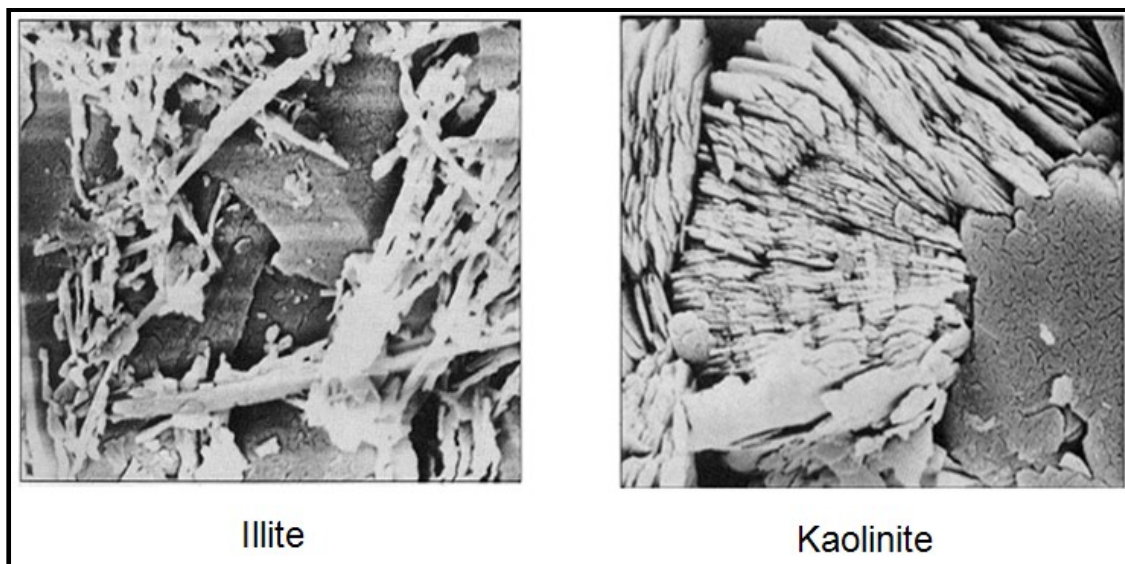
Fig. 3—Forms of clay minerals inside the sandstone formation (Civan 2000).

Amaefule et al. (1988) stated that rock-fluid interactions in sedimentary formations can be classified in two groups: (1) chemical reactions resulting from the contact of rock minerals with incompatible fluids, and (2) physical processes caused by excessive flow rates and pressure gradients. Illites are interlayered, **Fig. 4**. Therefore, illites combine the worst characteristics of the dispersible and the swellable clays. The illites are most difficult to stabilize.
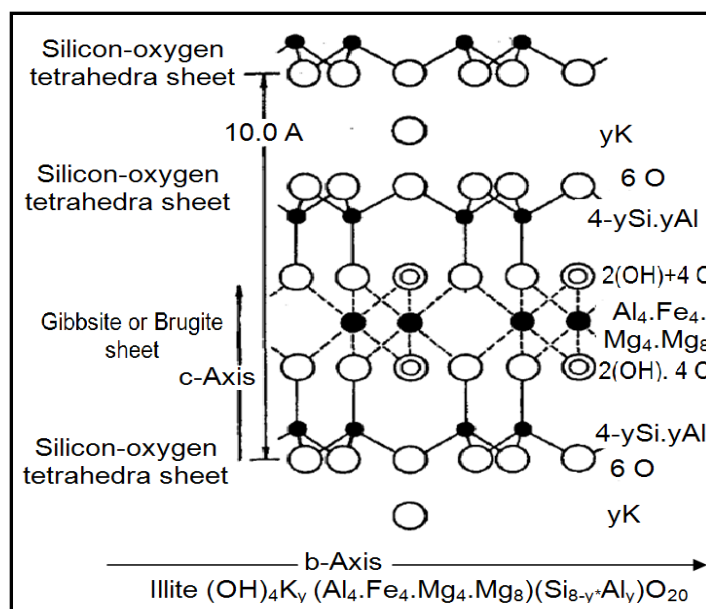
Fig. 4—Schematic description of the crystal structure of illite (Civan 2000).

Flowing HCl in cores containing illite and chlorite (high surface area, **Table 4,** Ezzat 1990 and Welton 1984) caused the pressure drop to increase due to the clay reaction product migration, formation of reaction product and/or increase in the viscosity. Illite and chlorite are attacked by HCl to produce an amorphous silica gel residue i.e. the aluminum layer extracted. The alumina layer if attacked, it will weaken the clay structure and make it more sensitive to fluid flow (Thomas et al. 2001). Thomas et al. (2001) showed that HCl has degraded Illite and chlorite in the tested cores from actual producing sandstone reservoirs. Degradation of Illite and chlorite led to potential core damage. Treating the actual reservoir cores by mud acid caused fines migration during the overflush.

Chelating Agents in Sandstone Stimulation

Parkinson et al. (2010) studied the use of chelating agents to stimulate sandstone formations with high calcite content. Pinda formation in West Africa has a wide range of carbonate content (varying from 2% to nearly 100%) and formation temperature is 300°F. This field was treated using 7.5 wt% HCl with foam, a sequence of job failures was noticed, with constant problems of tubular corrosion. Na_3HEDTA at pH 4 was tested using Berea sandstone cores and was compared with mud acid (9 wt% HCl + 1 wt% HF). The results showed that Na_3HEDTA was more effective in stimulating Berea core than mud acid and HCl.

The coreflood tests were conducted at 290°F, 2,000-psi confining pressure, and 500-psi backpressure with a flow rate range (0.5 to 5 ml/min). Using 0.8 wt% HF with the Chelant deconsolidated the treated core at the injection face of the core plug due to the increased concentration of HF. After the coreflood experiments they performed Na$_3$HEDTA was decided to be used alone in the field treatment.

The old stimulation fluid was 7.5 wt% HCl with corrosion inhibitors, surfactants, iron-control agent, and mutual solvent. The use of this system caused several corrosion-related coiled-tubing failures. HEDTA with 0.2 wt% corrosion inhibitor was used instead of 5 wt% with the 7.5 wt%-HCl and HEDTA showed less corrosion rate than HCl. After treating 6 wells in this filed the production rate from the six wells was increased from 2,881 BOPD (Pre-job production) to 4,531 BOPD (One year post-job production).

Ali et al. (2008) showed that low pH solutions of HEDTA (pH = 4) were capable of stimulating carbonate and sandstone formations at high temperatures. Because of reduced reaction rates and corrosion rates, these fluids effectively stimulated high temperature reservoirs without the damage to the well tubulars and formation integrity that is commonly caused by strong mineral acids.

High temperature sandstone acidizing is challenging due to the very fast reaction rates and instability of clays at these temperatures. Gdanski and Scuchart (1998) have shown that essentially all clays are unstable in HCl above 300°F. The ideal stimulation fluid would remove the near-wellbore damage without depositing precipitates in the formation, and preventing well production declines due to solids movements.

Ali et al (2002) stimulated Berea sandstone cores Na$_3$HEDTA and it gave results better than HCl. EDTA performed better than HCl in actual formations, because the formation is sensitive to HCl because of some silt and fines will react with low pH solution to form precipitates and reduce the final permeability. Wells treated with EDTA fluid produced an average of 1.84 MMscf/d more gas after the treatments. This benefit was approximately twice that observed in wells in the area treated with conventional sandstone stimulation fluids. EDTA was used to remove the calcium carbonate scale from the sandstone reservoirs caused by the drilling fluid and removed the damage caused during the drilling operations (Tyler et al. 1985).

HCl leached the metal aluminum from the clay or feldspar. EDTA or HEDTA removed only calcium from the core. HEDTA removed essentially calcium containing minerals (Calcite, dolomite, Ca-feldspar, etc..) and small amount of aluminosilicates. Removing aluminum may cause fines migration for the clay minerals. Damage was noticed after treatment of wells using HCl but not after Chelant treatments (Shaughnessy and Kline 1982). If the reservoir pressure was not high, the damage may be permanent, as the precipitates may never be produced back.

Frenier et al. (2004, 2000) showed that HEDTA removed the calcium, magnesium, and iron carbonate minerals without inducing damage through clay degradation and precipitated byproducts. Chelating agents were able to stimulate high temperature sandstone formations in the field; they removed the scale and stimulate the high-temperature wells.

Objectives

HCl-based fluids have been used in the oil industry long time ago. Using HCl in stimulation is not favorable in the following cases: high temperature reservoirs, illitic sandstone reservoirs, wells completed with Cr-13 tubing, sandstone with high percentage of calcite, and acid-sensitive crudes bearing formations. HCl can cause damage to sandstone reservoirs if its illite content is high. Therefore, the objectives of this study are to:

i.   Study the ability of GLDA to dissolve calcite over a wide range of pH and comparing this to other chemicals such EDTA, HEDTA, and HEIDA. The thermal stability of GLDA at high temperature will be investigated.

ii.   Investigate the ability of GLDA to form wormholes or channels in 20-in. and 6-in. calcite cores (high and low permeability).

iii. Study the factors affecting the wormhole formation in calcite cores by GLDA.

iv.   Study the effect of reservoirs fluid type on the stimulation of calcite cores by GLDA and HEDTA chelating agents.

v.   Developing analytical model to predict the flow of GLDA in calcite cores.

vi.   Determine the effectiveness of GLDA in stimulating dolomite cores.

vii. Study the possibility of using GLDA as a stand-alone stimulation fluid for sandstone cores and in combination with HF acid to remove the damage from sandstone cores.

CHAPTER II

EVALUATION OF A NEW ENVIRONMENTALLY FRIENDLY CHELATING AGENT FOR HIGH-TEMPERATURE APPLICATIONS

Introduction

Most of the current chelates have low biodegradability and some of them have very low solubility in 15 wt% HCl solutions. LePage et al. (2010) introduced a new environmentally friendly chelate: L-glutamic acid, N, N-diacetic acid or GLDA, which is manufactured from L-glutamic acid (MSG-Mono-Sodium Glutamate). They compared the new chelate (GLDA) with other chelates, including EDTA, hydroxyethylethylenediaminetriacetic acid (HEDTA), nitrilotriacetic acid (NTA) and ethanoldiglycinic acid (EDG). GLDA was very effective in dissolving calcium carbonate compared to other chelates and organic acids. In their results they showed that one gallon of 20 wt% GLDA dissolved up to 1.5 lb calcium carbonate, whereas one gallon of 15 wt% HCl can dissolve 1.8 lb calcium carbonate. Unlike other chelates, GLDA has better solubility in HCl over a wide pH range. Regarding environmental, safety and health issues, GLDA has favorable environmental characteristics as it is readily biodegradable.

All previous studies done using chelating agents as a stand-alone stimulation fluid were based on short core samples (maximum 5 in. length). No previous work considered measuring the concentration of the chelate in the coreflood effluent. Therefore, the objectives of this part are to: (1) examine the ability of GLDA to dissolve calcite over a wide range of pH values using a slurry reactor and rotating disk, and comparing this with EDTA, EDG and HEDTA, (2) determine the ability of GLDA to form wormholes in long calcium carbonate cores, (3) analyze the core effluent samples to understand the reaction of GLDA with calcite, (4) study the thermal stability of GLDA, and (5) address the environmental characteristics of GLDA.

Experimental Work

Materials

HEDTA (hydroxyethylethylenediaminetriacetic acid), GLDA (L-Glutamic acid N,N-diacetic acid), and EDG (ethanoldiglycinic acid, also known as HEIDA: hydroxyethyliminodiacetic acid) were obtained from AkzoNobel. The concentration of chelating agents used was 0.6M prepared from original solutions with different concentrations. Sodium chloride, calcium chloride and ferric chloride reagents were obtained from VWR International. Calcium carbonate cores (1.5 in. in diameter and 20 in. in length) were used in the coreflood experiments have a permeability range

of 3 to 10 md (Edward limestone). The viscosity of different GLDA solutions with different calcium concentrations was measured using a capillary tube viscometer (Ubbelhold type).

The rotating disk core samples were cut from blocks of Pink Dessert limestone with a diameter of 3.81 cm (1.5 in.) and a thickness of 2.54 cm (1 in.). The procedure reported by Fredd and Fogler (1998b) was followed as follows: one surface of each sample was first polished with sand paper then soaked in 0.1N HCl for 30 to 40 minutes then rinsed thoroughly with deionized water before reaction. This method ensures good reproducibility and eliminates problems associated with preparing the disk surfaces. 0.6M GLDA solutions at pH values of 1.7, 3.8, and 13 were prepared by dilution from an initial solution of 40wt% that was supplied from AkzoNobel. De-ionized water was used to prepare the GLDA solutions.

Dissolution of Calcite by Chelates

A slurry reactor was used to determine the ability of different chelates to dissolve calcium carbonate, **Fig. 5**. Portions of pink desert limestone cores were ground and particles of 30 mesh size were oven dried before use. GLDA/calcite slurries with a molar ratio of 1.5 were put in the reaction flask at $180^{o}F$; samples were removed at set time periods. Samples taken for testing from the slurry reactor were filtered using 70 μm filter paper. The clear filtrate was analyzed for the total calcium concentration using atomic absorbance spectrometer (AAnalyst 700-flame type) immediately after the test at room temperature. The chelating ability of the different chelates was calculated by the determination of the free calcium ion using an ion selective electrode (370 PerpHecT meter) and then subtracting the free calcium from the total calcium. Also, the total chelate concentration was determined using an iron potentionmetric titration method at pH 3. The pH of the samples was determined using PerpHecT Ross Electrode, and the density of samples was determined using DMA 35N densimeter. The effect of different parameters on the reaction of GLDA with calcite included: pH, sodium chloride and calcium chloride. To study the effect of sodium chloride and calcium chloride on the GLDA performance, 5 wt% salt solutions were prepared using sodium chloride or calcium chloride. All GLDA solutions were prepared using deionized water with total dissolved solids (TDS) of 20 ppm.
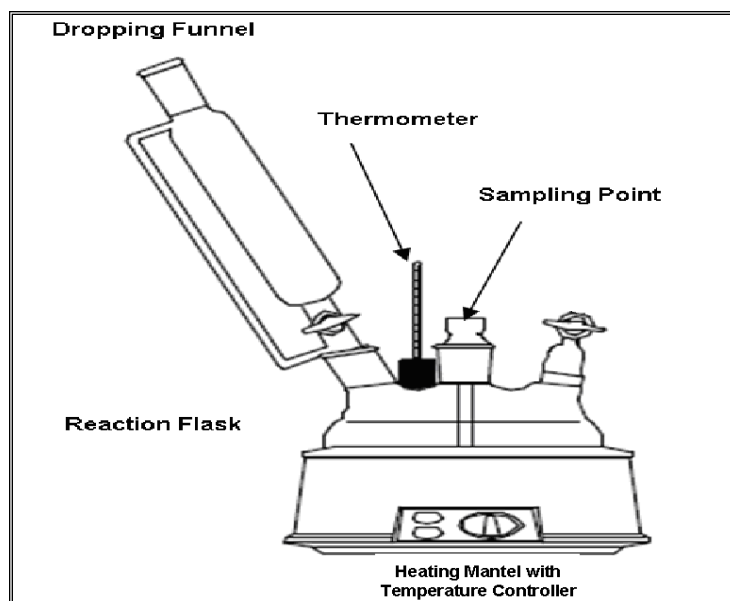
Fig. 5—Slurry reactor (modified after Frenier 2001).

Rotating Disk Experiments

Rotating disk apparatus RDR-100 (Core Lab Instruments (CLI) & Temco), shown in **Fig. 6**, was used to perform the reaction rate measurements. The instrument consists mainly of two chambers; one is a "reactor" vessel and the second is a reservoir" vessel. Both vessels were flushed with inert gas (nitrogen) before starting the experiment. Calcite disks were fixed in the core holder assembly in the reactor vessel using heat-shrinkable Teflon tubing. Reaction fluid was then poured in the reservoir vessel and both were heated up to the desired temperatures. Compressed N_2 was applied to pressurize the reservoir vessel to a pressure that was sufficient to transfer the acid to the reactor vessel and results in a reactor pressure above 1000 psig. Pressure greater than 1000 psig is necessary in the reaction vessel to ensure that the evolved CO_2 is kept in solution and does not affect the system hydrodynamic and the dissolution rate. The rotational speed was then set up to the selected value and the time was recorded starting the moment at which the valve between the reservoir and the reactor vessels was opened. Samples, each of approximately 2 ml, were withdrawn periodically up to 20 minutes for measuring the calcium concentration in the samples as function of time using Perkin-Elmer atomic absorption. Corrections were made to account for the change in volume of reaction medium due to sample withdrawing. A new core sample was used for each experiment. The initial surface area ($\frac{\pi d_{core}^2}{4}\ 1 - \phi$) of the sample was used to determine the initial dissolution rate.

Fig. 6—Rotating disk apparatus.

Thermal Stability Tests

The thermal stability of the chelates was determined by heating 10 ml of a 0.6M chelate solution in a 100 ml Teflon pressure vessel for 6 hours at 177°C (350°F) using a temperature controlled microwave resulting in a pressure of 350 psi. The thermal stability was measured in one series to avoid possible differences in the heating profile. The stability was calculated from the chelate concentration before and after heating as determined by complexometric-potentiometric end-point titration using a ferric chloride solution (LePage et al. 2010). A similar set of experiments was conducted at 400°F and 400 psi for 24 hours.

Coreflood Tests

Fig. 7 shows a schematic diagram for the coreflood. A back pressure of 1,000 psi was necessary to keep CO_2 in solution. The backpressure must be kept constant and it is desired to be 300 - 400 psi less than the overburden pressure. One Mity-Mite back pressure regulator model S91-W was installed on the upstream line. The pressure in the line controls the effluent flow and exerted the resistance for the purpose described above, maintaining constant pressure upstream; the pressure was the same as the nitrogen pressure. An Enerpac hand hydraulic pump was used to apply the required overburden pressure on the core. The pressure drop

across the core was sensed with a set of FOXBORO differential pressure transducers, models, IDP10-A26E21F-M1. There were two gauges installed with ranges 0-300 psi, and 0-1500 psi. Then the pressure drop across the core was monitored through the lab view software. Coreflood tests were run at different flow rates using different GLDA formulas at high temperatures. The temperature of the acidizing process must be maintained fairly constant to ensure the reliability of the results; therefore, two temperature controllers were used. The temperature of the preheated fluids coming from the accumulators was controlled by compact bench top CSC32 series, which has 4-digit display, 0.1° resolution with an accuracy of ± 0.25% full scale ± 1°C. It uses a type K thermocouple and two Outputs (5 A 120 Vac SSR). The coreflood tests were done at 200, 220, and 300°F. Before running the coreflood test, the core was first saturated with water and the pore volume was calculated. Computer tomographic scans were performed before and after the treatment to determine the propagation of the wormhole after the chemical treatment.
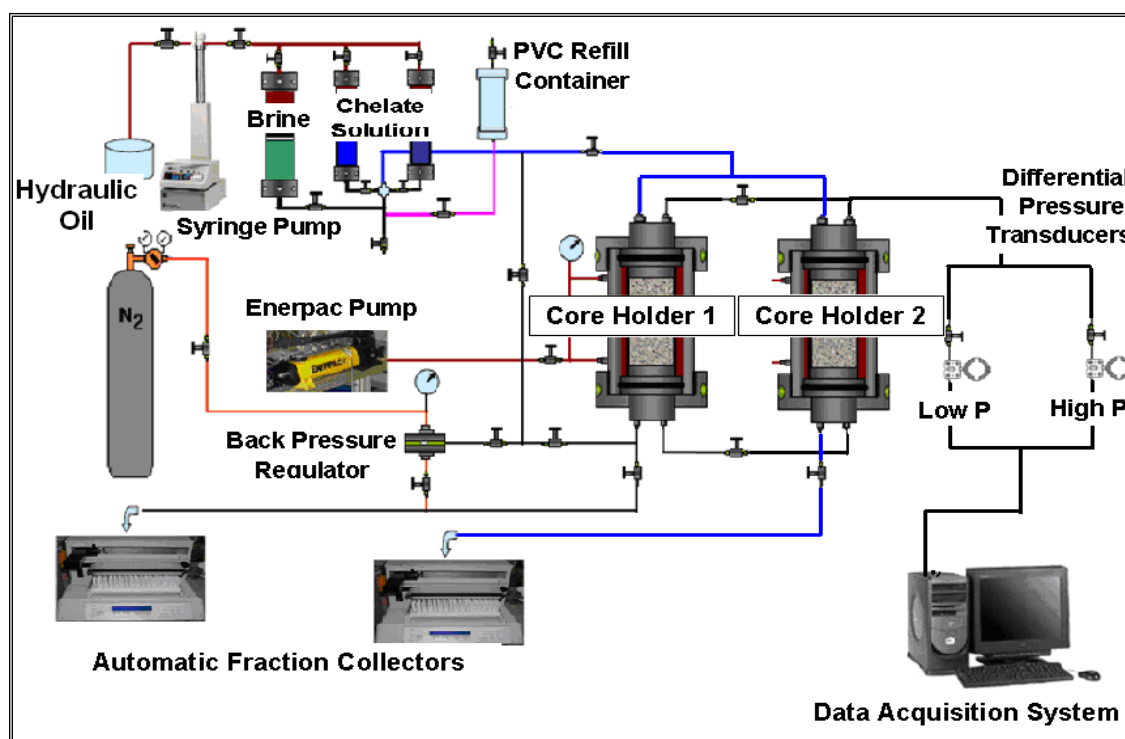
Fig. 7—Coreflood setup.

Lab view software was used to monitor the pressure drop across the core during the treatment and determine the core permeability before and after the treatment by using Darcy's equation for laminar, linear, and steady-state flow of Newtonian fluids in porous media:

$$k = 122.812 q \mu L_{core} / \Delta p d_{core}^2 \quad \text{.. (24)}$$

where k is the core permeability, md, q is the flow rate, cm^3/min, μ is the fluid viscosity, cP, L_{core} is the core length, in., Δp is the pressure drop across the core, psi and d_{core} is the core diameter, in.

Results and Discussion

Dissolution of Calcite by GLDA: Effect of GLDA pH

Fig. 8 shows the effect of the initial pH value on the calcium concentration for the samples collected during the reaction of GLDA with calcite. As noted by the concentration of calcium, the total calcite dissolved increased as the pH was decreased. This means that the acid portion of the chelating agent was participating in the calcium carbonate dissolution. A similar trend for the effect of initial pH on calcite dissolution by HEDTA was obtained by Frenier (2001). GLDA/calcite slurries at a 1.5 molar ratio were put in the reaction flask at 180°F. To maintain a constant molar ratio between the calcite and GLDA, each sample was collected from a single test to keep a constant GLDA/ calcite molar ratio. As shown in Fig. 8 the total calcium concentration increased with time until reaching a plateau value after 3 hours (equilibrium). The same behavior was noticed at all pH values. The total calcium concentration decreased as GLDA pH value was increased. There are two reaction regimes; at low pH the acidic dissolution prevails, whereas at high pH CaCO$_3$ is removed by complexation of calcium with the chelate. The reaction rate is primarily driven by the acidic dissolution. At low pH the reaction is fast and it slows down with increasing pH (Fredd and Fogler 1998c).
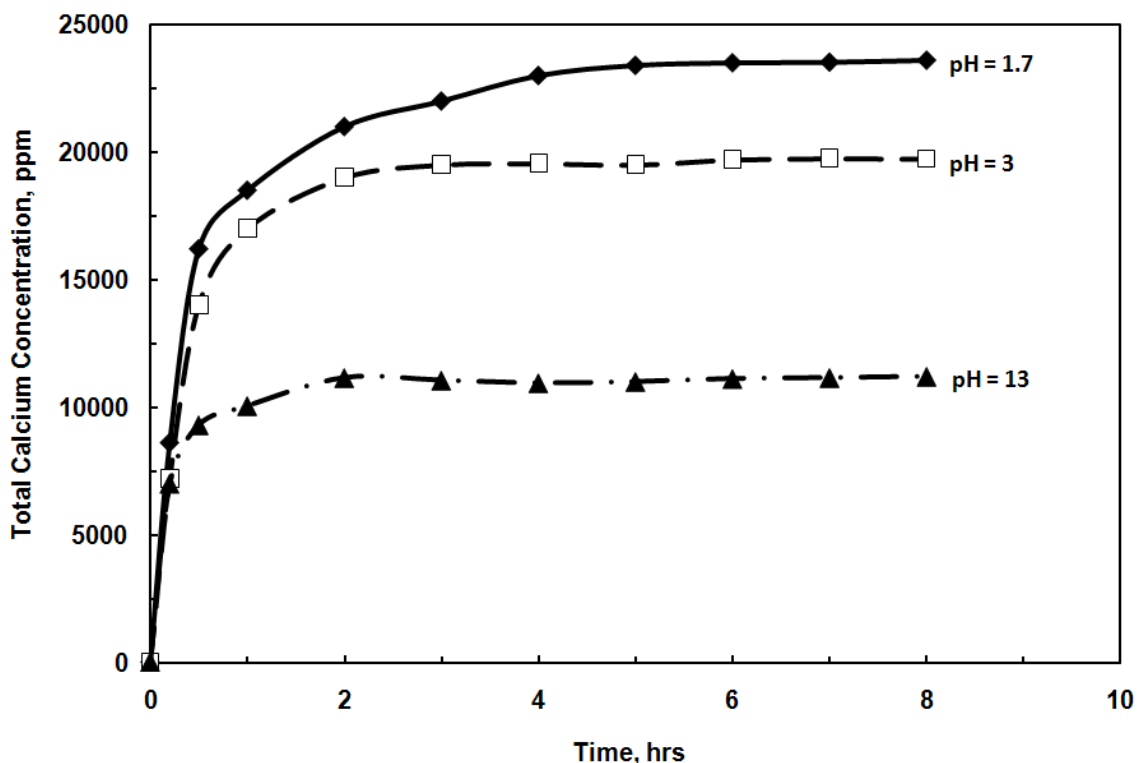
Fig. 8—Dissolution of calcite using 20 wt% GLDA at different initial pH values at 180°F.

Fig. 9 shows the complexed calcium concentrations at different pH values of GLDA at 180°F. The maximum amount of chelated calcium was noted at pH 13 where no free calcium remained. At high pH the dissolution mechanism was only by the chelation reaction. As the pH decreased the chelating ability decreased and free calcium concentration increased. At low pH the dissolution mechanism was due to both chelation and acid dissolution (mass transfer). The highest free calcium concentration was obtained with GLDA-calcium solutions at pH = 1.7.

Fig. 10 and Table 5 show the effect of the initial pH value on the calcite dissolution using 0.6M GLDA solutions. There was an S-shaped relationship between the ratio of complexed/maximum complexed calcium and equilibrium pH of the GLDA solutions. The maximum complexed calcium was obtained at pH of 13. As the pH increased the ratio became closer to 1, meaning less free calcium exists in solution at high pH. At low pH the ratio was very small as there was small amount of chelated calcium compared to the total calcium concentration. At low pH 1.7, the GLDA exists principally in an acid form and does not chelate Ca effectively because hydrogen ions occupy the carboxylic acid groups. As the pH increased, GLDA reached a maximum chelating ability as it becomes fully deprotonated.
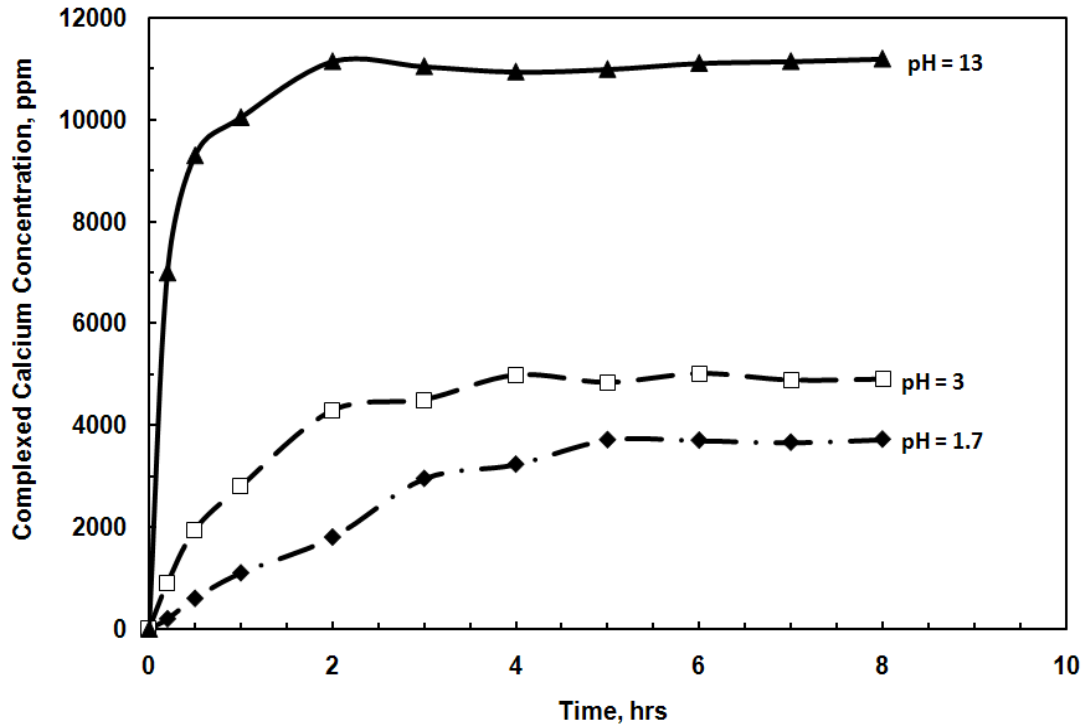
Fig. 9—Concentration of complexed calcium as a reaction of initial pH and time at 180°F.

Table 5—EFFECT OF pH ON THE CHELATION OF GLDA AT 180°F				
Initial pH	**Final pH**	**Total Ca, ppm**	**Chelated Ca, ppm**	**Chelated Ca/ Maximum Ca**
1.7	2.5	23600	4000	0.36
3.0	4.3	19730	4630	0.41
8.0	6.5	15200	9000	0.80
13	12.8	11200	11200	1.00
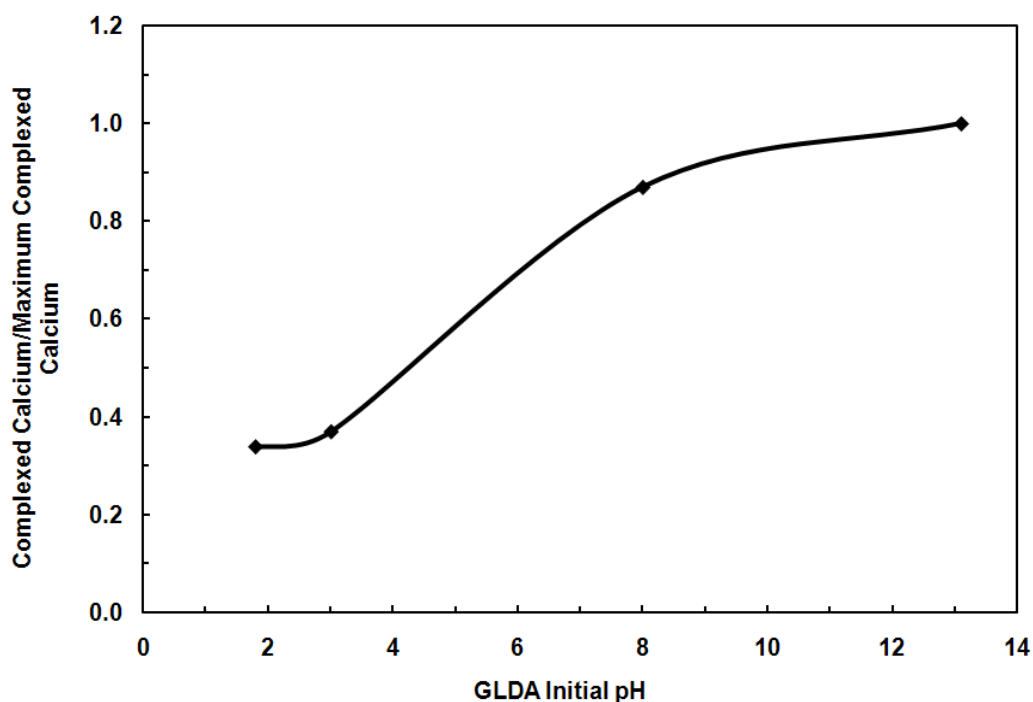
Fig. 10—Effect of initial pH on the chelating ability of 20 wt% GLDA at 180°F.

Effect of Simple Inorganic Salts

Fig. 11 shows the effect of adding 5 wt% NaCl on the dissolved calcium concentration for the samples that were collected from the reactor during the reaction of GLDA at different pH with calcite at 180°F. The addition of 5 wt% NaCl to 0.6M GLDA at pH 1.7 significantly accelerated the reaction as the equilibrium calcium concentration was reached after 10 minutes, whereas without NaCl it took 4 hours to reach this concentration. The calcium concentration was nearly the same in both cases. This acceleration was attributed to the increase in the ionic strength. Finally, it was found that sodium chloride did not affect the performance of GLDA of pH 13. The increase in calcium concentration as a result of adding sodium chloride also was observed by Willey (2004) during the dissolution of calcium sulfate by EDTA.

The addition of 5 wt% sodium chloride, 0.9M, will increase the ionic strength by 0.9M. Also, Willey (2004) stated that, there is a direct relation between the solution ionic strength and calcium solubility in solution, in other words, as the solution ionic strength increases the calcium solubility in that solution will increase.
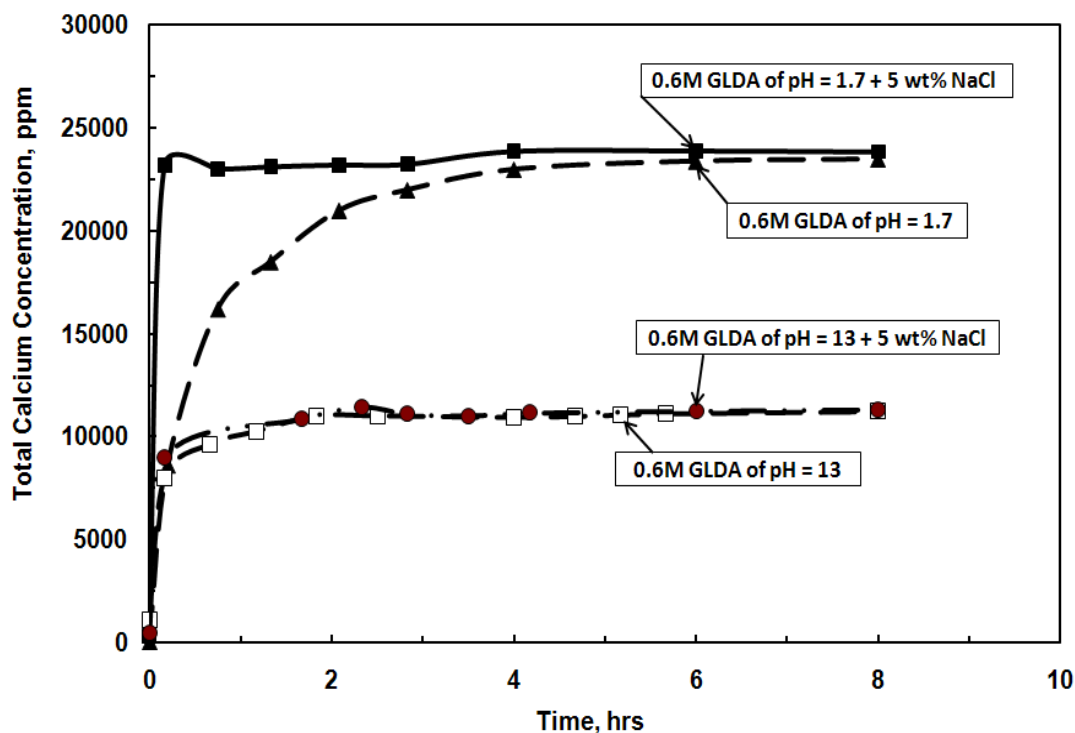
Fig. 11—Effect of 5 wt% NaCl on 0.6M GLDA reaction with calcite at 180°F.

Fig. 12 shows the effect of adding 5 wt% calcium chloride on the calcium concentration for the samples that were collected from the reactor during the reaction of GLDA of different pH with calcite at 180°F. For GLDA at pH = 1.7, it is shown that there was a small effect on the net calcium concentration (total dissolved calcium – calcium from 5 wt% $CaCl_2$). The calcium concentration increased slightly in the first two hours, as the GLDA chelated small amounts from the calcium in solution after that the concentration was almost the same for the two cases (with and without calcium chloride). In case of the pH 13, GLDA chelated all the calcium in solution from the calcium chloride and did not react with the calcite. The weight of the crushed calcium carbonate sample was the same before and after the test. The reaction at high pH was due to chelation only and there was no calcite dissolution as there was no H^+. The existence of calcium chloride in solution affects the reaction of GLDA (pH 13) with calcite greatly; it can completely hinder the reaction, as it is easier for the GLDA to chelate the calcium in solution rather than to chelate the calcium from the calcium carbonate. From Fig. 12 the amount of chelated calcium was the same during the whole test time and it was equal to the amount of calcium in the 5 wt% $CaCl_2$.
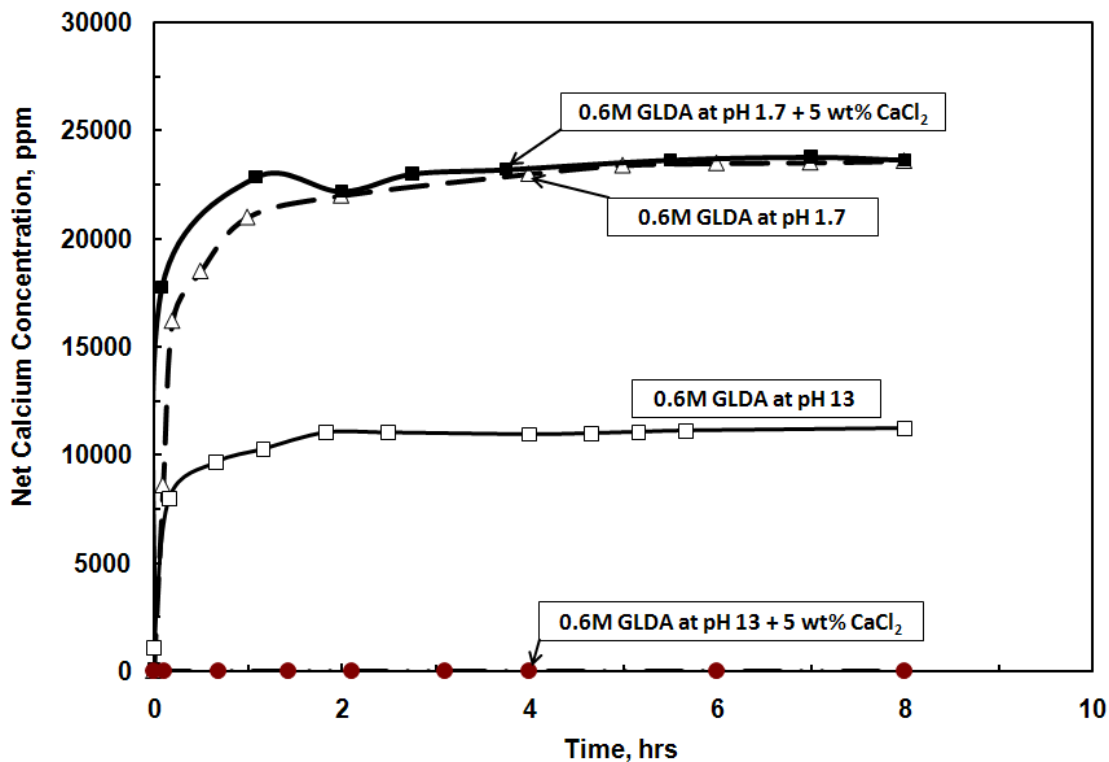
Fig. 12—Effect of 5 wt% CaCl$_2$ on GLDA reaction with calcite at 180°F.

Fig. 13 shows a comparison between 0.6 M GLDA (pH = 11), 0.6 M HEDTA (pH = 11), 0.6M EDTA (pH =11), and 0.6 M EDG (pH = 11) at 180°F. Chelate/calcite with 1.5 molar ratio was put in the reaction flask at 180°F. The ability of GLDA to dissolve calcite was almost the same like HEDTA (with two nitrogen atoms) but was greater than EDG (also like GLDA with only one nitrogen atom). Comparing GLDA with EDTA, EDTA dissolved more calcium than GLDA. GLDA is a good calcite dissolver compared to other chelating agents; in addition it is safer to use than EDG and more readily biodegradable than HEDTA and EDTA.
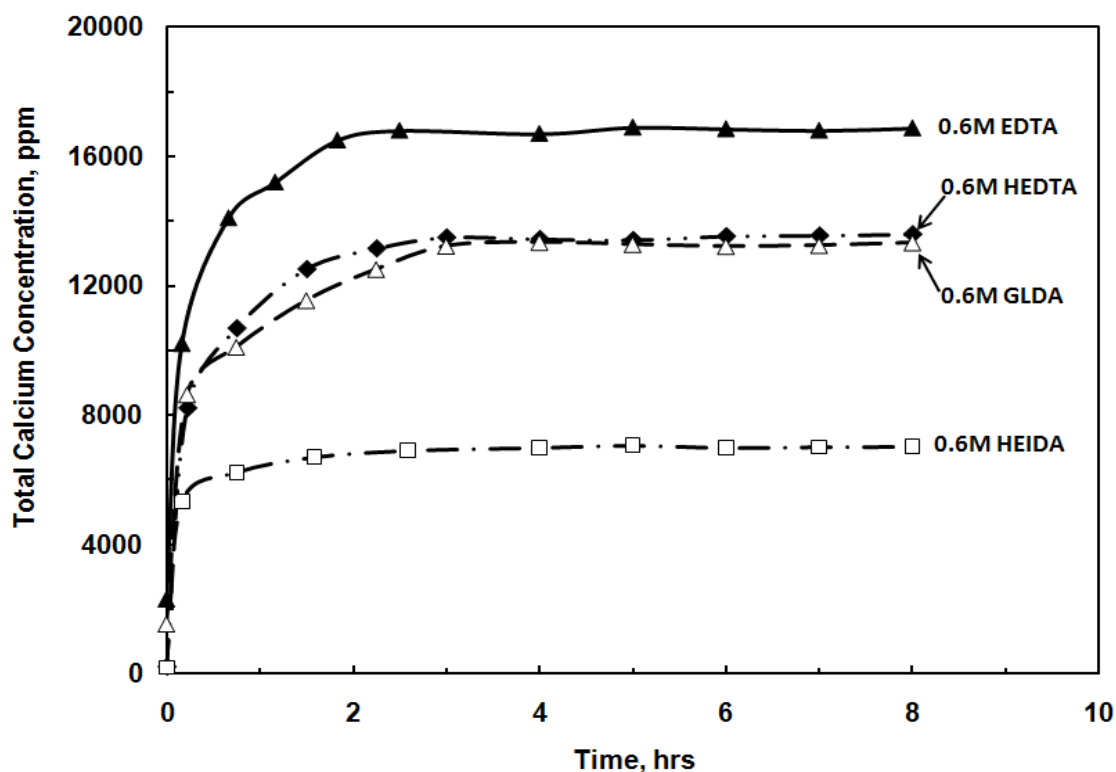
Fig. 13—Comparison between 0.6M GLDA (pH = 11), 0.6M HEDTA (pH = 11), 0.6M EDTA (pH = 11) and 0.6M EDG (pH = 11) at 180°F.

Effect of Disk Rotational Speed and pH

In general, increasing the rotating disk rotational speed has a positive effect on the rate of dissolution in case the reaction is mainly controlled by the mass transport process or controlled by both mass transport and surface reaction together. **Fig. 14** shows the behavior of the reaction between GLDA and calcite (Pink dessert limestone) for a range of disk rotational speeds of 100-1800 rpm at 200°F. Increasing the disk rotational speed from 100 to 1000 rpm increased the rate of dissolution 4 times at pH of 1.7 and 3 times at pH of 13. On the other hand increasing the pH of the reacting solution from 1.7 to 13 has significantly reduced the rate of dissolution. The reaction at pH (3.8, and 13) become less dependent on the disk rotational speed which indicates that at these pH values the kinetics of the surface reaction play a role in the overall rate. Fredd and Fogler (1998c) have reported a surface kinetic limited reaction of calcite with 0.25M EDTA at pH 12 and a mass and reaction limits at pH of 4. However, all the reaction experiments in their work were performed at room temperature (21 ± 2°C).
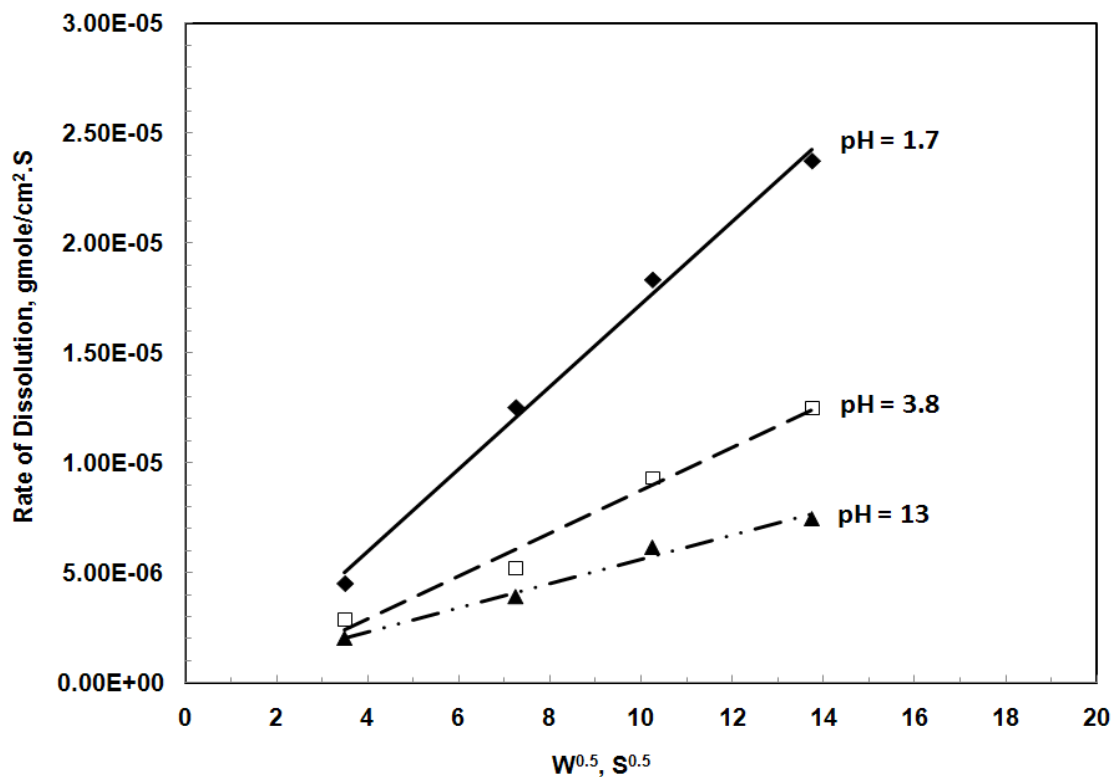
Fig. 14—Rate of calcite dissolution by 0.6M GLDA at 200°F.

Effect of Temperature on the Calcite Dissolution Rate

Increasing the temperature increased the overall rate of dissolution. **Fig. 15** shows the measured rate of reaction as a function of the disk rotational speed for two different temperatures at 80 and 200°F. At 1000 rpm, the rate of reaction at 200°F was 6 times the reaction at 80°F. This difference becomes more noticeable at higher rpm. The reaction rate at 1800 rpm and 200°F is almost one order of magnitude higher than the reaction at 80°F (27°C). GLDA dissolved more calcite at higher temperatures and this indicated the effectiveness of GLDA to be used at high temperatures without the fear of thermal degradation. **Fig. 16** shows the rate of calcite dissolution by GLDA (0.6M and pH 3 .8) in a wide range of temperature from 80°F to 300°F at a constant rotary speed of 1000 rpm.
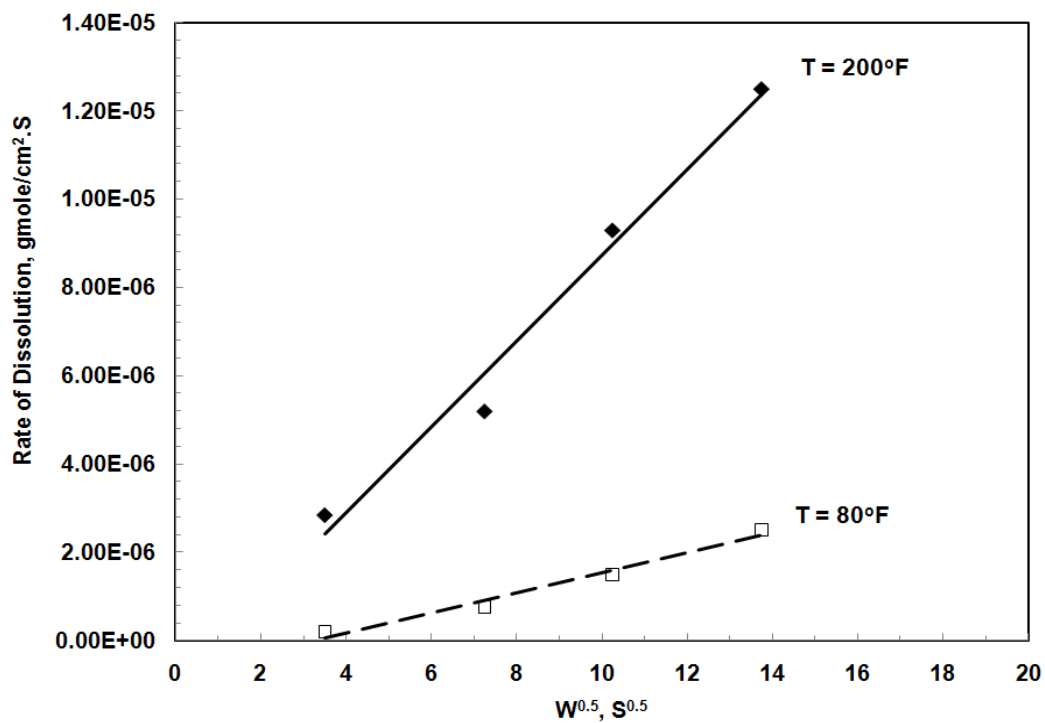
Fig. 15—Effect of temperature on the rate of dissolution of calcite by 0.6M GLDA of pH 3.8.
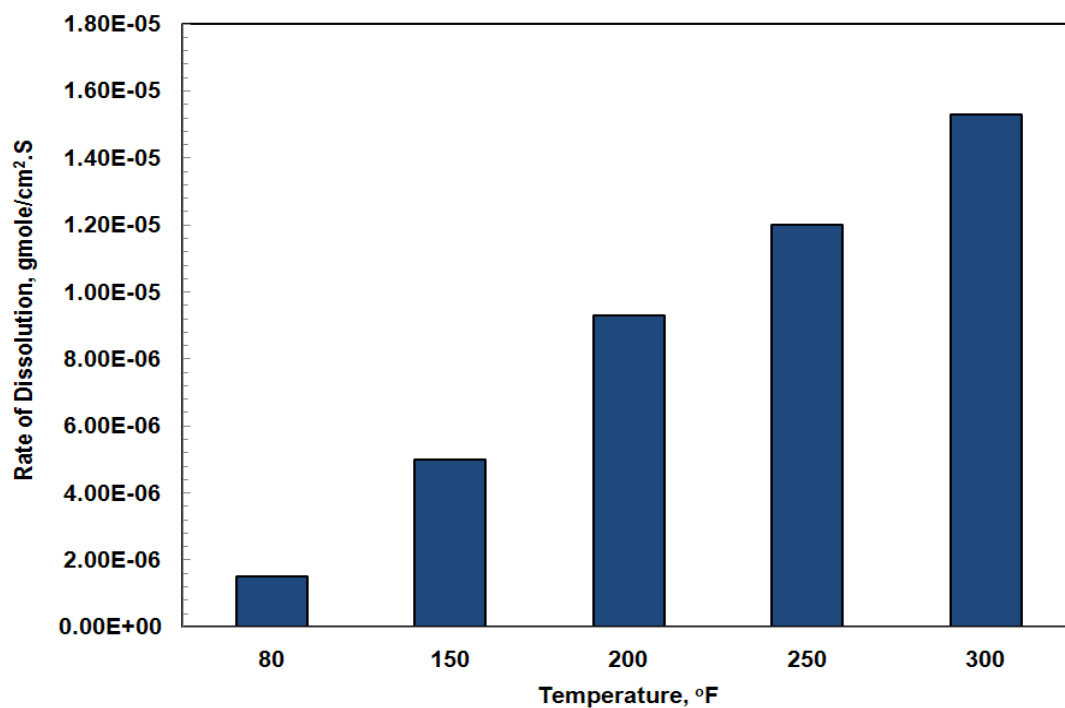
Fig. 16—Effect of temperature on the dissolution rate of calcite by 0.6M GLDA of pH 3.8 at 1000 rpm.

Thermal Stability Tests

Previous results (LePage et al. 2010) on the thermal stability of GLDA showed that it is comparable to the thermal stability of HEDTA. The results presented in **Fig. 17** demonstrate that the thermal stability of GLDA is influenced favorably in high ionic strength solutions like seawater and brines. Once applied in downhole stimulation of carbonate rock, GLDA will be complexed to calcium giving adequately thermally stable Ca-GLDA solutions. **Fig. 18** shows the thermal stability of different GLDA solution with an initial concentration of 0.6M at 400°F. GLDA solutions were heated up to 400°F for 24 hrs in a hot rolling oven. There is slight difference for thermal stability than before at high ionic strength solutions the thermal stability still high. The increased thermal stability at high ionic strength solutions or in the presence of NaCl was believed due to addition of NaCl will increase the ion strength which can lower the activity of the ions leading to changes in the pKa's. From the experiments we know that the initial pH has a strong influence on the thermal stability of the solution so it makes sense that changes in the pKa will have an effect on the thermal stability. On a molecular scale this means that the presence of protons on the reactive sites will "block" the degeneration reaction. The presence of an excess Na^+ might lead to the formation of more stable ion pairs, like (GLDA-Na_3)- (so sodium and GLDA are not completely dissociated). Again this might block the most reactive sites.
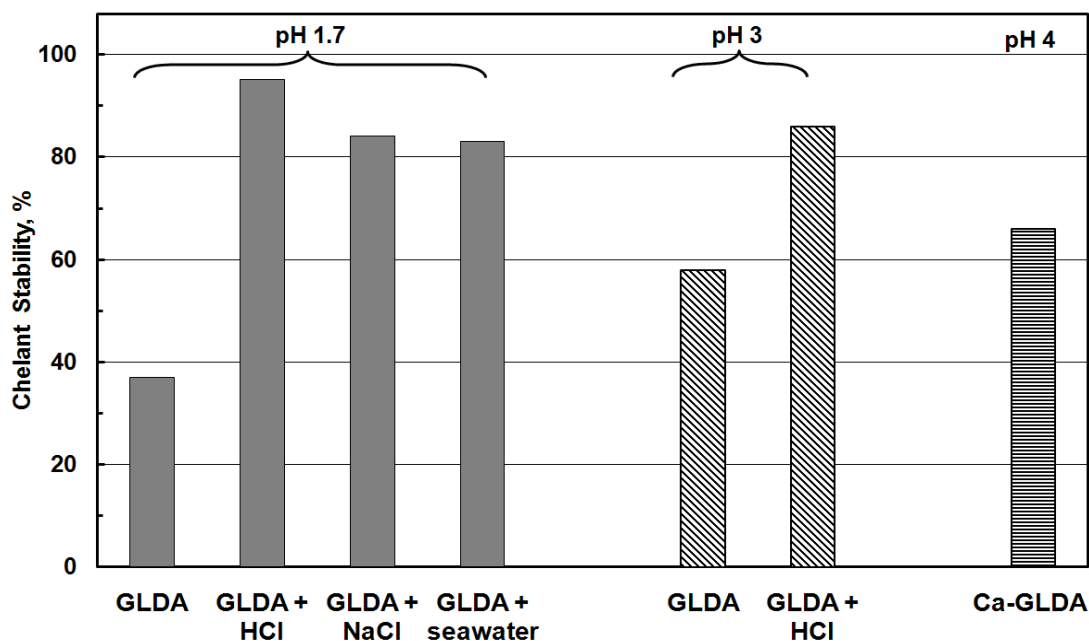
Fig. 17—Thermal stability of different GLDA solutions (0.6M) at 350°F after 6 hrs.
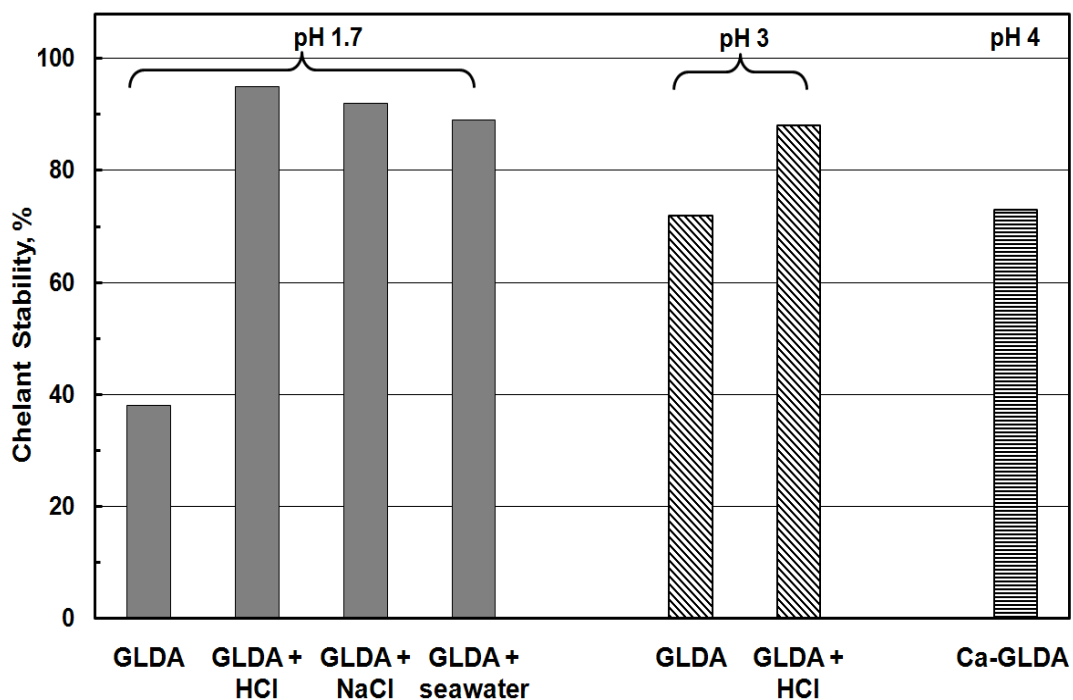
Fig. 18—Thermal stability of different GLDA solutions (0.6M) at 400°F after 24 hrs.

Coreflood Experiments

Table 6 gives the data for the coreflood experiments that were performed using the setup shown in Fig. 7. **Figs. 19 to 22** show the pressure drop across the core during the GLDA for the four coreflood experiments. The pressure drop initially increased during the introduction of GLDA and then decreased until the GLDA penetrated through the core (start of wormhole formation). The increase in the pressure drop can be attributed to the increased viscosity and density of the reacted GLDA solution. The viscosity and density measurements of GLDA (pH 1.7) with different concentrations of calcium at room temperature are reported in **Table 7** (the viscosity in this table for GLDA-Ca complex only, i.e. there is no free calcium only complexed calcium from calcium chloride solutions). As the amount of soluble calcium increased the viscosity of the solution is also increased and in turn the pressure drop across the core increased. During the reaction of GLDA with calcite the wormholes began to form and the pressure drop should begin to decrease, but the propagation rate of the wormhole was very small. As wormhole formation progressed the overall pressure drop rose more slowly until it began to decrease.

Table 6—DATA FOR COREFLOOD EXPERIMENTS				
Parameter	**Test #1**	**Test #2**	**Test #3**	**Test # 4**
Flow rate, cm^3/min	2	3	2	3
Temperature, ^{o}F	200	220	300	300
Core length, in.	20	20	20	20
Core diameter, in.	1.5	1.5	1.5	1.5
Initial core permeability, md	6.1	10.2	4.45	5
Porosity, vol%	19.7	20	18.2	17.3
Confining pressure, psi	2200	2200	2500	2500
Back pressure, psi	1100	1100	1100	1100
Core pore volume, cm^3	108	109.3	100	95
Injected chelate concentration, wt%	20	20	20	20
pH of chelate solution	1.7	1.7	1.7	1.7
Core permeability after the test, md	130	275	Large wormholes	
Pore volume to breakthrough (PV$_{bt}$)	2.1	3.2	1.4	1.68

Table 7—DENSIY AND VISCOSITY OF 20 WT% GLDA (PH = 1.7) SOLUTIONS WITH DIFFERENT CALCIUM CONCENTRATIONS AT 77°F		
Calcium Concentration, ppm	**Density, g/cm^3**	**Viscosity, cP**
0.0000	1.13	2.52
10,000	1.15	2.80
20,000	1.17	3.23
30,000	1.18	3.57
40,000	1.20	3.80
50,000	1.22	4.20
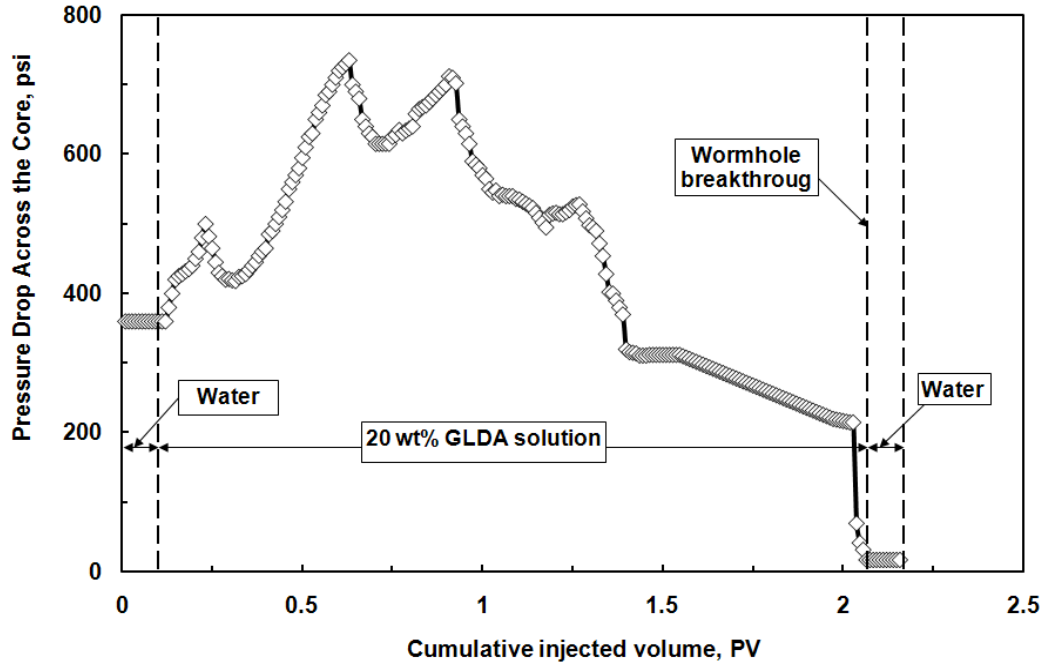
Fig. 19—Pressure drop across the core at 2 cm^3/min & 200°F for 20 wt% GLDA with pH = 1.7.
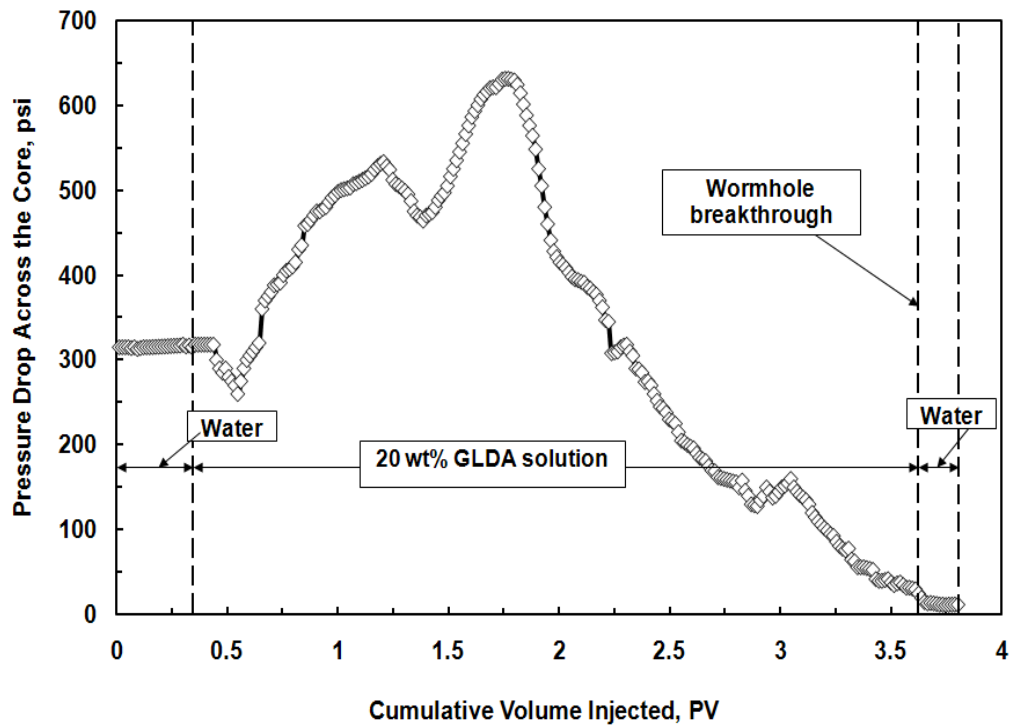
Fig. 20—Pressure drop across the core at 3 cm^3/min, 220°F for 20 wt% GLDA with pH = 1.7.
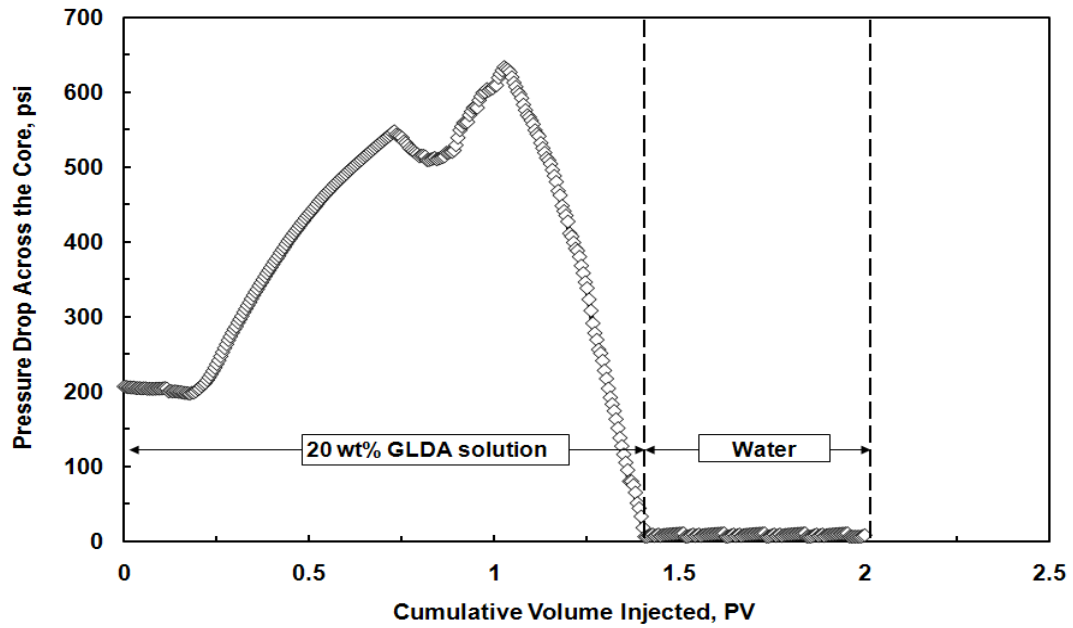
Fig. 21—Pressure drop across the core at 2 cm³/min & 300°F for 20 wt% GLDA at pH 1.7.
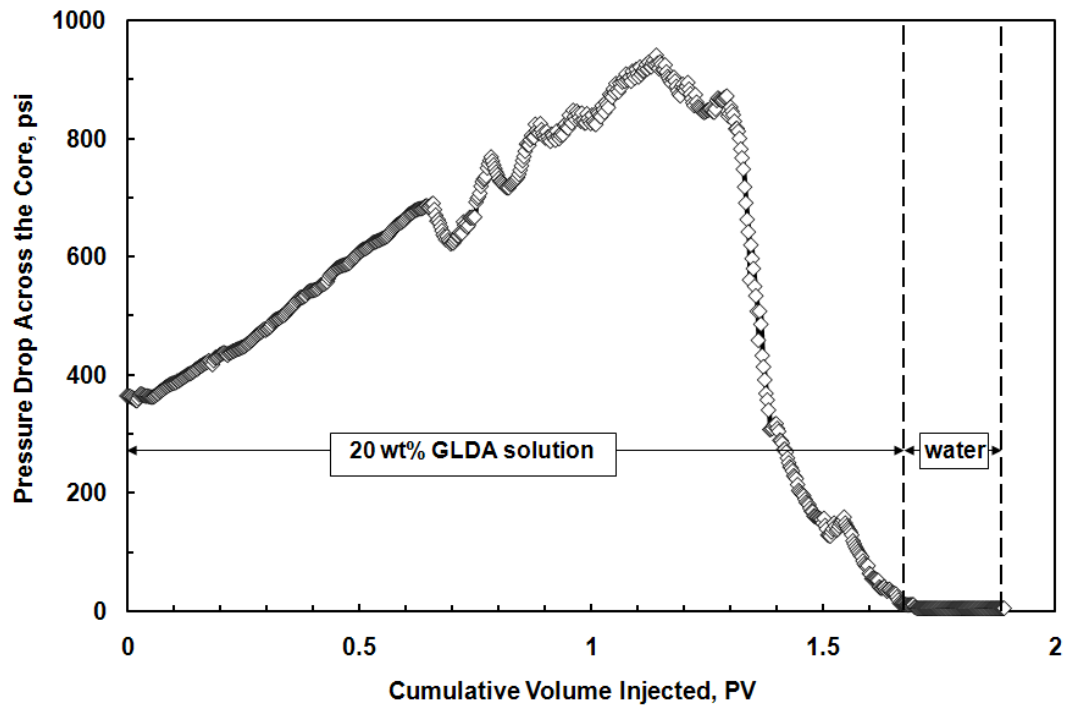
Fig. 22—Pressure drop across the core at 3 cm³/min & 300°F for 20 wt% GLDA at pH 1.7.

Figs. 23 - 26 show the calcium and the GLDA concentration for the coreflood tests. From these figures the calcium and GLDA concentrations reached a maximum at the GLDA breakthrough and started to decrease after the formation of wormholes. Introduction of de-ionized water further reduced the concentrations of calcium and GLDA until they reached the minimum value. The chelant concentration for the two coreflood tests reached a plateau value of 19 wt% for both tests at 200 and 220^oF which was 95% of the original concentration. At 300^oF, the concentration of GLDA in the coreflood effluent reached an average value of 18.5 wt% with a thermal stability of 93% at 2 cm^3/min, and reached an average of 18.8 wt% with 94% thermal stability at 3 cm^3/min. This indicated GLDA has a very good thermal stability during coreflood tests in good agreement with separate thermal stability test data (the GLDA that was used in this study is $H_3NaGLDA$ blended with HCl to get pH of 1.7, so there was NaCl in solution , as HCl kicked the sodium out). The amount of GLDA required to breakthrough the core was reduced from 2.1 PV at 200^oF to 1.4 PV at 300^oF at a flow rate of 2 cm^3/min. Increasing the temperature by 100^oF saved 0.7 PV from the GLDA at 2 cm^3/min. The same scenario in the case of 3 cm^3/min as the temperature was increased from 220 to 300^oF, the pore volume required to breakthrough the core was reduced from 3.2 to 1.68 PV. GLDA performed better at 2 cm^3/min because the increase in contact time allowed GLDA to react more with calcite. At 300^oF the amount of dissolved calcium at 2 cm^3/min reached a maximum value of 58,000 ppm and 53,000 ppm in the case of 3 cm^3/min.

Fig. 27 shows the 2D CT scan for the cores after the coreflood test with GLDA. The wormhole formation after the treatment is indicated by the black color. **Fig. 28** shows the 3D CT scan for the cores after the treatment. The wormhole has greater diameter in case of 3 cm^3/min and 220^oF, as there was more calcium (dissolved) in the effluent samples than the 2 cm^3/min and 200^oF. The amount of calcium that was dissolved at 2 cm^3/min was 7 g and 11.5 g for 3 cm^3/min. **Fig. 29** shows the core inlet and outlet after the coreflood at 300^oF. The wormhole formed at 2 cm^2/min was larger than that at 3 cm^3/min. This meant that GLDA performed better at low rates due to the increased contact time with core allowed more reaction of GLDA with calcite. There was no face dissolution or washouts at both rates.

Fig. 23—Total calcium concentration & GLDA concentration in the core effluent samples at flow rate of 2 cm3/min & 200°F for 20 wt% GLDA with pH = 1.7.
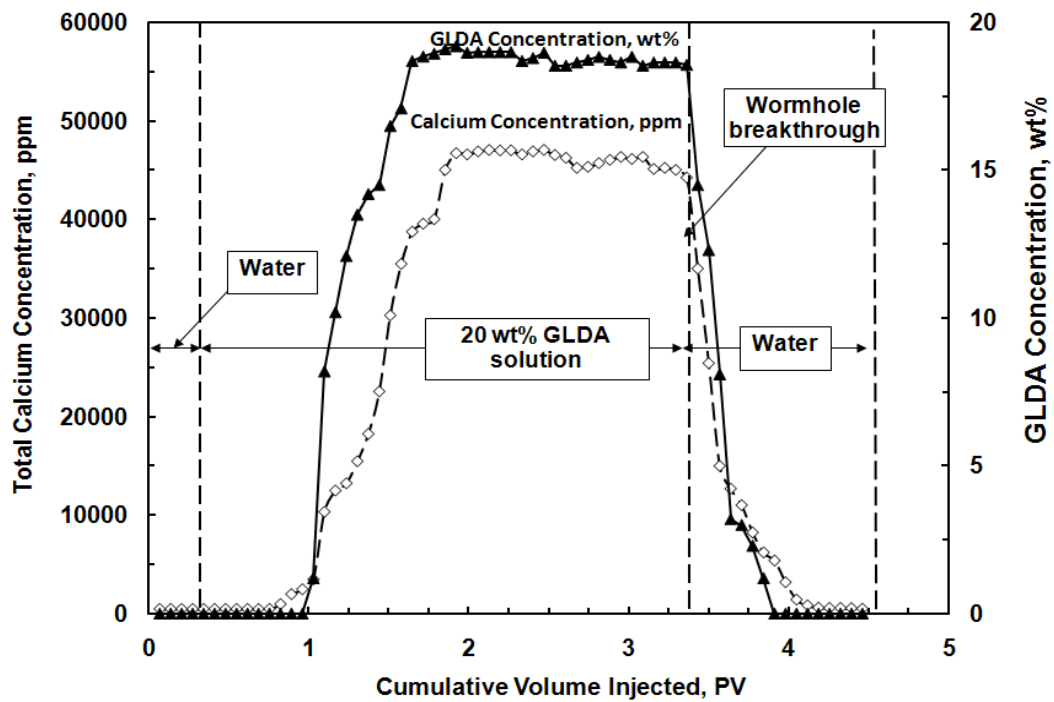
Fig. 24—Total calcium concentration & GLDA concentration in the core effluent samples at flow rate of 3 cm³/min & 220°F for 20 wt% GLDA with pH = 1.7.
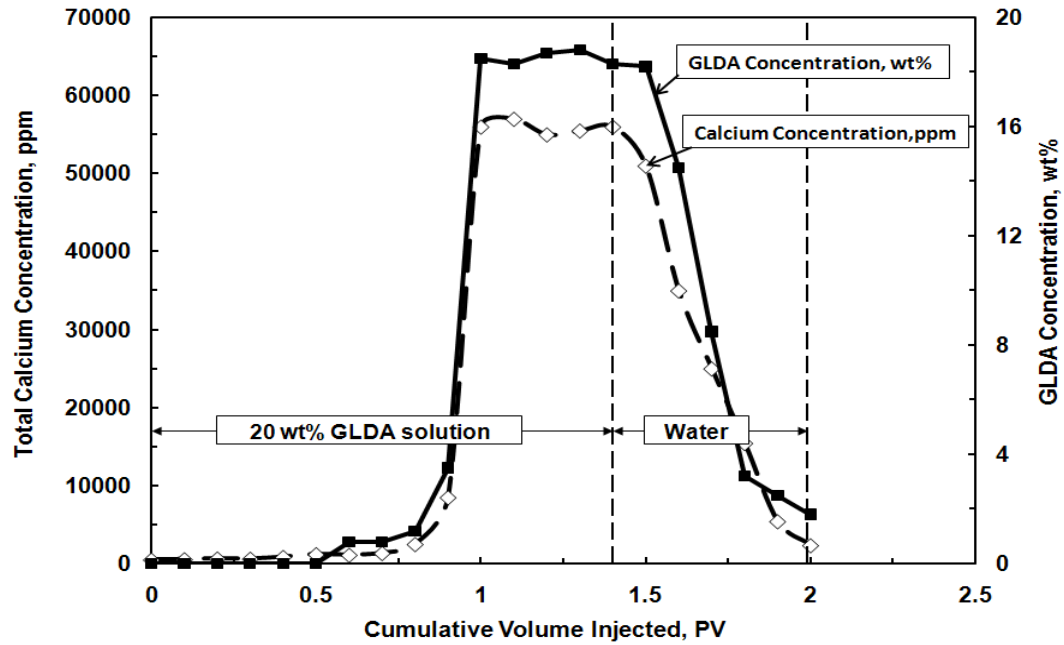
Fig. 25—Total calcium concentration & GLDA concentration in the core effluent samples at a flow rate of 2 cm³/min & 300oF for 20 wt% GLDA at pH 1.7.
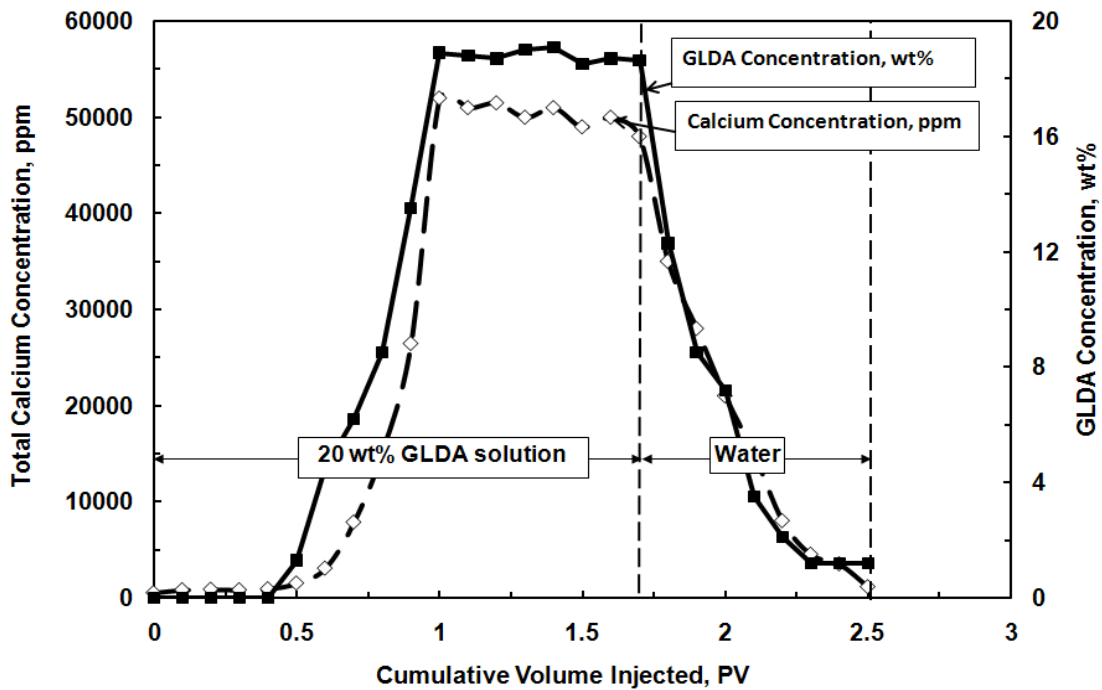
Fig. 26—Total calcium concentration & GLDA concentration in the core effluent samples at a flow rate of 3 cm³/min & 300°F for 20 wt% GLDA at pH 1.7.
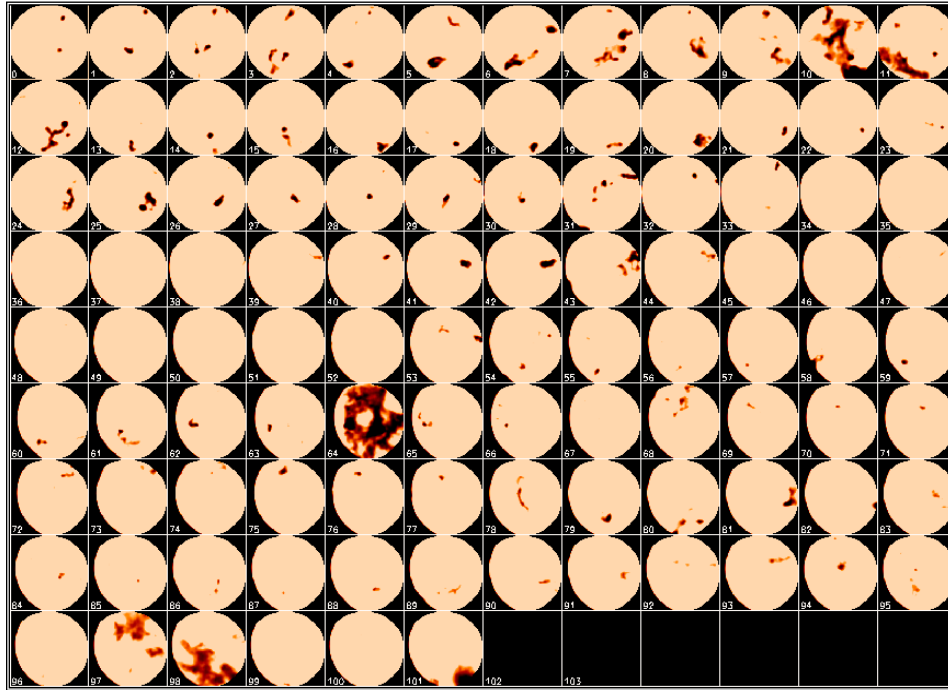
(a)
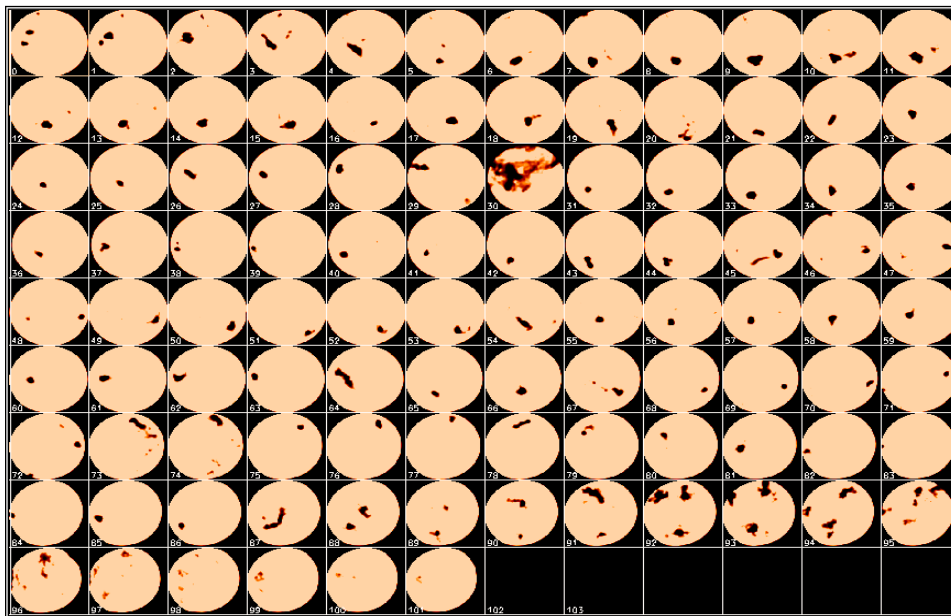
(b)

Fig. 27—A cross-sectional area for each slice along the core length after treatment for: (a) 2 cm^3/min & 200°F; (b) 3 cm^3 /min & 220°F.
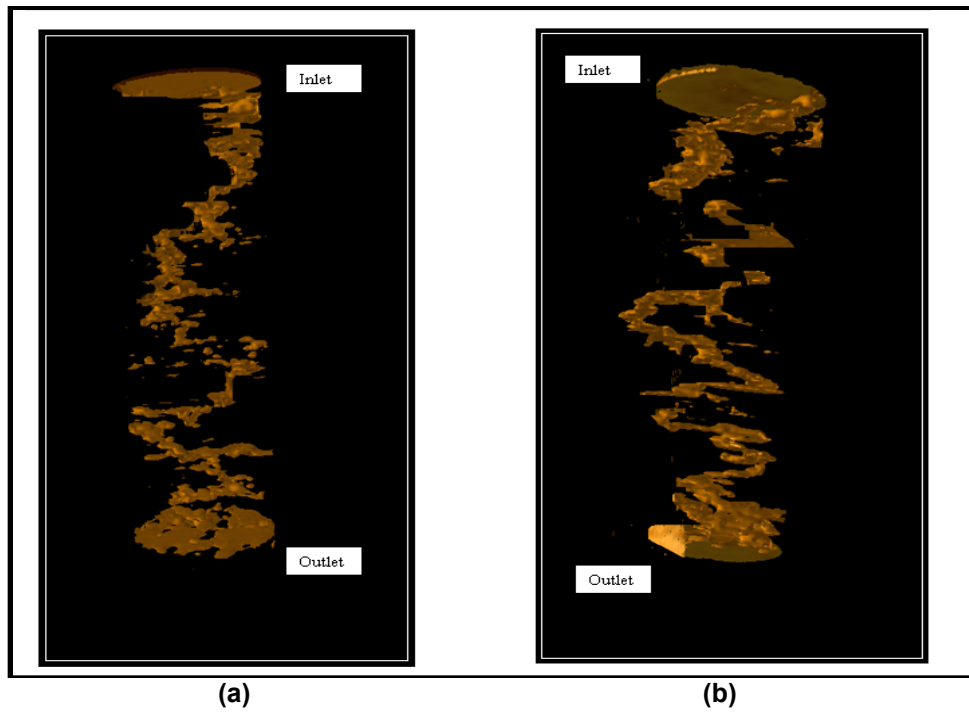
Fig. 28—3D CT scan after the coreflood test for: (a) 2 cm^3/min & 200°F; (b) 3 cm^3/min & 220°F.

(a)   (b)
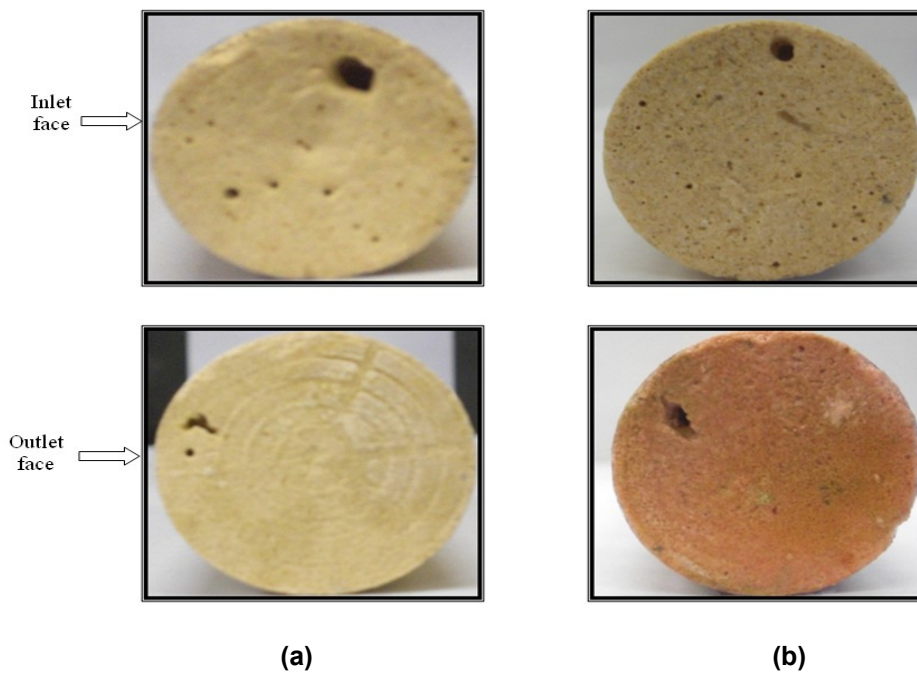
Fig. 29—Inlet and outlet core faces after the coreflood experiments with 20 wt% GLDA of pH = 1.7 at 300°F for (a) flow rate = 2 cm^3/min, (b) flow rate = 3 cm^3/min.

Biodegradability of GLDA

GLDA based on naturally occurring raw materials, is seen as a good basis for microorganisms to feed upon. Indeed, this is confirmed by the results obtained in several biodegradability studies that were performed with GLDA, see **Table 8**.

In a ready biodegradability test, i.e. the Closed Bottle test (OECD 301D), carried out in compliance with the principles of Good Laboratory Practice, GLDA was biodegraded > 60% at day 28 (**Fig. 30**). Hence this product should be classified as *readily* biodegradable. The biodegradation percentage in excess of 60% also demonstrates that GLDA is *ultimately* biodegradable (Van Ginkel et al. 2005). A test simulating conventional activated sludge treatment (OECD 303A) was performed. In this test biodegradation was followed by specific analysis of GLDA and by monitoring the change of dissolved organic carbon present in the effluent. At temperatures of 10 and 20°C, almost complete removal of GLDA was obtained. Consequently, GLDA will be removed almost completely under conditions prevailing in conventional activated sludge plants.

Table 8—THE BIODEGRADABILITY OF GLDA		
Biodegradability studies	**Method**	**Result**
Ready Biodegradability	OECD 301D	> 60% at day 14 *(readily* and *ultimately* biodegradable)*
Ready Biodegradability	OECD 301D	> 76% at day 28 *(readily* and *ultimately* biodegradable)*
Simulation test-aerobic sewage treatment; A activated sludge units	OECD 303A	> 80%
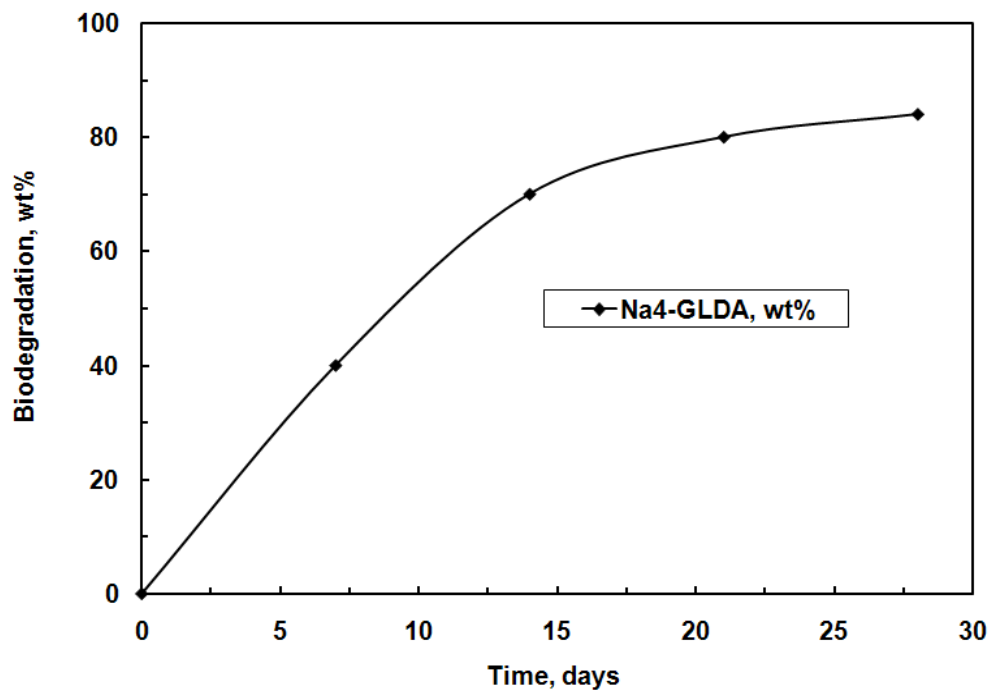
Fig. 30—Biodegradability of GLDA in OECD 301D in time.

Conclusions

L-glutamic acid diacetic acid (GLDA), a newly developed environmentally friendly chelate, was examined as an effective fluid for matrix treatments in deep oil and gas wells. Based on the results obtained, the following conclusions can be drawn:

1. GLDA had a very good ability to dissolve calcium from carbonate rock in a wide pH range by a combination of acid dissolution and chelation. The calcite dissolution increased with decreasing pH as a result of the contribution of the acid dissolution process. Under more alkaline conditions chelation became the dominant dissolution process.

2. The addition of 5 wt% sodium chloride did not affect the GLDA performance at pH 13, but significantly accelerated the reaction at pH 1.7.

3. The addition of 5 wt% calcium chloride stopped the reaction of GLDA with calcite at pH 13. GLDA chelated all the calcium in solution and did not react with calcium carbonate.

4. Compared to other chelating agents, GLDA dissolved more calcium than EDG but less than HEDTA at high pH values.

5. GLDA of pH = 1.7 was able to form wormholes at 2 and 3 cm^3/min through the 1.5 inch diameter core.

6. GLDA was found to be thermally stable at temperatures up to 350^oF.

7. GLDA is readily biodegradable and environmentally friendly.

CHAPTER III
EFFECTIVE STIMULATION FLUID FOR DEEP CARBONATE RESERVOIRS: A COREFLOOD STUDY

Introduction

A recently introduced chelating agent was examined to stimulate deep carbonate reservoirs. This chelating agent can be used at very low injection rates to avoid fracturing the target zone during the treatment, which may occur if HCl is used at high flow rates. The chelating agent used in part of the study was glutamic acid-N,N-diacetic acid (GLDA). Two sets of calcium carbonate cores were used one with 1.5 in. diameter and 20 in. length and the other set was 1.5 in. diameter and 6 in. length. Calcium carbonate cores such as Indiana limestone cores were used in this study. A dolomite core 1.5 in. diameter and 6 in. length was used to investigate the ability of this chelating agent to stimulate dolomite cores. The cores were treated with GLDA at various pH (1.7-13) and temperatures (180-300°F). The concentrations of dissolved calcium, and GLDA in the core effluent were measured for material balance determination. GLDA was compared with HCl and other chelants used in stimulation such as HEDTA, LCA, and acetic acid.

GLDA was found to be highly effective in creating wormholes over a wide range of pH (1.7-13) in calcite cores. Increasing temperature enhanced the reaction rate, more calcite was dissolved, and larger wormholes were formed for different pH with smaller volumes of GLDA solutions. GLDA was found to be equally effective in creating wormholes in short and long cores. GLDA at low pH values was found to be more effective than HEDTA, in addition GLDA has one nitrogen atom, therefore, and it is more biodegradable than HEDTA with two nitrogen atoms.

In this part, GLDA solutions were used to stimulate carbonate cores. The objectives of this part of the study are to: (1) study the effect of the pH of GLDA solutions on the formation of wormholes in calcite cores, (2) determine the effect of temperature on the amount of GLDA required to create wormholes, (3) assess the effect of the core length on the propagation of GLDA in calcite cores, (4) study the effect of initial core permeability on the process of dissolution of calcite by GLDA, (5) determine the optimum GLDA concentration, and (6) compare GLDA with HCl and other chelating agents that are used in stimulation.

Experimental Studies

Materials

Indiana limestone cores with a permeability range of 0.5 to 5 md, and Pink Desert limestone with high permeability were used. The core samples were cut in cylindrical shape with a 1.5 in. diameter and lengths of 6 and 20 in. Indiana limestone is a calcite cemented grain stone made up of fossil fragments and oolites with gray color. Indiana limestone samples in the XRD indicated that this rock type was made up predominantly of calcite (99 wt %). The permeability of the Indiana limestone cores ranged from 0.5 to 5 md and the porosity ranged from 0.12 to 0.22. The high permeability set of cores were cut from Pink Desert limestone outcrops. The color of Pink Desert cores was light pink, there was no bedding and depositional structure visible in the original depositional texture. The calcite was the cementing material and matrix at the same time. The permeability of the cores that were used in this study ranged from 35 to 120 md and the porosity ranged from 0.17 to 0.23.

GLDA solutions at a concentration of 20 wt% and pH values of 1.7, 3 and 13 were prepared from original solutions that were obtained from AkzoNobel. De-ionized water (TDS = 20 ppm) was used to prepare the 20 wt% GLDA solutions. The viscosity of different 20 wt% GLDA solutions with different calcium concentrations (at pH of 1.7, 3 and 13) was measured using a capillary tube viscometer (Ubbelhold type). The total calcium concentration was determined using atomic absorbance spectrometer (AAnalyst 700-flame type) immediately after the test. The GLDA solutions with different calcium concentrations were prepared using di-hydrated calcium chloride from VWR International. The free calcium concentration was determined using a calcium ion selective electrode (370 PerpHecT meter). The concentration of GLDA after the coreflood experiment was determined by complexometric-potentiometric end-point titration using a ferric chloride solution at pH = 3.

Coreflood Experiments

The coreflood set-up shown in **Fig. 7** was used to perform the coreflood experiments in this part.

Results and Discussion

Effect of pH Values of GLDA Solutions

Coreflood experiments with GLDA fluids of different pH (1.7-13) were run using the coreflood set-up shown in **Fig. 7**. **Table 9** gives the data for the 6 in. long cores for different pH levels of 20 wt% GLDA solutions. Six coreflood tests were run, two for each pH at 180 and 250°F. The different pH values represent different forms of GLDA: pH = 1.7 (H_4GLDA-acid form with a

molecular weight of 263), pH = 3 (NaH$_3$GLDA with a molecular weight of 285), and pH = 13 (Na$_4$GLDA-salt form with a molecular weight of 351). For each coreflood experiment, the pressure drop across the core was plotted using lab-view software. Samples of the coreflood effluent were analyzed for total and chelated calcium concentrations. The concentration of GLDA in the effluent samples was also measured to determine its stability, as well as density and pH.

Table 9—DATA FOR 6 in. COREFLOOD EXPERIMENTS									
Exp.#	pH	ϕ, vol%	$K_{initial}$	K_{final}	$K_{final}/K_{initial}$	Q, cm^3/min	PV$_{bt}$	Ca, g	T, ^{o}F
1	1.7	13.5	2.00	350	175	2	3.65	5.93	180
2	1.7	10.5	0.65	180	277	2	2.30	6.84	250
3	1.7	11.3	0.55	250	450	2	1.65	7.25	300
4	3.0	15.8	1.00	120	120	2	3.80	5.85	180
5	3.0	14.1	2.73	400	147	2	2.65	6.45	250
6	3.0	13.5	1.25	310	250	2	2.00	6.74	300
7	13	10.3	0.35	11.6	33	2	18.0	2.51	180
8	13	12.1	0.66	31.7	48	2	14.0	3.21	250
9	13	12.4	1.45	85	59	2	8.50	3.53	300

Fig. 31 shows the pressure drop across the core during the coreflood experiment for 20 wt% GLDA at pH = 1.7 at 2 cm^3/min and 180°F. The pressure drop initially increased during the introduction of GLDA and then decreased until the GLDA penetrated through the core. The increase in the pressure drop can be attributed to the increased viscosity of the reacted GLDA solution. The viscosity and density measurements of GLDA (pH = 1.7) with different concentrations of calcium at room temperature are reported in **Table 10** (the viscosity in this table for GLDA-Ca complex only, i.e. there is no free calcium only complexed calcium from calcium chloride solutions)**.** As the calcite was dissolved and calcium concentration of the GLDA fluid increased and so did the viscosity of the fluid. At the same time during the reaction of GLDA with calcite wormholes were formed and the pressure drop was then expected to decrease. The net result on whether the pressure drop was increasing, stabilizing or decreasing depends on the extent of dissolution in the length of the core. It was noted that as soon as the calcium started to come out of the core the pressure drop started to decrease. This was due to increased

permeability caused by wormholing begun to dominate over the increased viscosity of the GLDA fluid.

	Table 10—DENSITY AND VISCOSITY MEASUREMENTS OF 20 WT% GLDA (pH = 1.7, 3, AND 13) SOLUTIONS WITH DIFFERENT CALCIUM CONCENTRATIONS AT ROOM TEMPERATURE					
Ca, ppm	pH = 1.7		pH = 3		pH = 13	
	ρ, g/cm^3	μ, g/cm^3	ρ, g/cm^3	μ, g/cm^3	ρ, g/cm^3	μ, g/cm^3
0	1.132	2.52	1.125	3.20	1.126	1.88
5000	—	—	1.133	3.87	1.134	2.25
10,000	1.151	2.80	1.143	4.65	1.142	2.63
15,000	—	—	—	—	1.150	3.15
20,000	1.173	3.23	1.160	5.56	—	—
30,000	1.182	3.57	1.168	6.49	—	—
40,000	1.202	3.80	—	—	—	—
50,000	1.223	4.20	—	—	—	—
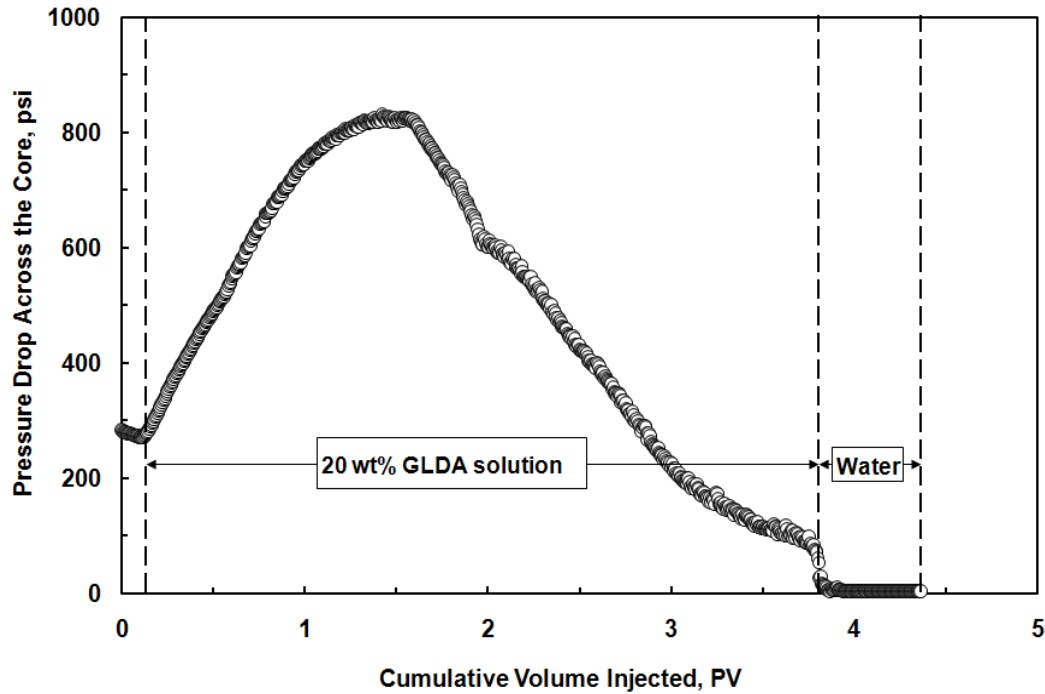
Fig. 31— Pressure drop across the core at a flow rate of 2 cm^3/min & 180°F for 20 wt% GLDA with pH = 1.7.

Fig. 32 shows the total calcium concentration, chelated calcium concentration and the GLDA concentration in the core effluent samples. The total calcium concentration reached a maximum value of 45,000 ppm indicating the effectiveness of GLDA to dissolve calcite under these conditions. At an effluent pH of 4.5 nearly 30% of the total dissolved calcium was found to be complexed by GLDA. The amount of chelated or complexed calcium was determined by subtracting the free calcium concentration from the total calcium concentration. The concentration of GLDA in the core effluent samples after the coreflood test reached the 20 wt% injection concentration indicating the stability of GLDA during the coreflood treatment.
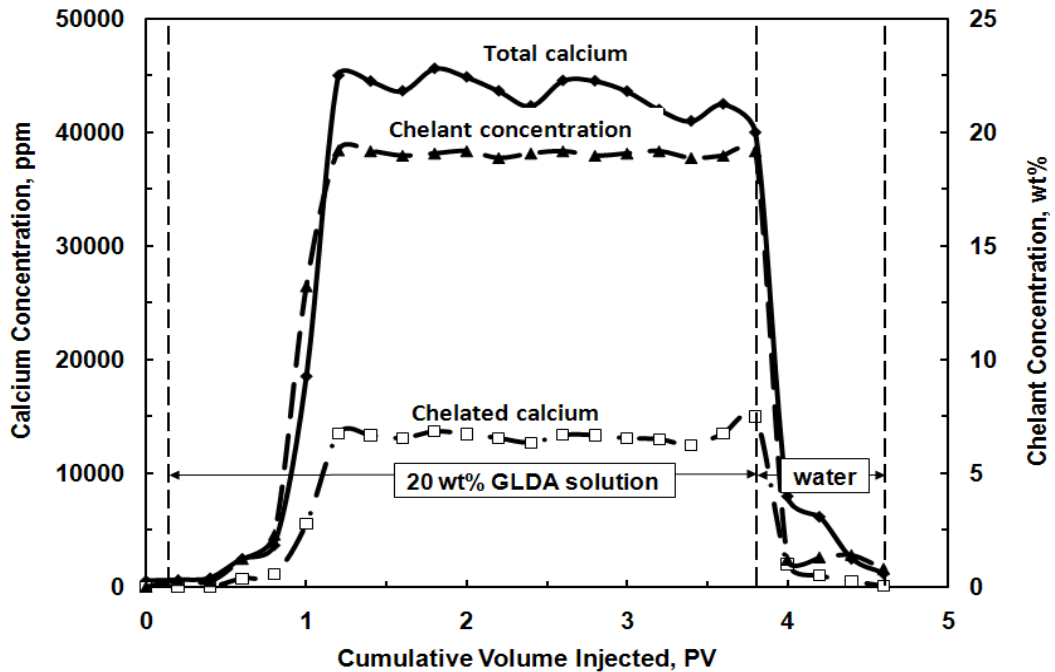
Fig. 32—Total and complexed calcium concentration & GLDA concentration in the core effluent samples at a flow rate of 2 cm³/min & 180°F for 20 wt% GLDA with pH = 1.7.

Fig. 33 shows the density and pH of the coreflood effluent samples for the same experiment. As calcium and GLDA breakthrough at PV = 1 the density of the effluent samples increased due to the presence of calcium ions in solution. The pH stabilized at a value around 4.5 because of the buffering effect of CO_2. At low pH, the theoretical reaction between calcium carbonate and a polycarboxylic acid is dictated by H^+ according to **Eq. 25**:

$$H_4Y + 2CaCO_3 \leftrightarrow 2H_2O + 2CO_2 + 2Ca^{2+} + Y^{4-} \dots\dots\dots\dots\dots\dots\dots\dots\dots\dots\dots (25)$$
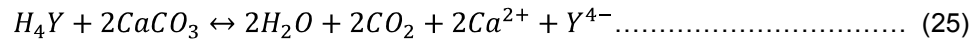
where H_4Y is a tetracarboxylic acid.
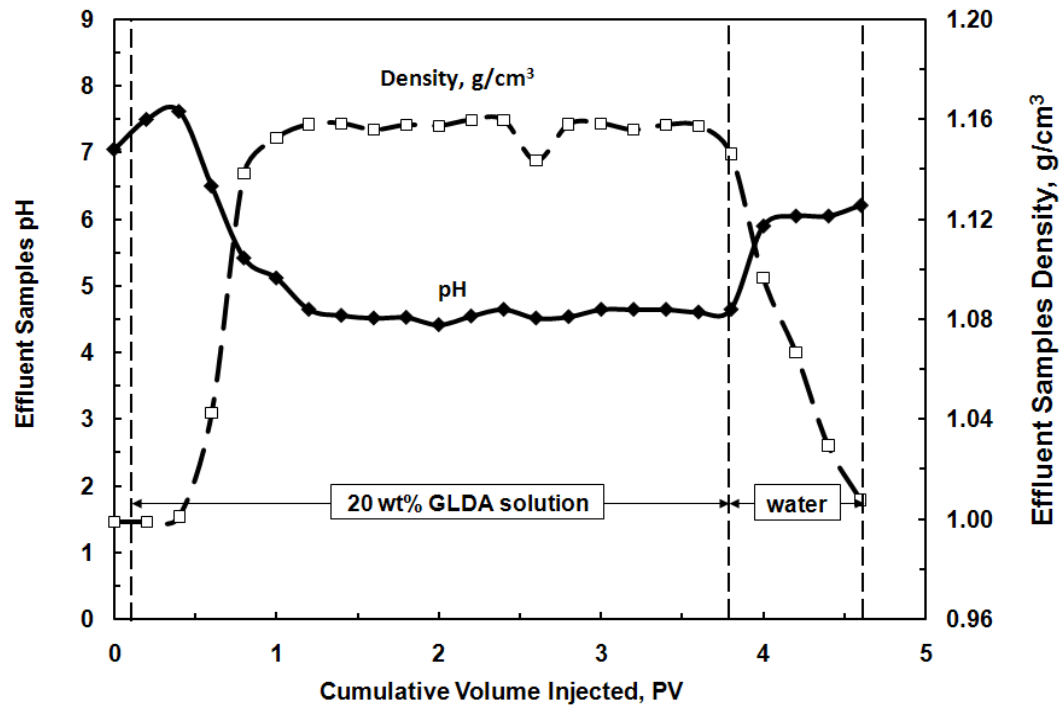
Fig. 33—Core effluent samples pH and density at a flow rate of 2 cm³/min & 180°F for 20 wt% GLDA with pH = 1.7.

A similar behavior in the coreflood experiment was observed with the 20 wt% GLDA solution at pH = 3. **Fig. 34** shows the pressure drop across the core during the flooding experiment. As before the pressure drop increased across the core, but in this case the ration of maximum pressure to initial pressure ($\Delta p_{max}/\Delta p_{initial}$) was greater than that in case of pH 1.7. The ratio of maximum pressure drop to initial pressure drop in the case of GLDA at pH 3 was 3.2 and it was 2.7 for pH 1.7. The increase in the pressure drop is attributed to the viscosity of GLDA at pH 3 at room temperature was greater than the viscosity of GLDA at pH of 1.7 as shown in **Table 10**.
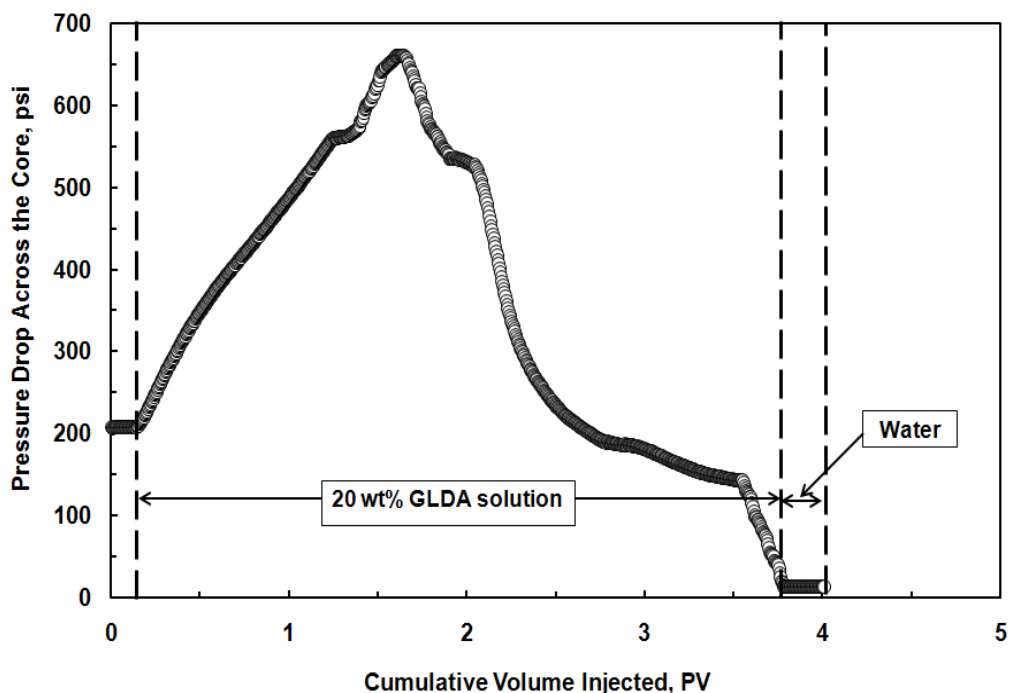
Fig. 34—Pressure drop across the core at a flow rate of 2 cm³/min & 180°F for 20 wt% GLDA at pH 3.

Fig. 35 shows the total calcium concentration, chelated calcium concentration and the GLDA concentration in the core effluent samples for these conditions. In this case the total calcium concentration reached a maximum value of 35,000 ppm, which was less than that observed at pH = 1.7. The effluent pH = 5.2 resulted in 40% of calcium being chelated by GLDA, versus 30% at pH = 1.7. Again the GLDA concentration after the coreflood effluent approached the 20 wt% showing a good stability of the GLDA chelate under these conditions.

Fig. 36 shows the density and pH for the coreflood effluent samples for 20 wt% GLDA solution (pH = 3) at 2 cm³/min and 180°F. The density of the GLDA solution increased to its maximum value (1.16 g/cm³) after the GLDA broke through the core. The effluent pH ranged from pH 5 to 5.5 being greater than the pH 4.5 observed when pH = 1.7 GLDA fluid was used. The pH in this case was greater than that when pH = 1.7 was used because the amount of hydrogen attack to the calcite was lower with the GLDA of pH 3 than that with GLDA of pH 1.7 and the amount of evolved CO_2 was less than that evolved when the GLDA of pH = 1.7 was used.
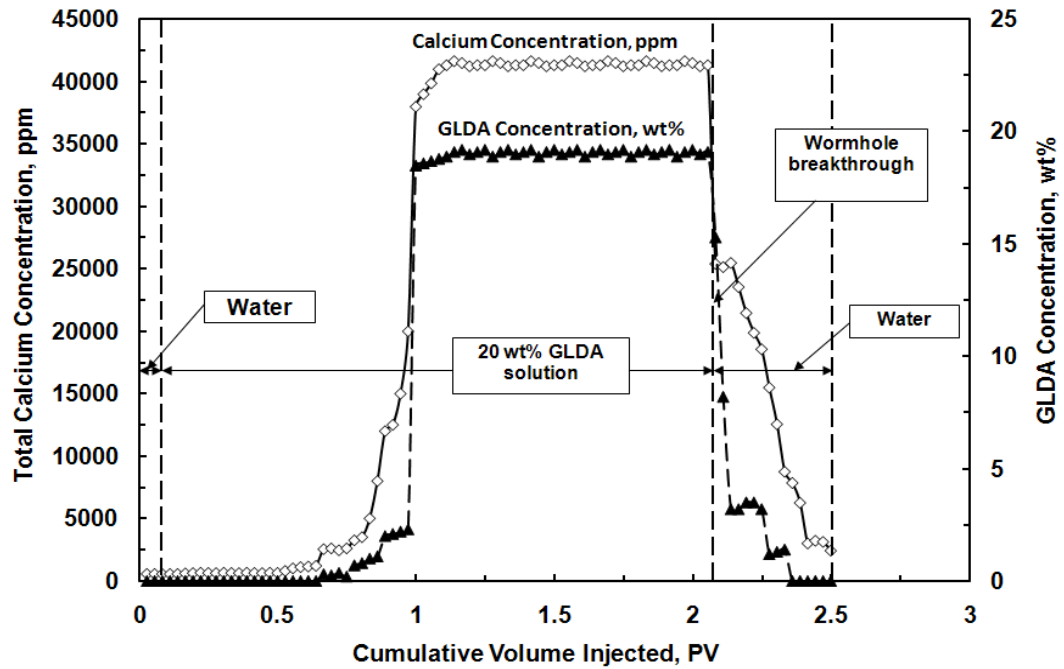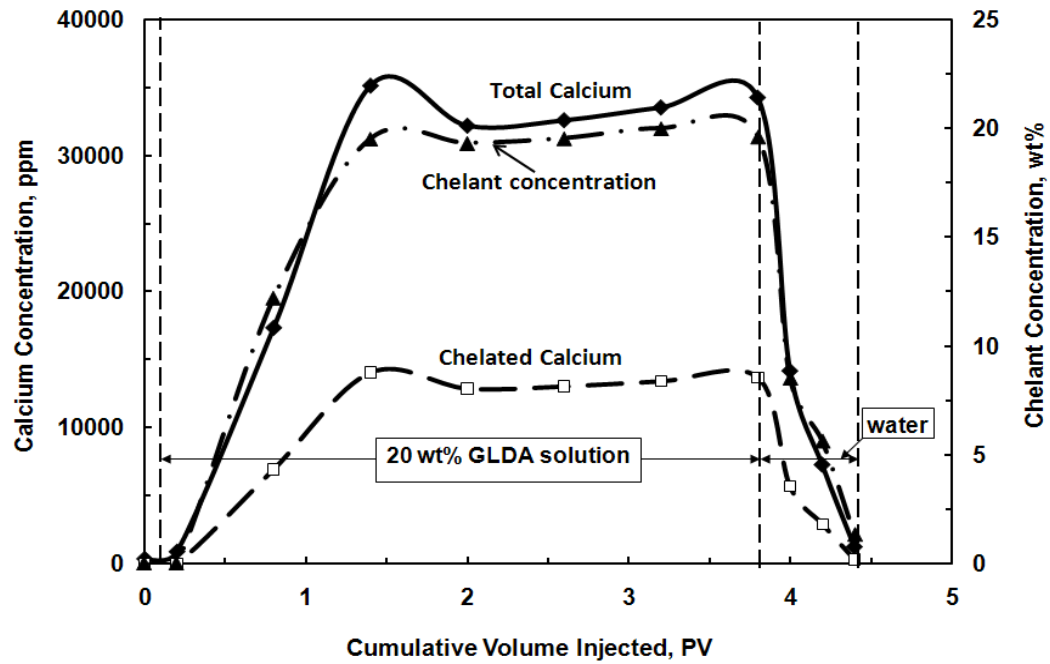
Fig. 35—Total and complexed calcium concentration & GLDA concentration in the core effluent samples at a flow rate of 2 cm^3/min & 180°F for 20 wt% GLDA at pH 3.
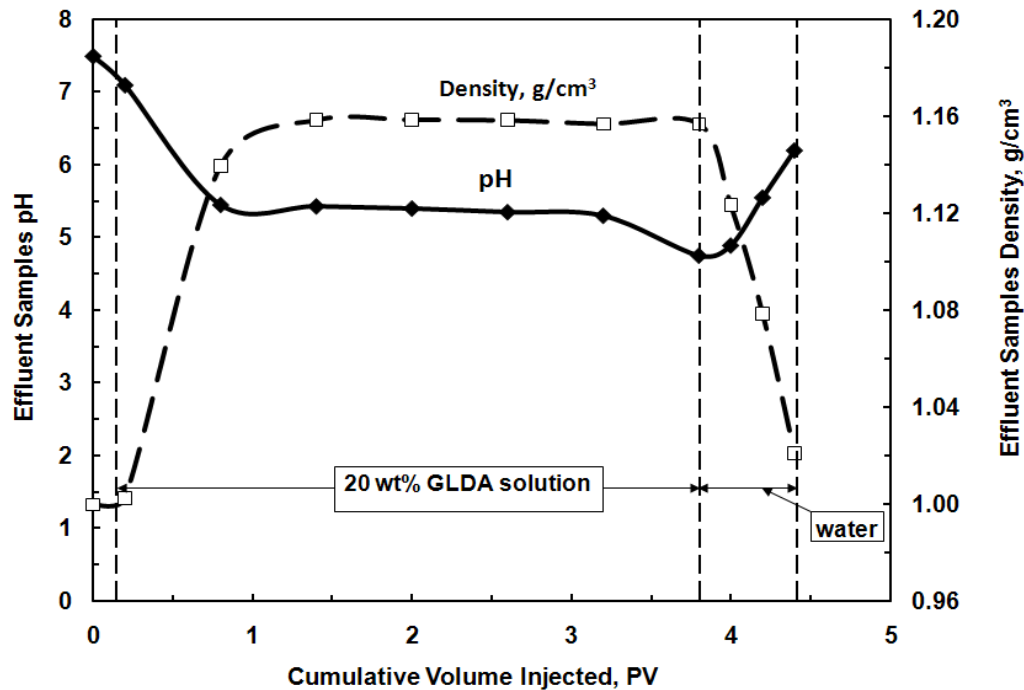

Fig. 36—Core effluent samples pH and density at a flow rate of 2 cm^3/min & 180°F for 20 wt% GLDA at pH 3.

Fig. 37 shows the pressure drop across the core during the coreflood experiment for 20 wt% GLDA solutions at pH 13 at 2 cm^3/min and 180°F. The behavior of the pressure drop after starting the injection of this fluid was somewhat different than that observed with fluids at pH 1.7 and 3. The increase in the pressure drop at pH 13 was small compared to the lower pH fluids. The pressure drop reached 1,050 psi after ~ 3 PV and then began to slowly decrease. This can be attributed to the viscosity of 20 wt% GLDA, pH = 13 is smaller than that in case of pH = 1.7 and 3, **Table 10**. From **Fig. 38** the maximum amount of dissolved calcium in the case of 20 wt% GLDA of pH = 13 was 10,000 ppm, the viscosity slightly increased, therefore, the increase in the pressure drop was not large. Also, the total calcium dissolved equaled to the amount of chelated calcium because in this case the dissolution mechanism was due to chelation only. This can be confirmed by **Fig. 39**, in which the pH of the core effluent samples was 12.5 to 13. In this case, there was no CO2 to buffer the solution. Also, the density of the effluent samples was smaller compared with that in case of pH = 1.7 and pH = 3 as there was lower calcium concentration in the effluent samples.
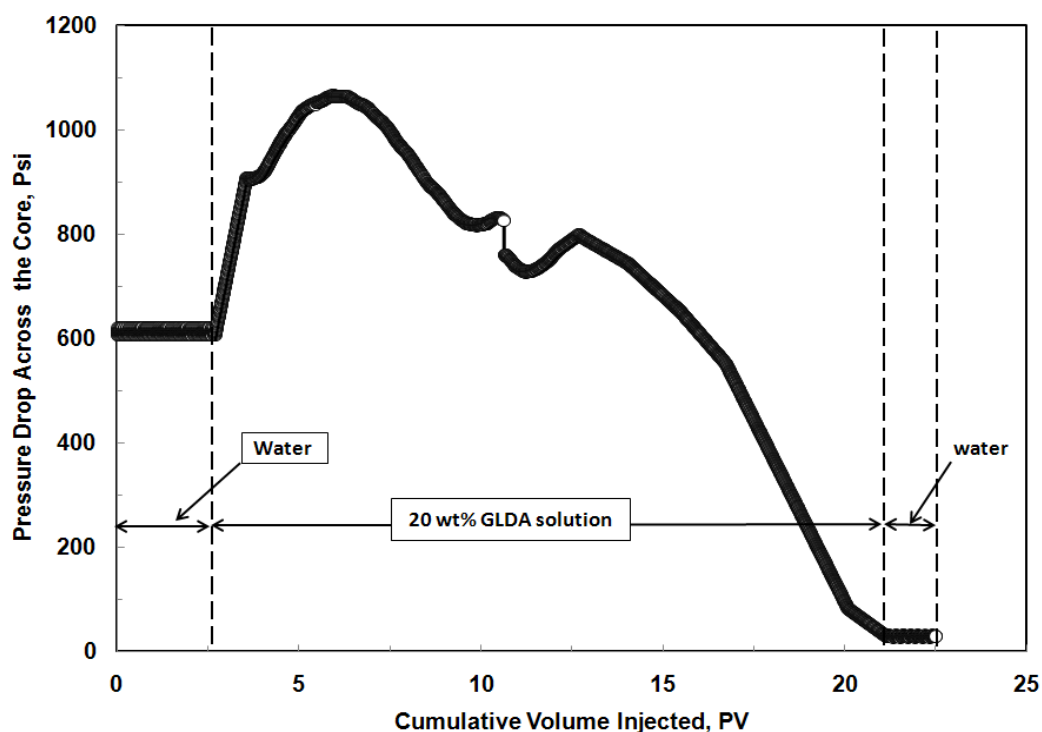
Fig. 37—Pressure drop across the core at a flow rate of 2 cm^3/min & 180°F for 20 wt% GLDA at pH 13.
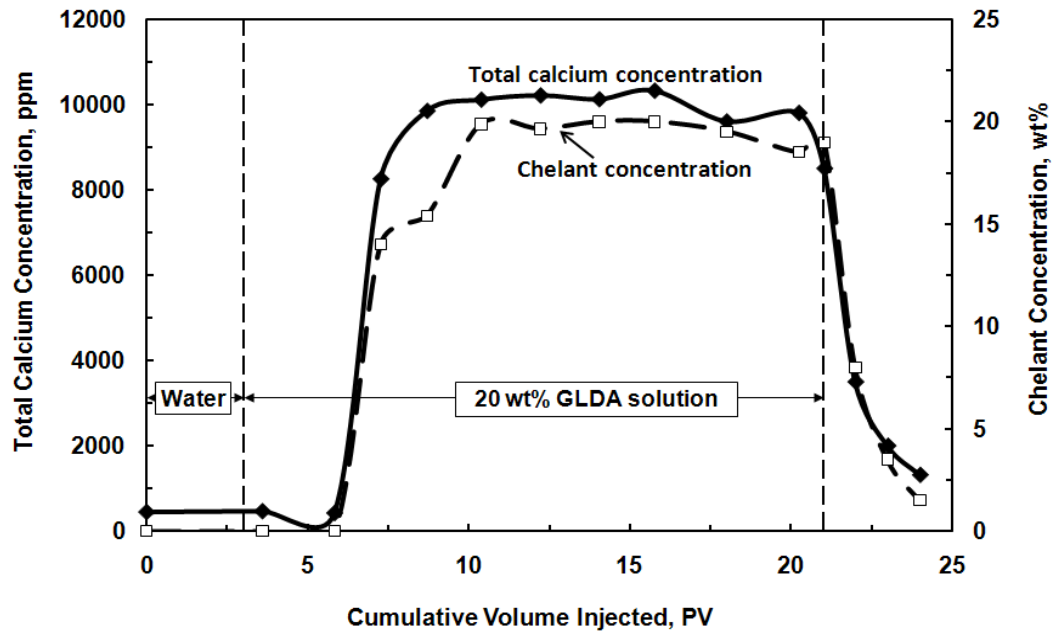
Fig. 38—Total calcium and GLDA concentrations in the core effluent samples at a flow rate of 2 cm^3/min & 180°F for 20 wt% GLDA at pH 13.
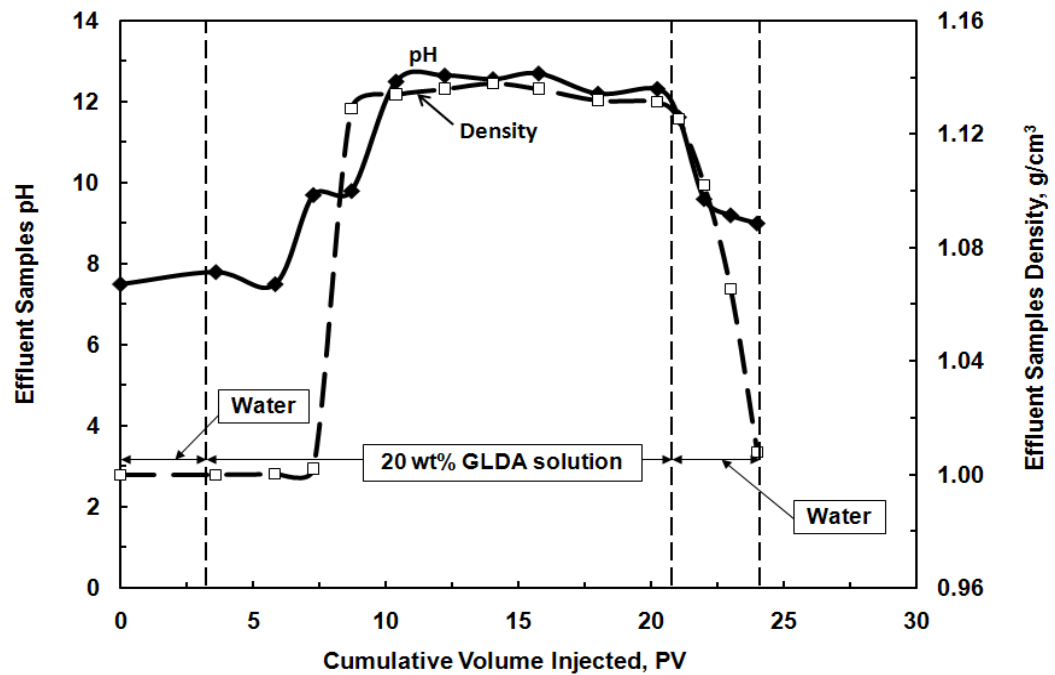
Fig. 39—Core effluent samples pH and density at a flow rate of 2 cm^3/min & 180°F for 20 wt% GLDA at pH 13.

Figs. 40 - 42 summarize the effect of the pH of the GLDA solutions on the dissolution of calcite and wormhole formation in calcium carbonate cores. The volume of 20 wt% GLDA required to form wormholes increased as the pH was increased. Specifically the volume of fluid required at pH = 1.7, 3 and 13 was 3.65, 3.8 and 18 PV, respectively. We can conclude that the acid form of GLDA (pH = 1.7) was more effective in dissolving calcite than at pH = 13. It was more effective in terms of the volume of GLDA required to breakthrough the core was less in case of GLDA at pH 1.7.The enhanced dissolution of calcite at pH = 1.7 was due to the H$^+$ attack, but was due nearly entirely to chelation at pH = 13. Therefore the reaction was very slow at pH = 13 and it took this large PV to form wormholes.

The influence of chelating agents on the rate of calcite dissolution is highly dependent upon the pH of the solution. For aminopolycarboxylic acids, these variations are due primarily to changes in ionic species involved at the surface reaction (Fredd and Fogler 1998c). The form of the ionic species is dictated by a series of dissociation reactions, which for a chelating agent with four carboxylic acid groups like GLDA are:

$$H_4Y \leftrightarrow H_3Y^{1-} + H^+ \dots\dots\dots\dots\dots\dots\dots\dots\dots\dots\dots\dots\dots\dots\dots \text{(26)}$$

$$H_3Y^{1-} \leftrightarrow H_2Y^{2-} + H^+ \dots\dots\dots\dots\dots\dots\dots\dots\dots\dots\dots\dots\dots\dots \text{(27)}$$

$$H_2Y^{2-} \leftrightarrow HY^{3-} + H^+ \dots\dots\dots\dots\dots\dots\dots\dots\dots\dots\dots\dots\dots\dots \text{(28)}$$

$$HY^{3-} \leftrightarrow Y^{4-} + H^+ \dots\dots\dots\dots\dots\dots\dots\dots\dots\dots\dots\dots\dots\dots \text{(29)}$$

where H_mY^{m-n} represents the chelating agent molecule, m is the number of acidic protons, and n is number of carboxylic acid groups, i.e. 4.

On the high pH side the reaction is primarily driven by the chelation process, which generally has a much lower reaction rate than the acid dissolution process and gives 1:1 ratio between the chelate and calcium ions:

$$Y^{4-} + CaCO_3 \leftrightarrow CaY^{2-} + CO_3^{2-} \dots\dots\dots\dots\dots\dots\dots\dots\dots\dots\dots \text{(30)}$$

In the intermediate pH range both processes will participate in the overall dissolution process. As pH increased from 1.7 to 13, the GLDA successively deprotonated from H_4Y to Y^{4-} thereby losing the ability to donate H$^+$ ions as pH increased. The reaction rate of GLDA at high pH was dominated by chelation and was expected to be significantly slower than at low pH. **Fig.**

42 shows the amount of dissolved calcium was maximum at pH 1.7 but minimum at pH 13. At pH 1.7 GLDA was predominantly in the form of H_4Y. At pH 13, GLDA successively deprotonated to the Y^4. The dissolution of calcite at high pH (pH =13) was due to complexation only.
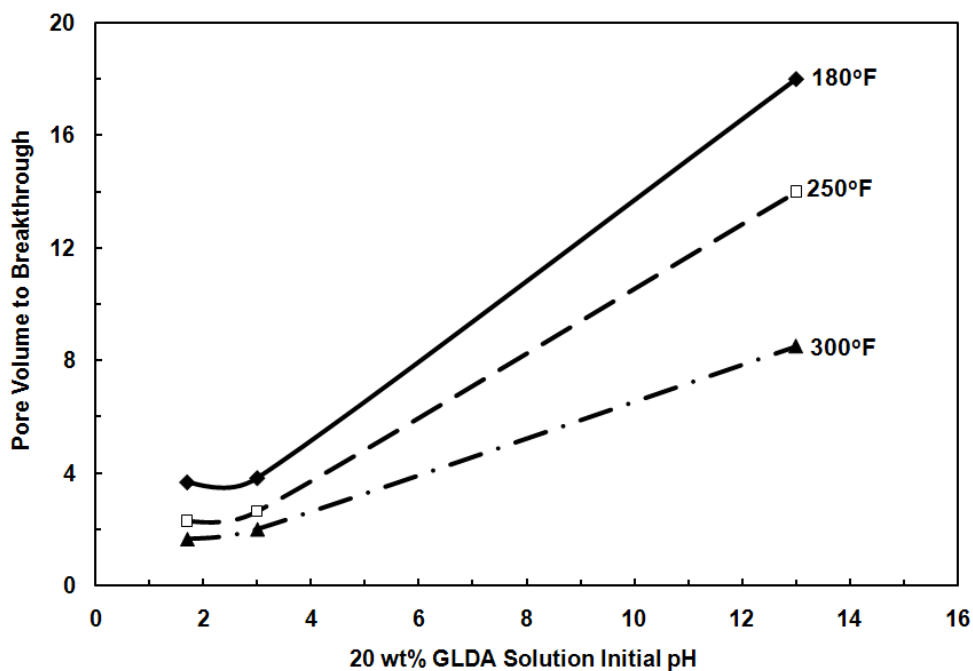
Fig. 40—Effect of 20 wt% GLDA solution pH on the pore volume to breakthrough the core at a flow rate of 2 cm^3/min at 180, 250, and 300°F.
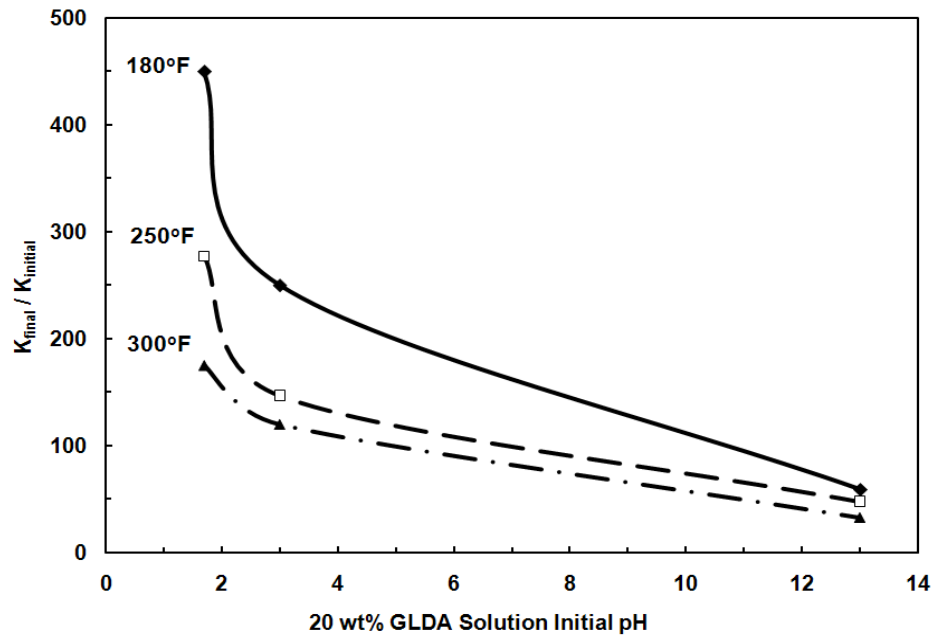
Fig. 41—Effect of 20 wt% GLDA solution pH on the ratio between final and initial permeability of the core at a flow rate of 2 cm³/min at 180, 250, and 300°F.
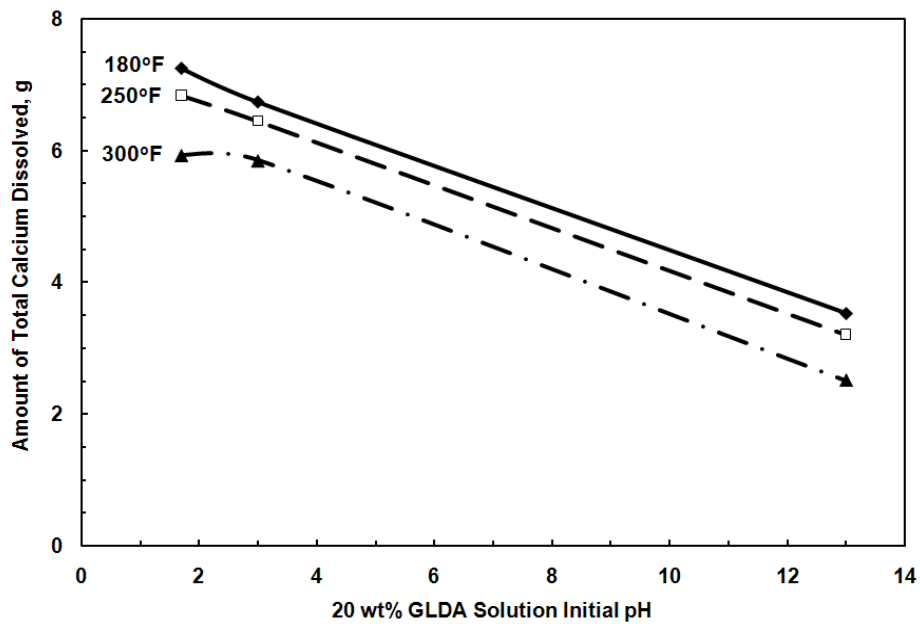
Fig. 42—Effect of 20 wt% GLDA solution pH on the amount of calcium dissolved from the core at a flow rate of 2 cm³/min at 180, 250, and 300°FEffect of Temperature.

Similar coreflooding experiments were performed at 250 and 300°F. Higher temperatures enhanced calcite dissolution by GLDA at all pHs examined. **Figs. 40 to 42** show the effect of increasing temperature on the performance of GLDA. As the temperature was increased from 180 to 300°F, the volume of GLDA required to form wormholes decreased to 1.65, 2 and 8.5 PV for pH = 1.7, 3, and 13, respectively. This indicated that GLDA was very effective at wormhole creation at high temperatures and required less pore volume than at low temperatures. The amount of dissolved calcium increased by 1.32, 0.89, and 1.02 g for pH = 1.7, 3 and 13, respectively as the temperature was increased from 180 to 300°F. The permeability ratio attained its highest value at 300°F and pH = 1.7.

GLDA solution at pH = 3 was very effective in creating wormholes at 180, 250, and 300°F compared with other chelating agents. The amount of 20 wt% GLDA at pH = 3 required to breakthrough the core was 3.8 and 2.65 PV at 180 and 250°F, respectively at a flow rate of 2 cm³/min. Our results are in agreement with the same trends obtained for other chelates such as 20 wt% Na₃HEDTA (pH = 2.5) (Frenier et al. 2001). Therefore, GLDA at pH 3 was found to be very effective and required less volume to create wormholes through the cores. **Fig. 43** shows the core inlet and outlet faces after the coreflood treatments for three different cores with 20 wt% GLDA at 2 cm³/min for different GLDA pH (1.7, 3, and 13). The wormhole had the maximum diameter at pH of 1.7 and there were very small wormholes in case of pH 13.

Fig. 43—Inlet and outlet core faces after the coreflood experiments with 20 wt% GLDA at 2 cm³/min at 300°F for (a) pH = 1.7, (b) pH = 3, and (c) pH = 13.

Similar coreflooding experiments were performed at 250 and 300°F. Higher temperatures enhanced calcite dissolution by GLDA at all pHs examined. **Figs. 40 to 42** show the effect of increasing temperature on the performance of GLDA. As the temperature was increased from 180 to 300°F, the volume of GLDA required to form wormholes decreased to 1.65, 2 and 8.5 PV for pH = 1.7, 3, and 13, respectively. This indicated that GLDA was very effective at wormhole creation at high temperatures and required less pore volume than at low temperatures. The amount of dissolved calcium increased by 1.32, 0.89, and 1.02 g for pH = 1.7, 3 and 13, respectively as the temperature was increased from 180 to 300°F. The permeability ratio attained its highest value at 300°F and pH = 1.7.

GLDA solution at pH = 3 was very effective in creating wormholes at 180, 250, and 300°F compared with other chelating agents. The amount of 20 wt% GLDA at pH = 3 required to breakthrough the core was 3.8 and 2.65 PV at 180 and 250°F, respectively at a flow rate of 2 cm^3/min. Our results are in agreement with the same trends obtained for other chelates such as 20 wt% Na$_3$HEDTA (pH = 2.5) (Frenier et al. 2001). Therefore, GLDA at pH 3 was found to be very effective and required less volume to create wormholes through the cores. **Fig. 43** shows the core inlet and outlet faces after the coreflood treatments for three different cores with 20 wt% GLDA at 2 cm^3/min for different GLDA pH (1.7, 3, and 13). The wormhole had the maximum diameter at pH of 1.7 and there were very small wormholes in case of pH 13.

Fig. 43—Inlet and outlet core faces after the coreflood experiments with 20 wt% GLDA at 2 cm^3/min at 300°F for (a) pH = 1.7, (b) pH = 3, and (c) pH = 13.

Stimulation of Long Calcite Cores

GLDA solutions of pH = 1.7 were also used to create wormholes in long calcium carbonate cores of 20 in. length. **Table 11** gives the data for three coreflood experiments using 20 in. long cores. **Fig. 44** shows the 3D pictures for the wormholes formed after the coreflood experiments. GLDA was equally effective in creating wormholes in long cores and short cores. Three different injected rates were used in the coreflood experiments. Wormholes were formed at the three different rates. There was only one dominant wormhole in the three coreflood experiments at 200°F. Generally at the three injection rates, the volume of GLDA required to create wormholes was less for long cores (20 in.) compared to that for short cores (6 in.). This can be attributed to the increased contact time due to the increased pore volume of the long core.

To investigate the effect of core length on the volume of GLDA required to breakthrough the core, two coreflood experiments were performed at pH 1.7 at a flow rate of 2 cm^3/min at 250°F. The pore volume of the 20 in. core was 95 cm^3 and the pore volume of the 6 in. core was 25 cm^3. The pore volume of the long core was more than three times the short one. In turn, the contact time of GLDA with the long core will be higher than that with the short core at the same flow rate. The pore volumes required to breakthrough the core in case of the 20 in. core was 2 PV and that for the 6 in. core was 2.45 at the same conditions. The decrease in the number of pore volumes in the long cores was due to the increased contact time. The same scenario was repeated at pH 3, two coreflood experiments were performed at a flow rate of 1 cm^3/min at 250°F. The pore volumes required to breakthrough the core in case of the 20 in. long core was 1.6 PV and that for the 6 in. core was 2.3. The pore volume of the 20 in. core was also more than three times that of the 6 in. core. This meant that GLDA performed better with the long cores than short cores. The performance of GLDA at pH 3 with 20 in. cores was better than that at pH 1.7. The reduction in pore volumes required 0.7 PV and 0.45 PV at pH 3 and 1.7, respectively. Finally, increasing the core length at any rate will be better for the GLDA to create wormholes and it allowed more time for reaction. GLDA was not degraded during the coreflood experiments and its concentration was almost the same after the coreflood so it can penetrate deep and bypass the damaged zone if injected for long time.

Table 11—COREFLOOD DATA FOR 20 IN. LONG CALCITE CORES			
Parameter	Exp.#1	Exp.#2	Exp.#3
Flow rate, cm^3/min	1	2	3
Initial pH of GLDA solution	1.7	1.7	1.7
Temperature, ^{o}F	200	200	200
Initial core permeability, md	1.2	6.1	5.2
Porosity, vol %	12.5	19.7	18.5
Final core permeability, md	650	130	150
Pore volume to breakthrough, PV_{bt}	3.52	2.1	2.96

(a)   **(b)**   **(c)**
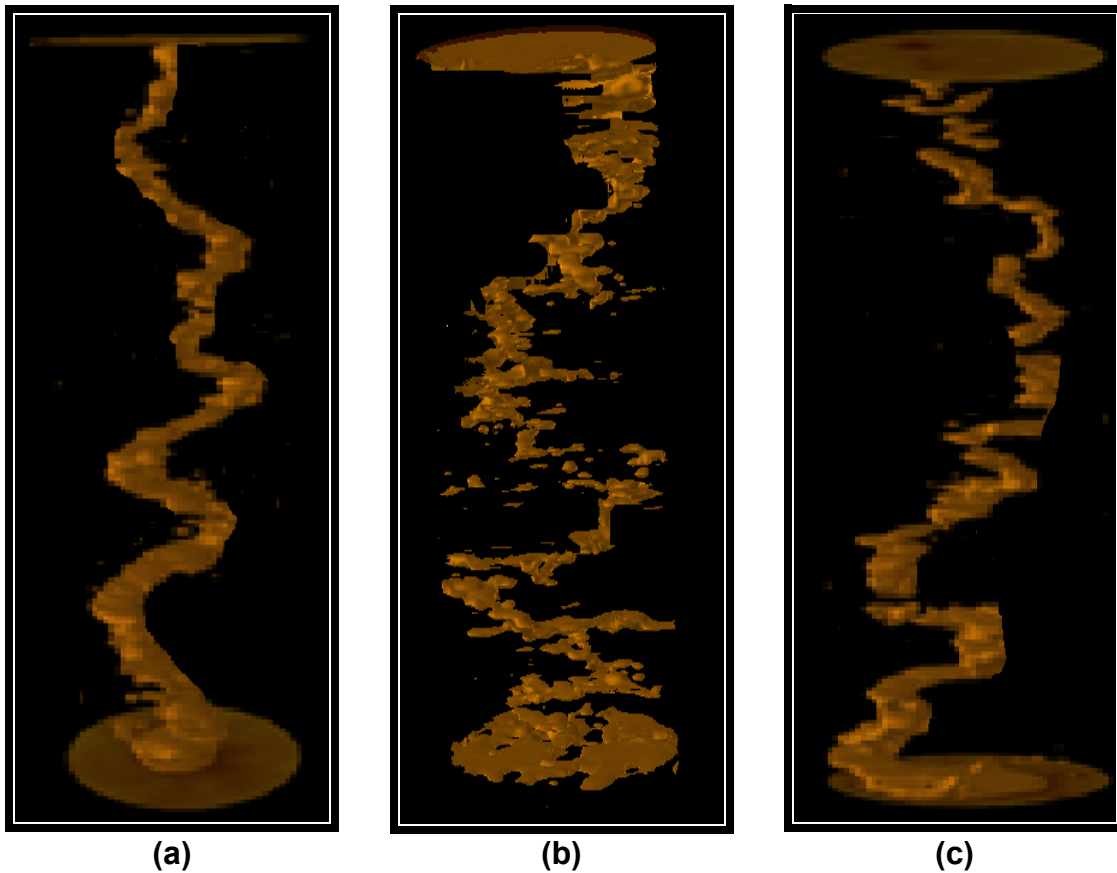
Fig. 44—3D CT scan after the coreflood test for: (a) 1 cm^3/min, (b) 2 cm^3/min, and (c) 3 cm^3/min, for GLDA at pH 1.7 & 200°F.

Effect of GLDA Concentration

Various concentrations of GLDA: 10, 15, 20, and 30 wt% were studied at pH 1.7 and 3. **Table 12** has listed the outcome of the coreflood experiments performed to study the effect of GLDA concentration on the volume of GLDA required to form wormholes. **Fig 45** shows the effect of GLDA solution concentration on the pore volumes of GLDA necessary to breakthrough the core at 2 cm^3/min and 250°F. For higher concentrations the reaction rate decreased because of the reduced fluid activity caused by the retarding effects of the dissolved reaction products and the increased GLDA viscosity. Similar trends were obtained by Mostofizadeh and Economides (1994). They used different concentrations of HCl 4, 15 and 30 wt. % to stimulate calcite cores. They found that 15 wt. % HCl performed better than 4 and 30 wt% HCl. At 30 wt% GLDA solution concentration the volume required to breakthrough the core was 3.85 and 4 PV at pH 1.7 and 3, respectively. The lower the concentration the higher the pore volume required to breakthrough the core, at 10 wt% GLDA solutions the volume of GLDA required to create wormholes increased to 5.85 and 7.35 PV for pH values of 1.7 and 3, respectively. The optimum concentration at which the lowest volume of GLDA needed to create wormholes was at 20 wt% for both pH values. **Fig. 46** shows the amount of maximum dissolved calcium in the coreflood effluent samples at different concentrations of GLDA solutions. At a flow rate of 2 cm^3/min and 250°F the maximum dissolved calcium was at 20 wt% concentration indicating that this is the optimum concentration that should be used to obtain the highest rate of calcite dissolution. At concentrations greater or less than 20 wt% GLDA the dissolution process was less effective. From Fig. 46 the reaction of GLDA at pH 3 with calcite was not reduced by the same magnitude as it was at pH 1.7. GLDA at pH 1.7 resulted in more calcium dissolved which then increased the fluid's viscosity and thus likely retarded the reaction more than GLDA at pH 3, which has lower dissolution ability compared to that at pH 1.7 (Mahmoud et al. 2010b).

Table 12—COREFLOOD DATA FOR THE EFFECT OF GLDA CONCENTRATION AT DIFFERENT pH VALUES

GLDA solution concentration, wt%	Temperature, °F	Flow rate, cm³/min	Initial pH of GLDA solution			
			1.7		3	
			Maximum Ca²⁺, ppm	PV$_{bt}$	Maximum Ca²⁺, ppm	PV$_{bt}$
10	250	2	32000	5.85	18000	7.35
15	250	2	35000	3.10	25000	3.55
20	250	2	45000	2.30	32000	2.65
30	250	2	24000	4.50	28000	4.00
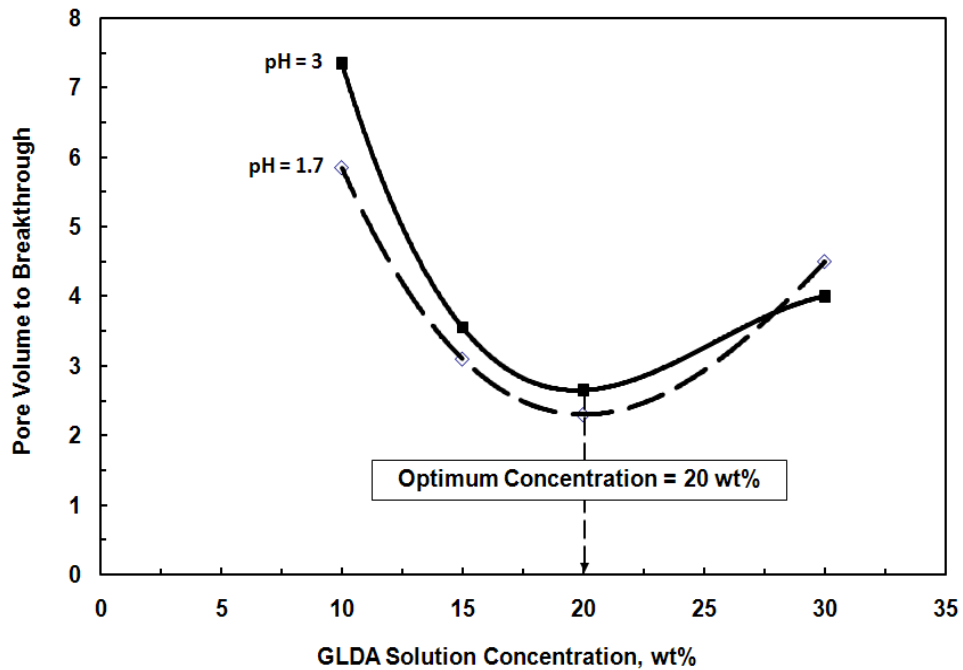
Fig. 45—Effect of GLDA concentration on the volume of 20 wt% GLDA solutions required to form wormholes at a flow rate of 2 cm³/min and 250°F.
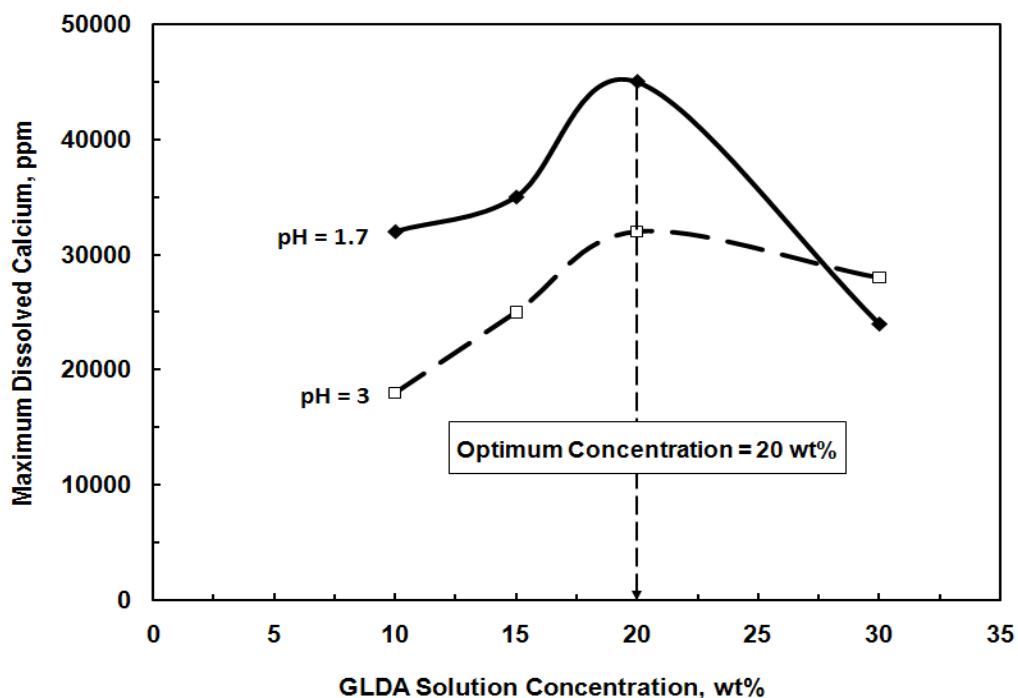
Fig. 46—Effect of GLDA concentration on the amount of calcium dissolved in the coreflood effluent at a flow rate of 2 cm³/min and 250°F.

Effect of Initial Core Permeability

The effect of core permeability was obvious in the amount of calcium dissolved and the pore volumes required to breakthrough in case of high and low core permeability. At the same conditions, the amount of dissolved calcium was greater in case of high permeability cores than with low permeability cores. In turn, the pore volumes required to breakthrough the core was greater in case of high permeability than cores with low permeability. Porosity and permeability were greater in the Pink Desert set of cores than in Indiana limestone set. The optimum flow rate for the lesser permeable Pink Desert cores was 3 cm³/min. The optimum injection rate for the Indiana limestone cores was less than 2 cm³/min, and the behavior of flow rate and PV_{bt} was different than in case of Pink Desert cores as shown in **Tables 13 and 14**. Increasing the core permeability increased the area-to-volume ratio (Mostofizadeh and Economides 1994) and the volume of GLDA required to breakthrough the core in the high permeability cores was greater than that required for low permeability cores.

Rock typing which is $(k/\phi)^{0.5}$ (Permadi and Susilo 2009) was calculated for each set of cores. It was found that the rock typing was greater in the case of Pink Desert set of cores than Indiana limestone set. The higher the rock typing the higher the dissolved calcium under the

same conditions. Tables 13 and 14 show the rock properties for high and low permeability cores with the typing factor for each set of samples. For example, at 1 cm^3/min for a Pink Desert core the typing factor was 20.85 and the amount of dissolved calcium was 7.53 g, whereas for Indiana limestone cores with a typing factor of 2.58 the amount of dissolved calcium was 6.05 g.

Table 13—COREFLOOD DATA FOR PINK DESERT CORES, 20 WT% GLDA OF pH 1.7 AT 180°F

Exp.#	K_i, md	K_f, md	K_f/K_i	q, cm^3/min	ϕ, fraction	PV_{bt}	Ca, gm	Typing factor
1	120	1000	8.33	0.75	0.20	4.35	8.20	24.50
2	100	1500	15.0	1.00	0.23	4.25	7.53	20.85
3	50	990	19.8	2.00	0.20	3.95	6.65	15.81
4	36	820	23.1	3.00	0.19	3.75	6.23	13.76
5	50	890	17.8	5.00	0.22	5.00	5.74	15.07
6	50	655	13.1	6.00	0.22	5.55	5.23	15.07
7	55	570	10.4	7.50	0.20	6.20	5.10	16.58
8	56	430	7.68	10.0	0.21	8.00	4.85	16.33

Table 14—COREFLOOD DATA FOR INDIANA LIMESTONE CORES, 20 WT% GLDA OF pH 1.7 AT 180°F

Exp.#	K_i, md	K_f, md	K_f/K_i	q, cm^3/min	ϕ, fraction	PV_{bt}	Ca, gm	Typing factor
1	2.00	300	150	0.50	0.14	3.15	6.35	3.78
2	1.80	280	156	0.75	0.15	2.95	6.25	3.46
3	1.00	250	250	1.00	0.15	2.85	6.05	2.58
4	2.00	350	175	2.00	0.14	3.00	5.95	3.78
5	5.50	450	82	3.00	0.13	3.20	5.23	6.50
6	5.20	300	58	5.00	0.15	4.50	5.15	5.89
7	3.70	200	54	7.50	0.10	6.50	4.10	6.08

Comparing GLDA with HCl and Other Chelates

The 0.6M GLDA at pH 3 was compared with other chelates such as 0.6M HEDTA at pH 4 and 0.6M HEDTA at pH 2.5 at 2 cm^3/min and 250°F. The pore volumes required to breakthrough the calcite cores at these conditions were 3.3, 6, and 9.5 PV for the 0.6M GLDA at pH 3, 0.6M HEDTA at pH 4, and 0.6M HEDTA at pH 2.5, respectively. Therefore, the GLDA performance was better than HEDTA. The problem with HEDTA there is its low biodegradability and low thermal stability at low pH values while GLDA is readily biodegradable and thermally stable (LePage et al. 2010).

Fig. 47 shows a comparison between 0.6M GLDA/pH 1.7, 0.6M GLDA/pH 3, 0.6M GLDA/pH 3.8, 0.6M HEDTA/pH 4, 0.6M HEDTA/pH 2.5, 10 wt% long chain carboxylic acid (LCA), and 10 wt% acetic acid at 250°F and 2 cm^3/min. GLDA at pH values 1.7 and 3, and 3.8 outperformed all the other chelants in terms in volume used to create wormholes and breakthrough the core. Another interesting result in this figure, decreasing the pH value for GLDA from 3.8 to 1.7 enhanced the performance of GLDA in creating wormholes with less pore volume. On the other hand, for HEDTA decreasing the pH value from 4 to 2.5 diminished the performance of HEDTA at the same coreflood conditions. For 0.6M HEDTA at pH 4, 7 PV were required to breakthrough the core, whereas at pH 2.5, 11 PV were required to breakthrough the core. This means GLDA performed better at low pH values than HEDTA in the coreflood experiments under the same conditions.
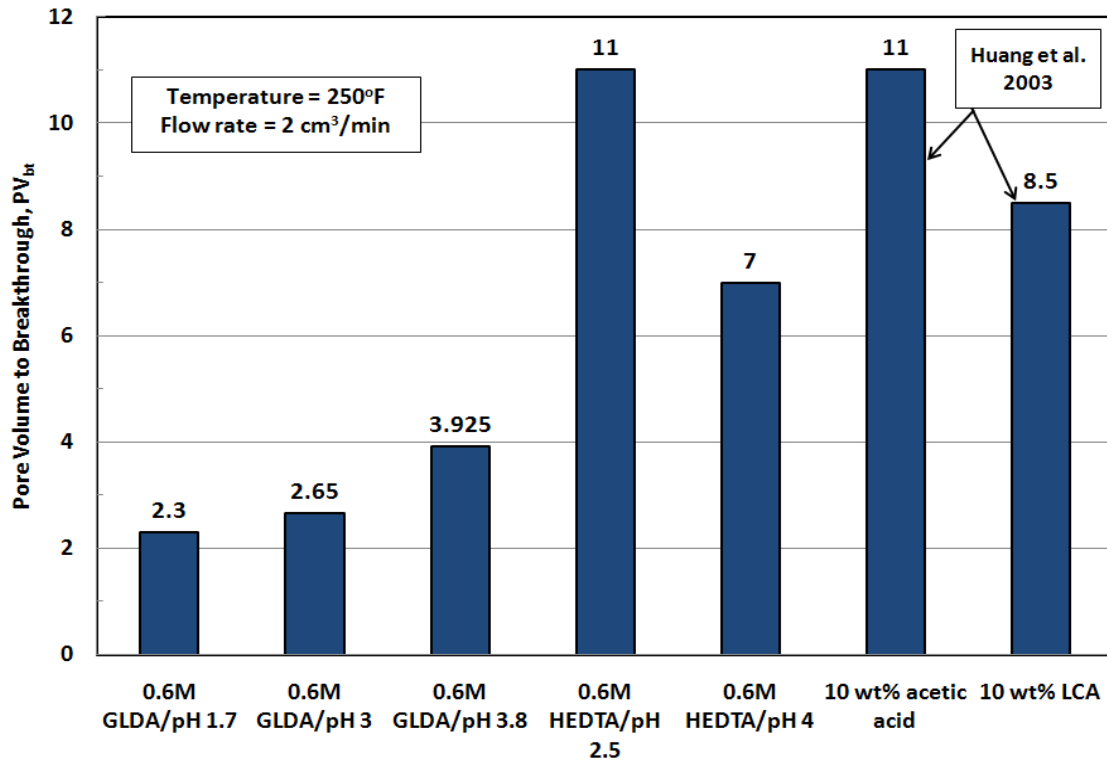
Fig. 47—Comparison between GLDA and other chelating agents used in stimulation.

Fig. 48 shows a comparison between the wormhole for a calcite core treated by 15 wt% HCl and 20 wt% GLDA at pH 1.7. The coreflood experiments were both performed at 2 cm^3/min. The 20 wt% GLDA was tested at 200°F while the 15 wt% HCl was tested at room temperature. There was no face dissolution in the core that was treated by GLDA and the wormhole was constant in diameter along the core length but the washout is clearly shown in the case of 15 wt% HCl even when injected at room temperature. The wormhole diameter decreased as the HCl penetrates through the core in case of 15 wt% HCl and the width of the wormhole decreased to one quarter of its original width. The width of wormhole was almost the same from the core inlet to the core outlet in case of 20 wt% GLDA. The pore volumes required to breakthrough the core were 1.8 and 2.1 in case of 15 wt% HCl at room temperature and 20 wt% GLDA solutions at 200°F, respectively, Fig. 48.
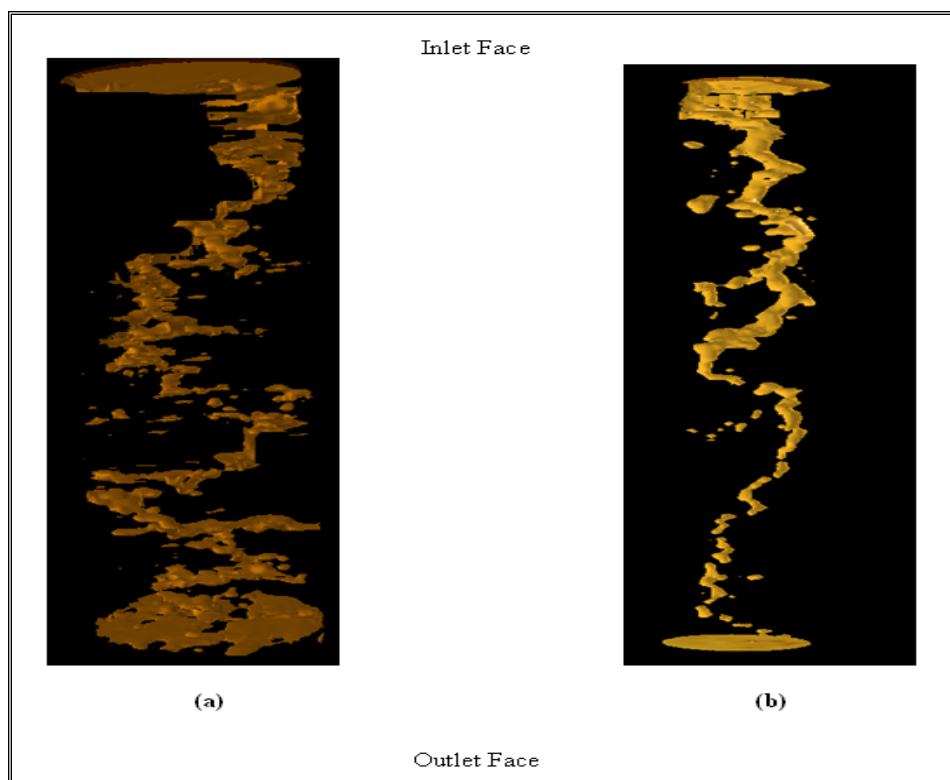
Fig. 48—3D Images for the wormholes formed by (a) 20 wt% GLDA at pH 1.7, 2 cm^3/min and 200°F, and (b) 15 wt% HCl at 2 cm^3/min and 72°F.

Conclusions

In this part, the effectiveness of GLDA solutions to stimulate carbonate cores was tested at various pH levels and temperatures. Tests were conducted on calcite (6 in. and 20 in.) and dolomite (6 in.) cores. GLDA was compared with other commercial chelants like HEDTA, acetic acid, and LCA. The following are the conclusions that were drawn from this study:

1. The 20 wt% GLDA fluids of pH 1.7 and 3 were very effective in dissolving calcite and creating wormholes.

2. The higher the pH the lower the reaction rate with calcite and the more pore volumes required to create wormhole.

3. Unlike HCl, GLDA fluids at pH 1.7 and 3 created dominant wormholes with fewer pore volumes at low rates without face dissolution or washout. This was noted up to 300°F. Therefore, low pump rate can be used without the fear of face dissolution.

4. High temperatures increased the reaction rate of GLDA with calcite and decreased the number of pore volumes to create wormholes.

5. GLDA was effective in creating wormholes in short (6 in.) and long (20 in.) calcium carbonate cores.

6. Initial core permeability was found to have a strong effect on the reaction of GLDA with calcite. The higher the permeability, the higher the volume of GLDA required to create wormholes.

7. Comparing GLDA to other chelates, GLDA was the most effective at low pH values (1.7, 3, and 3.8) under the same coreflood conditions.

CHAPTER IV

OPTIMUM INJECTION RATE OF A NEW CHELATE THAT CAN BE USED TO STIMULATE CARBONATE RESERVOIRS

Introduction

Different chelating agents were used as alternatives for HCl in matrix acidizing to create wormholes in carbonate formations. Previous studies demonstrated the use of ethylenediaminetetraacetic acid (EDTA), hydroxy ethylenediaminetriaacetic (HEDTA) and glutamic acid-N,N- diacetic acid (GLDA) as stand-alone stimulation fluids to stimulate carbonate reservoirs. The main problem of using EDTA and HEDTA is their low biodegradability.

GLDA was introduced as a stand-alone stimulation fluid for deep carbonate reservoirs where HCl can cause corrosion and face dissolution problems. In this study, calcite cores, 1.5 in. diameter with 6 or 20 in. length were used to determine the optimum conditions where the GLDA can breakthrough the core and form wormholes. GLDA solutions of pH values of 1.7, 3, and 3.8 were used. The optimum conditions of injection rate and pH were determined using coreflood experiments. Damköhler number was determined using the wormhole length and diameter from the CT scan 3D and 2D images. GLDA also was used to stimulate parallel cores with different permeability ratios (up to 6.25). The effect of adding 5 wt% sodium chloride on the GLDA performance in the coreflood experiments was investigated.

GLDA was found to be very effective in creating wormholes at pH = 1.7, 3, and 3.8, different injection rates, and temperatures up to 300°F. Increasing the temperature increased the reaction rate and less volume of GLDA was required to breakthrough the core and form wormholes. Unlike HCl, there was no face dissolution or washout in the cores even at low injection rates (0.5 cm^3/min). An optimum injection rate and Damköhler number were found at which the pore volume required to create wormholes was the minimal. GLDA at pH 1.7 and 3 created wormholes with a small number of pore volumes (at 1 cm^3/min GLDA at pH 1.7 required 1.5 PV at 300°F, and at pH 3 it required 1.8 PV). Compared to acetic acid and long chain carboxylic acid, the volume of GLDA at pH 3 required to create wormholes was less than that required in the case of acetic acid, and long chain carboxylic acid at the same conditions. GLDA was found to be effective in stimulating parallel cores up to 6.25 permeability contrast (final permeability/initial permeability). Adding sodium chloride to GLDA stabilized the solution at 300°F and performed better in the coreflood experiments.

The objectives of this part are to: (1) determine the optimum injection rate for the GLDA at different pH values, (2) determine the rate of dissolution of GLDA with calcite using rotating disk, (3) determine the effect of temperature on the optimum injection rate, (4) assess the ability of GLDA to stimulate parallel cores without adding diverting agents at different permeability ratios (1.45, 1.8, and 6.25), and (5) study the effect of adding sodium chloride on GLDA performance during the coreflood experiments.

Experimental Studies

Materials

Indiana limestone with permeability of 0.5 to 5 md and Desert Pink limestone with an average permeability of 100 md were used in all experiments. The core samples were cut in cylindrical shape with dimensions of 1.5 in. diameter and 6, 20 in. length.

GLDA solutions of different pH (1.7, 3, and 3.8) were prepared from original solutions that were obtained from AkzoNobel. De-ionized water (TDS < 20 ppm) was used to prepare the 20 wt% GLDA solutions. The 20 wt% GLDA was prepared from stock solution of 40 wt%.

Parallel Coreflood Experiments

The setup shown in **Fig. 7** was used to conduct the parallel coreflood experiments. Two new cores were used in each experiment, the core permeability was measured using de-ionized water. Permeability ratios (high permeability core/low permeability core) of 1.45, 1.8, and 6.25 were used in the coreflood experiments. The experiments were run at different injection rates and 200°F. GLDA solutions with concentration of 20 wt% and pH 3.8 were used in these experiments. The collected samples from the coreflood effluent were analyzed for injection rate by dividing the collected volume from the effluent for each core by time. The total calcium concentration was measured using the atomic absorption (AAnalyst 700). The injection of GLDA solutions continued until the wormholes breakthrough the two cores.

Damköhler Number Calculations

Damköhler number can be determined using **Eq. 31** (Fredd and Fogler 1999):

$$N_{Da} = \frac{\pi d_{wh} L_{wh} \kappa}{q} \quad \text{..} \quad (31)$$

where; d_{wh} is the diameter of wormhole, cm, L_{wh} is the length of wormhole, cm, q is the flow rate, cm^3/s, κ, is the overall dissolution rate constant, cm/s.

The overall dissolution rate constant, κ can be determined using **Eq. 32** (Fredd and Fogler 1999):

$$\kappa = \frac{1+\frac{1}{\nu K_{eq}}}{\frac{1}{k_{cR}}+\frac{1}{\nu K_S}+\frac{1}{\nu K_{eq}k_{cP}}} \quad\text{.. (32)}$$

where; k_{cR} and k_{cP} are the mass-transfer coefficients for reactants and products, respectively, k_s is the surface reaction rate constant, ν is the stoicheomteric ratio of products to reactants, and K_{eq} is the reaction-equilibrium constant.

The mass transfer coefficients for reactants and products can be determined from Levich's solution for laminar flow in a tube as follows (Levich 1962):

$$k_{c,i} = \frac{1.86 D_{e,i}^{2/3}}{d_{wh}}\left(\frac{4q}{\pi L_{wh}}\right)^{1/3}, i = R, P \quad\text{.. (33)}$$

where; $D_{e,i}$ is the effective diffusion coefficient for reactants and products.

The diffusion coefficient for the GLDA will be assumed the same as EDTA, which is 6 x 10^{-6} cm^2/s. also we will assume the diffusion coefficient for the reactants is the same for products. The surface reaction rate constant, k_s, will be assumed the same as the EDTA (pH = 4) which is 1.4 x 10^{-4} cm/s. The reaction equilibrium constant was assumed the same as that of EDTA (pH = 4) which is 1 x 10^{10}. The length and diameter of the wormholes can be determined from the CT scan 3D images. To justify the use of the constants of EDTA for GLDA we did a dissolution test in a small slurry reactor using 30 mesh crushed calcite with 0.25M EDTA (pH 4) and 0.6M GLDA (pH 1.7). In the first 30 min of the test we got a calcium concentration of 25,000 ppm total calcium at 180°F for both EDTA and GLDA. Therefore it is reliable to consider the reaction rate of GLDA at pH 1.7 is close to that of EDTA at pH 4.

The optimum injection rate can be scaled to the field injection rate using the following equation (Mostofizadeh and Economides 1994):

$$q_w = 7.55 \; x \; 10^{-5} q_{core}\frac{r_w h_f}{r_{core}L_{core}} \quad\text{.. (34)}$$

where; q_w is the injection rate required in the field, bbl/min, r_w is the well radius, in. h_f is the formation thickness, ft, q_{core} is the optimum injection rate from the coreflood test, cm^3/min, r_{core} is the core radius, in., L_{core} is the core length, in.

The injection rate required in the field to stimulate certain formations based on radial coreflood experiments can be determined as follows (Frick et al. 1994):

$$q_{radial} = q_{linear} \frac{2 r_w L_{radial}}{R_{linear}^2} \dots\dots\dots\dots\dots\dots\dots\dots\dots\dots\dots\dots\dots\dots\dots\dots\dots\dots \quad (35)$$

where; q_{radial} is the injection rate in a radial core, q_{linear} is the injection rate in a linear coreflood, r_w is the well radius, L_{radial} is the length of radial core, and R_{linear} is the radius of linear core.

Results and Discussion

Optimum Injection Rate for Different pH Values (6-in. Cores)

The optimum injection rate for different stimulation fluids has been determined by many investigators. The importance of identifying the optimum injection rate is to achieve the maximum penetration of the stimulation fluid through the treated zone. The volume of the stimulation fluid required to create deep, uniform wormholes is minimum at the optimum injection rate, therefore, it is necessary to determine the optimum injection rate for the new stimulation fluid (GLDA).

GLDA exhibited an optimum injection rate at different pH values. **Fig. 49** shows the optimum injection rate for 20 wt% GLDA at pH 1.7 at different temperatures using Indiana limestone cores at 1 cm^3/min. The pore volume at breakthrough (PV$_{bt}$) at the optimum rate was 2.85 PV at 180°F, at injection rates below the optimum, for example at 0.5 cm^3/min, the PV$_{bt}$ was 3.15 PV at the same temperature. At injection rates greater than the optimum, for example at 7.5 cm^3/min, the PV$_{bt}$ was 6.5 PV. A similar trend was obtained for EDTA by Fredd and Fogler (1998a) and Huang et al. (2003). The optimum injection rate of 1 cm^3/min for GLDA at pH 1.7 allows the use of GLDA in low fracture pressure formations where HCl can cause face dissolution. The trend for GLDA was different from that for HCl, at low injection rates HCl caused face dissolution and required higher volumes to create wormholes. GLDA when injected at low injection rates did not require this large pore volume as HCl did. Low injection rates in the case of GLDA allow more time for reaction and dissolved larger amounts of calcite than at high injection rates. The reaction rate of GLDA is slower compared to HCl, therefore, injecting GLDA at low injection rates allowed more time for the reaction and in turn less volume of the fluid was required to create wormholes.

At injection rates below the optimum, the pore volume required to breakthrough the core was higher than that at the optimum. At low injection rates GLDA formed more than one wormhole in the core inlet and in the first one inch of the core, but only one wormhole penetrated through the core. There was one dominating wormhole that penetrated through the core, the other wormholes did not penetrate through the core and they consumed more volumes of GLDA. At the optimum injection rate there was one dominating wormhole, therefore, the pore volume required to create this wormhole was minimum. At injection rates greater than the optimum, the pore volume required to create wormholes was greater than that at the optimum rate. At higher injection rates the increase in the pore volume was greater compared to the increase in pore volume for injection rates below the optimum one. At higher injection rates, there was not enough time for the GLDA to react with the rock and GLDA was able to dissolve just small amounts of the rock. To form a dominant wormhole more volumes of GLDA were required to compensate for the decrease in contact time. From the CT scan images at 4 cm^3/min, the wormhole diameter was smaller compared to that at 2 cm^3/min. The wormhole diameter for cores have an average permeability of 5 md, was 6 mm at 2 cm^3/min and 3 mm at 4 cm^3/min at 250°F.

GLDA has several advantages over HCl in that decreasing the rate below the optimum rate, for example at 0.5 cm^3/min, did not create face dissolution as HCl did, but it consumed 0.3 PV of GLDA more than that at the optimum rate at 180°F. Decreasing the injection rate below the optimum injection rate in the case of HCl increased the pore volume to breakthrough by an order of magnitude (Wang et al. 1993).
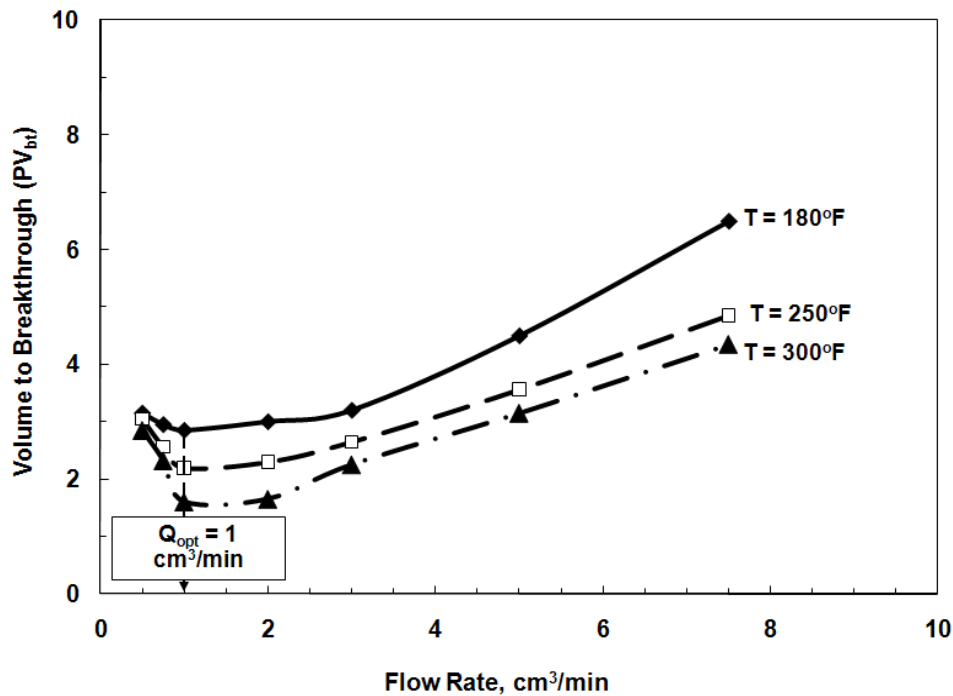
Fig. 49—Pore volume to breakthrough with 20 wt% GLDA solutions at pH 1.7 at various temperatures using Indiana limestone cores.

Fig. 50 shows the optimum injection rate for 20 wt% GLDA solutions at pH 3. The optimum injection rate is not clearly obvious for GLDA at pH 3. A range from 0.5 to 2 cm^3/min existed for the optimum injection rate because the difference in PV_{bt} was small at the three rates 0.5, 1, and 2 cm^3/min. The pore volumes to breakthrough were 3.26, 3.11, and 3.35 PV at 0.5, 1, and 2 cm^3/min, respectively. Although the difference was small in this range, the minimum was 1 cm^3/min, therefore, we can conclude that for the 20 wt% GLDA at pH 3, the optimum injection rate range from 0.5 to 2 cm^3/min. Also, the ratio between the final and initial core permeabilities was maximum at 1 cm^3/min. Decreasing the injection rate below the optimum, 0.5 cm^3/min, did not increase the PV_{bt} significantly as GLDA at pH 3 did because the reaction rate of GLDA at pH 1.7 was faster than that at pH 3 (Mahmoud et al. 2010c).
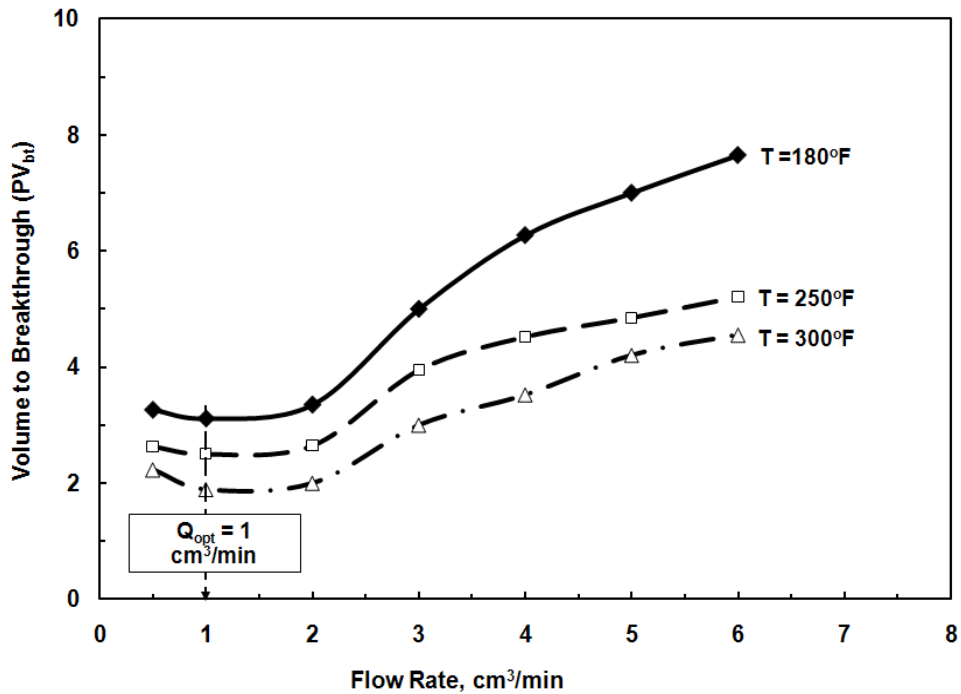
Fig. 50—Pore volumes to breakthrough with 20 wt% GLDA solutions, pH 3 at various temperatures using Indiana limestone cores.

Fig. 51 shows the optimum injection rate for Pink Desert calcite cores using 20 wt% GLDA at pH 1.7 at 180, 250, and 300°F. The optimum injection rate was 3 cm³/min. The optimum injection rate for Pink Desert was greater than that for Indiana limestone cores at the same conditions. The increase in the optimum injection rate for the Pink Desert high permeability cores was attributed to the increase in area-to-volume ratio. Increasing the core permeability increases the pore size and in turn the area of contact between the rock and the fluid will increase. The relationship between the pore diameter and rock permeability can be determined using **Eq. 36** (Permadi and Susilo 2009):

$$d_p = 0.18 \sqrt{\frac{k}{\phi}} \quad \text{..} \quad (36)$$

where; d_p is the average pore diameter, microns, k is the rock permeability, md, and ϕ is the rock porosity, volume fraction.

In turn more GLDA was required to form wormholes at the same conditions. More calcite was dissolved in the high permeability cores; therefore more pore volumes were required to create wormholes. The pore volume to breakthrough in case of Pink Desert cores was higher

than that for Indiana limestone cores at the optimum injection rate. The pore volume to breakthrough at 2 cm^3/min and 300°F for the Pink Desert core was 3 PV and that for the Indiana core at the same conditions was 1.75 PV.
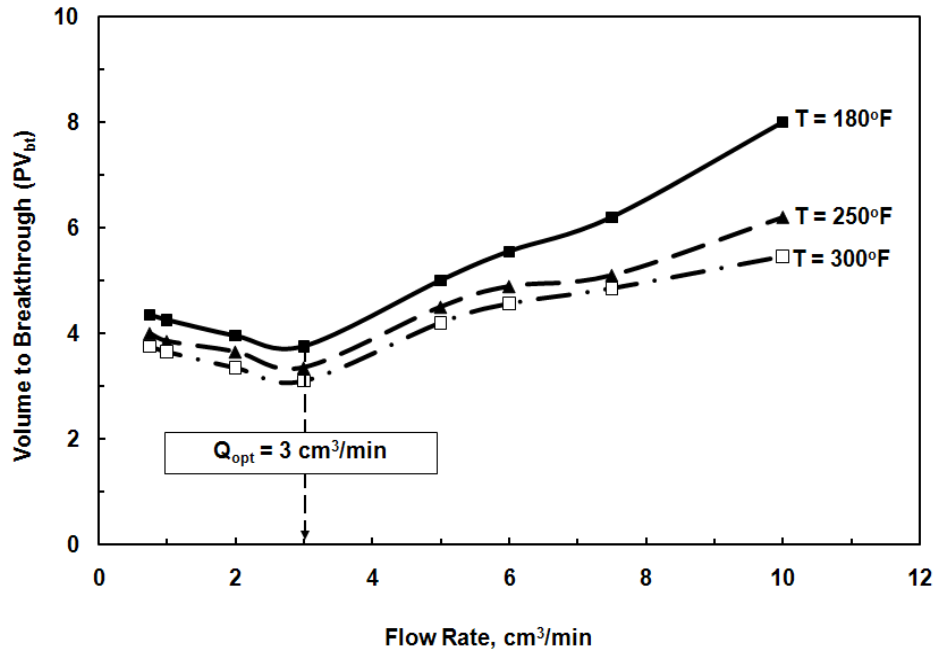
Fig. 51—Pore volumes to breakthrough with 20 wt% GLDA solutions, pH 1.7 at various temperatures using Pink Desert limestone cores.

Effect of Core Length

Investigating the effect of core length on the volume of the fluid required to form wormholes is important, because when we inject the fluid into the formation we need the maximum penetration for this fluid to bypass the damaged zone. In this study, we are the first to study the effect of core length on the propagation of a chelating agent inside the calcite cores.

Fig. 52 shows the volume of GLDA for 6 and 20 in. at different injection rates. Indiana limestone cores treated by 20 wt% GLDA at pH 3 and 250°F. The 20-in. cores gave a trend similar to the 6-in. cores, both cores almost have the same range for the optimum injection rate. The pore volume of the long cores was more than three times that of the short cores, therefore, the contact time for GLDA with calcite was higher in the long cores than in the short cores. At 2 cm^3/min the pore volume of the 6 in. core was 20 cm^3, and the pore volume of the 20 in. core was 70 cm^3. Increasing the contact time in the case of long cores allowed GLDA to dissolve

more calcite than that in short cores. Moreover, the volume of the fluid required to penetrate through the core and form wormholes was less in the case of the 20 in. cores compared to the 6 in. cores. At injection rate of 2 cm³/min the volume of GLDA to breakthrough the core was 1.6 PV in the 20-in. core, and 2.60 PV in the 6-in. core. Therefore, soaking GLDA through the damaged zone will dissolve more calcite and minimize the volume required to bypass the damage. Another factor affecting the volume of GLDA required to breakthrough the 20-in. core was the diffusion coefficient of GLDA.

In the long calcite cores the average calcium concentration in the coreflood effluent was 43,000 ppm after injecting one pore volume of the fluid. The average calcium concentration in the 6-in. cores at the same conditions for the same pH value was 25,000 ppm. The increased calcium concentration in the case of long cores decreased the diffusion of GLDA, and reduced the pore volume required to breakthrough the core.

The relation between the calcium concentration and diffusion coefficient was introduced by Conway et al. (1999). This relation can be given by the following equation:

$$D_{H^+} = exp\left[\frac{2918.54}{T} - 0.589\frac{\overline{Ca^{2+}}}{H^+} - 0.789\frac{\overline{Mg^{2+}}}{H^+} + 0.0452\,H^+ - 4.995\right]$$

.... (37)

Increasing the calcium concentration in the case of long cores increased the viscosity of the GLDA solution and in turn the fluid diffusion decreased. The wormholes formed in the 20-in cores had smaller diameters than those in the 6-in. cores at the same conditions of injection rate, temperature, pH, and initial permeability.
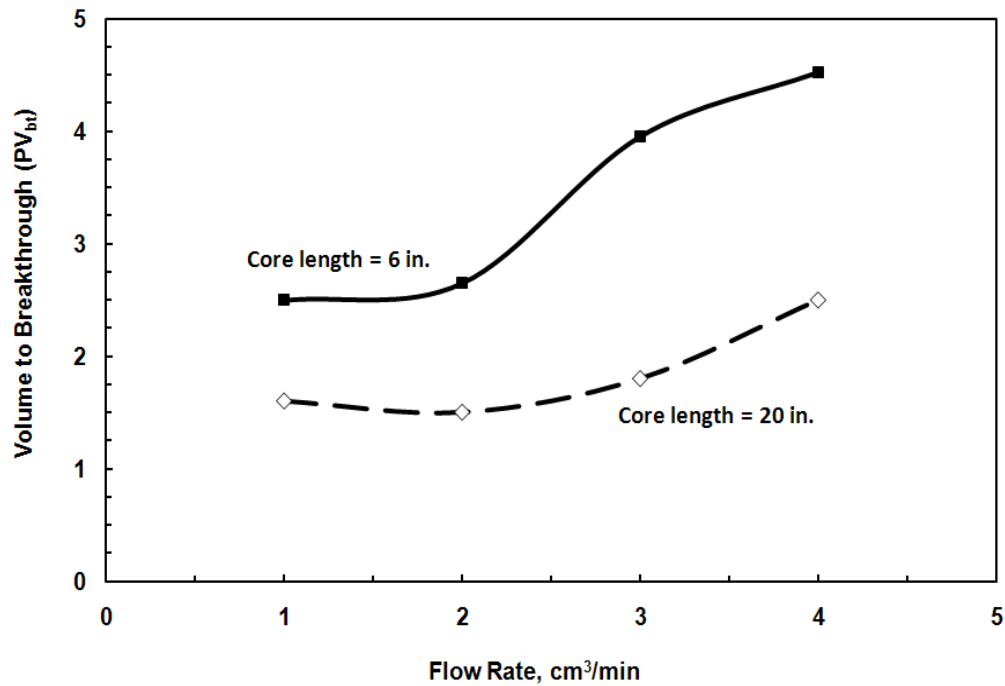
Fig. 52—Volume to breakthrough with 20 wt% GLDA solutions, pH 3 at 250°F for 20 in. and 6 in. length Indiana limestone cores.

These results can be better explained by the core Peclet number, N_{pe}, which can be defined as follows:

$$N_{pe} = \frac{vL_{core}}{D_l}$$ .... (38)

where; v is the frontal advance velocity = $q/(A\phi)$ is the injection rate, cm^3/s, A is the cross sectional area, cm^2, ϕ is the porosity, volume fraction, L_{core} is the core length, cm, and D_l is the longitudinal dispersion coefficient, cm^2/s.

The velocity and the dispersion coefficients are the same for the short and long cores, therefore, the core Peclet number for the long 20-in. core was 3.3 times that of the short 6-in. core. Increasing the core Peclet number will minimize the dispersion and diffusion of the fluid in the porous media (Binder and Vampa 1989), and in turn less volume of the fluid was required to create wormholes. These effects were due to the reduced diffusion rates in the bulk solution, also we can attribute that to the reduced fluid loss from the main wormhole in the case of long cores (Hoefiner and Fogler 1985).

Effect of Temperature on the Optimum Injection Rate

It is important to investigate the effect of temperature on the performance of the stimulation fluid when injected at high temperatures. The injection rate should be adjusted according to the temperature of the formation because for fluids such as HCl and EDTA, the optimum injection rate changed with temperature (Wang et al. 1993 and Fredd and Fogler 1999).Figs. 49 to 51 show the optimum injection rate at different pH values and temperatures. Increasing the temperature from 180 to 300°F did not affect the optimum injection rate (the calcium concentration in the coreflood effluent was increased with temperature) at different pH values. The optimum injection rate remained the same but increasing the temperature increased the reaction rate and reduced the pore volume required to breakthrough the core. Increasing the temperature during stimulation of calcite cores by HCl increased both the optimum injection rate, and the pore volume to breakthrough (Wang et al. 1993). The optimum injection rate for EDTA increased by increasing the temperature from 72 to 175°F, but the pore volume to breakthrough decreased by increasing the temperature (Fredd and Fogler 1999). In the case of GLDA at pH 1.7, increasing the temperature from 180 to 300°F decreased the pore volumes required to form wormholes from 2.85 to 1.6 PV for Indiana limestone cores and the optimum rate did not change from 1 cm^3/min. The same scenario was repeated at pH 3 as shown in Fig. 50. Increasing the temperature at pH 3 enhanced the reaction of GLDA with calcite and decreased the pore volumes required to breakthrough the core. Fig. 51 shows the optimum injection rate at different temperature, the increase in temperature did not change the optimum injection rate for Pink Desert cores, which remained constant at 3 cm^3/min. Increasing the temperature decreased the pore volumes to breakthrough at 3 cm^3/min from 3.75 to 3.1 cm^3/min. Unlike HCl and EDTA, GLDA at different pH values has a fixed optimum injection rate, and this rate was not affected by increasing the temperature from 180 to 300°F.

Calculation of the Damköhler Number

The creation of wormholes in calcite cores using HCl, EDTA, and acetic acid was found to be dependent on the Damköhler number. There was a strong function between the fluid volume required to create wormholes and the Damköhler number (Fredd and Fogler 1999).

The Damköhler number was calculated using **Eq. 31** based on the final wormhole dimensions. The average wormhole diameter was measured from the CT scan. The wormhole diameter was determined for each slice from the 2D image for each core and then the average wormhole diameter was determined by averaging the wormhole diameters in the scanned slices. **Fig. 53** shows the 3D wormhole images for the Pink Desert cores that were treated by 20 wt% GLDA solutions of pH = 1.7 at 180°F. The Damköhler numbers at different injection rates were

calculated using **Eqs. 31-33**. The same was done for long calcite cores (20 in.), the Damköhler number was calculated based on the diameter from the CT 3D images for the 20-in. cores, **Fig. 54**. The optimum Damköhler number for Pink Desert cores was 0.275 at 3 cm^3/min and 0.280 for the 20-in. Indiana limestone cores. At this rate, the pore volumes required to breakthrough the core and create wormhole was the minimum. Using **Eq. 34** to scale this optimum injection rate to the field with a formation thickness of 100 ft and 0.328 ft wellbore radius, the optimum injection rate was 0.5 bbl/min. The optimum injection rate can be predetermined from the optimum Damköhler number by first calculating the optimum injection velocity using **Eq. 39** (Glasbern et al. 2009):

$$U_{opt} = \frac{130 D_e L_{core}}{d_{core}^2} \quad \text{..} \quad (39)$$

where; U_{opt} is the optimum injection velocity, cm/s, D_e is the diffusion coefficient of the product/reactants, cm^2/s, L_{core} is the core sample length, cm, and d_{core} is the core diameter, cm. The optimum injection rate can be determined using **Eq. 40**:

$$Q_{opt} = 47.1 d_{core}^2 U_{opt} \quad \text{..} \quad (40)$$

where; Q_{opt} is the optimum injection rate, cm^3/min.
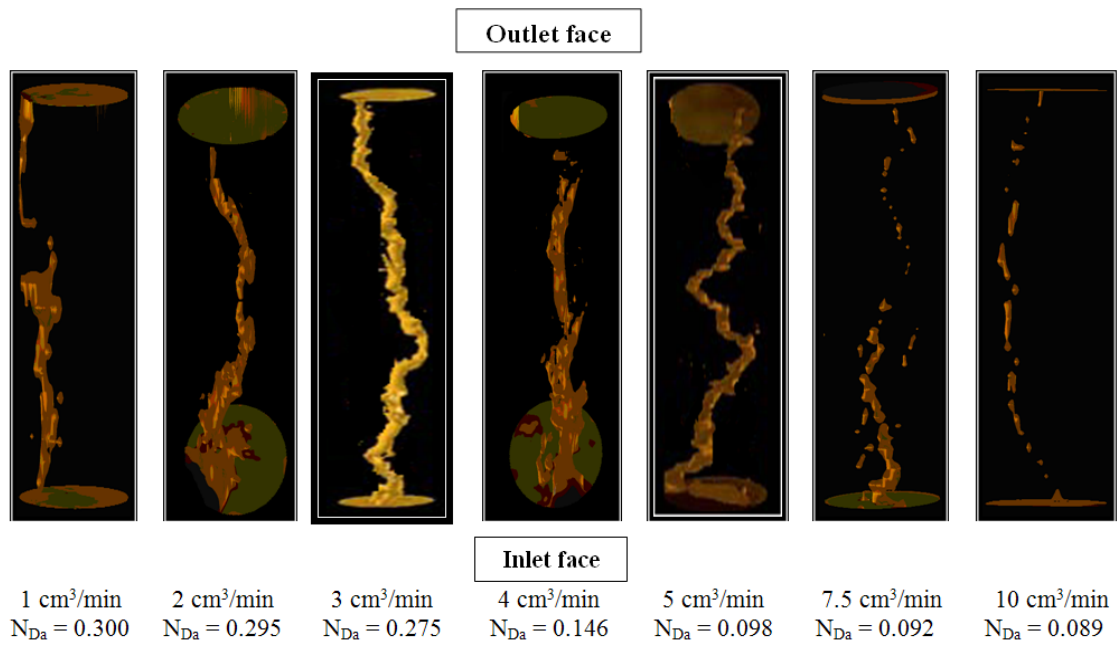
Fig. 53—3D CT scans for 6-in. Pink Desert cores at 180°F using 20 wt% GLDA at pH =1.7.
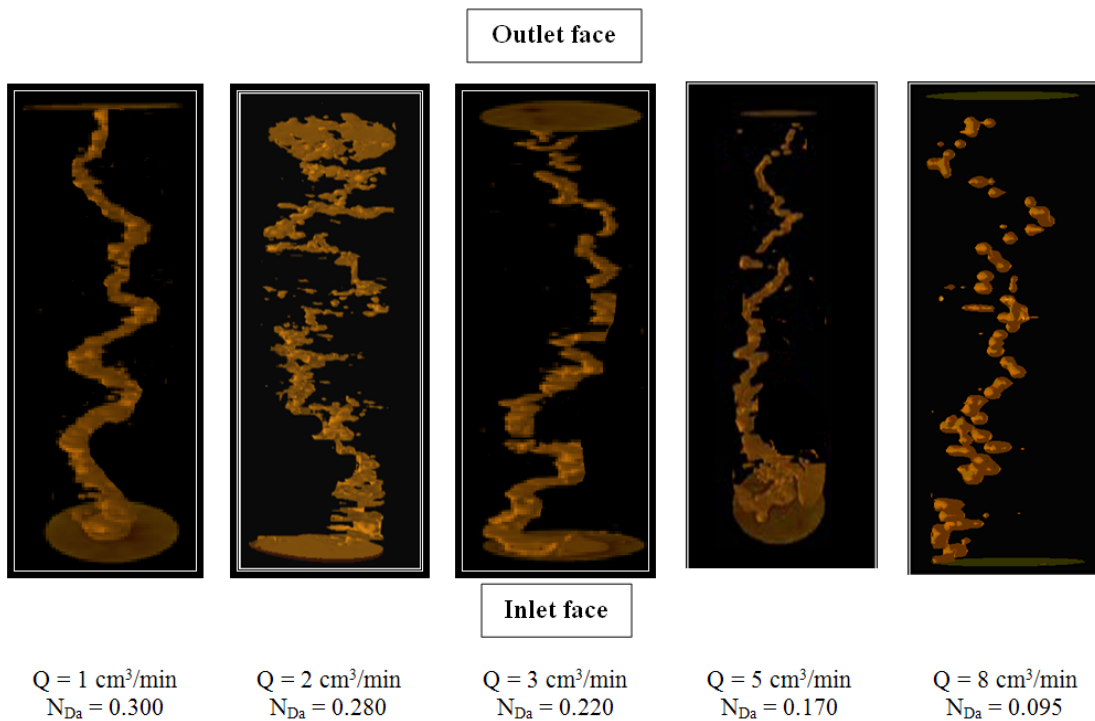
Fig. 54—3D CT scan after the coreflood experiments for 20-in. Indiana limestone cores at 200°F using 20 wt% GLDA at pH =1.7.

Fig. 55 shows the dependence of the wormhole structure on the inverse of Damköhler number. The number of pore volume to breakthrough was plotted versus 1/Damköhler number for 20 wt% GLDA of pH 1.7 at 180°F. There was a similar trend like the injection rate with pore volume in this case, Fig. 51. Increasing the Damköhler number means high dissolution rate and low pore volumes required to breakthrough the core. At low Damköhler numbers the dissolution capacity was lower and the volume required to beakthrough increased. The wormhole structure was more dominant at high Damköhler numbers compared to that at low Damköhler numbers. For the 6 in. core length and 1.5 in. diameter, the optimum injection velocity was 3.8×10^{-3} cm/s and the optimum injection rate was 2.6 cm^3/min. The optimum injection velocity and optimum injection rate were calculated from Eqs. 39 and 40, respectively using an optimum Damköhler number of 0.29.
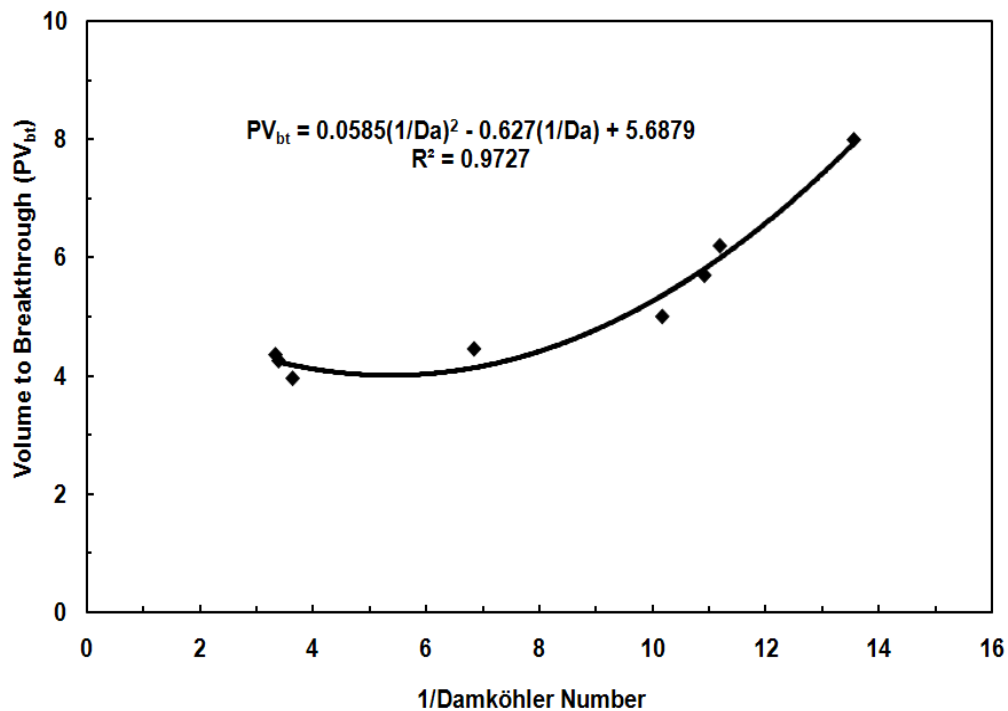
Fig. 55—Dependence of the number of pore volumes to breakthrough on the inverse of Damköhler number for Pink Desert cores, 20 wt% GLDA of pH = 1.7 at 180°F.

Pore Volumes to Breakthrough for Different Stimulation Fluids

Fig. 56 shows a comparison between 20 wt% GLDA at pH 3 and 10 wt% long chain carboxylic acid (LCA), 10 wt% acetic acid (Huang et al. 2003) at 250°F. GLDA outperformed LCA and acetic acid, as the pore volume to breakthrough was lower than those for LCA and acetic acid. Decreasing the injection rate increased the pore volumes required to breakthrough the core in both LCA and acetic acid and did not affect GLDA.
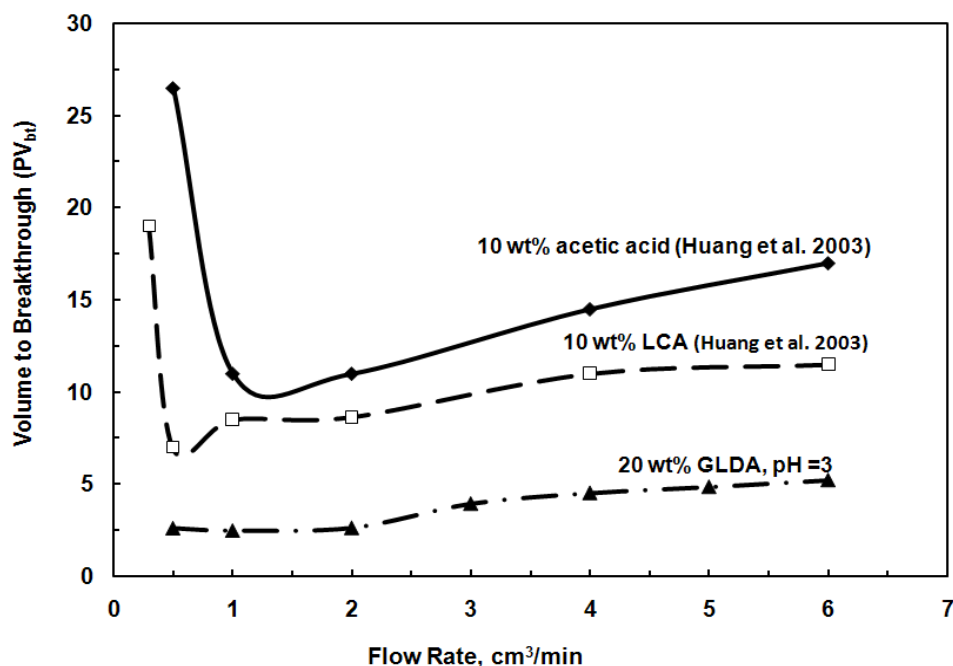
Fig. 56—Pore volume to breakthrough as a function of injection rate at 250°F.

Fig. 57 shows the 2D CT scan images for the 6-in. pink desert calcite cores treated by 15 wt% HCl and 20 wt% GLDA at pH 1.7 at 200°F and a injection rate of 1 cm^3/min. Face dissolution was obvious in case the 15 wt% HCl but there was no face dissolution in the case of 20 wt% GLDA. The core initial permeability was 55 md in case of HCl coreflood and it was 58 md in case of GLDA. The wormhole diameter decreased in case of 15 wt% HCl as the wormhole penetrated through the core. The wormhole in the case of 20 wt% GLDA had had a constant diameter through the entire core length.
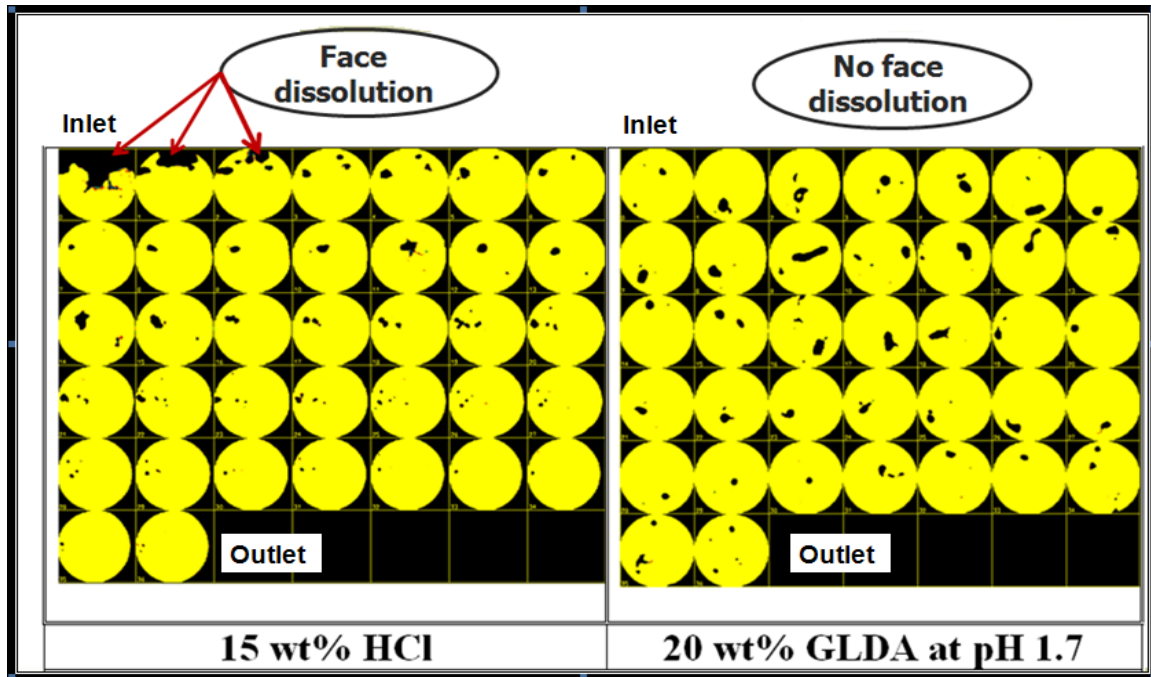
Fig. 57—Difference in wormhole pattern between HCl and GLDA at 1 cm^3/min and 200°F.

Factors Affecting the Wormhole

Fig. 58 shows the effect of temperature on the wormhole size at injection rate of 2 cm^3/min and at pH 3. The permeabilities of the two cores were close in values at 0.45 and 0.5 md. As temperature was increased from 200 to 300°F, the wormhole diameter increased. The wormhole size at 200°F was less than 1.5 mm but it reached more than 5 mm at 300°F. Increasing the temperature by 100°F increased the wormhole size more than three times, indicating the effectiveness of GLDA in creating large wormholes at high temperatures. At 200°F the cross section of wormholes was almost uniform circle; as the temperature was increased to 300°F, the shape of wormholes cross section started to change from circular to irregular shapes and more than one wormhole was formed. At 300°F GLDA reacted with the rock and created many wormholes.

$k_{initial}$ = 0.45 md, q = 2 cm^3/min @ T = 200°F, pH 3 | $k_{initial}$ = 0.5 md, q = 2 cm^3/min @ T = 300°F, pH 3
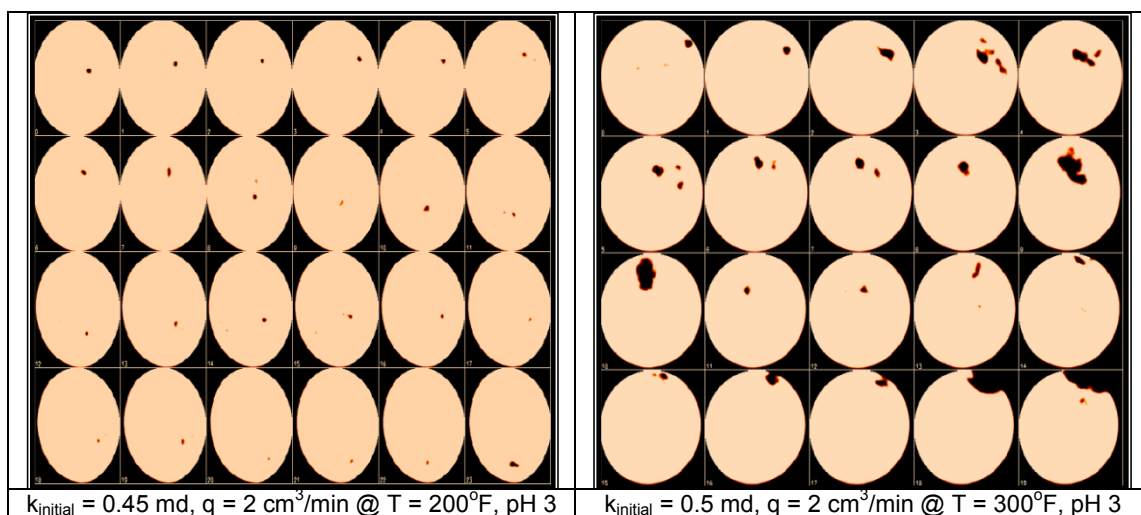
Fig. 58—Effect of temperature on the wormhole size. Large wormholes were created at 300°F because of the higher reaction rate.

Fig. 59 shows the effect of the injection rate on the wormhole size. Fixing other parameters, the effect of injection rate on the wormholes shape and size was studied. At 2 cm^3/min the wormholes formed by 20 wt% GLDA at pH 3 were larger than that at 4 cm^3/min. Increasing the injection rate from 2 to 4 cm^3/min decreased the contact time between GLDA and calcite, which in turn reduced the reaction time. At 2 cm^3/min injection rate, more than one wormhole with irregular shape was formed. At 4 cm^3/min the wormholes started to take regular rounded shapes but smaller sizes than that at 2 cm^3/min.

Fig. 60 shows the effect of initial core permeability on the wormhole size. Two cores with permeabilities of 0.45 and 4.7 md were selected at 2 cm^3/min and 200°F using 20 wt% GLDA at pH 3. The wormhole size of the high permeability core (4.7 md) was larger than that of the low permeability core (0.45 md) at the same conditions. As the core permeability increased, the area-to-volume ratio increased and the surface area exposed to the reaction increased. In turn bigger wormholes were formed at high permeability than at low permeability. Increasing the core permeability also increased the amount of GLDA required to form wormholes at the same conditions. The pore volumes required to form the smaller size wormholes in the low permeability core (0.45 md) at 2 cm^3/min and 200°F were 2.65 PV. The pore volumes to create bigger wormholes in the case of the high permeability core (4.7 md) were 3.35 PV at the same conditions.

$k_{initial}$ = 5 md, q = 2 cm^3/min @ T = 200°F, pH 3 | $k_{initial}$ = 5.2 md, q = 4 cm^3/min @ T = 200°F, pH 3
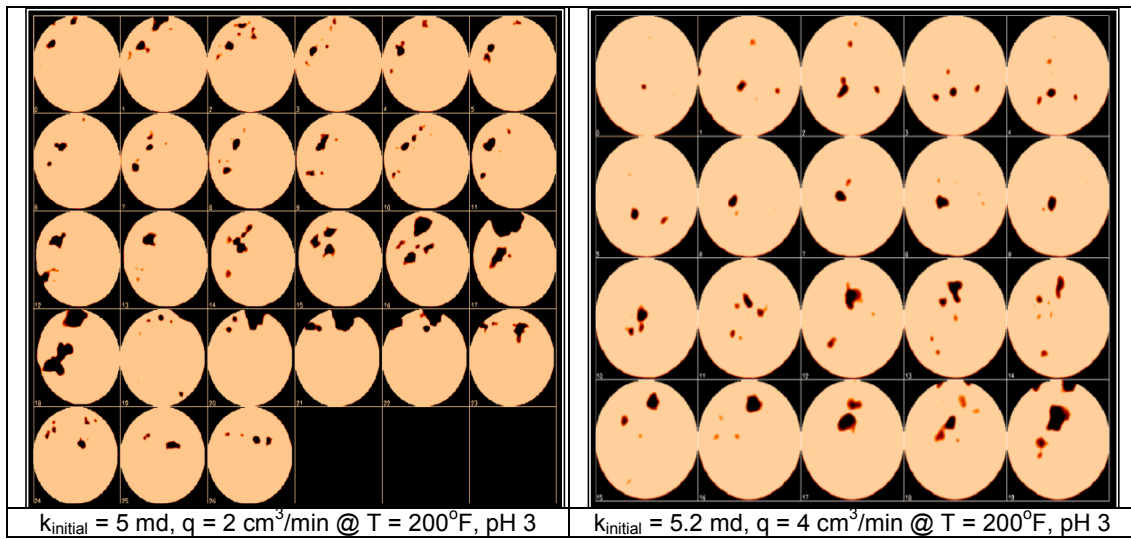
Fig. 59—Effect of injection rate on the wormhole size. At low rate bigger wormholes were created due to the increased contact time allowed more calcite to be dissolved.

$k_{initial}$ = 0.45 md, q = 2 cm^3/min @ T = 200°F, pH 3 | $k_{initial}$ = 4.7 md, q = 2 cm^3/min @ T = 200°F, pH 3
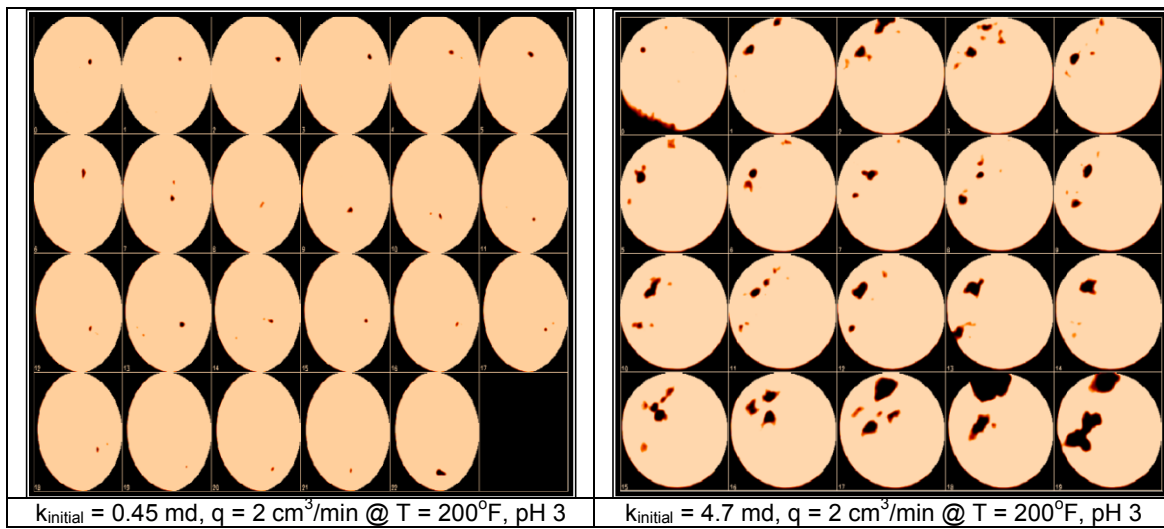
Fig. 60—Effect of initial permeability on the wormhole size. High permeability allowed more time for reaction and created large wormholes.

Fig. 61 shows the effect of GLDA pH on the wormhole size. Mahmoud et al. (2010a) investigated the chemical reaction of GLDA with calcite at different pH values. At low pH (1.7) the reaction of GLDA with calcite was attributed to the hydrogen ion attack and at higher pH (13) the reaction was complexation only. A minor difference between the wormhole sizes in 1.7 and 3 pH values was noticed. At pH of 3 GLDA has 3 hydrogen ions in the carboxylic groups and it has also hydrogen attack. Increasing GLDA pH from 1.7 to 3 did not create noticeable changes in the wormhole shape and size. Extra pore volume of 0.1 PV was required to create the wormhole at pH 3. The pore volumes to breakthrough at 2 cm^3/min and 200°F in case of GLDA at pH 3 was 3.55 PV and was 3.45 PV at pH 1.7 at the same conditions.

| $k_{initial}$ = 0.8 md, q = 2 cm^3/min @ T = 200°F, pH 1.7 | $k_{initial}$ = 0.75 md, q = 2 cm^3/min @ T = 200°F, pH 3 |
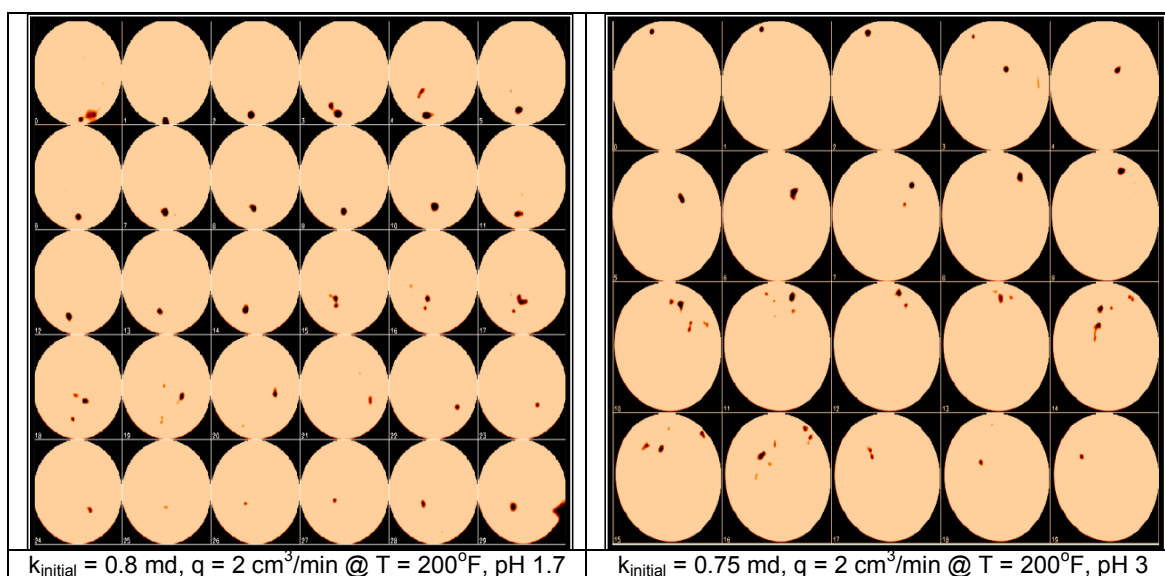
Fig. 61—Effect of 20 wt% GLDA solution initial pH on the wormhole size. There was a small difference in the wormhole size in both cases.

Effect of NaCl on the Performance of GLDA During Coreflood

GLDA solutions with a concentration of 20 wt% at pH 3.8 were used and NaCl concentration of 5 wt% was used. Two coreflood experiments were performed using the prepared solutions at injection rate of 2 cm^3/min and 300°F. **Fig. 62** shows the total calcium concentration for the two coreflood experiments. The wormhole broke through the core at 3 PV and 3.5 PV for 20 wt% GLDA without NaCl and with 5 wt% NaCl respectively. Adding 5 wt% NaCl enhanced the performance of GLDA and saved 0.5 PV. The calcium concentration reached a maximum of 25,000 ppm in case of GLDA with 5 wt% NaCl, and 17,000 ppm in case of GLDA without NaCl.

The presence of sodium chloride enhanced the thermal stability of the GLDA at 300°F (Mahmoud et al. 2010d).
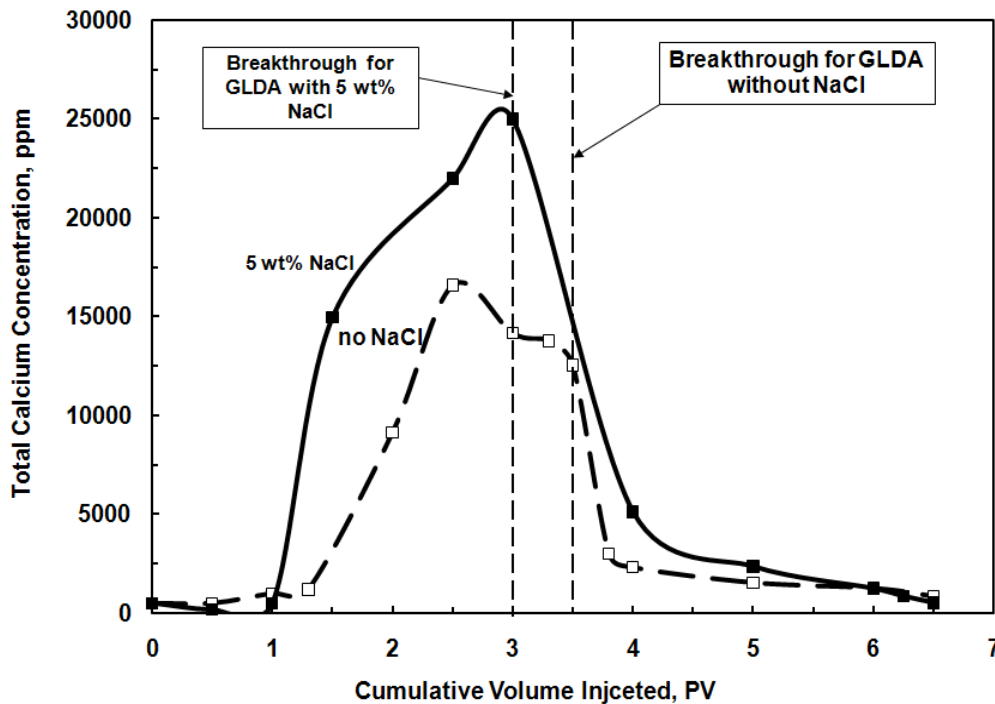
Fig. 62—Effect of NaCl on GLDA (20 wt%, pH =3) performance during coreflood experiments at 2 cm³/min and 300°F.

Fig. 63 shows the effect of adding 5 wt% NaCl on the wormhole shape and size. The coreflood experiments were run using 20 wt% GLDA at pH 3.8 at injection rate of 2 cm³/min, and 300°F. The core initial permeability was 3 md for the GLDA without NaCl, and it was 3.2 md for the GLDA with 5 wt% NaCl. Adding 5 wt% NaCl enhanced the reaction of GLDA with calcite through increasing its thermal stability. The wormhole that was created in the case of adding 5 wt% NaCl had a larger diameter than that created without adding NaCl (NaCl increased the thermal stability of GLDA (Mahmoud et al. 2010d), and at 300°F the reaction rate was high, so the GLDA reacted with the rock more to create irregular shape wormholes). Fredd and Fogler (1998b) investigated the effect of adding sodium chloride to EDTA in the rotating disk experiments. They found that increasing the sodium chloride concentration from 0 to 0.7M (~4.1 wt%), the reaction rate of EDTA with calcite decreased by about 25%. The decrease in the

reaction rate was attributed to the association of Na$^+$ with EDTA and transport of Na-EDTA complexes.

| 20 wt% GLDA, pH = 3.8 | 20 wt% GLDA, pH = 3.8 + 5 wt% NaCl |
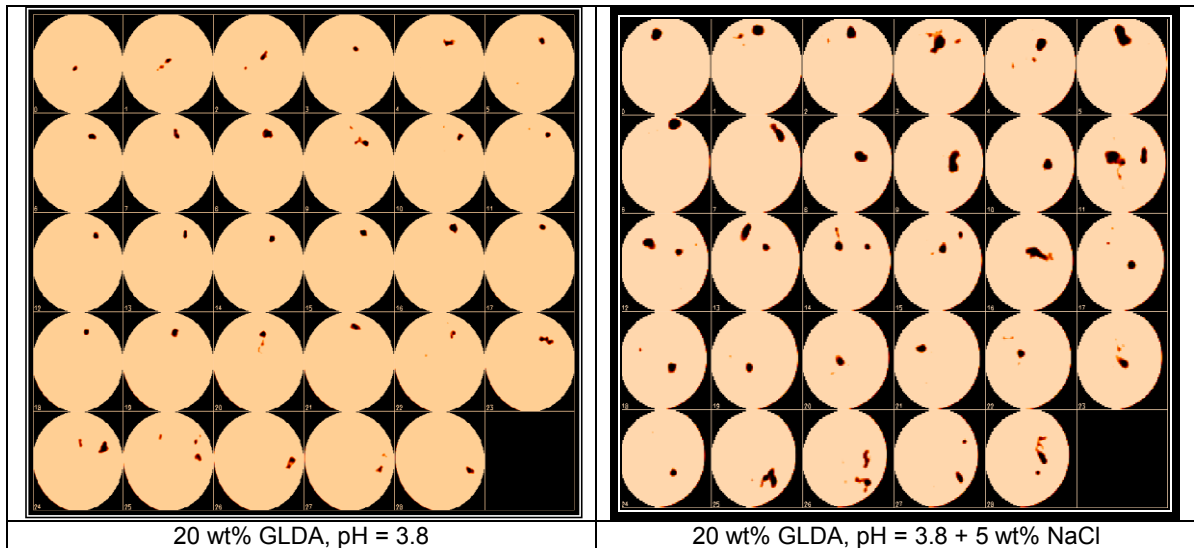
Fig. 63—Effect of NaCl on the wormhole shape and size. Coreflood experiments were run using 20 wt% GLDA at pH 3.8, 2 cm^3/min, and 300°F using 6-in. cores.

Parallel Coreflood

The low-reactive nature of GLDA in addition to the build in its viscosity after complexing calcium can be invested in stimulating parallel cores with low permeability contrast. The viscosity of GLDA increased during the reaction of GLDA with calcite due to the calcium complexation, the viscosity relationship with the calcium concentration of GLDA at pH 3.8 at room temperature can be given by **Eq. 41**:

$$\mu = 0.0001 \ Ca \ + 3.4 \ \dots\dots\dots\dots\dots\dots\dots\dots\dots\dots\dots\dots\dots\dots\dots \ (41)$$

where; [Ca] is the calcium concentration, ppm, and μ is the viscosity of GLDA solution, cP.

We got equation 41 by measuring the viscosity of GLDA at pH 3.8 at different calcium concentrations starting from 0 up to 60,000 ppm and the relationship was linear. The first experiment was performed at 3 cm^3/min and 200°F. **Fig. 64** shows the distribution of the injection rate for the two cores during the coreflood experiment. Before switching to 20 wt% GLDA the injection rate ratio between the high permeability and low permeability core was near

the permeability ratio which was 1.45. The distribution of the injection rate before switching to GLDA can be determined analytically using **Eq. 42**:

$$\frac{Q_1}{Q_2} = \frac{\frac{\Delta p_1 k_1 A_1}{\mu_1 L_1}}{\frac{\Delta p_2 k_2 A_2}{\mu_2 L_2}} = \frac{k_1}{k_2} \quad \text{...} \quad (42)$$
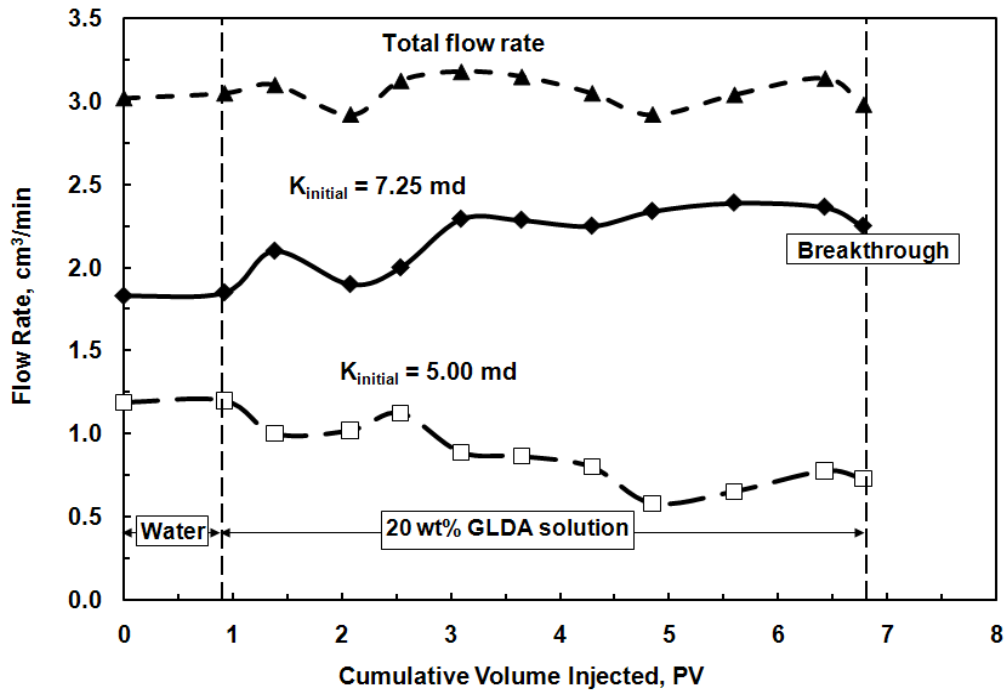
Fig. 64—Distribution of the total injection rate (3 cm^3/min) into cores 1 and 2; 20 wt% GLDA at pH 3.8; and 200°F.

The total injection rate while injecting water through the core should be the summation of the injection rates from the two cores; $Q_T = Q_1 + Q_2$. Before switching to GLDA, the total injection rate coming out from the two cores was almost 3 cm^3/min, the same as the total injection rate, and the ratio was almost the same as the permeability ratio. After switching to GLDA, the ratio was not the same like injecting water. Due to the build in viscosity as the reaction proceeded with the high permeability core, the fluid diverted itself to the lower permeability one. The increase in viscosity forced the GLDA to injection in both the high permeability and low permeability cores at the same time. In this experiment the wormhole broke through the two cores at the same time. The injection came from the two cores until the breakthrough of the

wormhole, then the injection rate in the high permeability core increased and decreased because of the increase in viscosity after the reaction with calcite.

Fig. 65 shows the total calcium concentration in the effluent samples from the two cores. The GLDA broke through the two cores at the same time after the injection of one pore volume. The calcium concentration reached a maximum of 32,500 ppm in the two cores, indicating equal reaction rate in both cores. The calcium concentration remained constant in the effluent of the two cores until the wormhole breakthrough.
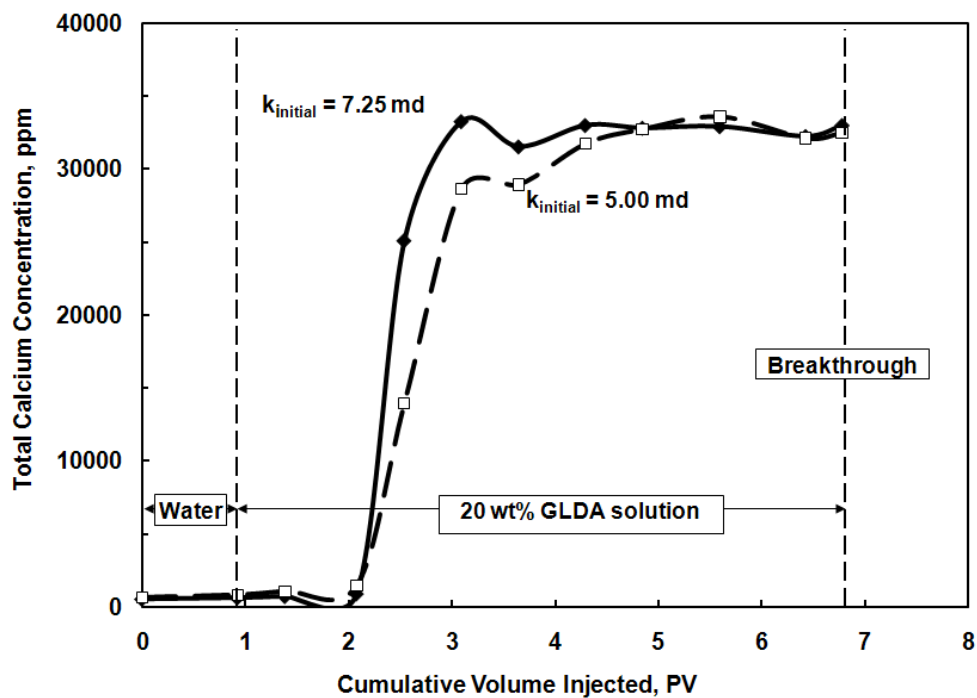
Fig. 65—Total calcium concentration in the effluent of cores 1 and 2; 20 wt% GLDA at pH 3.8; 3 cm^3/min and 200°F.

Fig. 66 shows the injection rate distribution for 1.8 permeability ratio cores at 2 cm^3/min and 200°F. The same scenario repeated here, although the permeability ratio was higher than the first experiment, there was a flow coming from the two cores. The injection distribution in the effluent from the two cores indicated a good ability of GLDA to stimulate different permeability contrasts. The injection rate in the low permeability core increased from the average value of 0.7 cm^3/min to an average value of 0.85 cm^3/min after injecting GLDA through the two cores. This meant that GLDA at pH 3.8 was able to divert the injection from the high permeability core to the low permeability one without adding diverting agents. No cross-linker or breaker was required as

in the case of polymer-based acids, or mutual solvent as in the case of surfactant-based acids. GLDA was able to divert the injection in the low permeability core in a 1.8 permeability ratio injection, where polymer-based acid can cause damage and filter out on the face of these cores.
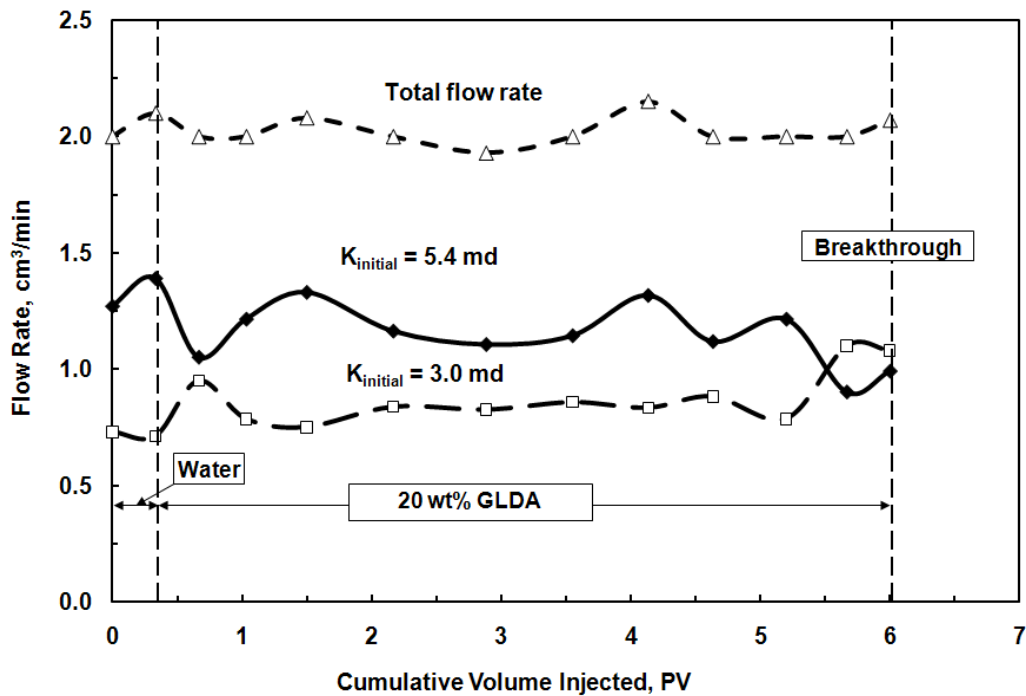
Fig. 66—Distribution of injection rate in cores 1 and 2; 20 wt% GLDA at pH 3.8; 2 cm³/min and 200°F.

Fig. 67 shows the calcium concentration in the effluent samples for the two cores reaching similar results to the first experiment. The injection rate and temperature were the same and the only difference in this case is that the permeability ratio increased from 1.45 to 1.8. GLDA broke through the two cores at the same time and the calcium concentration stabilized at a maximum value of 32,500 ppm for the two core effluent samples.
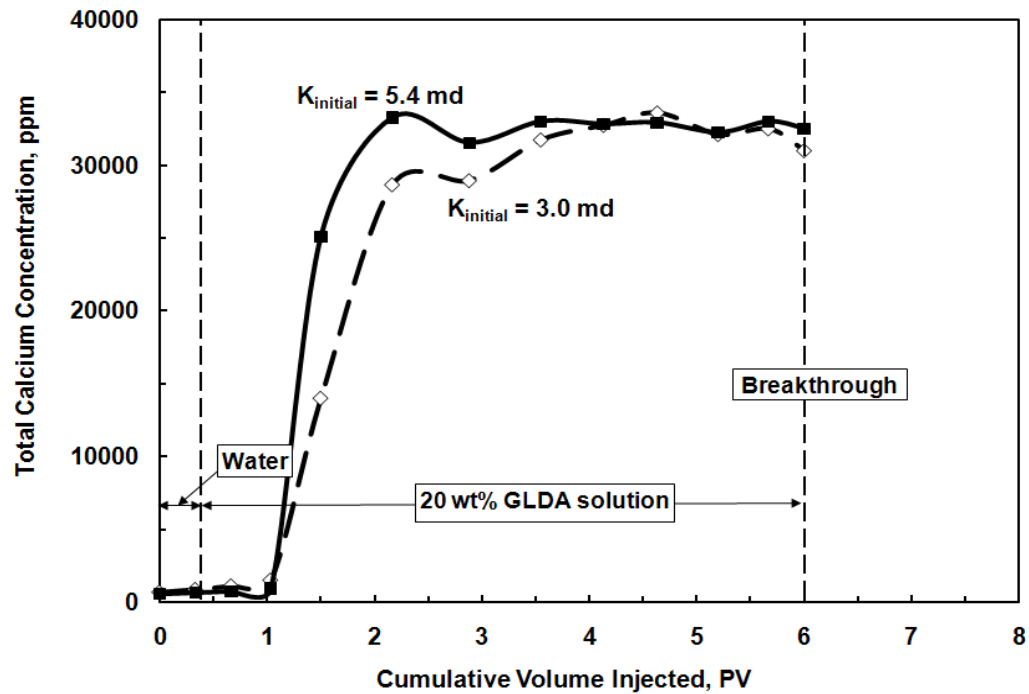
Fig. 67—Distribution of total calcium concentration in each core; 20 wt% GLDA at pH 3.8; 2 cm^3/min and 200°F.

Fig. 68 shows the 3D CT scan images for the wormholes created during the parallel coreflood experiment at 2 cm^3/min and 200°F. The permeability ratio between the two cores was 1.8. The wormholes propagated 100% of the total core length in both cores and the breakthrough occurred in both cores in the same time. The 3D CT scan images showed the effectiveness of GLDA in stimulation two cores with different permeabilities without using chemical diverters.
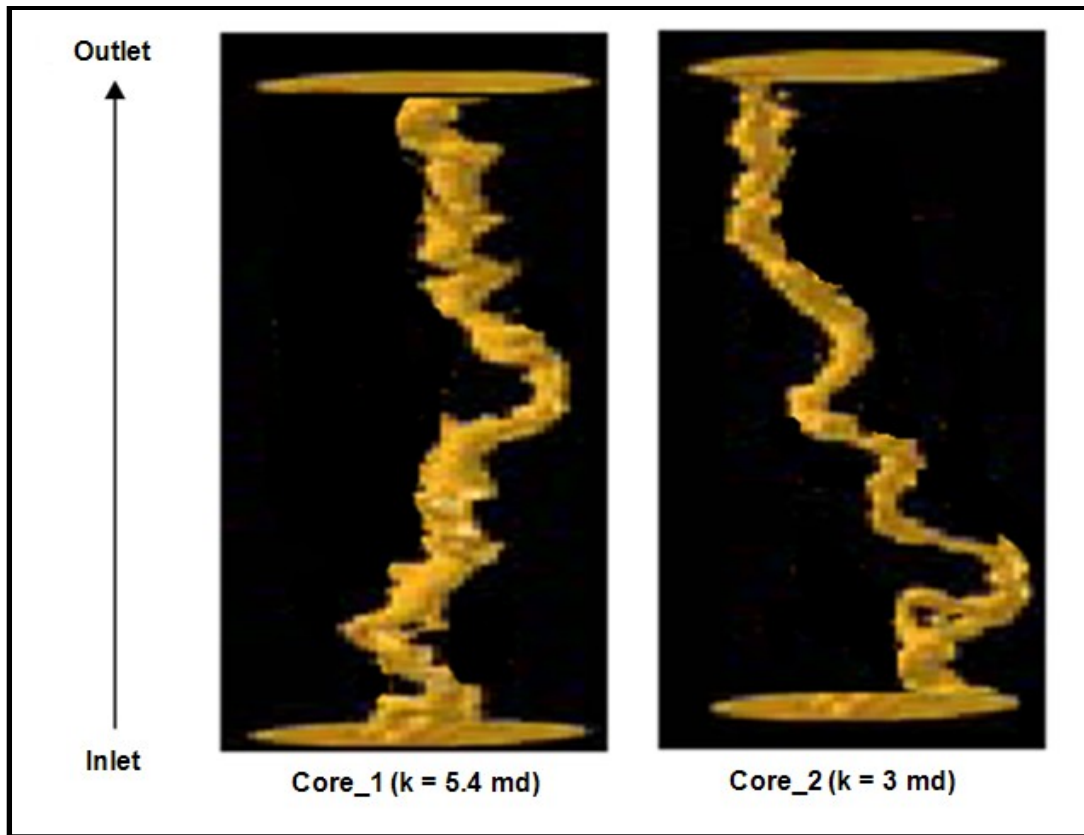
Fig. 68—3D images for the wormholes created in each core during the parallel coreflood experiment.

Two more coreflood experiment were performed using two sets of cores, the first set one of permeability of 50 md and the other one had a permeability of 8 md (permeability ratio = 6.25). The second set of cores had cores with permeabilities 50 and 15 md (permeability ratio = 3.33). GLDA at pH of 3.8 and 20 wt% was used to stimulate both cores in the parallel coreflood at 200°F. GLDA broke through the two cores at the same time proportionally according to the ratio between core permeabilities. The amount of calcite dissolved in the core in 50 md permeability was 10.8 g, and it was 3.1 g in the 8 md permeability core. AT permeability contrast of 6.25 (50 and 8 md) GLDA showed good results in both cores and wormholes formed in the two cores. The permeability of the 50 md core increased to 850 md, and the permeability of the 8 md increased to 365 md after the coreflood experiment at injection rate of 2 cm^3/min as shown in **Table 15**. The 20 wt% GLDA at pH 3.8 also formed wormholes in the cores that had 3.33 permeability contrast (50 and 15 md) in the same time, but the wormhole diameter for the 50 md core was greater than that for the 15 md core, **Fig. 69**.

Table 15—SUMMARY OF PARALLEL COREFLOOD EXPERIMENTS					
Exp. #	Permeability contrast	$K_{initial}$, Core #1	$K_{initial}$, Core #2	K_{final} , Core #1	K_{final} , Core #2
1	6.25	50.0	8.0	850	365
2	3.33	50.0	15.0	910	425
3	1.80	5.40	3.0	1300	1150
4	1.45	7.25	5.0	1100	760
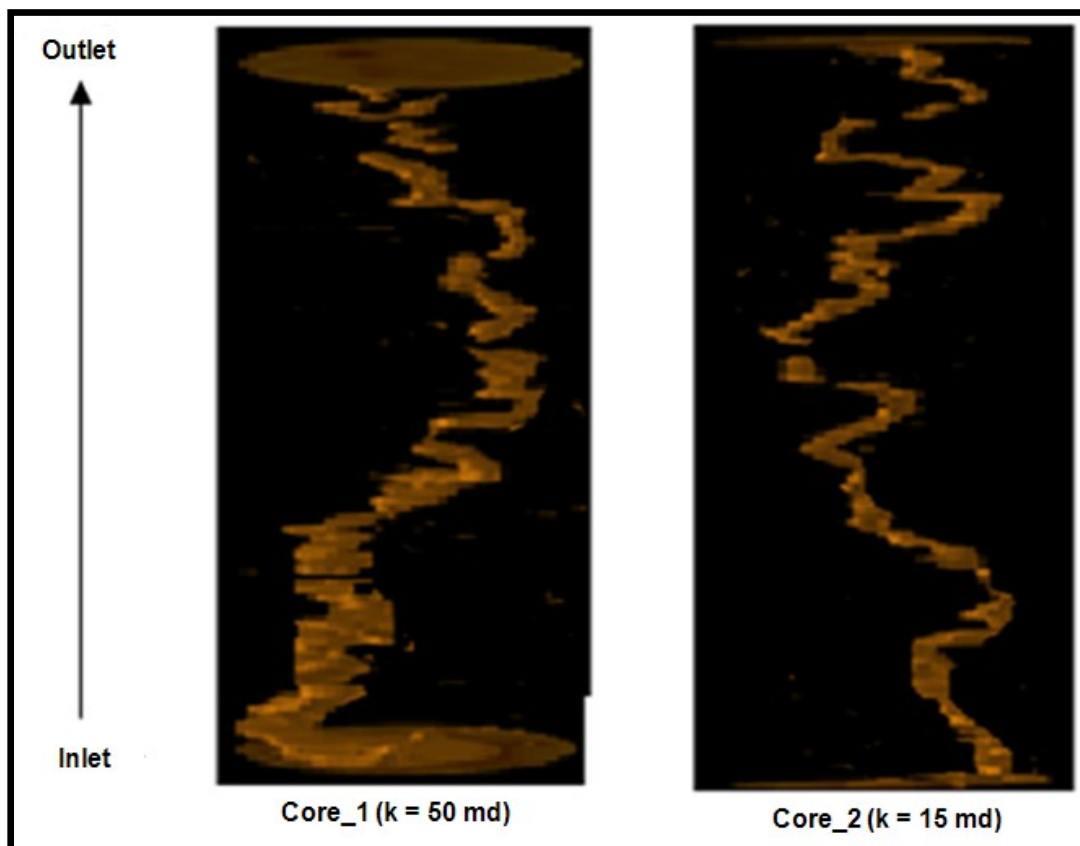
Fig. 69—3D images for the wormholes created in each core during the parallel coreflood experiment.

Conclusions

Coreflood tests were conducted using calcite cores, GLDA solutions of pH values 1.7, 3, and 3.8. Cores of 6 and 20 in. length were used based on the results obtained, the following conclusions can be drawn:

1. There was an optimum rate for the GLDA to create wormholes at different pH values.
2. The optimum injection rate was not affected by increasing temperature from 180 to 300°F.
3. Increasing the core length from 6 to 20 in. decreased the volume of GLDA required to create wormholes due to the increased Peclet number.
4. There was a relationship between the creation of wormholes in calcite cores using GLDA and the inverse of Damköhler number.
5. GLDA was able to stimulate parallel calcite cores at low permeability contrast (up to 6.25).
6. GLDA at pH 3 outperformed 10 wt% acetic acid and long chain carboxylic acid at high temperatures.
7. Adding 5 wt% NaCl to GLDA enhanced the performance of GLDA of pH 3.8 during the coreflood experiments. Less volume of GLDA was required in case of adding 5 wt% NaCl.

CHAPTER V

EFFECT OF RESERVOIR FLUID TYPE ON THE STIMULATION OF CALCITE CORES USING CHELATING AGENTS

Introduction

Different fluids have been introduced in the oil industry to be used as alternatives to HCl. Chelating agents such as EDTA (ethylene diamine tetraacetic acid), HEDTA (hydroxyl ethylene diamine triacetic acid), and GLDA (glutamicacid-N,N-diacetic acid) have been introduced to be used as stand-alone stimulation fluids. These fluids can be used to stimulate water injectors, oil, or gas producers, therefore, the effect of the type of reservoir fluid on the stimulation process should be investigated.

In this part of the study, 0.6M of GLDA, EDTA, and HEDTA were used in the coreflood experiments on carbonate rocks at 300°F. The cores were saturated with water, oil, or gas to determine the effect of reservoir fluid type on the performance of the chelating agents with the carbonate cores. The effect of using 10 vol% mutual solvent (ethylene-glycol-monobutyl-ether) in the preflush on the stimulation process was examined. An analytical model for the reaction of GLDA with calcite was developed to predict the propagation of GLDA in carbonate cores.

The results showed that GLDA performed better in the oil-saturated cores due to the reduced diffusion. GLDA at pH of 4 stimulated calcite cores better than HEDTA at 300°F and at different injection rates. The results obtained with carbonate cores saturated with nitrogen gas were almost similar to those obtained when the cores were saturated with water. The analytical model results showed good match with the experimental results, therefore, this model can be used to predict the performance of the chelating agent in carbonate stimulation. This model can be used to predict the volume of the fluid required to create wormholes in the reservoir with certain length and diameter. The volume of the fluid from the model and experimental results showed a good match. The pressure performance during the treatment also can be predicted using the developed model.

The objectives of the current study are to: (1) study the wormholing and dissolving capacity of the 20 wt% GLDA at pH 1.7, (2) investigate the effect of saturating the cores with actual crude oil on the creation of wormholes, (3) compare the optimum injection rate of HEDTA and GLDA at 300°F using Indiana limestone cores, (4) determine the best chelating agent that can be used to stimulate oil-saturated cores, and (5) identify the effect of flushing the oil-saturated cores by 10 vol% mutual solvent on the stimulation of carbonate cores by chelating agents.

Experimental Studies

Materials

The chelating agents that were used in this study were GLDA, HEDTA, and EDTA of concentration 0.6M prepared from an initial stock concentration of 40 wt%. Calcium carbonate cores such as Pink Desert limestone, Austin Chalk, and Indiana limestone cores of 6 in. length and 1.5 in. diameter were used in the coreflood experiments. The crude oil used in this study has a composition that showed in **Table 16**. The API and specific gravities of the used oil were 27.5 and 0.89. The mutual solvent used in this study was ethylene glycol mono butyl ether of 10 vol% concentration.

Table 16—COMPOSITION OF CRUDE OIL	
Component	**Volume %**
Hexane	5.07%
Cyclopentane, methyl-	1.39%
Cyclohexane	5.42%
Hexane, 3-methyl-	1.69%
Heptane	3.78%
Cyclohexane, methyl-	4.62%
Octane	4.99%
p-Xylene	7.67%
Nonane	5.55%
Decane	4.86%
Undecane	4.23%
Dodecane	4.45%
Undecane, 2,6-dimethyl-	1.49%
Tridecane	4.12%
Tetradecane	3.31%
Pentadecane	3.65%
Hexadecane	2.94%
Heptadecane	2.80%
Octadecane	2.01%
Nonadecane	2.28%
Eicosane	2.16%
Heneicosane	2.10%
Docosane	3.60%
Pyrene	10.63%
Octacosane	2.01%
Hentriacontane	1.43%
Hexacosane	1.73%

Experimental Procedures

A complete description for the coreflood set-up that was used in this study was given in **Fig. 7**. The following are the procedures that we followed in the coreflood experiments:

1. The core was first dried in the oven at 200°F, then take the dry weight of the core.

2. The core was vacuumed and saturated with de-ionized water using the Hassler core holder, using back pressure of 500 psi and 1500 psi overburden, then take the weight of saturated core and determine the pore volume.

3. Saturating the core by oil was performed using the coreflood, the oil was injected into the core at 0.5 cm^{3}/min to insure proper displacement of water for the Pink Desert cores and 0.1 cm^{3}/min for the Indiana limestone cores. Three pore volume of oil were injected into the core in each core.

4. The oil and residual water saturations were determined.

5. The core was heated up to 300°F for 3 hrs to ensure the stabilization of temperature.

6. GLDA, HEDTA, and EDTA at pH 4 and 0.6M concentrations were used to stimulate the oil-saturated calcite core at 300°F.

7. The same chelant were used to stimulate water-saturated cores to compare with that saturated with oil.

8. GLDA, HEDTA, and EDTA were injected until the wormhole breakthrough.

9. In the second set of the experiments three pore volume of 10 vol% mutual solvent were injected into the oil-saturated cores to remove the oil followed by the injection of 0.6M chelating agent.

10. For gas experiments nitrogen gas was used. The core was first saturated by de-ionized water and heated up to 300°F until stabilization then the core was flooded by nitrogen gas until no more water coming out from the core.

11. The nitrogen gas injection continues until no more water coming out from the core, the back pressure in this case was 1000 psi and the nitrogen injection pressure was kept constant as the same that for water before switching to nitrogen.

12. The effluent samples collected were analyzed for calcium using the AAalyst 700.

Analytical Model

The dissolving power of the 20 wt%-GLDA at pH 1.7 will be determined in this part. To determine the dissolving power of GLDA we have to know the stoichiometric equation of the GLDA with calcite which can be given as follows:

$$H_4GLDA + 2CaCO_3 \leftrightarrow GLDA - Ca^{2+} + Ca^{2+} + 2CO_2 + 2H_2O \ldots\ldots\ldots (43)$$
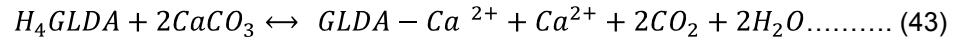
From this equation we can conclude that one mole of H_4GLDA can dissolve two moles of calcite. The gravimetric dissolving power (β) of 100 wt% GLDA can be determined using **Eq. 44** (Hill et al. 1993):

$$\beta = \frac{MW_{CaCO_3} \cdot \alpha_{CaCO_3}}{MW_{GLDA} \cdot \alpha_{GLDA}} \ldots\ldots\ldots\ldots\ldots\ldots\ldots\ldots\ldots\ldots\ldots\ldots\ldots\ldots\ldots\ldots\ldots (44)$$

where; MW_{CaCO3} is the molecular weight of the calcium carbonate = 100.09 lbmole, MW_{GLDA} is the molecular weight of the acid GLDA = 263 lbmole, α_{CaCO3} is the stoichiometric coefficient of $CaCO_3$ = 2, and α_{GLDA} is the stoichiometric coefficient of GLDA = 1. The gravimetric dissolving power for 100 wt% H_4GLDA (β_{100}) is 0.755 lbmole $CaCO_3$/lbmole GLDA, and that for the 20 wt% GLDA (β_{20}) is 0.151 lbmole $CaCO_3$/lbmole GLDA.

The volumetric dissolving power (X) which is the volume of mineral dissolved by a given volume of GLDA can be determined from **Eq. 45** (Hill et al. 1993):

$$X = \beta \frac{\rho_{GLDA}}{\rho_{CaCO_3}} \ldots\ldots\ldots\ldots\ldots\ldots\ldots\ldots\ldots\ldots\ldots\ldots\ldots\ldots\ldots\ldots\ldots (45)$$

Fig. 70 shows the gravimetric and volumetric dissolving power for GLDA at pH 1.7 at different concentrations. The relations between both volumetric and gravimetric dissolving powers with the GLDA concentration were almost linear relationship.
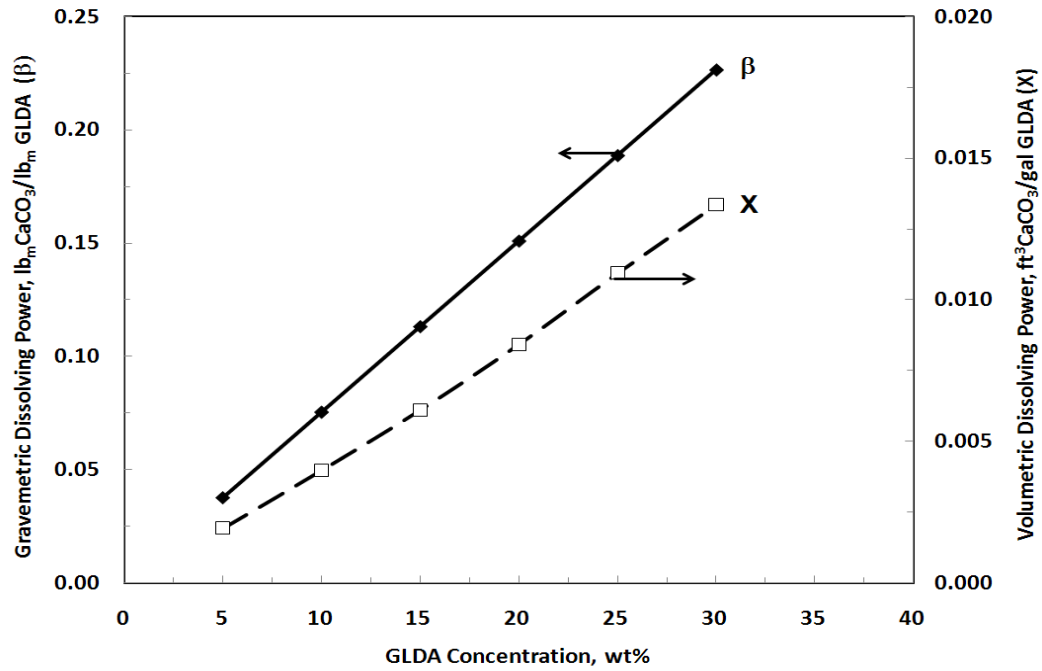
Fig. 70—Volumetric and gravimetric dissolving powers for different GLDA concentrations, pH = 1.7.

The volumetric dissolving power of the 20 wt%-GLDA at pH 1.7 is 0.0631 ft^3 CaCO$_3$/ft^3 20 wt%-GLDA. If we need to penetrate the formation with a one foot penetration depth the volume of GLDA required can be determined using the volumetric dissolving power and the following equations:

$$V_{GLDA} = \frac{V_{CaCO_3}}{X} \quad \text{...} \quad (46)$$

$$V_{CaCO_3} = \pi \left(r_{GLDA}^2 - r_w^2 \right) (1 - \phi) x_{CaCO_3} \text{...} \quad (47)$$

where; V_{GLDA} is the volume of GLDA required to dissolve V_{CaCO3} volume of calcite, X is the volumetric dissolving power of GLDA, r_{GLDA} is the radius from the wellbore to be acidized, r_w is the wellbore radius, ϕ is the formation porosity, and x_{CaCO3} is the volume fraction of calcite in the formation.

A coreflood experiment was run using Indiana limestone core of 20 in. length and 1.5 in. diameter, the core had a porosity of 20 vol%. The coreflood experiment was run at an optimum injection rate of 2 cm^3/min and 250°F the amount of the dissolved calcite was 30 g which is 2.5 wt% of the total core weight. The volume of the dissolved calcite from the 20-in. Indiana core was 11.1 cm^3 which was 2 vol% of the total volume of the core (579 cm^3). At 250°F and at the optimum injection rate the volume of GLDA required to penetrate 3 ft inside a formation has characteristics like the Indiana core that we used in our experiment in a 0.328 ft radius well can be determined using **Eqs. 46 and 47**. The volume of calcite to be dissolved from **Eq. 47** will be 0.55 ft^3/ft. The volume of GLDA required to create wormholes through the formation at the mentioned conditions will be 8.7 ft^3/ft of formation thickness or it will be 65 gal GLDA/ft.

The volumetric model developed by Hill et al. (1993) can be used to predict the volume of GLDA required to create wormholes. The following equation can be used:

$$\frac{V}{h} = \pi \phi \ r_{wh}^2 - r_w^2 \ PV_{bt} \ \dots\dots\dots\dots\dots\dots\dots\dots\dots\dots\dots\dots\dots\dots\dots\dots\dots \ (48)$$

Using the volumetric model the amount of GLDA required to create channels through 3.328 ft radius from the wellbore was 13.8 ft^3/ft or 103 gal GLDA/ft of formation thickness. **Fig. 71** shows the volume of GLDA required to create wormholes through the formation at different temperatures and different injection rates using the volumetric model, **Eq. 48**. The prediction in Fig. 71 was done for 3 ft penetration for the GLDA from the wellbore (r_w = 0.328 ft) and a formation porosity of 0.20. At low injection rates the volume of the fluid required to penetrate 3 ft inside the formation was lower than that at higher injection rates. It is better for GLDA to be injected at low injection rates to use less volume of the fluids.
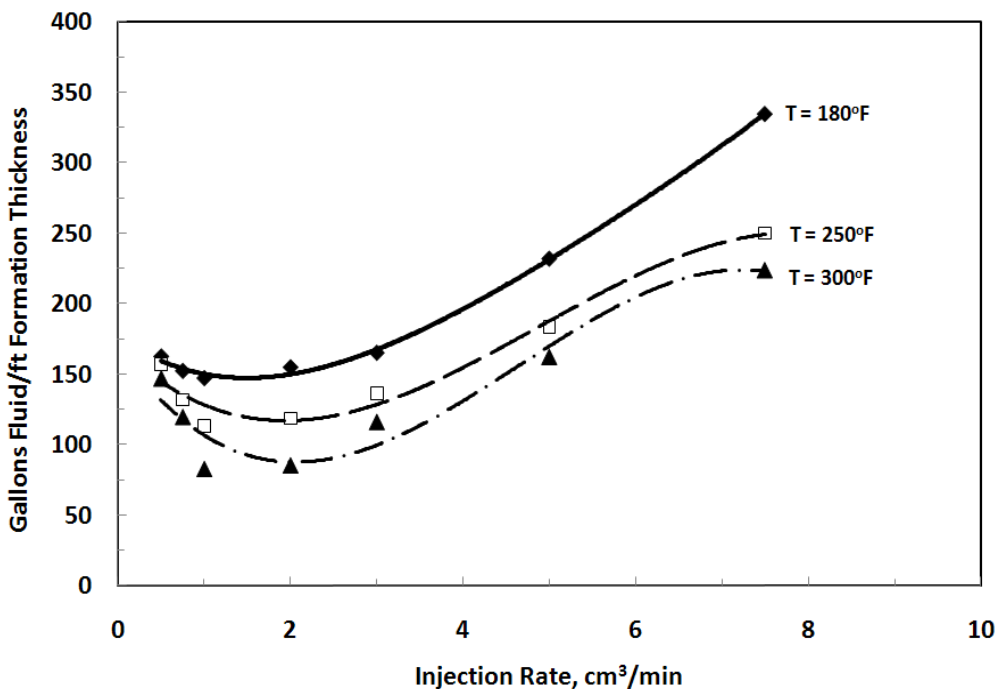
Fig. 71—Volume per foot of 20 wt% GLDA at pH 1.7 required to penetrate 3 ft into a 20% porous formation at different temperatures.

The acid capacity number (N_{ac}) which is the volume of the rock dissolved per the volume of the acid present for GLDA at pH of 1.7 can be determined using **Eq. 49** (Hill et al. 1993):

$$N_{ac,GLDA} = \frac{\phi \beta_\% \rho_{GLDA}}{1-\phi \ \rho_{rock}} = \frac{\phi X}{1-\phi} \quad \text{..} \quad (49)$$

where; ϕ is the formation porosity, β is the gravimetric dissolving power, ρ_{GLDA}, is the GLDA density, g/cm^3, ρ_{rock}, is the rock density, g/cm^3, and X is the volumetric dissolving power.

The acid capacity number for 20 wt% H_4GLDA in a calcite formation of 20 vol% porosity will be 0.0158.

Different models can be used to determine the wormholing rate (v_{wh}) during carbonate acidizing, Buijse and Glasbern (2005) developed the following semi-empirical equation:

$$v_{wh} = \frac{v_{i,opt}^{1/3}}{PV_{bt}} v_i^{2/3} \left[1 - exp \left(-4 \frac{v_i^2}{v_{i,opt}^2} \right)^2 \right] \quad \text{.......................................} \quad (50)$$

where; $v_{i.opt}$ is the optimum interstitial velocity = $Q_{opt}/(A\phi)$, Q_{opt} is the optimum injection rate, cm^3/min, A is the cross sectional area, cm^2, ϕ is the porosity, v_i is the interstitial velocity, cm/min = $Q/(A\phi)$, and PV_{bt} is the pore volume to breakthrough.

Hung et al. (1989) related the wormhole growth rate (v_{wh}) to the acid capacity number by the following equation:

$$v_{wh} = v_{i,tip}\ \frac{C_{tip}}{C_0}\ N_{ac} \quad\quad\quad (51)$$

where; C_0 and C_{tip} are the injection acid concentration, and the actual acid concentration at the tip of the wormhole. In the case of GLDA acid the concentration is constant inside the wormhole because it is not consumable we measured the concentration of H_4GLDA in the effluent sample and it was close to 20 wt%, therefore **Eq. 51** can be written in the following form:

$$v_{wh} = v_{i,tip}N_{ac} \quad\quad\quad (52)$$

The interstitial velocity at the tip of wormhole ($v_{i,tip}$) can be determined as follows (Furui et al. 2010):

$$v_{i,tip} = v_i\ \frac{d_{core}}{d_{wh}} \quad\quad\quad (53)$$

where; d_{core} is the core diameter, cm, and d_{wh} is the wormhole diameter, cm.
The wormholing rate can be determined also by combining equations 52 and 53 to give the following equation:

$$v_{wh} = v_i\ \frac{d_{core}}{d_{wh}}\ N_{ac} \quad\quad\quad (54)$$

Substituting the interstitial velocity in terms of flow rate and core diameter in Eq. 54, the wormhole growth rate can be written as follows:

$$v_{wh} = \frac{4QN_{ac}}{\pi\phi d_{core}d_{wh}} \quad\quad\quad (55)$$

The pore volume to breakthrough (PV_{bt}) can be determined from the wormholing rate and interstitial velocity as follows (Buijse and Glsabern 2005):

$$PV_{bt} = \frac{v_i}{v_{wh}} \dots\dots\dots\dots\dots\dots\dots\dots\dots\dots\dots\dots\dots\dots\dots\dots\dots\dots \quad (56)$$

Table 17 and **Fig. 72** show the actual and predicted pore volume to breakthrough using **Eq. 56**. There was a good match showing the validity of the derived equation to be used as an effective tool to predict the PV_{bt} based on fluid velocity and wormholing rate during the treatment of carbonate cores using GLDA. From Eq. 56, the PV_{bt} is function of injection rate, acid capacity number, wormhole size, core size, and core porosity. **Table 17** shows the predicted PV_{bt} at for different Indiana limestone cores at different injection rates.

Table 17—PREDICTED AND CATUAL VALUES FOR THE PV_{bt} USING GLDA		
Experiment number	**Actual PV_{bt}, PV**	**Predicted PV_{bt}, PV**
1	6.85	6.64
2	10.5	11.62
3	3.35	3.65
4	3.20	4.15
5	5.22	5.81
6	8.00	9.13
7	3.10	4.15
8	3.40	3.32
9	3.65	4.20
10	3.40	3.85
11	3.22	2.99
12	3.10	3.65
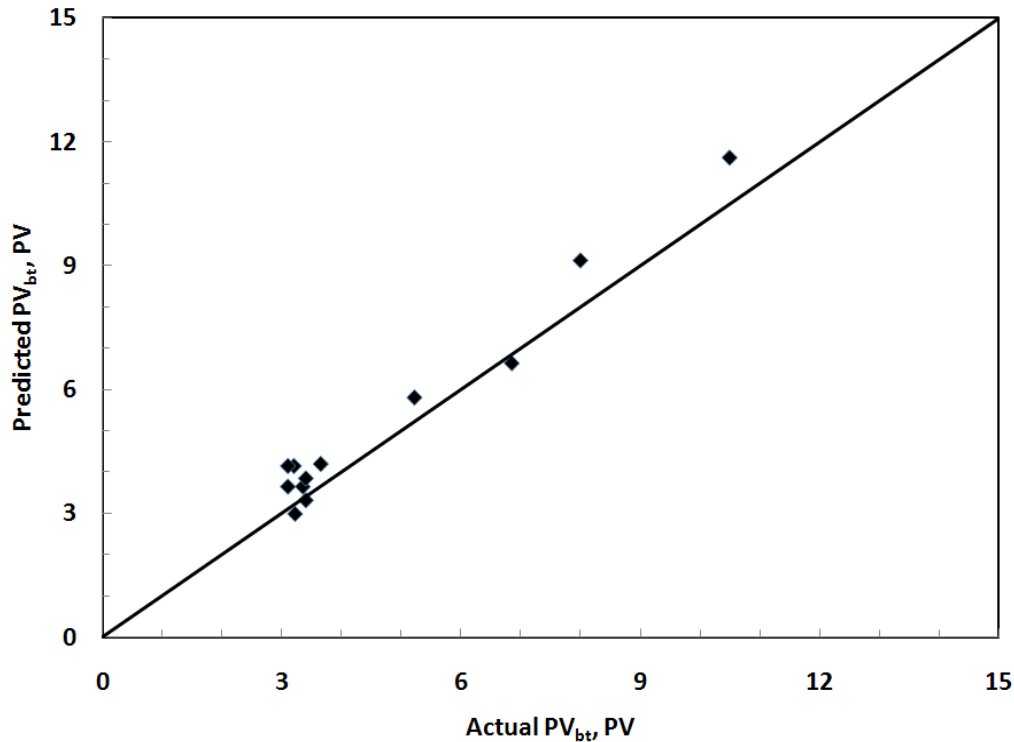
Fig. 72—Prediction of the PV$_{bt}$ from Equation 56 and the PV$_{bt}$ from the actual experimental data showing good match.

Prediction of the Pressure Drop Across the Core

The pressure drop across the core can be predicted using Darcy's equation for linear incompressible flow. The viscosity of the GLDA solutions with different calcium concentrations were measured at different temperatures up to 70°C. The calcium concentration in the coreflood effluent samples was measured and constructed versus pore volume. The viscosity that was used in predicting the pressure drop was that of the solutions in the coreflood effluent. The viscosity of the effluent samples can be determined also from the correlation obtained from **Fig. 73** and extrapolated to the required temperature. The viscosity in this figure was determined by preparing different GLDA solution with a total calcium concentration shown in the figure. The H$_4$GLDA first was neutralized by crushed calcite then the calcium concentration was increased to the required value by adding calcium chloride. The following equations will be used to predict the pressure drop across the core:

1. The pressure drop in the region that the calcium concentration increased from zero to the maximum value (viscosity-build up region) can be determined as follows:

$$\Delta p = \Delta p_{wh} + \Delta p_{GLDA} + \Delta p_{water} = 0 + \frac{122.812Q\mu_{GLDA} \ L_{GLDA}-L_{wh}}{kd_{core}^2} +$$

$$\frac{122.812Q\mu_{water} \ L_{core}-L_{GLDA}}{kd_{core}^2} \ \dots\dots\dots\dots\dots\dots\dots\dots\dots\dots\dots\dots\dots\dots\dots\dots\dots \ (57)$$

2. The pressure drop in the second region in which the fluid has its maximum viscosity and constant until the wormhole breakthrough can be determined as follows:

$$\Delta p = \Delta p_{wh} + \Delta p_{GLDA} = 0 + \frac{122.812Q\mu_{GLDA-max} \ L_{core}-L_{wh}}{kd_{core}^2} \ \dots\dots\dots\dots \ (58)$$

where; Q is the injection rate, cm^3/min, μ_{GLDA} is the GLDA viscosity, cP and can be determined from **Fig. 73** , L_{GLDA} is the invaded length of GLDA, L_{core} is the core length, in., k is the initial core permeability, md, d_{core} is the core diameter, in., L_{wh} is the wormhole length, in., Δp_{wh} is the pressure drop across the wormhole, psi, Δp_{GLDA} is the pressure drop in the region invaded by the GLDA-Ca complex solution, psi, and Δp_{water} is the pressure drop in the water region, psi.
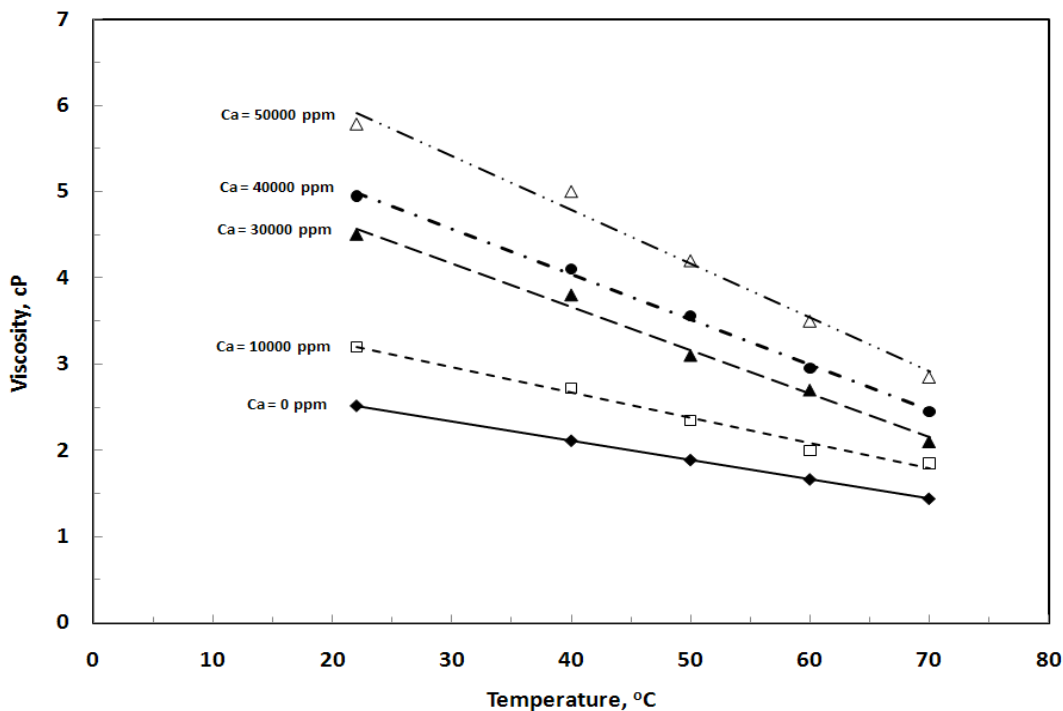
Fig. 73—Relationship between the GLDA viscosity and solution temperature at different calcium concentration for 20 wt% GLDA at pH 1.7. These data were constructed using capillary tube viscometer.

The assumptions included in predicting the pressure drop are:

1. Pressure drop across the wormhole is zero.
2. The wormhole formation is linear with time.
3. The viscosity of GLDA increased linearly with time until the GLDA breakthrough the core ($\mu_{GLDA-max}$) after that the GLDA viscosity is constant until the wormhole breakthrough and depends on the calcium concentration.
4. The relation between the GLDA viscosity and temperature can be given from **Fig. 73** and can be extrapolated for temperature higher than 70°C.
5. There is no effect for the CO_2 at back pressure of 1000 psi or the CO_2 is soluble in GLDA solutions at 1000 psi back pressure.
6. GLDA-Ca complex has a constant viscosity and does not react with the rock ahead of the fresh GLDA entering the core, so the rock permeability is constant.

Model Validation

The model was used to predict the pressure drop across a 6 in. Indiana limestone core at 180°F and injection rate of 2 cm^3/min treated by GLDA at pH 1.7. The calcium concentration for the coreflood effluent samples is shown in **Fig. 74** showing average calcium concentration of 42,000 ppm. At that calcium concentration we can choose the correlation for viscosity from Fig. 73 or we can use the measured value of the viscosity. Using Equations 57 and 58 the pressure drop across the core can be determined. **Fig. 75** shows the actual and the predicted pressure drop across the core for this case. There was a good match between the predicted and the actual pressure drop confirming the validity of the developed model to predict the pressure drop during treatment of the core using GLDA solutions. The pressure drop across the core also was predicted for an Indiana limestone core treated by 20 wt% GLDA of pH 1.7 at 220°F and 3 cm^3/min. The actual and predicted pressure data are shown in **Fig. 76** showing validity for the developed model to be used to predict the pressure drop across the core at different GLDA pH values. The calcium concentration in the coreflood effluent for the pressure drop data in Fig. 75 was measured and had an average value of 43,000 ppm from the GLDA breakthrough until the wormhole breakthrough. The viscosity of the 43,000 ppm Ca-GLDA solutions can be determined from Fig. 73 by interpolation. Assuming that the GLDA-Ca complex is not reactive with the rock is a reasonable assumption because we prepared a solution of 50,000 ppm GLDA-Ca by putting crushed calcite in H_4GLDA solution until equilibrium and we add calcium chloride solution until the total calcium concentration reached 50,000 ppm. After that the solution was stirred with a crushed calcite in the slurry reactor for two hours. Then the solution was removed from the reactor and filtered using 70 μm filter paper and was analyzed for the total and free calcium. The

total calcium was the same which was 50,000 ppm, and this means that the GLDA solution did not touch the crushed calcite, i.e., there was no reaction.
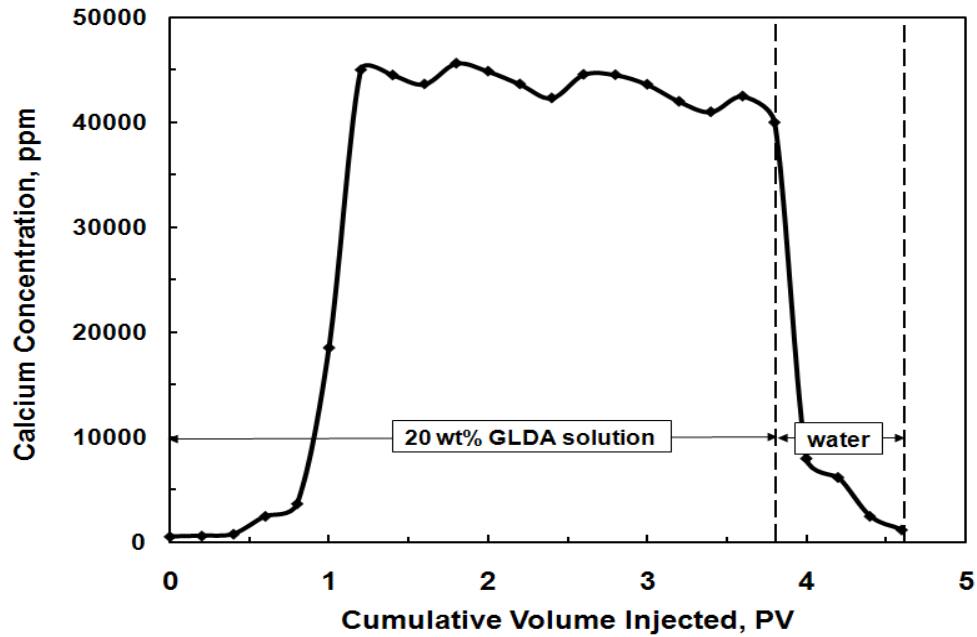
Fig. 74—Calcium concentration in the coreflood effluent for a calcite core treated by 20 wt% GLDA of pH 1.7 at 180°F. The calcium concentration was constant after injecting 1.2 PV until the wormhole breakthrough.
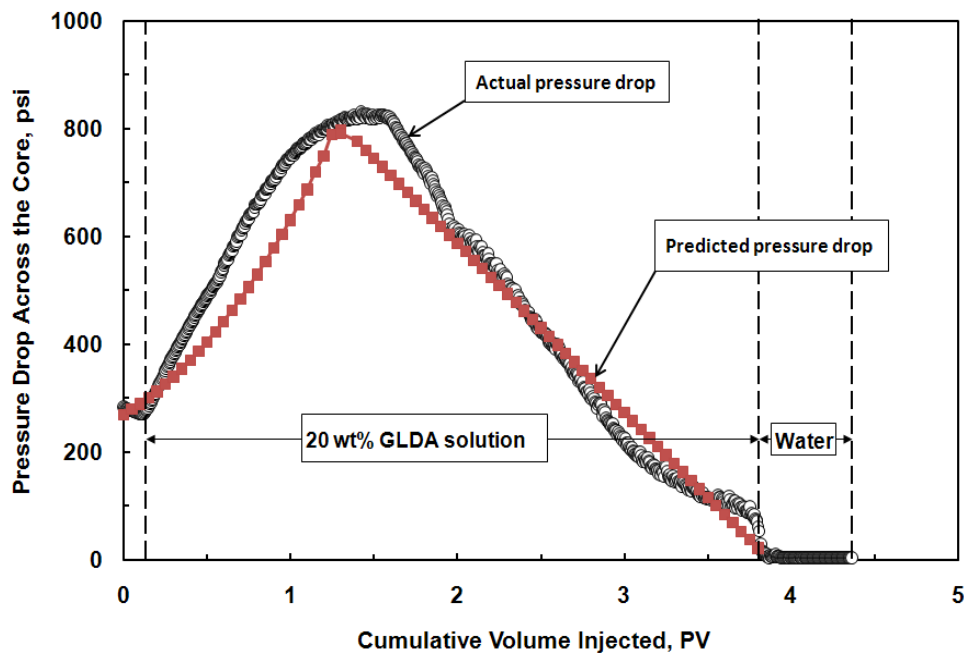
Fig. 75—Actual and predicted pressure drop across the core for a calcite core treated by 20 wt% GLDA of pH 1.7 at 2 cm³/min and 180°F. There was a good match between the actual and predicted profiles showing a good validation for the developed model.
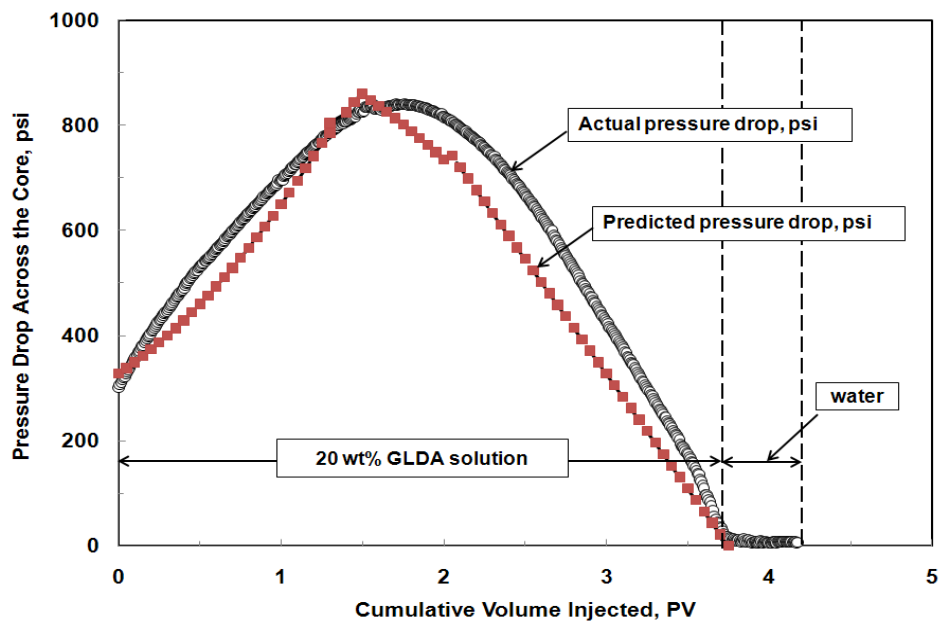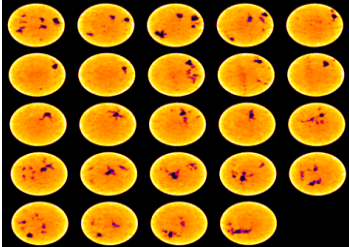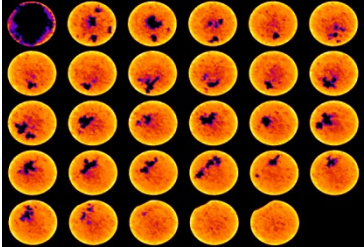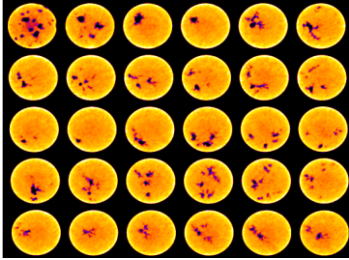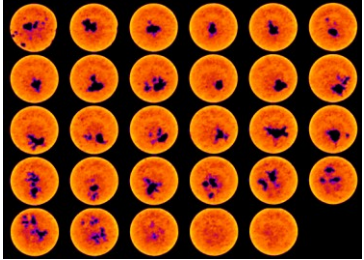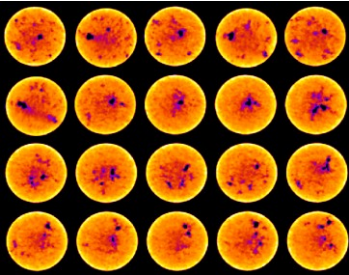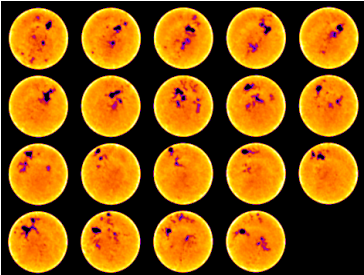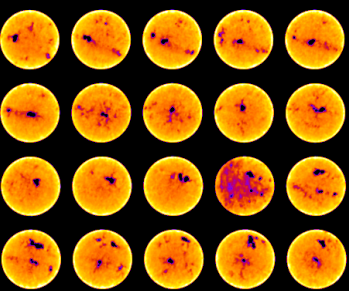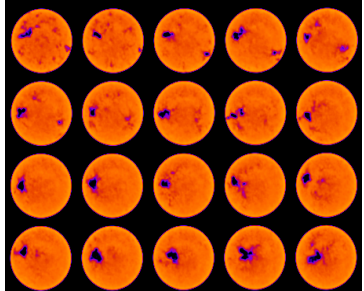
Fig. 76—Actual and predicted pressure drop across the core for a calcite core treated by 20 wt% GLDA of pH 1.7 at 3 cm³/min and 220°F. There was a good match between the actual and predicted profiles showing a good validation for the developed model.

Results and Discussion of the Experimental Part

Stimulation of Indiana Cores (Water Saturated) by GLDA and HEDTA

Indiana limestone cores with average permeability of 1 md and average porosity of 13 vol% were used in this study. The coreflood experiments were run using 0.6M GLDA at pH 4 at temperatures of 200 and 300°F. The experiments were run at different injection rates from 1 to 5 cm^3/min. The maximum final core permeability was at 2 cm^3/min but the minimum pore volume to breakthrough (PV_{bt}) was at 3 cm^3/min. At low injection rates below the optimum GLDA at pH 4 created more than one wormhole in the core inlet and there was one dominant wormhole. **Fig. 77** shows the pore volume of GLDA required to create wormholes through the core as a function of injection rate. At 1 cm^3/min the pore volume to breakthrough was 4.2 PV at 300°F compared to 3.35 PV at 3 cm^3/min, considering the 3 cm^3/min the optimum injection rate for 0.6M GLDA at pH 4. At injection rates lower than the optimum, 0.5, and 1 cm^3/min, there were more than one wormhole in the first few slices as shown in the 2D CT scan images in **Table 18**. Therefore more volumes of GLDA were required to create those non-dominant wormholes, and there was only one dominant wormhole at that rate. In the case of HEDTA the wormhole diameter was bigger than that in the case of GLDA showing uncontrolled reaction at low rates. The PV_{bt} at low injection rates, 0.5, and 1 cm^3/min, was smaller in the case of GLDA compared to that in the case of HEDTA showing a good controlled reaction of GLDA even at low injection rates. At injection rate of 0.5 cm^3/min there was clear face dissolution in the case of 0.6M HEDTA at 300°F as shown in Table 18. At injection rates greater than the optimum, 5 cm^3/min, the pore volume to breakthrough was 5.22 PV. At this rate only one dominant wormhole was formed from the core inlet face to the outlet face, and the wormhole size was smaller compared to that formed at the optimum injection rate (3 cm^3/min), Table 18. At injection rates higher than the optimum the amount of dissolved calcium was small compared to that at the optimum because at higher rates the reaction time for GLDA with the rock was smaller. Increasing temperature from 200 to 300°F increased the reaction rate of the 0.6M GLDA with calcite and decreased the pore volume to breakthrough at different injection rates. The decrease in the pore volume to breakthrough with increasing the temperature from 200 to 300°F was not high meaning a controlled reaction rate even at high temperatures.

Table 18—COREFLOOD SUMMARY FOR INDIANA LIMESTONE TREATED BY 0.6M GLDA and 0.6M HEDTA at pH 4 and 300°F

Q, cm³/min	PV_bt, GLDA	PV_bt, HEDTA	2D CT Scan Images GLDA	2D CT Scan Images HEDTA
0.5	4.5	12.5		
1	4.2	10.50		
3	3.35	3.20		
5	5.22	8.00		
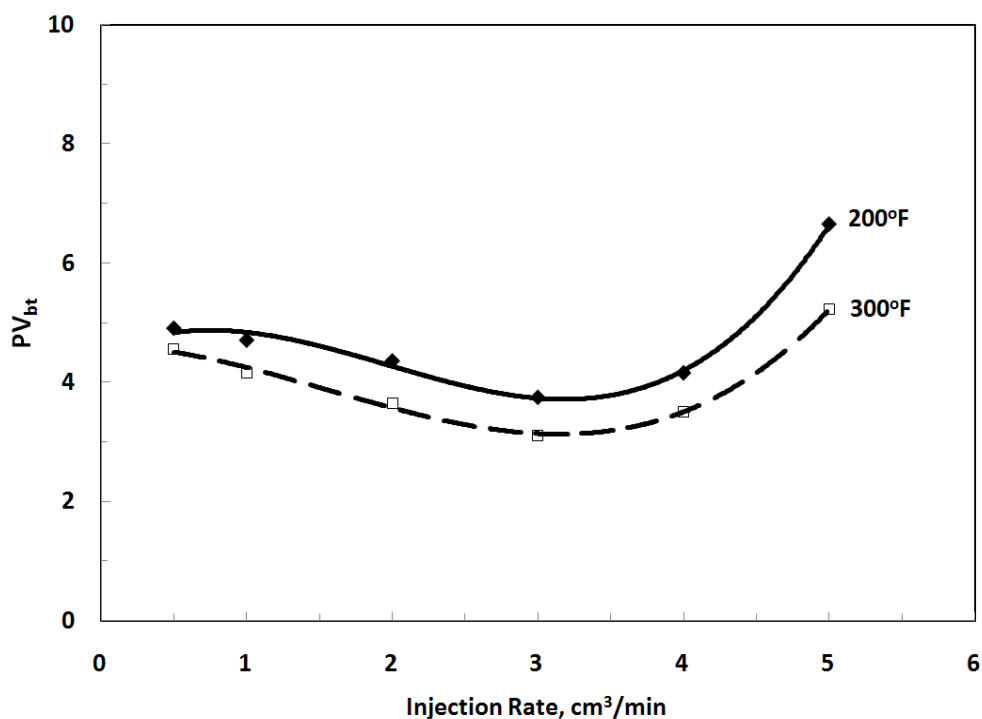
Fig. 77—Relationship between the pore volume to breakthrough the core and injection rate of 0.6M GLDA (pH = 4) at different temperatures using 6-in.Indiana limestone cores.

Fig. 78 shows the coreflood results of the stimulation of 6-in. Indiana limestone cores by 0.6M HEDTA of pH 4 at 200 and 300°F. Results similar to that obtained with the 0.6M GLDA at pH 4 were obtained here. The optimum injection rate for the 0.6M HEDTA was 3 cm^3/min at 300°F and almost the same at 200°F. Increasing the temperature from 200 to 300°F enhanced the reaction rate of the 0.6M HEDTA with calcite and less volume of the fluid was required to create wormholes at different injection rates. The degree of concavity in the case of HEDTA in the curves at different temperatures was higher than that in the case of GLDA. This can be attributed to at the injection rates lower than the optimum HEDTA required more volumes to create wormholes. **Fig. 79** shows the difference of 0.6M GLDA and 0.6M HEDTA at different injection rates and 300°F at pH 4. At the optimum range from 2 to 3 cm^3/min the performance of the two chelating agents was almost the same in terms of the required pore volume to breakthrough the core (PV$_{bt}$). At injection rates below and above that range there was a noticeable difference between GLDA and HEDTA. At injection rates higher than the optimum GLDA has a more controlled reaction with calcite than HEDTA. The PV$_{bt}$ for the 0.6 M HEDTA increased from 3.2 PV at 3 cm^3/min to 10.5 PV at 1 cm^3/min (almost increased three times), while for the 0.6M GLDA the PV$_{bt}$ increased from 3.35 PV at 3 cm^3/min to 4.2 PV at 1 cm^3/min.

As shown in Table 18, the 2D images for HEDTA at 1 cm^3/min showed a big wormhole compared to that created by GLDA at the same conditions. This big wormhole created by HEDTA required a lot of volume to be created as it required three times the volume required at the optimum rate (3 cm^3/min). The wormhole created by HEDTA at 1 cm^3/min was not dominant as in the last three slices which is one tenth of the core length (0.6 in.) we could not see the wormhole because it was very thin. Most of the volume of HEDTA was consumed in enlarging the existed wormhole rather than creating a dominant wormhole. At injection rate of 3 cm^3/min (optimum injection rate) the wormhole diameter was the same for both 0.6M HEDTA and 0.6M GLDA.
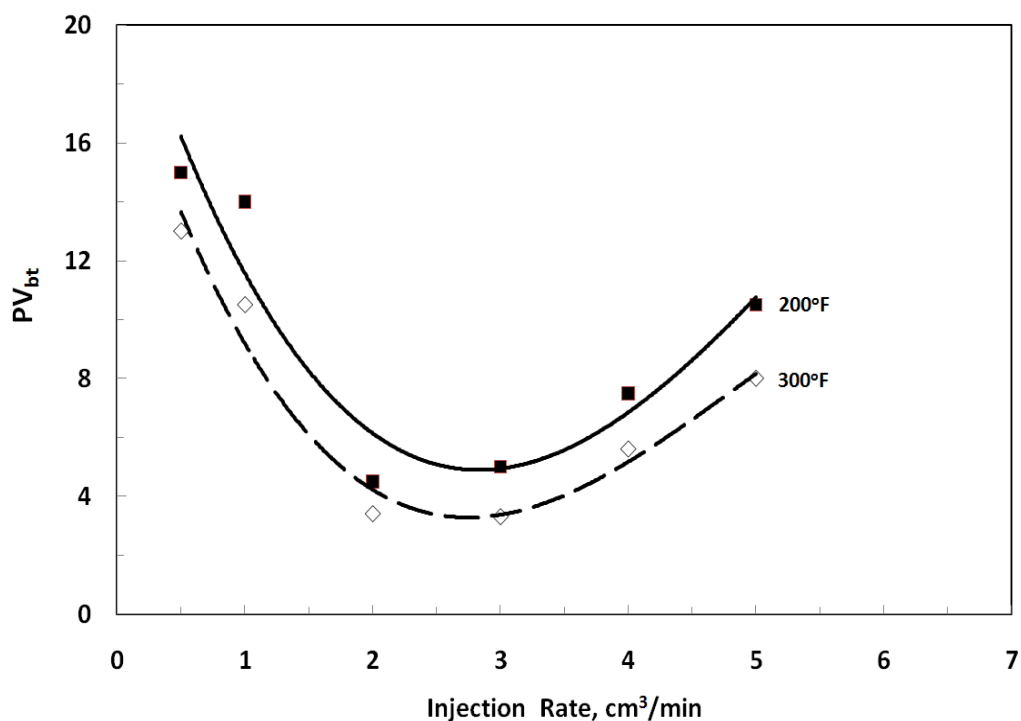
Fig. 78—Relationship between the pore volume to breakthrough the core and injection rate of 0.6M HEDTA (pH = 4) at different temperatures using 6-in.Indiana limestone cores.
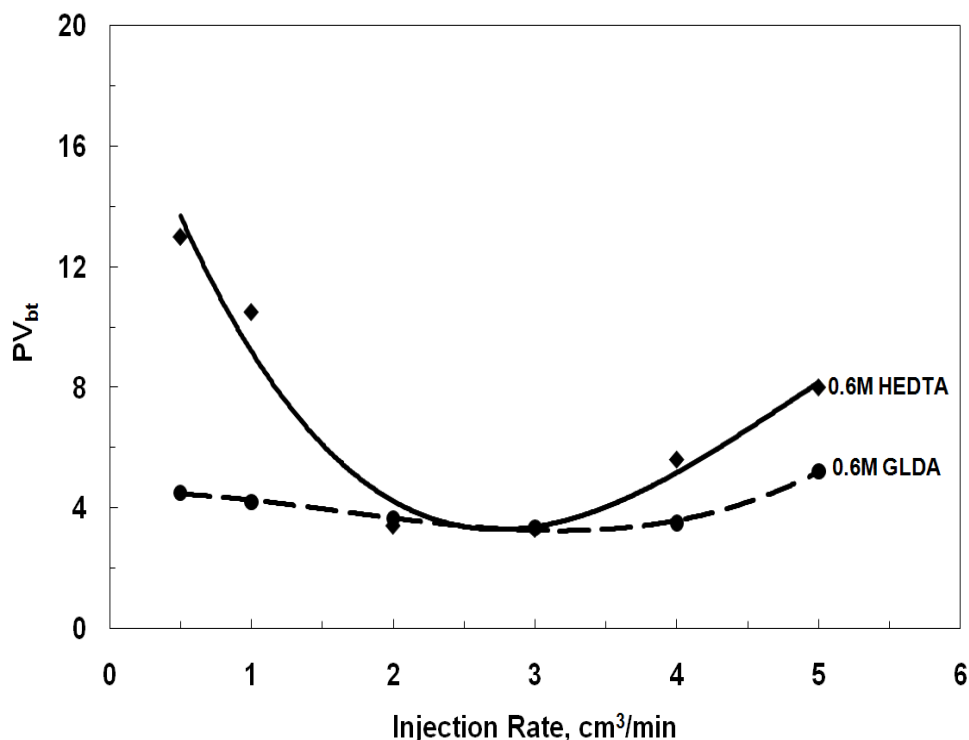
Fig. 79—Comparison between 0.6M GLDA and 0.6M HEDTA chelating agents at 300°F and pH 4.

Stimulation of Pink Desert (High Permeability-Water Saturated) Calcite Cores by Different Chelating Agents

Three different chelating agents of 0.6M concentration and pH 4 were used to stimulate water-saturated Pink Deseret limestone cores. The cores had an average permeability of 95 md and average porosity of 25 vol%. The cores used in the coreflood experiments have 1.5 in. diameter and 6 in. length. The coreflood experiments were run at 300°F and 5 cm^3/min. **Fig. 80** shows the volume of 0.6M GLDA, EDTA, and HEDTA required to create channels along the total core length. The volume required to breakthrough the core (PV$_{bt}$) was 4, 6, and 9.5 for 0.6M GLDA, 0.6M HEDTA, and 0.6M EDTA respectively. The 0.6M GLDA performed better than HEDTA and EDTA at pH of 4 in the high permeability Pink Desert calcite cores. The enhanced performance of GLDA at low pH value can be attributed to its higher solubility (**Fig. 81**) and higher thermal stability at low pH values compared to EDTA and HEDTA (Jim et al. 2010). The 0.6M HEDTA created wormholes with diameter bigger than that created by the 0.6M GLDA at the same conditions, therefore, the PV$_{bt}$ in the case of HEDTA was higher than that for GLDA. More volume of HEDTA was required just to enlarge the wormhole from the core inlet to the core outlet. In the case of the 0.6M EDTA the pore volume of EDTA required to breakthrough the core

was high because of the solubility of EDTA. The prepared solutions of GLDA, HEDTA, and EDTA were left for 3 hours after the preparation, the EDTA precipitated a white precipitate and for both HEDTA and GLDA there was no precipitate meaning a good solubility at 0.6M concentration.
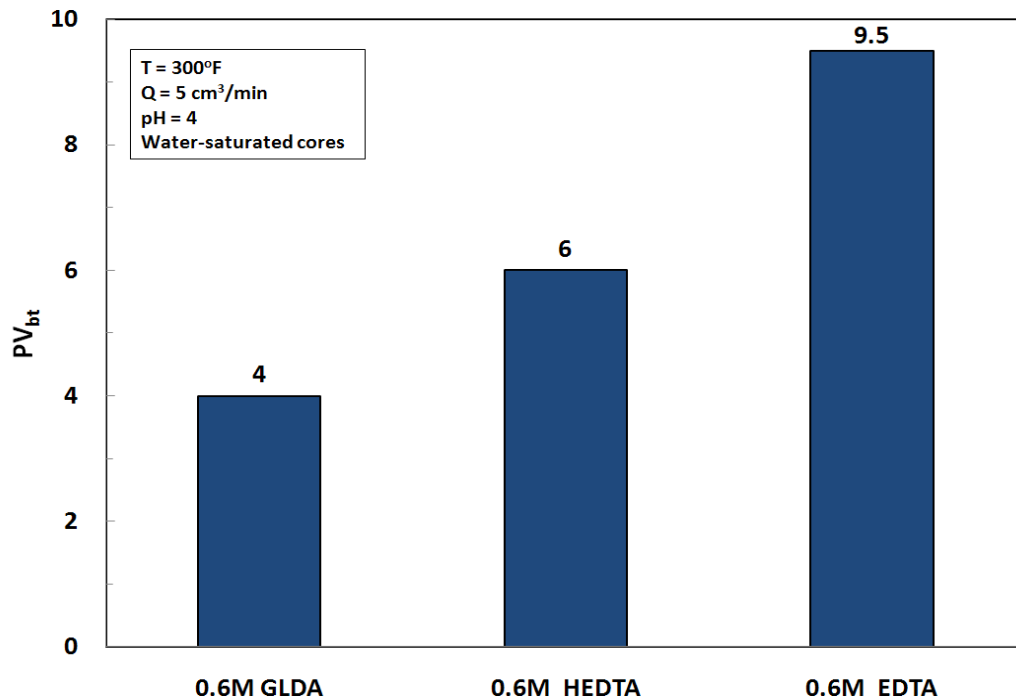
Fig. 80—Pore volumes required to create wormholes for different chelating agents using Pink Desert calcite cores at 300°F. The cores were saturated by de-ionized water.
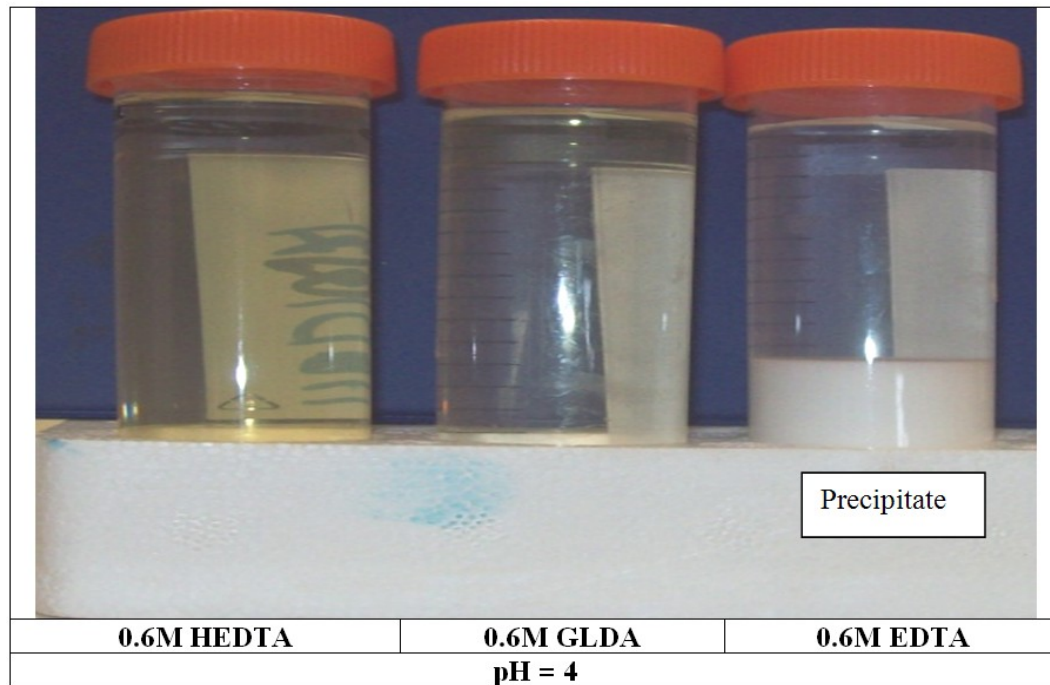
Fig. 81—Solutions of GLDA, HEDTA, and EDTA at pH of 4 showing low solubility of EDTA at pH 4 after 10 hours.

Stimulation of Oil-Saturated Indiana Cores by GLDA and HEDTA

In this part the effect of saturating the Indiana cores by oil was studied at 300^oF. The cores were saturated first by water and then flushed by oil at 0.1 cm^3/min, three pore volume of oil were injected into the core after that the cores were soaked in the oven at 200^oF for 24 hours and 15 days. **Table 19** shows the results of the coreflood experiments for the Indiana cores saturated with water and oil treated by 0.6M GLDA and 0.6M HEDTA at an injection rate of 2 cm^3/min and 300^oF. The Indiana core that was treated by 0.6M GLDA at pH 4 had a pore volume of 22 cm^3 and the residual water after flushing the core by oil was 5 cm^3 (S_{wr} = 0.227). After soaking the core for 15 days and then flush the core by water at 300^oF and 2 cm^3/min only 6 cm^3 of the oil was recovered and the volume of residual oil was 10 cm^3 (S_{or} = 0.46), this is high fraction of the pore volume indicating an oil-wet core. The pore volume to breakthrough (PV_{bt}) for the Indiana cores that was treated by GLDA was 3.65 PV for the oil-saturated core, and 3.10 PV for the oil-saturated core. The presence of oil in the core reduced the PV_{bt} for the cores treated by 0.6M GLDA at pH of 4, thus the GLDA performance was enhanced in the oil-saturated cores by creating a dominant wormhole. The enhancement in the performance can be attributed to the reduced fluid diffusion in the presence of oil. The 2D CT scan images showed that the wormhole diameter was not affected by saturating the core by oil or water. The Indiana core saturated by

oil that was treated by 0.6M HEDTA at pH 4 required the same PV as the water-saturated core to breakthrough the core. The PV_{bt} for both the oil and water-saturated core was 3.4 PV. As shown in Table 19 the 0.6M HEDTA at pH 4 was able to create wormholes in both oil and water saturated cores with the same volume, which meant that the oil has no effect on the performance of HEDTA in the coreflood experiment at 300^oF.

The effect of soaking time of the Indiana oil-saturated cores was studied by soaking the core for 24 hours, and 15 days. The pore volume of the Indiana core that was soaked for one day was also 22 cm^3, the core was saturated by the same procedures and the same type of oil as that soaked for 15 days. The oil saturation after flushing the core by 25 PV water at 2 cm^3/min was 0.227 compared to 0.455 for the 15 days-soaked core. The S_{or} of 0.227 indicated a water-wet core. The pore volume required to create wormholes was 3.22 PV for the core that was soaked for 24 hours and 3.10 PV for the 15 days-soaked cores. Soaking the oil-saturated core for long time increased the amount of the residual oil saturation and decreased the volume of the fluid required to create wormholes. **Table 20** shows the summary of the effect of soaking time on the performance of GLDA with oil-saturated cores. The wormhole diameter was bigger in the case of 15 days-soaked core indicating that GLDA performed better in the oil-wet cores than the water-wet cores.
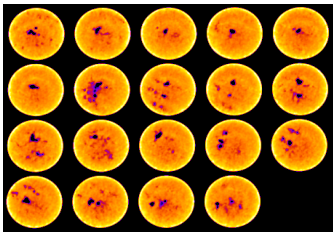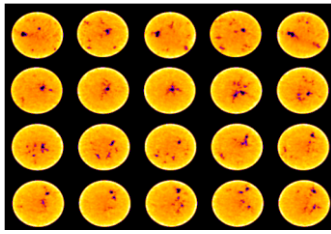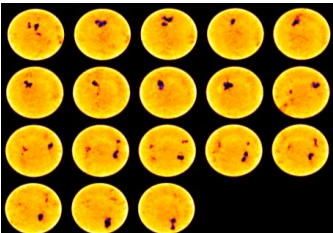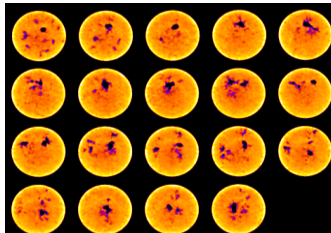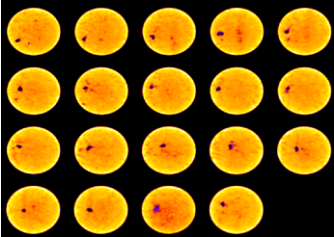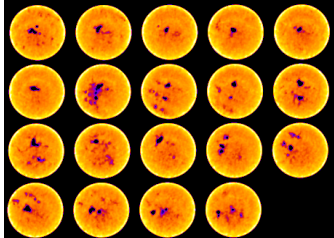
Table 19—EFFECT OF SATURATING THE CORE BY OIL ON THE PERFORMANCE OF 0.6M GLDA AND 0.6 HEDTA AT 300°F, pH 4 and 2 cm^3/min

Reservoir fluid type	Oil-Saturated Core	Water-Saturated Core
2D CT scan images, GLDA		
2D CT scan images, HEDTA		
PV_{bt}, GLDA, PV	3.10	3.65
PV_{bt}, HEDTA, PV	3.40	3.40

Table 20—EFFECT OF SOAKING TIME ON THE WORMHOLE CREATION USING INDIANA-OIL SATURATED CORES TREATED BY 0.6M GLDA AT pH 4 , 2 cm^3/min, AND 300°F

Soaking time, days	2D CT scan images	PV$_{bt}$, PV	Residual oil saturation (S$_{or}$)
1		3.22	0.23
15		3.10	0.46

Effect of Gas

In this part the effect of stimulation of gas saturated cores by GLDA and HEDTA was studied. The Indiana limestone cores were first saturated by water and then flushed by nitrogen gas until no more water coming out from the core. The coreflood experiments of the gas-saturated Indiana limestone cores were run using 0.6M GLDA and 0.6M HEDTA at pH 4, and 300°F at different injection rates. **Table 21** shows the results of the Indiana limestone cores treated by 0.6M GLDA and 0.6M HEDTA at 300°F at 2 cm^3/min. There was a small difference between the PV$_{bt}$ in the case of water-saturated and gas-saturated cores. There was a small increase in the PV$_{bt}$ in the case of gas-saturated cores in both cases, GLDA and HEDTA.

Table 21—EFFECT OF SATURATING THE CORE BY GAS ON THE PERFORMANCE OF 0.6M GLDA AND 0.6 HEDTA AT 300°F, pH 4 and 2 cm^3/min

Reservoir fluid type	Gas-Saturated Core	Water-Saturated Core
2D CT scan images, GLDA		
2D CT scan images, HEDTA		
PV$_{bt}$, GLDA, PV	3.83	3.65
PV$_{bt}$, HEDTA, PV	3.80	3.40

Fig. 82 shows the total calcium concentration in the coreflood effluent for Indiana limestone cores treated by 0.6M GLDA of pH 4 at 2 cm^3/min and 300°F. The calcium concentration was slightly higher in the case of water-saturated core than that in the gas-saturated core by 1000 ppm. **Figs. 83 and 84** show the relationship between the PV$_{bt}$ and injection rate for 0.6M GLDA and 0.6M HEDTA using water and gas-saturated cores at 300°F. Generally we can conclude that saturating the core by nitrogen gas did not affect the performance of 0.6M GLDA and 0.6M HEDTA at pH 4 with the Indiana limestone cores.
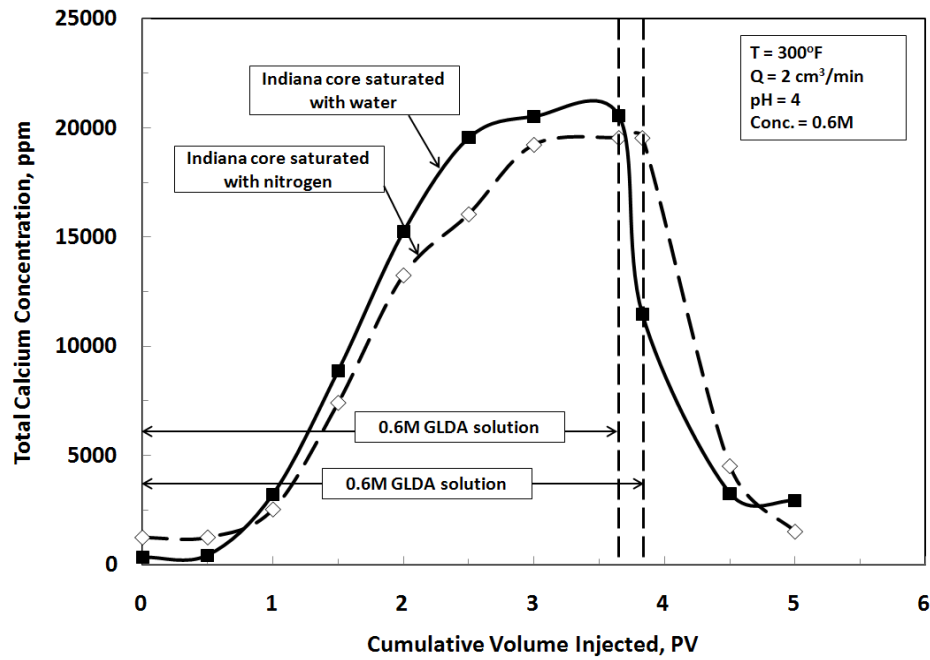
Fig. 82—Effect of gas on the amount of calcium concentration during the coreflood experiment for Indiana limestone cores treated by 0.6M GLDA at 2 cm³/min and 300°F.
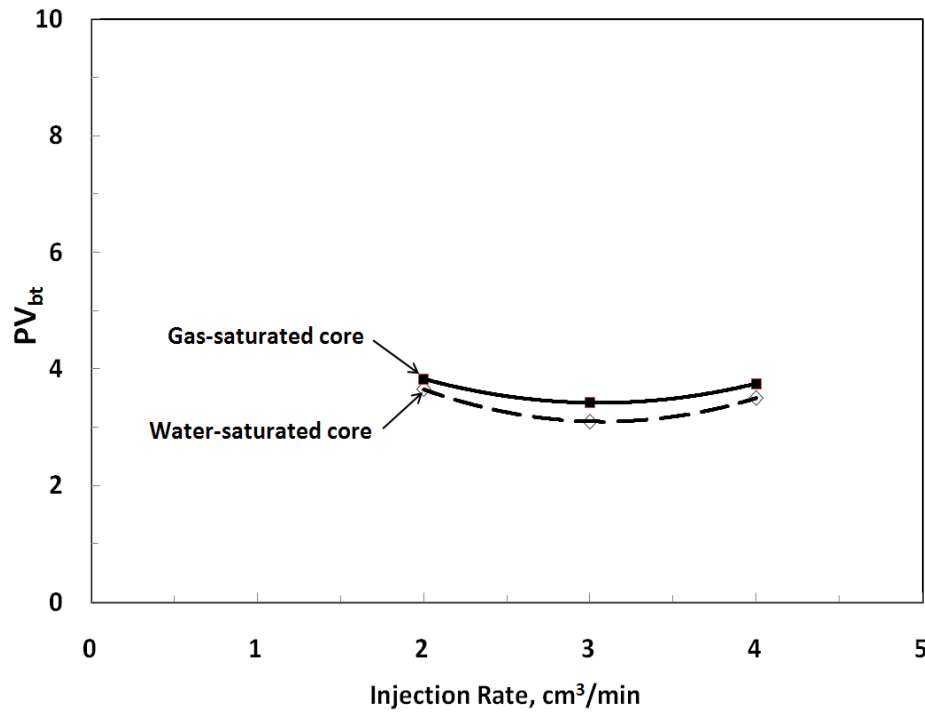
Fig. 83—Effect of gas on the PV$_{bt}$ during the coreflood experiment for Indiana limestone cores treated by 0.6M GLDA (pH = 4) at 300°F.
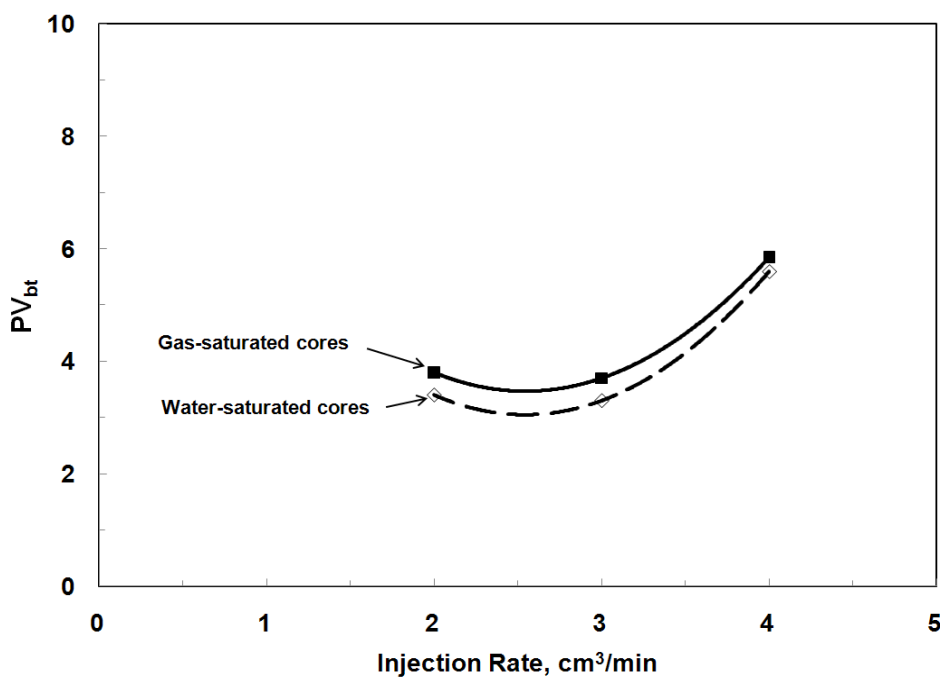
Fig. 84—Effect of gas on the PV$_{bt}$ during the coreflood experiment for Indiana limestone cores treated by 0.6M HEDTA (pH = 4) at 300°F.

Stimulation of Pink Desert (High Permeability-Oil Saturated) Calcite Cores by Different Chelating Agents

The effect of saturating the Pink Desert cores by oil and water on the performance of GLDA, HEDTA, and EDTA was studied in this part. The solutions of 0.6M EDTA, GLDA, and HEDTA of pH 4 at 5 cm^3/min and 300°F were used in the coreflood experiments. **Fig. 85** shows a comparison between the three chelants, the PV$_{bt}$ was the lowest in the case of 0.6M GLDA (3.8 PV), the PV$_{bt}$ in the case of HEDTA was 5.5 PV and wormholes with bigger diameter were created than that in the case of GLDA. 0.6M EDTA solution was prepared from 40 wt% solution of initial pH 11 using HCl and used immediately in the coreflood experiment after preparation. The PV$_{bt}$ in the case of EDTA was 9 PV because of the lower solubility and the lower thermal stability of the low pH solutions of EDTA (Jim et al 2010).
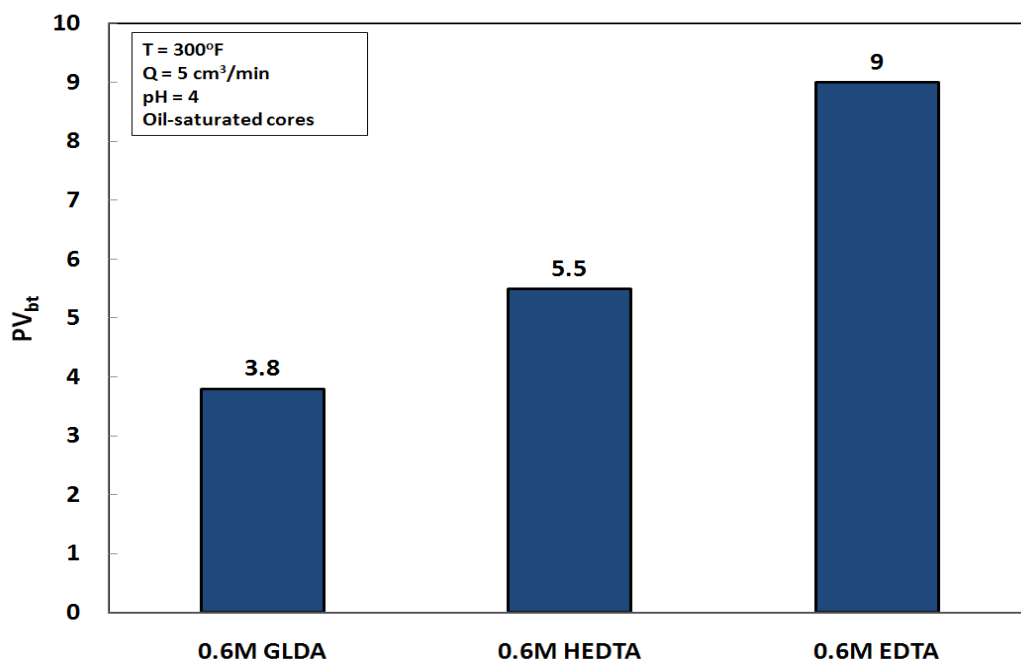
Fig. 85—Pore volumes required to create wormholes for different chelating agents using Pink Desert calcite cores at 300°F. The cores were saturated by crude oil and soaked for 15 days in the oven at 200°F.

The coreflood experiments were repeated using oil-saturated cores with the three chelating agents used above. Similar results were obtained but with slightly lower PV_{bt}. The PV_{bt} decreased from 4, 6, and 9.5 PV in the case of water-saturated cores to 3.8, 5.5, and 9 PV in the case of oil-saturated cores for 0.6M GLDA, HEDTA, and EDTA at pH 4 and 300°F. The average permeability of the used cores was 50 md. The oil-saturated cores were flushed by 3 PV 10% mutual solvent to remove the oil from the core at 300°F and after that the core was flowed by chelating agent. In this case we almost got the same results as in Fig. 78, indicating that the 3 PV 10 vol% mutual solvent removed almost all the oil inside the core, **Fig. 86**.
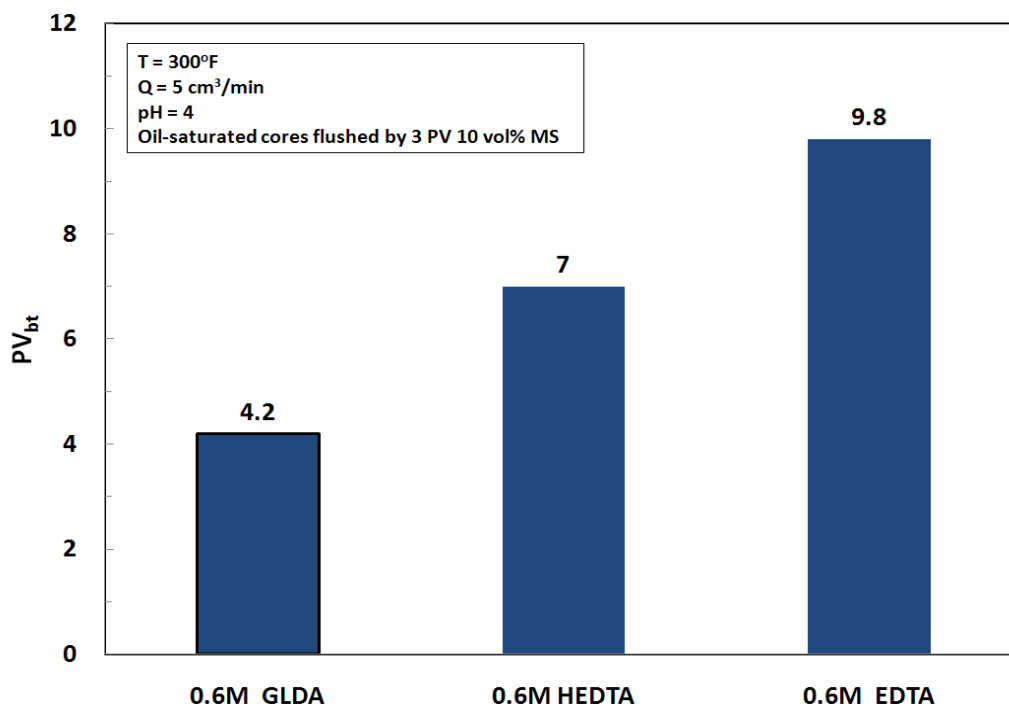
Fig. 86—Effect of flushing the oil-cores by mutual solvent on the volume of the fluid required to create wormholes for different chelating agents.

Fig. 87 shows the total calcium concentration in the coreflood effluent samples for the Pink Desert cores treated by EDAT, GLDA, and HEDTA of 0.6M concentration and pH 4. The highest calcium concentration was obtained in the case of GLDA and HEDAT at an average value of 27,500 ppm and the lowest was obtained in the case of EDTA at an average value of 13,000 ppm because of the lower solubility of the EDTA at low pH values.
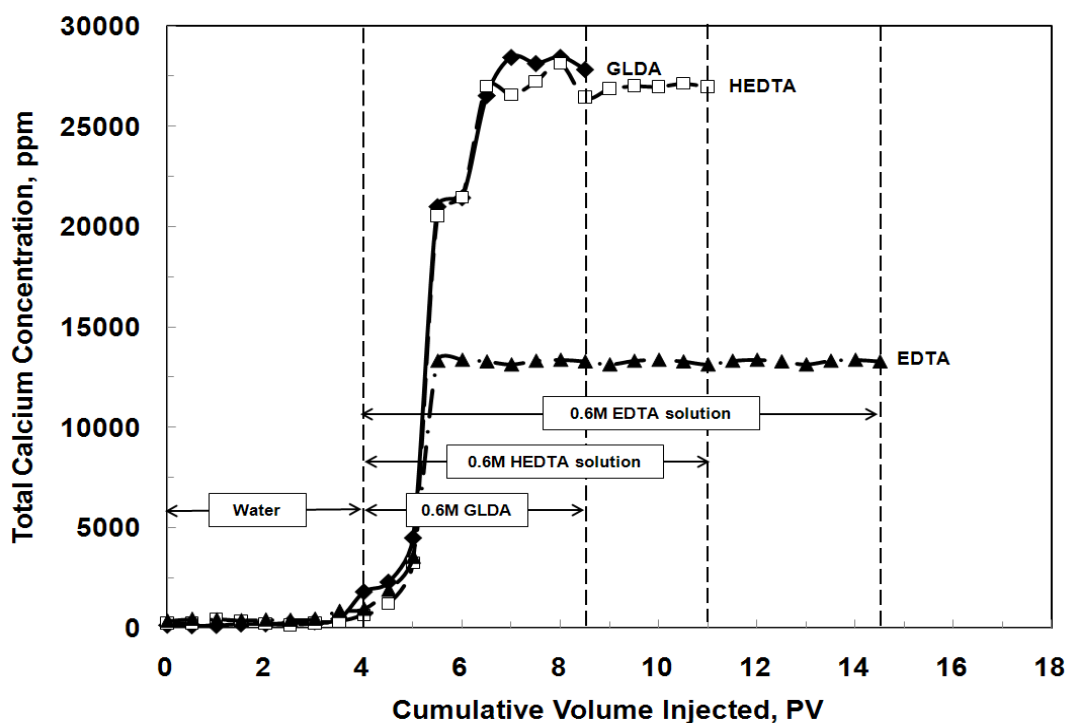
Fig. 87—Different coreflood stages showing the effect of flushing the cores by mutual solvent on the amount of calcium in the coreflood effluent.

Conclusions

In this paper the effect of saturating the calcite core by water, oil, and gas on the performance of GLDA, HEDTA, and EDTA was studied at 300°F. Analytical model was developed to predict the propagation of GLDA in calcite cores and showed good results. The following are the conclusions that were drawn from this study:

1. The analytical model results showed good match with the experimental data indicated the validity of this model.

2. GLDA performed better than HEDTA at low injection rates (0.5 and 1 cm^3/min) and performed the same at the optimum injection rates (2 and 3 cm^3/min).

3. Saturating the core by oil enhanced the performance of the chelating agents in both high and low permeability cores.

4. Chelating agents performance did not change during saturating the cores by nitrogen gas.

5. GLDA at low pH values performed better than HEDTA and EDTA at high temperatu

CHAPTER VI

EFFECT OF LITHOLOGY ON THE FLOW OF CHELATING AGENTS IN POROUS MEDIA DURING MATRIX ACID TREATMENTS

Introduction

Chelating agents such as GLDA, EDTA, and HEDTA have been used to stimulate calcite cores as alternatives to HCl. HCl based stimulation fluids are very corrosive at high temperatures and should be loaded with many additives to reduce corrosion problems. GLDA chelating agent was used to stimulate calcium carbonate cores up to temperature of $300^{o}F$ and at low rates without any face dissolution problems. The dissolution of dolomite by chelating agents has not been thoroughly investigated. Preliminary experiments with EDTA at ambient temperature revealed no significant dolomite dissolution. The dissolution mechanism is probably inhibited by the low stability of the magnesium chelate at that temperature.

In this part we will investigate the ability of GLDA (glutamic-N,N-diaacetic acid) to stimulate dolomite cores as well as calcite cores. GLDA of different pH (1.7, 3 and 13) was used for this study. Dolomite and Indiana limestone cores with dimensions of 1.5 in. diameter and 6 in. length were used. The coreflood experiments were run at different flow rates and different temperatures to determine the optimum rate that the GLDA can create wormholes in both dolomite and calcite cores. Complete fluid analysis for the coreflood effluent was done to study the reaction of GLDA with both dolomite and calcite.

GLDA was very effective in stimulating both dolomite and calcite cores at different pH over a wide range of temperatures (180, 250 and $300^{o}F$). There was an optimum injection rate at which the amount of GLDA needed to create wormholes was minimum. Also, GLDA effectively chelated magnesium and calcium from dolomite cores. GLDA was stable up to temperatures of $300^{o}F$ and the concentration of GLDA after the treatment was the same as that before the treatment, further confirming thermal stability of GLDA at this temperature.

The objective of this part of the study is to:

(1) evaluate the use of GLDA as a stand-alone stimulation fluid for dolomite reservoirs, (2) the effect of GLDA initial pH value on wormhole creation and permeability increase, (3) analyze the coreflood effluent to show the thermal stability and the amount of dissolved calcium and magnesium, and (4) compare the performance of GLDA in both dolomite and calcite cores.

Experimental Studies

Materials

Dolomite cores with permeability range of 50 to 100 md were used in the coreflood experiments. The core samples were cut in a cylindrical form with dimensions of 1.5 in. diameter of 6 and 20 in. lengths.

Different pH values (1.7, 3, 3.8, and 13) of 20 wt% GLDA solutions were prepared from original solutions that were obtained from AkzoNobel. De-ionized water (TDS < 20 ppm) was used to prepare the 20 wt% GLDA solutions.

Dissolution of Dolomite by GLDA

A slurry reactor (**Fig. 5**) was used to determine the ability of GLDA to dissolve dolomite. Complete description for the reactor was given in Chapter II. Portions of Silurian dolomite cores were ground and particles of 20 mesh size were oven dried before use. GLDA/dolomite slurries with a molar ratio of 2 were put in the reaction flask at 125, and 180°F; samples were removed at set time periods. Samples taken for testing from the slurry reactor were filtered using 70 μm filter paper. The clear filtrate was analyzed for both calcium and magnesium concentrations using atomic absorbance spectrometer (AAnalyst 700-flame type) immediately after the test. To study the effect of sodium chloride on the GLDA performance, 5 wt% salt solutions were prepared using sodium chloride. All GLDA solutions were prepared using de-ionized water with total dissolved solids (TDS) of 20 ppm.

Characteristics of Core Samples

Silurian dolomite cores were used in this study. The core permeability ranged 50 to 100 md and average porosity of 20%. The dolomite cores were scanned before the coreflood experiments and cores with fractures were excluded and were not used in the study. The coreflood set up (**Fig. 7**) and the procedure to conduct coreflood experiments were given in Chapter II.

Results and Discussion

Effect of GLDA pH Value on the Dolomite Dissolution

Fig. 88 shows the effect of initial pH value of 20 wt% GLDA solutions (pH 1.7 and 13) on the dolomite dissolution process at 180°F. GLDA at pH 1.7 dissolved more calcium and magnesium than GLDA at pH 13. The total calcium and magnesium concentrations stabilized at 11,500 and 6,600 ppm respectively at pH 1.7. GLDA at pH 13 dissolved less calcium and magnesium, the total calcium and magnesium concentration reached maximum values at 1,500 and 800 ppm

respectively. The calcium and magnesium concentrations were higher at pH 1.7 than that at pH 13, because of the dissolution at low pH was due to both complexation and hydrogen ion attack (four hydrogen in the carboxylic groups-H_4GLDA). The reaction at high pH was due to complexation only (no hydrogen in the carboxylic groups-Na_4GLDA). A complete explanation for the process of GLDA reaction with calcite at different pH values was given by Mahmoud et al. (2010a).

According to the stoichiometric reaction in **Eq. 59**, the molar ratio of calcium/magnesium should be 1. Molar ratio of 1 should be attained in the case of HCl, but here GLDA has more affinity for calcium than magnesium.

$$4HCl + CaMg\ (CO_3)_2 \rightarrow CaCl_2 + MgCl_2 + 2CO_2 + 2H_2O .... \quad (59)$$
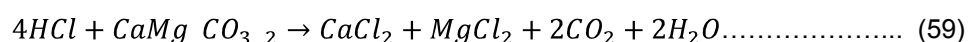
The stability constant of GLDA with calcium is 5.9, and with magnesium is 5.2. Thus GLDA tends to prefer Calcium over Magnesium. The dissolution at pH 1.7 is predominantly due to hydrogen ion attack, in which GLDA reacts as acid; therefore the molar ratio should be close to 1. The calcium/magnesium molar ratio at pH 1.7 was 1.045, because the reaction was due to complexation and hydrogen ion attack (12.5 % complexation and 87.5% hydrogen ion attack, Mahmoud et al. 2010a). The part of complexation contributing in the reaction gave the affinity of GLDA to calcium more than magnesium; therefore, the molar ratio was slightly higher than 1. The reaction at GLDA of pH 13 was due to complexation only; therefore, the calcium/magnesium molar ratio should be more than 1 and close to the ratio of Ca-GLDA stability constant/Mg-GLDA stability constant. The ratio between stability constants for calcium and magnesium was 5.9/5.2 = 1.13. The calcium magnesium molar ratio at pH 13 was 1.125 which was close to 1.13.
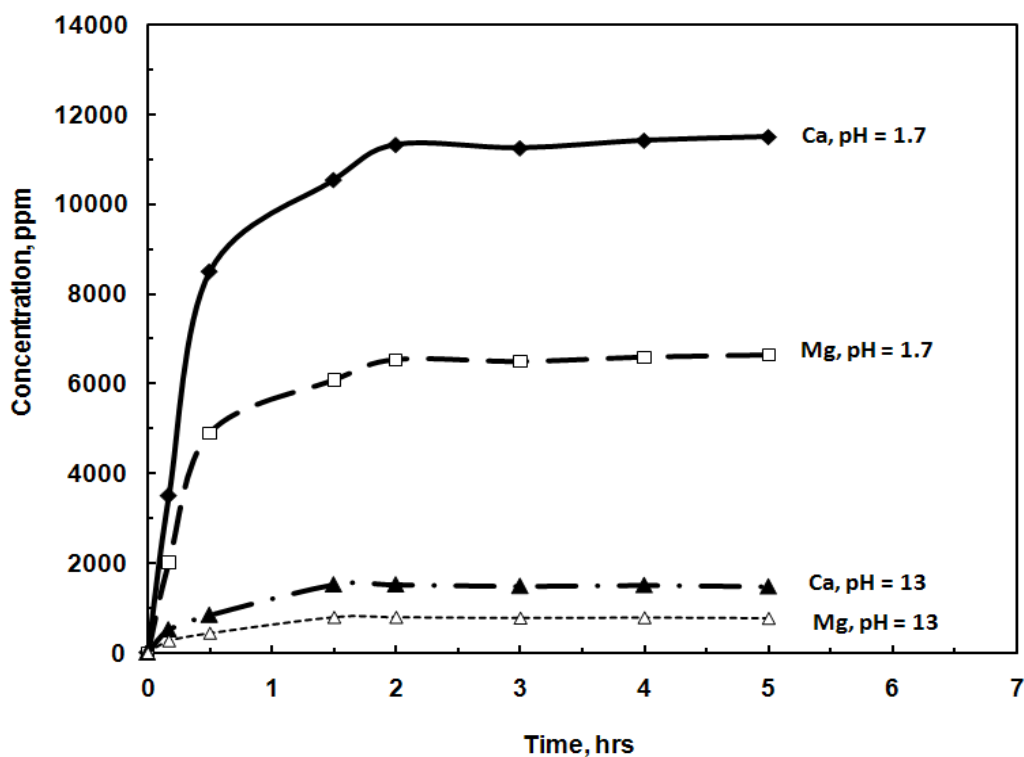
Fig. 88—Effect of initial pH value of GLDA on dolomite dissolution at 180°F.

Effect of Salts

Fig. 89 shows the effect of adding 5 wt% NaCl to 20 wt% GLDA at pH 3.8 on the dolomite dissolution at 180°F. Adding sodium chloride to the GLDA solution increased the amount of dissolved magnesium and calcium by 400 ppm only. This can be attributed to that at 180°F, GLDA at pH 3.8 did not degraded and still thermally stable. Adding 5 wt% NaCl enhanced the thermal stability, and kept the concentration of GLDA constant at 20 wt%. Without adding salt, after heating GLDA to 180°F the concentration was measured after heating and it was 19 wt%. The amount of calcium and magnesium dissolved when adding 5 wt% NaCl was 400 ppm greater than that when no salt was added.
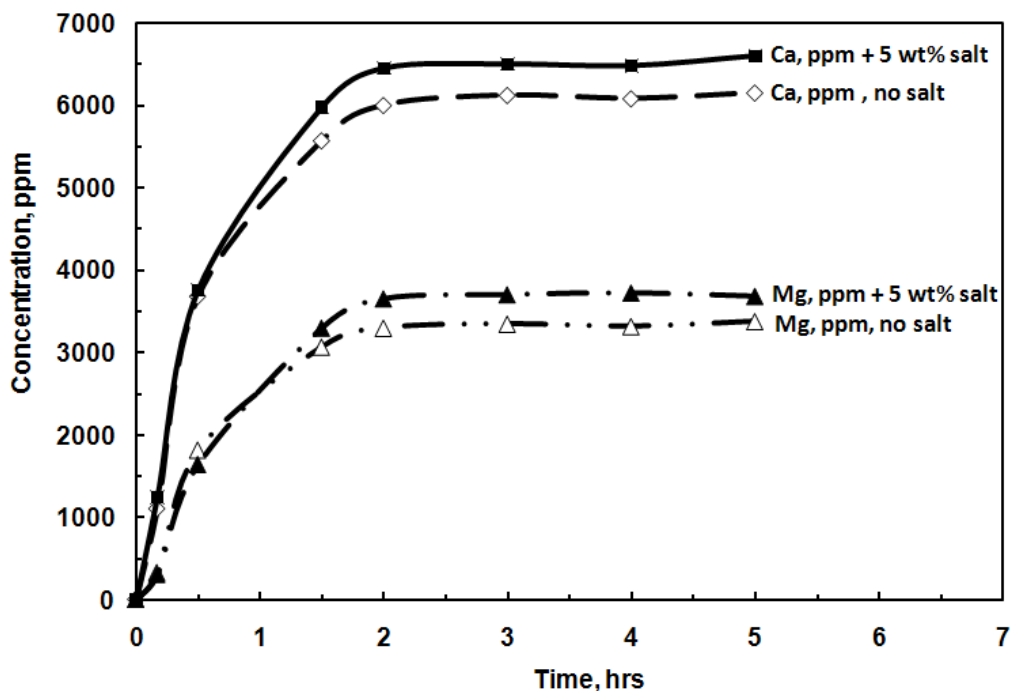
Fig. 89—Effect of salt on dolomite dissolution by GLDA (pH = 3.8) at 180°F.

Comparison between Calcite and Dolomite Dissolution by GLDA

Fig. 90 shows the calcite dissolution by 20 wt% GLDA at pH 1.7 and 13 at 180°F. At the same conditions the amount of dissolved calcium from calcite was greater than both the amount of calcium and magnesium dissolved from dolomite. The calcium concentration in case of calcite stabilized at 22,000 ppm, which was greater than the amounts of both calcium (11,500 ppm) and magnesium (6,600 ppm) that were dissolved from dolomite at the same conditions. As discussed in literature the reaction rate of HCl with calcite was greater than with dolomite at temperatures below 200°F, the same applied here for GLDA. The reaction of GLDA with dolomite produced less amount of cations than that produced in the case of calcite at the same temperature.
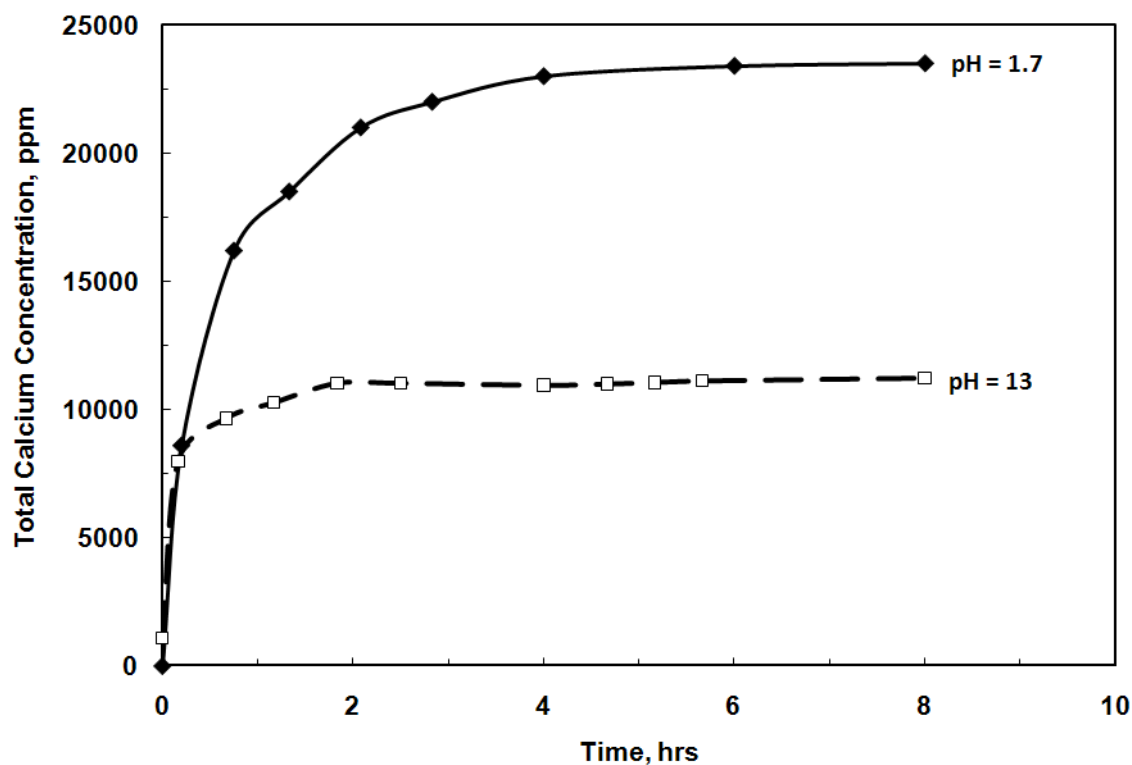
Fig. 90—Calcite dissolution by 20 wt% GLDA at 180°F.

Effect of Temperature on Dolomite Dissolution by GLDA

Fig. 91 shows the effect of increasing the temperature from 125 to 180°F on the amount of dissolved calcium and magnesium by 20 wt% GLDA at pH 3.8. Lund et al. (1973) showed that increasing the temperature during the reaction of HCl with dolomite increased the reaction rate by orders of magnitude. The reaction of GLDA with dolomite at 180°F produced more calcium and magnesium than at 125°F. Increasing the temperature from 125 to 180 °F increased the amount of dissolved calcium from 4,200 to 6,150 ppm, and increased the amount of dissolved magnesium from 2,250 to 3,350 ppm. Increasing the tempearture from 125 to 180°F increased the amount of dissolved calcium and magnesium by more than 30%. GLDA reaction with dolomite was similar to that of HCl with dolomite as the reaction increased with increasing the temperature.
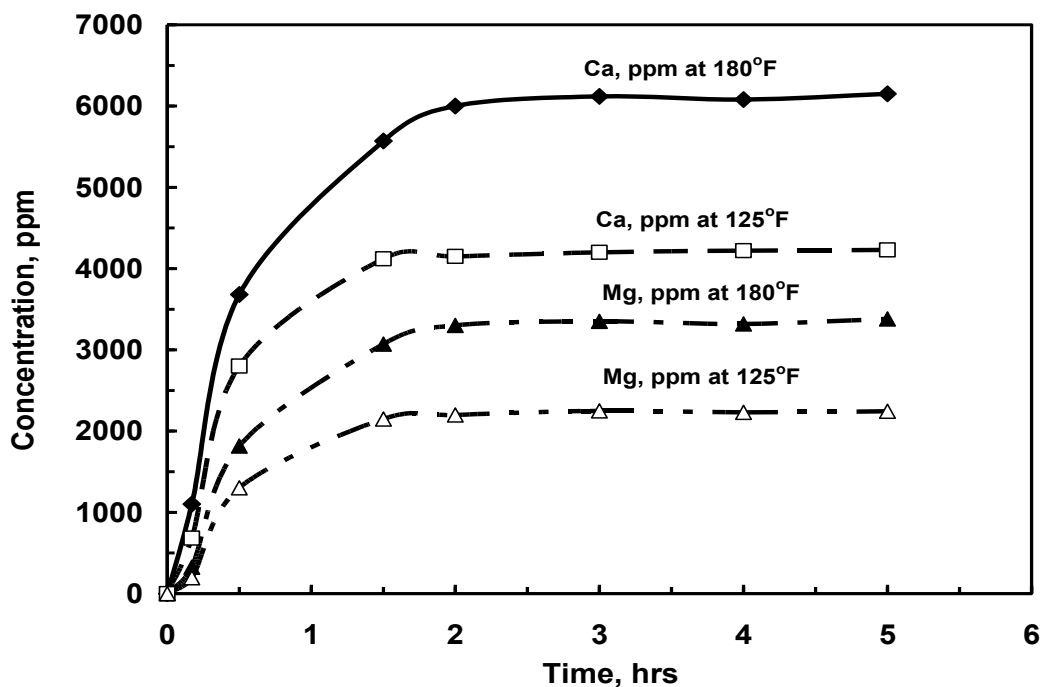
Fig. 91—Effect of temperature on dolomite dissolution by 20 wt% GLDA at pH 3.8.

Optimum Injection Rate in the Coreflood

Fig. 92 shows the volume of GLDA required to create wormholes as a function of injection rate for 20 wt% GLDA at pH 3 and 200°F. Increasing the injection rate from 1 to 9 cm^3/min resulted in increase in the pore volume required to create wormholes from 7.8 to 15.5 PV. The optimum injection rate for 1N HCl at 70°C (158°F) was well defined at 3.8 cm^3/min (Hill and Schechter 2000). In case of both calcite and dolomite GLDA performed better at low injection rates than at high injection rates. This can be attributed to the increased time of reaction allowed more calcium and magnesium to be dissolved. From this figure, the reaction of GLDA with dolomite was lower than that with calcite, because of the volume required to create wormholes was high in the case of dolomite than calcite. The PV$_{bt}$ in the case of dolomite was almost twice that for calcite at 200°F. Injecting GLDA at injection rates above this rate resulted in sharp increase in the pore volumes required to breakthrough the core. Injecting GLDA at low rates allowed more contact time between the fluid and dolomite and enhanced the dissolution process.
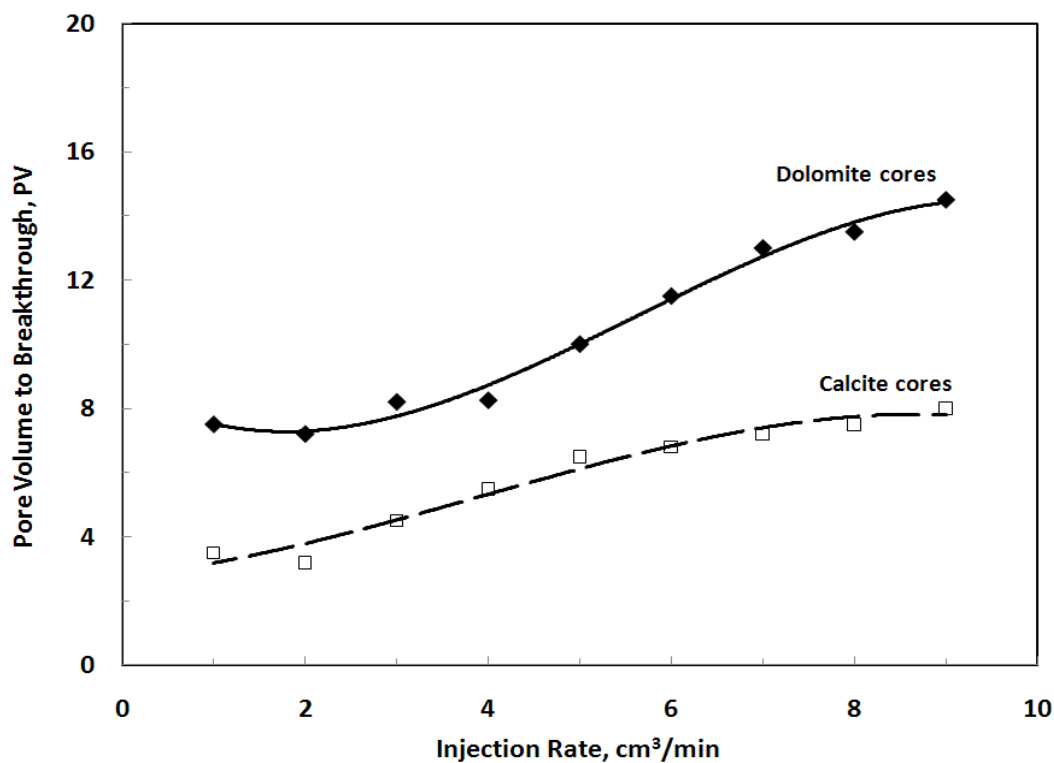
Fig. 92—Optimum injection rate for GLDA at pH 3 at 200°F.

Effect of GLDA pH Value on the Coreflood Experiments

Coreflood experiments were run using 20 wt% GLDA solutions at 5 cm^3/min and 300°F to investigate the effect of GLDA initial pH value on the creation of wormholes during the coreflood experiments. Coreflood experiments were run at GLDA initial pH values of 1.7, 3, 3.8, 11, and 13.

    Fig. 93 shows the calcium and magnesium concentrations at pH 1.7. Seven pore volumes were injected to breakthrough the core, and the core permeability was increased from 75 to 785 md ($k_{final}/k_{initial}$ = 10). The amount of calcium reached a maximum value at 18,000 ppm and the magnesium reached a maximum value at 12,500 ppm.
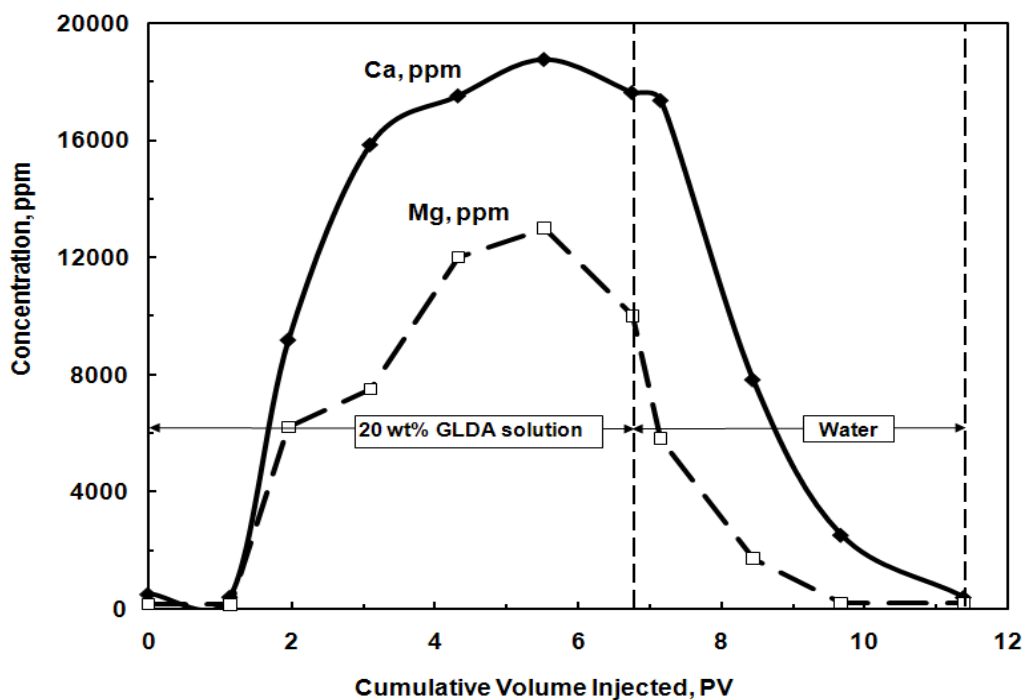
Fig. 93—Effluent analysis for GLDA at pH 1.7 and 5 cm³/min at 300°F.

Fig. 94 shows image profile for a slice from the dolomite core before the coreflood experiments. In this image there was no fractures, no vugs, and this applied for all slices taken from this core. The CT number had an average value of 2,500 before the coreflood experiments. **Fig. 95a** shows the 2D CT scan image after the coreflood experiment. There are a lot of wormholes formed after injecting the core by GLDA. Twenty slices were imaged by the CT scan tomography, and there was at least one wormhole in each slice indicating the effectiveness of GLDA to create wormholes in dolomite cores at low pH.
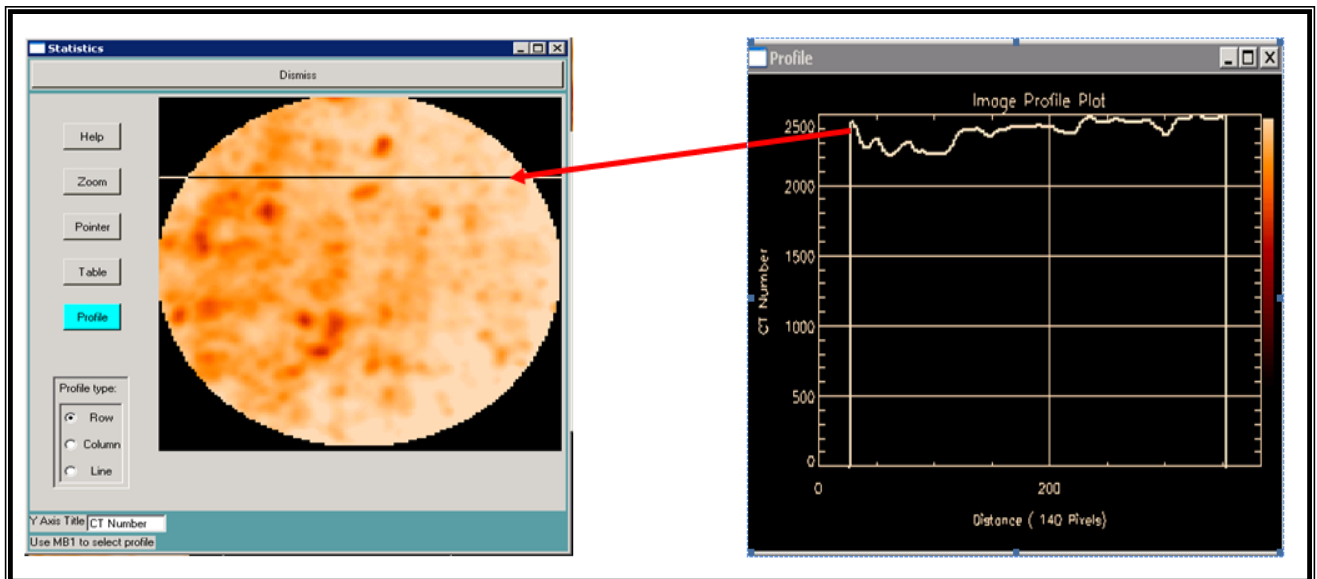
Fig. 94—Image profile for a slice of dolomite core before the coreflood experiment.

| (a) injection rate = 5 cm^3/min | (b) injection rate = 2 cm^3/min |
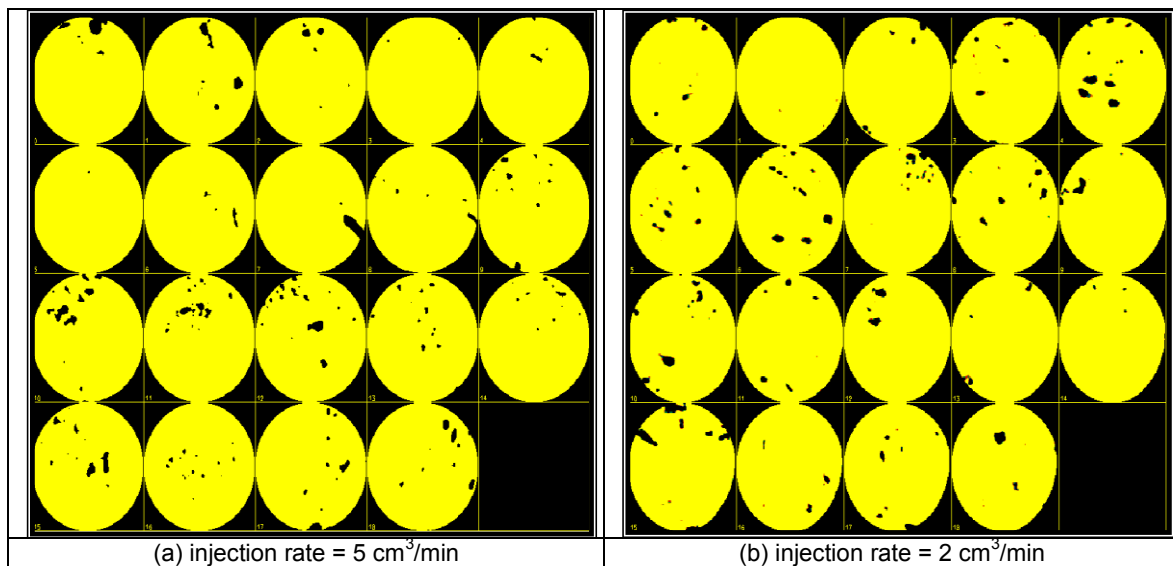
Fig. 95—2D CT scan images after the coreflood experiment at 300°F, GLDA pH = 1.7.

Fig. 96 shows the calcium and magnesium concentrations for the same previous conditions (1.7 pH and 300°F) but at lower flow rate (2 cm^3/min). Lowering the injection rate from 5 to 2 cm^3/min increased the amount of calcium and magnesium in the effluent samples. The calcium concentration increased from 18,000 to 25,000 ppm after decreasing the injection rate from 5 to 2 cm^3/min. The same applied for magnesium concentration it increased from 12,500 to 14,500 ppm after decreasing the injection rate. **Fig. 95b** shows the 2D CT scan images for the core after the coreflood experiment at 2 cm^3/min. The wormholes number increased due to decreasing the injection rate. The core permeability increased from initial permeability of 50 md before the coreflood experiment to a final permeability of 730 md after the experiment ($k_{final}/k_{initial}$ = 15).
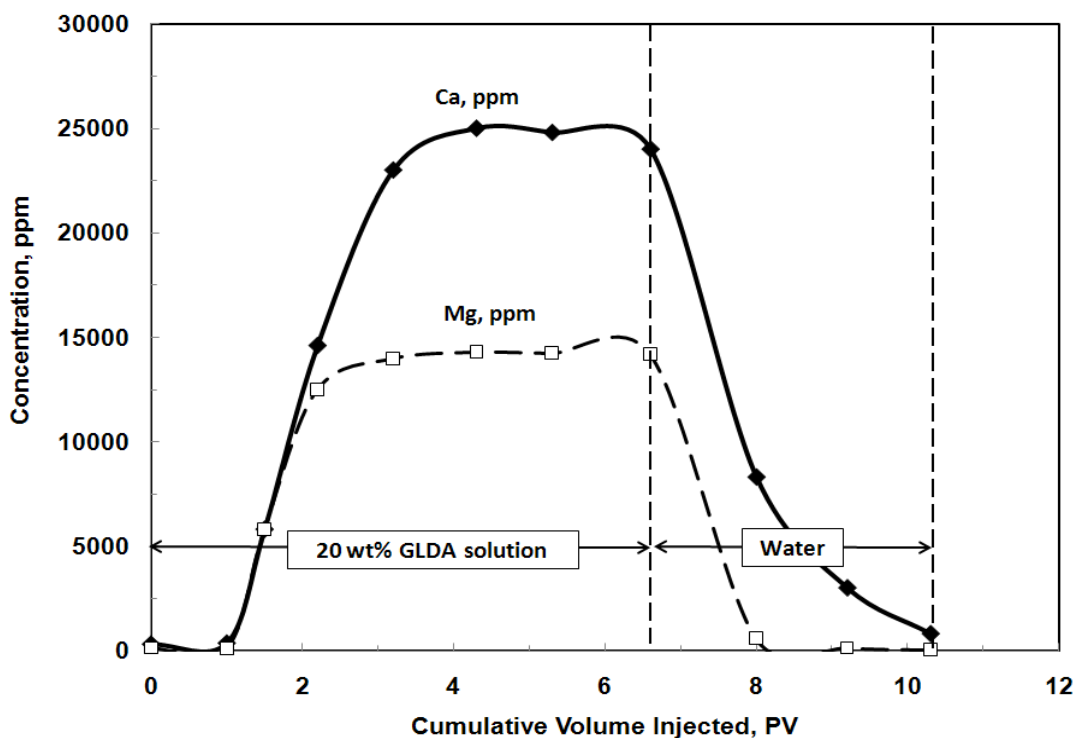
Fig. 96— Effluent analysis for GLDA at pH 1.7 and 2 cm^3/min at 300°F.

Fig. 97 shows the coreflood effluent analysis for calcium and magnesium. The coreflood experiment was performed using 20 wt% GLDA at pH 3 at 5 cm^3/min, and 300°F. The performance of the GLDA at pH 3 was close to GLDA at pH 1.7 at the same conditions of injection rate. The calcium concentration reached a maximum value of 16,400 ppm (it was 18,000 ppm in case of GLDA at pH 1.7), and the magnesium concentration reached a maximum

value of 9,500 ppm (it was 12,500 ppm in case of GLDA at pH 1.7). The difference in the ability of GLDA at pH 3, and 1.7 to dissolve dolomite and produce calcium and magnesium was small. This can be attributed to that the structure of GLDA at pH 3 still contains three hydrogen atoms in the carboxylic groups ($H_3NaGLDA$), which also, can act as acid. The core permeability increased from 55 to 490 md with $k_{final}/k_{initial} = 9$.
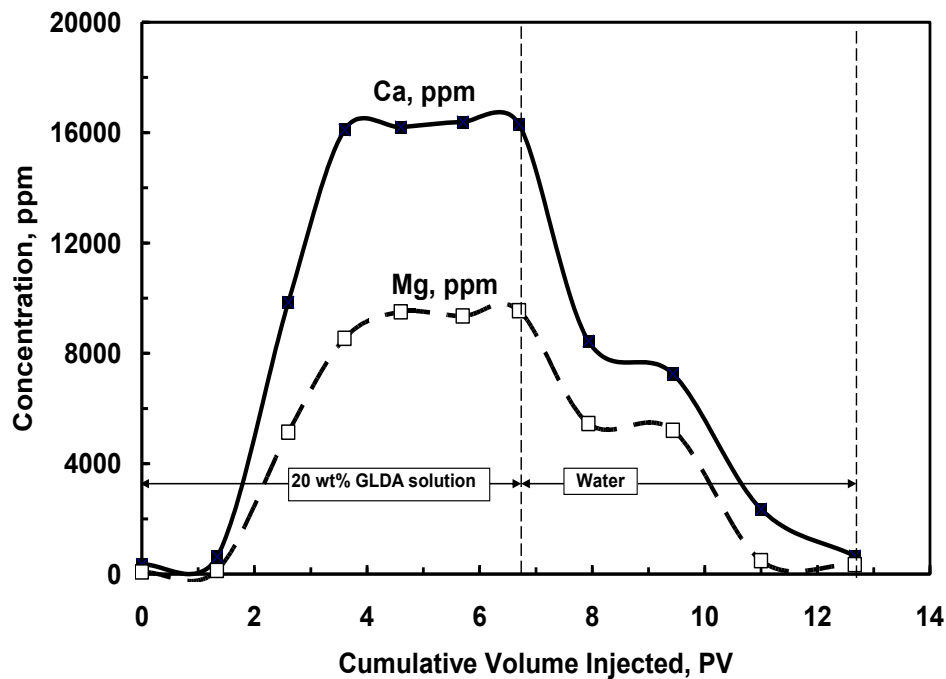
Fig. 97—Effluent analysis for GLDA at pH 3 and 5 cm^3/min at 300°F.

Fig. 98 shows the total concentrations of calcium and magnesium in the coreflood effluent samples. The coreflood experiments shown in Fig. 98 were performed using 20 wt% GLDA at pH 13 at injection rate of 2 and 5 cm^3/min, and 300°F. At injection rate of 5 cm^3/min the calcium concentration reached a maximum value at 1,900 ppm (compared to 18,000 ppm at pH 1.7). GLDA at pH 13 has no hydrogen (Na_4GLDA) and the reaction was due to complexation only. The same for magnesium concentration it reached its maximum value at 950 ppm (compared to 12,500 at pH 1.7). GLDA at pH 13 had low efficiency in stimulating dolomite cores compared with GLDA at pH 1.7, and 3. Decreasing the injection rate from 5 to 2 cm^3/min allowed more time for complexation and more calcium and magnesium were complexed. The calcium concentration reached 2,150 ppm and the magnesium concentration increased from 950 at 5 cm^3/min to 1,150

ppm at 2 cm^3/min. The core permeability increased from 65 to 110 md at 5 cm^3/min ($k_{final}/k_{initial}$ = 1.7), while it increased from 85 to 168 md at 2 cm^3/min ($k_{final}/k_{initial}$ = 2.0). Decreasing the injection rate from 5 to 2 cm^3/min, enhanced the complexation of calcium and magnesium by GLDA at pH 13, and it also enhanced the permeability increase. There was no wormholes in this case, we just investigated the effect of injecting 7.5 PV on enhancement the permeability of the dolomite core.
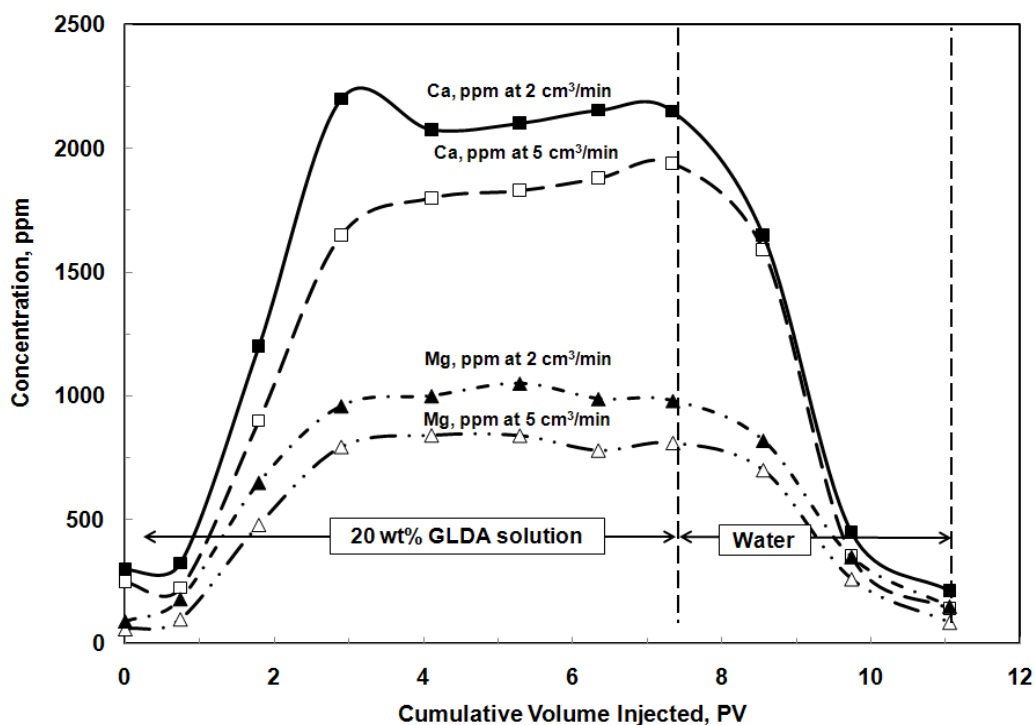
Fig. 98—Effluent analysis for GLDA at pH 13 and injection rates of 5, and 2 cm^3/min at 300°F.

Thermal Stability of GLDA

The coreflood effluent samples were analyzed for the GLDA concentration. The effluent analysis for GLDA concentration showed a high thermal stability at high pH values (11&13), the concentration before and after the coreflood experiments was 20 wt%. The GLDA at pH 11 and 13 showed high thermal stability after the coreflood experiments performed at 300°F. GLDA at pH 1.7 used in the coreflood experiments was GLDA at pH 3 blend with HCl to get pH of 1.7, the analysis in the coreflood effluent samples after the coreflood experiments showed a concentration of 19 wt%. The initial concentration was 20 wt%; therefore, GLDA at pH 1.7

showed thermal stability of 95% at 300°F in the coreflood experiments. GLDA at pH 3 and 3.8 also, showed a good thermal stability, as the average samples concentration in the coreflood effluent was 19 wt% showing a 95% thermal stability at 300°F in the coreflood experiments.

Effect of GLDA pH value on the Ca/Mg Molar Ratio

Coreflood experiments were performed using 20 wt% GLDA at five pH values (1.7, 3, 3.8, 11, and 13). The coreflood experiments were run at 5 cm³/min and 300°F. **Table 22** shows the total amounts of calcium and magnesium that were dissolved during the coreflood experiments. **Fig. 99** shows the calcium magnesium molar ratios for the samples collected after the coreflood experiments. The amount of the dissolved calcium and magnesium were the highest at pH 1.7, because GLDA at pH 1.7 reacts with dolomite with both hydrogen donation and complexation. The amount of the dissolved calcium and magnesium was the lowest at pH 13 because the reaction of GLDA with dolomite was due to complexation only and there was no hydrogen donation.

The calcium/magnesium molar ratio was the lowest at pH 1.7 and was 1.055 which is closer to 1. GLDA at pH 1.7 performed close to HCl at which the calcium/magnesium ratio should be 1. The calcium/magnesium molar ratio increased as the GLDA initial pH value increased, it reached its maximum value of 1.137 at pH 13. As the GLDA pH value increased the reaction due to complexation increased, and reached maximum at pH 13. The calcium/magnesium molar ratio at pH 13 (1.137) was close to the ratio between Ca-GLDA stability constant and Mg-GLDA stability constant (5.9/5.2 = 1.135).

Table 22—CALCIUM/MAGNESIUM MOLAR RATIO DURING THE COREFLOOD EXPERIMENTS			
GLDA Initial pH Value	Amount of calcium Dissolved, g	Amount of Magnesium Dissolved, g	Calcium/Magnesium Molar Ratio
1.7	3.780	2.150	1.055
3	2.050	1.160	1.062
3.8	1.053	0.577	1.092
11	0.650	0.347	1.125
13	0.531	0.280	1.137
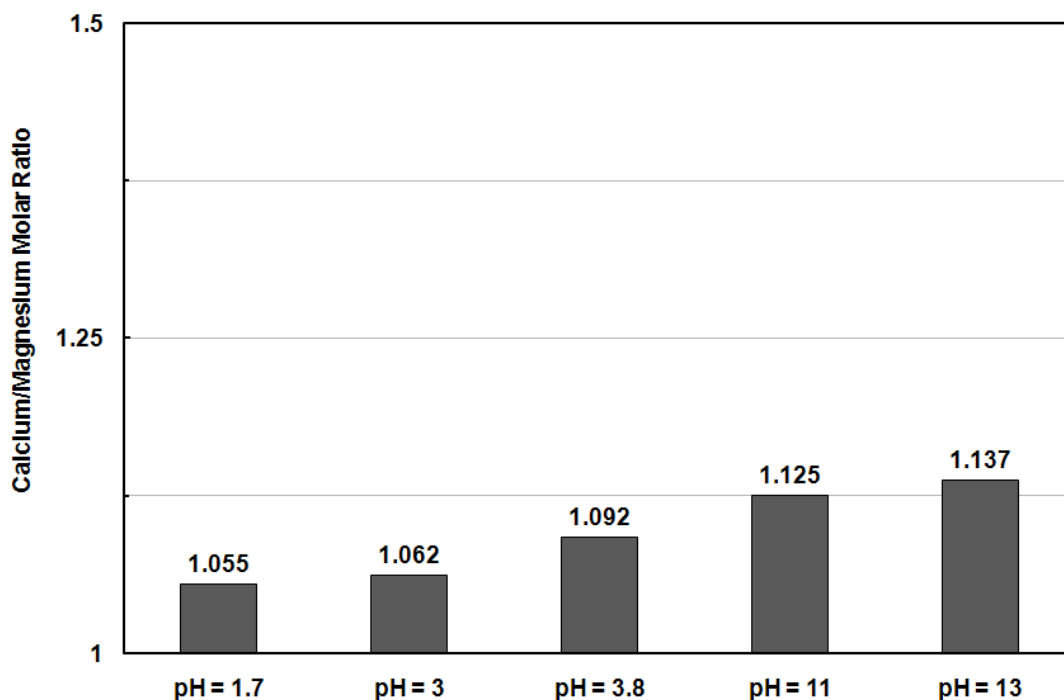
Fig. 99—Calcium/magnesium molar ratio for the coreflood effluent samples at 5 cm³/min and 300°F at different 20 wt% GLDA solutions pH.

Conclusions

In this part GLDA was used to stimulate dolomite cores at high temperatures. GLDA was effective in stimulating both dolomite and calcite cores. The following are the conclusions that were drawn from this part of the study:

1. GLDA reaction with calcite was higher than that with dolomite at 180°F.

2. GLDA at different pH values (1.7, 3, 3.8, 11, and 13) effectively stimulated dolomite cores as it chelated both calcium and magnesium.

3. Unlike HCl, GLDA has no well-defined optimum injection rate with dolomite. Decreasing the rate enhanced the dissolution and decreased the volume required to create wormholes.

4. GLDA was thermally stable during the coreflood experiments up to 300°F.

5. The calcium/magnesium molar ratio was the lowest and close to 1 at pH 1.7 (1.055), and was the highest and close to Log $K_{Ca-GLDA}$/Log $K_{Mg-GLDA}$ (1.135) at pH 13 which was 1.137.

CHAPTER VII

SANDSTONE ACIDIZING USING A NEW CLASS OF CHELATING AGENTS

Introduction

The objective of stimulation of sandstone reservoirs is to remove the damage caused to the production zone during drilling or completion processes. Many problems may occur during sandstone acidizing with HCl/HF mud acid. Among those problems: decomposition of clays in HCl acids, precipitation of fluosilicates, precipitation of aluminum fluorides, silica-gel filming, colloidal silica-gel precipitation, and mixing between various stages of the treatment.

In this part of the study GLDA was used to stimulate sandstone cores. Berea sandstone cores were used in this study. Different GLDA solution pH values (1.7, 3, 3.8, 11, and 13) were used. The sandstone cores were scanned before and after the treatment to investigate the effect of GLDA on the core using the CT scan. The effluent samples were analyzed for calcium, magnesium, aluminum, and iron using the ICP to show the ability of GLDA on the complexation of these ions. Coreflood experiments were run at temperatures ranged from 200 to 300°F and the concentration of GLDA was determined after the treatment. The effect of flow rate, volume of GLDA, and GLDA pH was investigated on the Berea sandstone cores. Different correlations were used to determine the core permeability after the treatment, and the correlation that gave the minimum error was determined.

GLDA showed a strong ability in chelating calcium, magnesium, and iron, but chelated small amounts of the aluminum ions from the sandstone cores. At 300°F GLDA at different pH values was able to enhance the core permeability. Decreasing the injection rate from 5 to 2 cm^3/min increased the contact time between the fluid and the rock and increased the amount of dissolved ions. X-ray CT scan showed a porosity increase after the treatments. The concentration of GLDA after the coreflood experiment was almost the same before the treatment showing a high thermal stability up to 300°F in the coreflood experiment. Lambert correlation was found to be the best correlation to predict for the core permeability after treating Berea sandstone cores by 20 wt% GLDA solutions.

In this part, GLDA chelating agent will be tested on sandstone cores, therefore, the objective of this part is to: (1) assess the use of GLDA chelating agent in stimulating Berea sandstone cores, (2) study the effect of initial GLDA pH value, injection rate, volume of GLDA, and temperature on the permeability enhancement of Berea cores, (3) use the CT scan to evaluate the use of GLDA to stimulate Berea sandstone cores, and (4) find the best correlation that can be used to determine the core permeability treated by GLDA.

Experimental Studies

Materials

GLDA Chelating agent was used in this part of the study was supplied from AkzoNobel. The original concentration of the chemical was 40 wt% at the different pH values. A concentration of 0.6M GLDA was used at different pH values. Core plugs were cut in a cylindrical form from Berea sandstone blocks of dimensions 9 x 9 x 9 in. The XRD results for the Berea sandstone cores are listed in **Table 23**.

Table 23—MINERAL COMPOSITION FOR DIFFERENT SANDSTONE CORES	
Mineral	**Wt%**
Quartz	86
Dolomite	1
Calcite	2
Feldspar	3
Kaolinite	5
Illite	1
Chlorite	2

Experimental Procedure

Coreflood experiment were performed using the set up shown in **Fig. 7**, the core was first loaded into a Hassler sleeve core holder at an overburden pressure of 2,000 psig and temperatures up to 300°F. The core was subjected to vacuum for an hour. Then, it was saturated with injection water until the brine permeability became constant. The brine used in the experiments was 5 wt% NaCl. A 1000 psi back pressure was applied in the coreflood experiments to achieve good saturation and displacement of the fluid and to keep CO_2 in solution. The pore volume of the core was determined after saturating the core by dividing the difference between the saturated core and dry core by the brine density (1.034 g/cm^3 at 22°C). The cores were CT-scanned dry, saturated with 5 wt% NaCl, and after the treatment. Before flooding the cores by chelating agent solution, the core was heated-up to the test temperature for at least three hours to ensure the stabilization of the core and fluid temperatures. The effluent samples were collected in all the coreflood experiments to analyze for calcium, magnesium, iron, aluminum, and silicon using the ICP.

Results and Discussions

Using GLDA to Stimulate Berea Sandstone Cores

The first coreflood experiment was run using 0.6M GLDA at pH 3.8 at 300°Fand 5 cm^3/min. GLDA was able to chelate calcium, magnesium, iron, and small amount of aluminum from the sandstone core, **Fig. 100**. GLDA start to react with the minerals in Berea core such as calcite, dolomite, chlorite, etc, and chelated calcium, magnesium, iron, and aluminum. The concentration of calcium, magnesium, iron, and aluminum started to increase after injecting one pore volume of GLDA. Injecting 7 PV of GLDA at 300°F increased the core permeability from an initial value of 95 to 145 md. The amount of ions that were chelated or dissolved by the 0.6M GLDA were 1.98, 1.93, 0.7, and 0.135 g of calcium, iron, magnesium, and aluminum respectively. **Figs. 101 and 102** show the CT scan results for a slice of the Berea core before and after the treatment by GLDA. The CT number decreased from an average initial value of 1720 to an average value of 1610 confirming the effectiveness of GLDA in stimulating the Berea sandstone core.
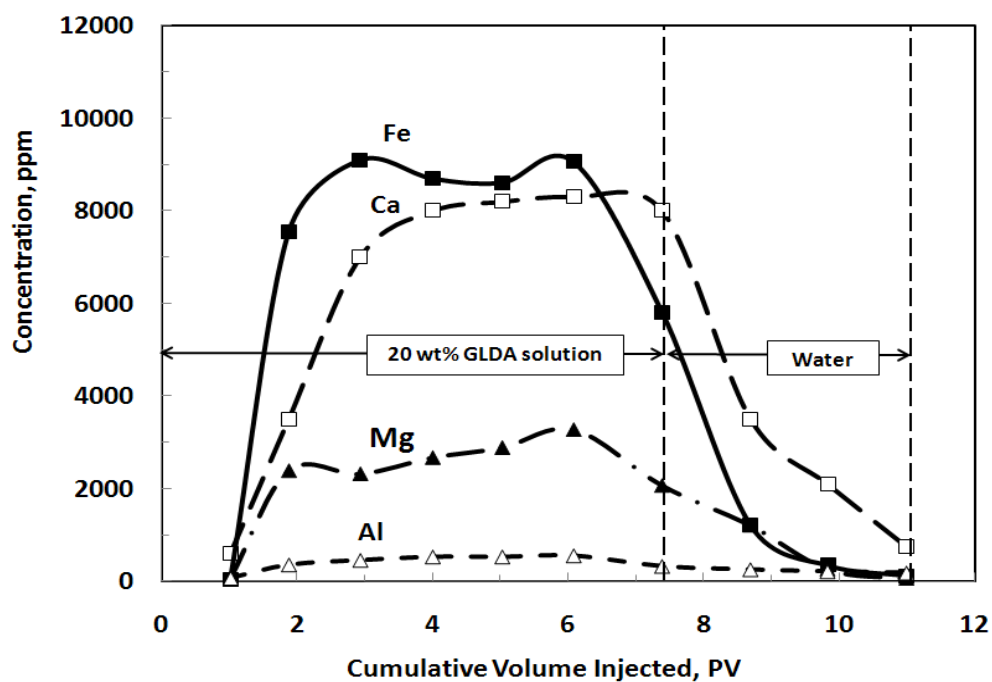
Fig. 100—Analysis of the coreflood effluent samples for Berea sandstone cores treated by 0.6M GLDA at pH 3.8, 300°F, and 5 cm^3/min.
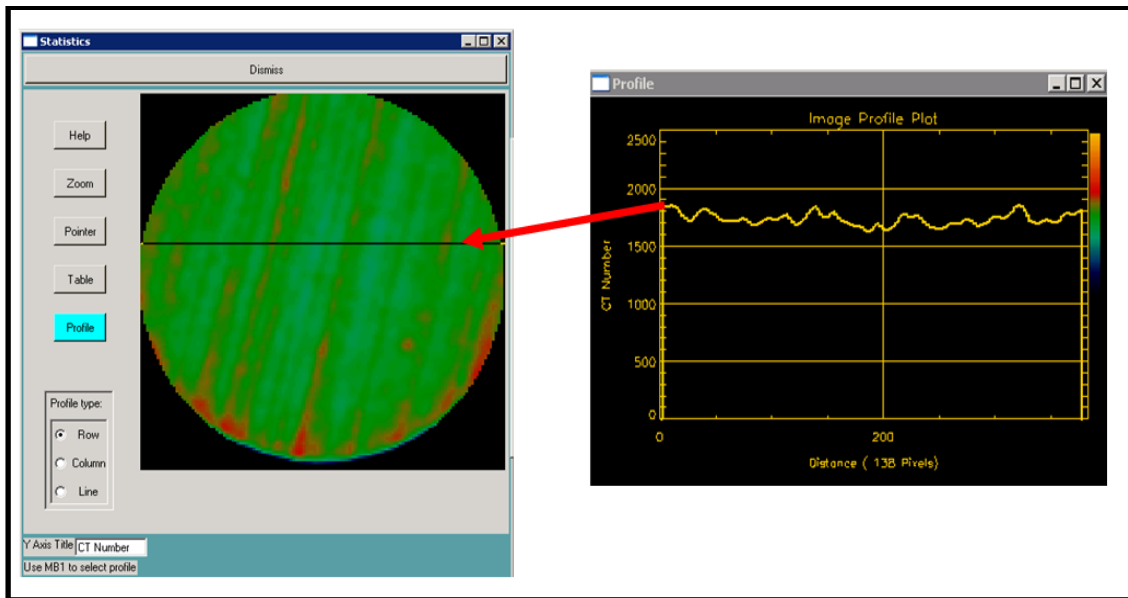
Fig. 101—2D image for a slice of saturated Berea sandstone core before the treatment showing average CT number of 1720.
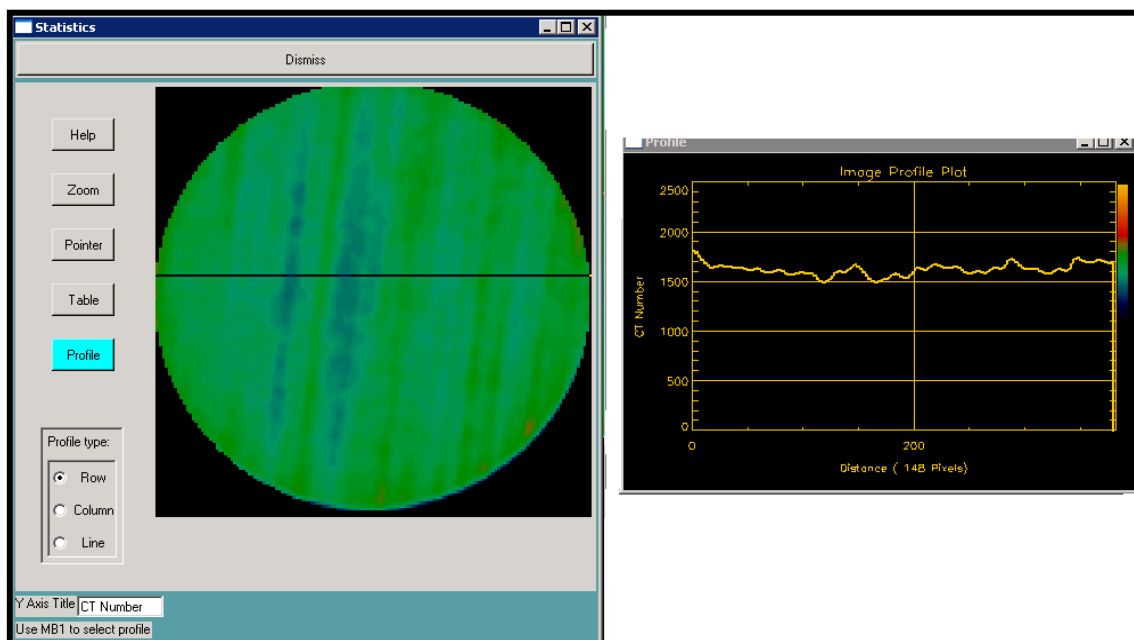
Fig. 102—2D image for a slice of saturated Berea sandstone core after the treatment showing average CT number of 1610.
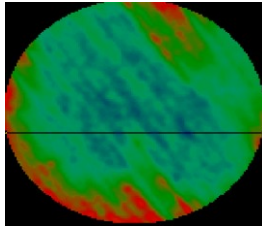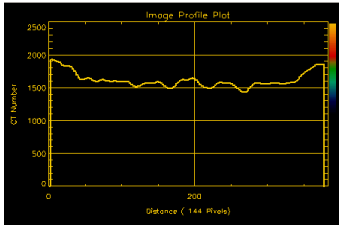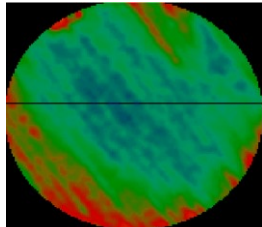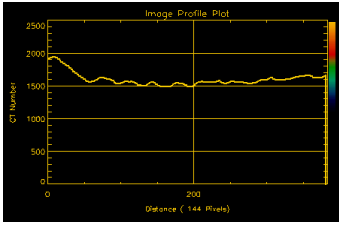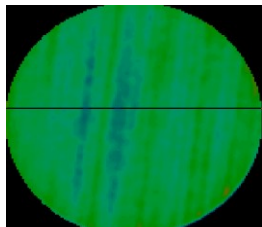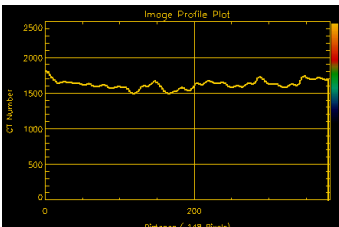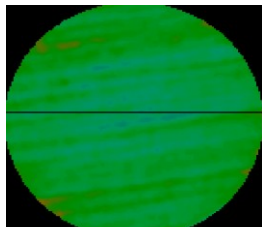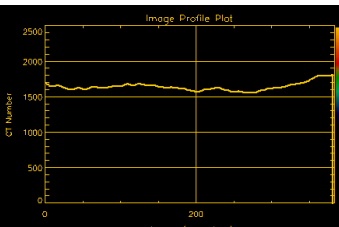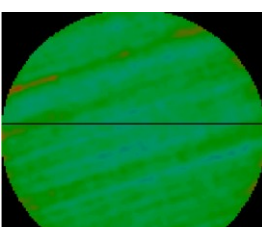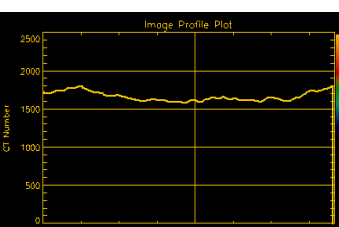
Effect of GLDA pH Value on the Permeability Ratio of Berea Cores

Fig. 103 shows the effect of initial pH value of 0.6M GLDA on the Berea sandstone cores at a flow rate of 5 cm^3/min and 300°F. Five pH values of 0.6M GLDA were used, namely: 1.7, 3, 3.8, 11, and 13. All the GLDA solutions used increased the permeability of Berea sandstone cores indicating the compatibility of all pH values of the GLDA solutions with the clays found in the Berea sandstone cores. **Table 24** shows the rock properties of the five coreflood experiments were run at the same conditions and the volume of injected GLDA in all experiments was 7 PV. GLDA at pH 1.7 was able to double the permeability of the Berea sandstone core, increasing the pH from 1.7 to 13 decreased the efficiency of GLDA, but still there was an increase in the permeability ratio. GLDA at high pH did not cause precipitations inside the core, CT scan images for cores treated by GLDA at different pH value showed a decrease in the CT number and there was no anomalies in the images which means there was no precipitation even at high pH values (11and 13). GLDA at pH 11 and 13 almost performed the same during the coreflood experiments as it increased the permeability with the same ratio ($K_{final}/K_{initial}$ = 1.16). **Table 25** shows the increase in the average CT number for different cores treated by different pH values using 0.6M GLDA at 300°F and 5 cm^3/min. The decrease in CT number was the maximum at pH 1.7 as it decreased from 1720 to an average value of 1510. Increasing the pH value from 1.7 to 13 reduced the decrease in the CT number as it decreased from 1735 to 1705 at pH 13. The results from the CT number in Table 25 confirmed the results obtained in Fig. 102 showing a strong relation between the final core permeability and the CT number of the Berea sandstone cores.

Table 24—EFFECT OF INITIAL pH VALUE OF 0.6M GLDA SOLUTIONS ON THE PERMEABILITY RATIO FOR BEREA SANDSTONE CORES AT 5 cm^3/min AND 300°F

pH	$k_{initial}$, md	k_{final}, md	$k_{final}/k_{initial}$
1.70	82	165	2.01
3.00	82	160	1.95
3.80	95	145	1.54
11.0	95	110	1.16
13.0	95	110	1.16

Table 25—EFFECT OF INITIAL pH VALUE OF 0.6M GLDA SOLUTIONS ON THE AVERAGE CT NUMBER FOR BEREA SANDSTONE CORES AT 5 cm³/min AND 300°F

Initial pH	Slice Image	Slice Profile	CT no. before	CT no. after
1.70			1725	1510
3.00			1715	1540
3.80			1720	1610
11.0			1750	1710
13.0			1735	1705
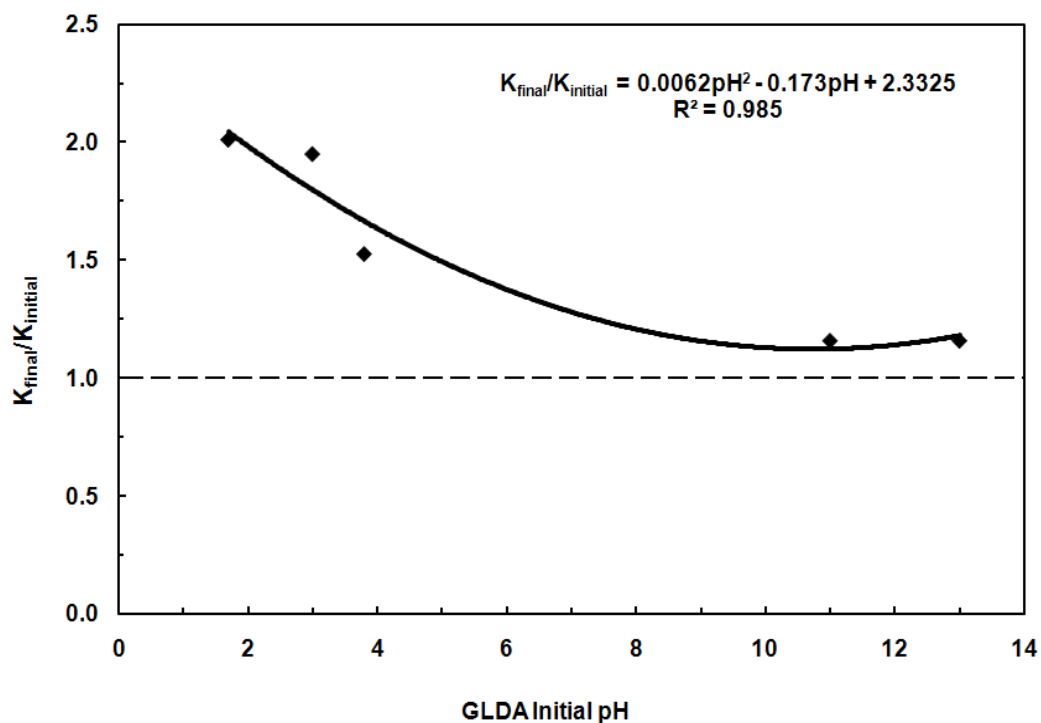
Fig. 103—Effect of the initial pH value of GLDA on the permeability ratio for Berea sandstone cores treated at 300°F and 5 cm³/min using 0.6M GLDA.

Effect of Injection Rate on the Permeability Ratio of Berea Cores

Fig. 104 shows the effect of injection rate of 0.6M GLDA at pH 3.8 on the permeability ratio of Berea sandstone cores. Three coreflood experiments with three different injection rates were performed. The injection rates used are 2, 5, and 8 cm³/min, and the injected GLDA volume was constant in the three coreflood experiments, i.e., 7 PV were injected in each experiment. The core permeability increased in the three experiments at the three injection rates. The maximum increase in the core permeability was attained at the lowest injection rate, 2 cm³/min, in which the contact time between the GLDA and the Berea core was increased and allowed more time for reaction. At 2 cm³/min the GLDA solution dissolved more calcium, magnesium, and iron than at 8 cm³/min. The permeability ratio was 1.86, 1.54, and 1.2 at injection rates of 2, 5, and 8 cm³/min respectively. From these results we recommend that GLDA should be injected at low injection rate to attain the maximum possible increase in permeability for the treated sandstone formations. At all injection rates there was no fines migration or any disturbance in the pressure performance indicating the compatibility of GLDA with clays (kaolinite, chlorite, and illite) existed in the Berea sandstone cores.
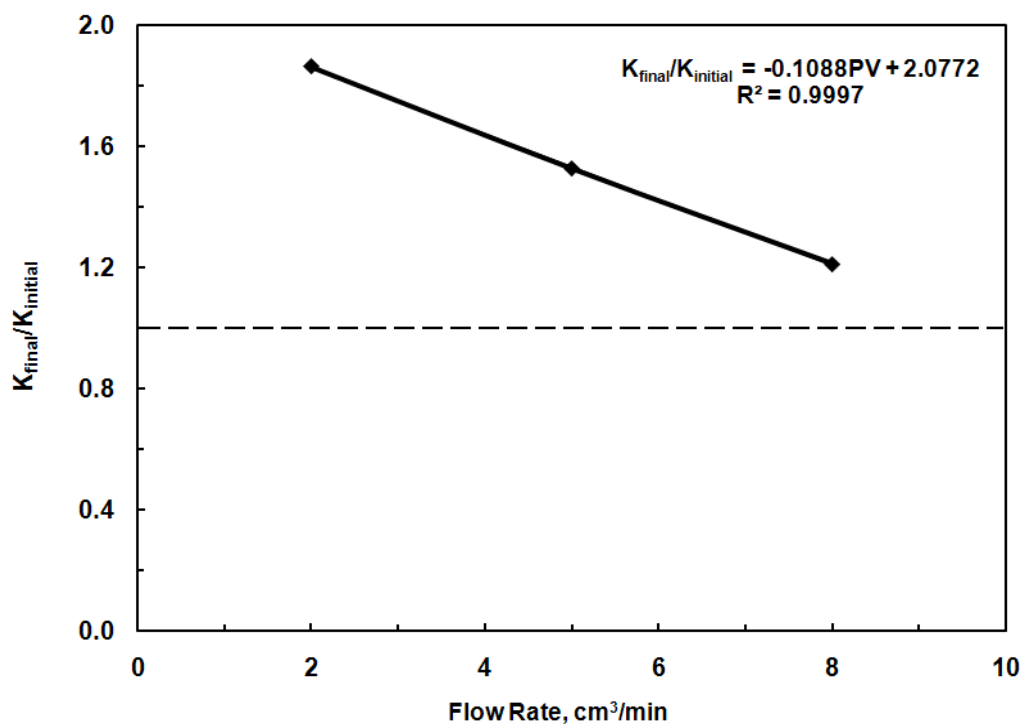
Fig. 104—Effect of injection rate on the permeability ratio for Berea sandstone cores treated at 300°F and 5 cm³/min using 0.6M GLDA at pH 3.8.

Effect of the Injected Volume of GLDA on the Permeability Ratio

Fig. 105 shows the effect of injected volume of 0.6M GLDA at pH 3.8 on the permeability ratio of Berea sandstone cores. All the coreflood experiments were performed at 5 cm³/min, and 300°F. Different pore volumes of GLDA were injected through the Berea sandstone cores, namely; 1.5, 4.5, 7, and 10 PV. The relation between the permeability ratio ($K_{final}/K_{initial}$) and injected volume of GLDA was a second degree polynomial. Injecting 10 PV of 0.6M GLDA (pH = 3.8) at 5 cm³/min and 300°F increased the core permeability more than twice ($K_{final}/K_{initial}$ = 2.16).

Fig. 106 shows the amount of dissolved ions as a function of the injected volume of GLDA at the same previous conditions. Generally we can say that the ability of GLDA to chelate iron was greater than its ability to chelate calcium and magnesium. This can be attributed to the stability constant of GLDA with iron ($LogK_{Fe-GLDA}$ = 11.7) is greater than the stability constant of GLDA with calcium ($LogK_{Ca-GLDA}$ = 5.9). The amount of iron was greater than that of calcium at the different injected PV of GLDA. Injecting more volume of GLDA through the Berea sandstone cores while other factors are constant increased the amount of dissolved calcium, iron, and magnesium in the coreflood effluent samples. The molar ratio of calcium to magnesium was

greater than unity here because there are two sources for calcium calcite and dolomite and the sources of magnesium are dolomite and chlorite. It was easy for GLDA to chelate calcium from calcite and dolomite rather than to chelate magnesium from chlorite.

$$K_{final}/K_{initial} = 0.0171PV^2 - 0.0865PV + 1.3153$$
$$R^2 = 0.9983$$
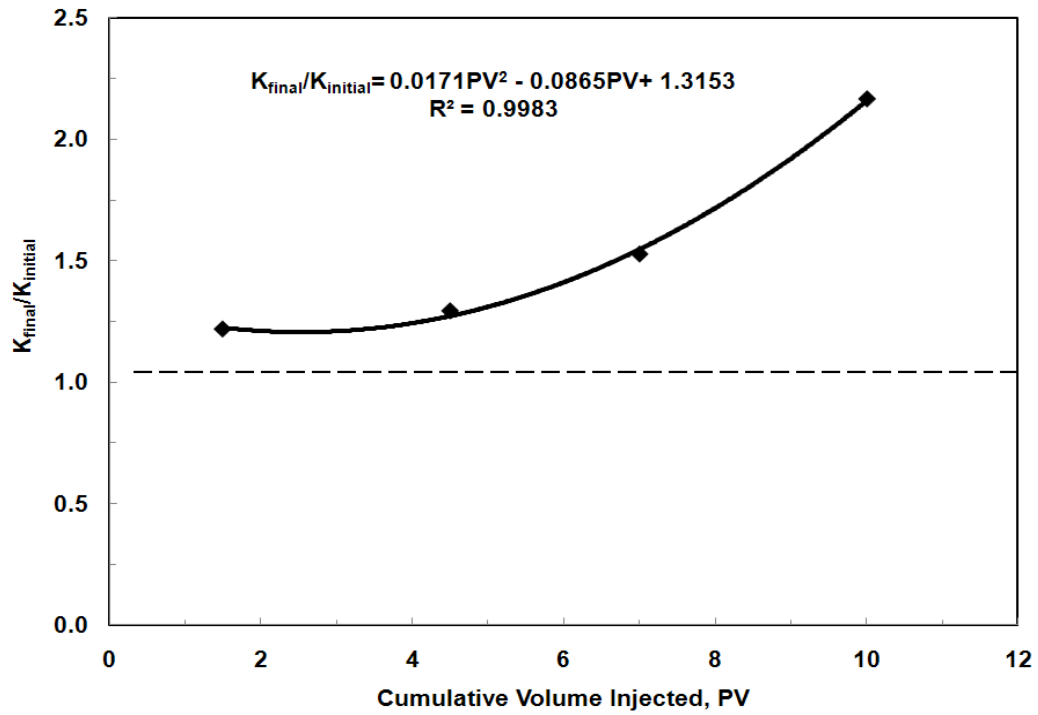
Fig. 105—Effect of the injected volume of GLDA on the permeability ratio for Berea sandstone cores treated at 300°F and 5 cm³/min using 0.6M GLDA at pH 3.8.
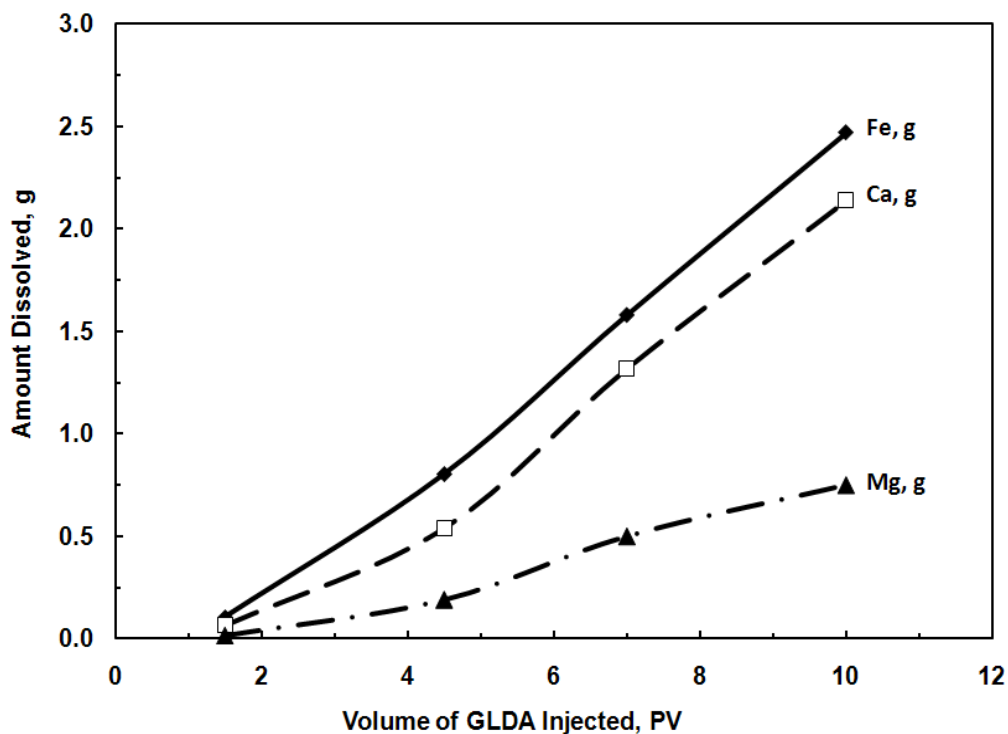
Fig. 106—Effect of the injected volume of GLDA on the amount of dissolved cations for Berea sandstone cores treated using 0.6M GLDA at pH 3.8 and 5 cm³/min.

Effect of Temperature on the Stimulation of Berea Sandstone Cores

Fig. 107 shows the results of the three coreflood experiments performed at 200, 250, and 300°F using 0.6M GLDA at pH 3.8 and at injection rate of 5 cm³/min. The effect of increasing temperature from 200 to 300°F on the permeability ratio of the Berea cores was small. Increasing the temperature increased the reaction rate of GLDA and increased the amount of dissolved calcium, iron, and magnesium as shown in **Fig. 108**. Increasing the temperature increased the reaction rate of GLDA with calcite, dolomite, and chlorite minerals in the Berea sandstone core.

From the coreflood experiments we can summarize the order of the factors that affecting the permeability ratio of the Berea sandstone cores using 0.6M GLDA. We can put the factors in order as follows from the highest to the lowest effect; volume of GLDA (PV), GLDA pH, injection rate, and temperature. Unlike the reaction of GLDA with calcite the most important factor was the temperature because it enhanced the reaction rate of GLDA with calcite (Mahmoud et al. 2010a). In Berea sandstone cores the calcite concentration is very small (1 to 2 wt%), therefore, the effect of temperature will be smaller compared to that in case of calcite cores. Increasing the

temperature from 200 to 300°F at the same conditions increased the average calcium concentration from 7000 to 8000 ppm. This can be attributed to the smaller concentration of calcite and dolomite minerals in the Berea sandstone cores used in this study. The calcium concentration in the effluent analysis came from the dissolution of dolomite and calcite minerals by GLDA. Increasing the temperature from 200 to 300°F increased the reaction rate of GLDA with calcite more than dolomite, therefore, the total increase in calcium concentration was smaller compared to that in case of the reaction of GLDA with calcite. Increasing the temperature from 200 to 300°F during the calcite coreflood experiment of GLDA at pH 3.8 and 5 cm^3/min, increased the average calcium concentration from 15,000 to 20,000 ppm.

$$K_{final}/K_{initial} = 2E\text{-}05T^2 - 0.0084T + 2.3684$$
$$R^2 = 1$$
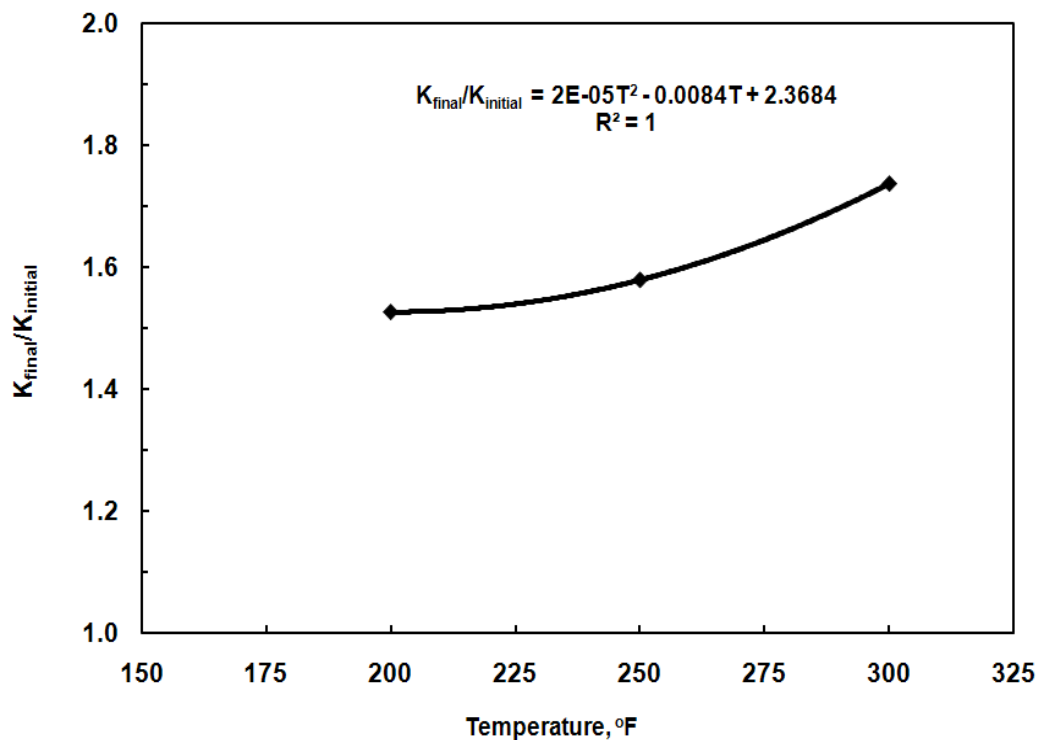
Fig. 107—Effect of temperature on the permeability ratio of Berea sandstone cores treated using 0.6M GLDA at pH 3.8 and 5 cm^3/min.
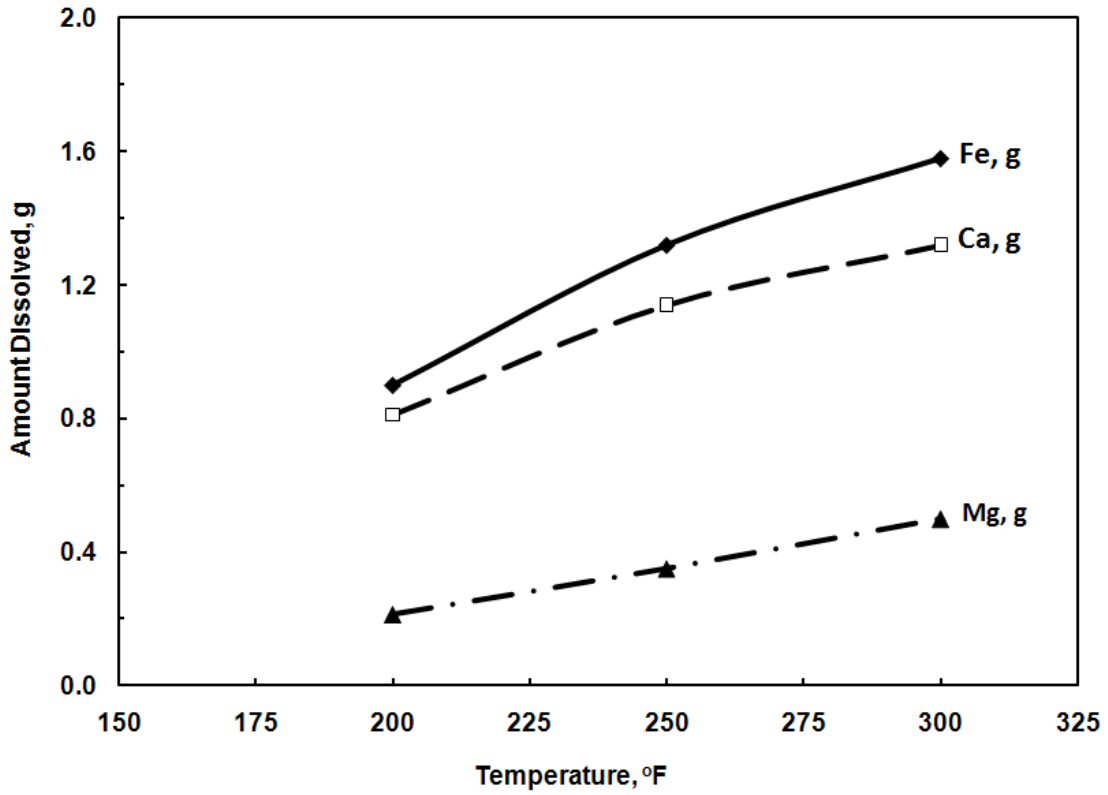
Fig. 108—Effect of temperature on the amount of dissolved cations for Berea sandstone cores treated at 5 cm³/min using 0.6M GLDA at pH 3.8.

Improvement in Skin Damage and Production Rate Using GLDA

The skin damage in sandstone reservoirs can be determined using **Eq. 61** (Hill et al. 1993):

$$S = \left(\frac{k_d}{k_t} - 1\right) \ln\frac{r_t}{r_w}$$

.... (61)

where; S = skin effect due to damage, k_d = damaged zone permeability, md, k_t = treated zone permeability, md, r_t = damaged radius, assume = 6 in., and r_w is the well radius, assume = 3 in.

Using Eq. 61 assuming the damaged length to be the core length, 6 in., and the well radius is 3 in., the skin damage can be determined at GLDA pH values of 1.7, 3, 3.8, 11, and 13.

The production rate of an oil well can be determined using **Eq. 62** (Hill et al. 1993):

$$q_o = \frac{7.08kh}{\mu \beta_o} \frac{p_e - p_{wf}}{\ln \frac{r_e}{r_w} + s} \quad \dots\dots\dots\dots\dots\dots\dots\dots\dots\dots\dots\dots\dots\dots\dots\dots\dots\dots \quad (62)$$

where; q_o= oil production rate, bbl/day, k = formation permeability after treatment, Darcy, p_e = average reservoir pressure, psi, p_{wf} = wellbore flowing pressure, psi, μ = oil viscosity, cP, β_o = oil formation volume factor, bbl/stb, and S = skin damage, dimensionless. The effect of GLDA initial pH value can be showed by assuming a producing oil well from a layer with a thickness of 100 ft, draw down pressure (p_e – p_{wf}) of 1500 psi, oil viscosity of 5 cP, oil formation volume factor of 1.15 bbl/stb, and $\ln(r_e/r_w)$ = 8.

     Fig. 109 shows the production rate and skin damage as a function of the initial pH of 0.6M GLDA at 300°F and 5 cm³/min. The maximum production rate and the least skin damage were attained at GLDA of pH 1.7. GLDA at low pH values (1.7, 3, and 3.8) enhanced the production rate and removed the damage better than GLDA at high pH values (11 and 13).
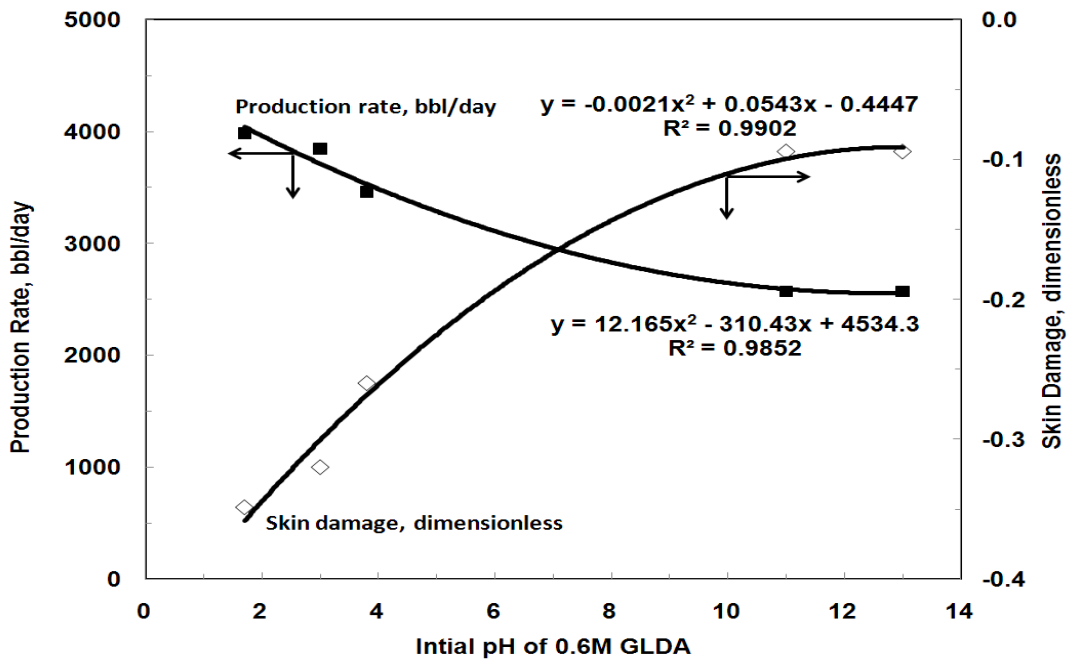
Fig. 109—Effect of initial pH value of 0.6M GLDA on skin damage and oil production rate for Berea sandstone cores treated at 300°F and 5 cm³/min.

Permeability Prediction for Berea Cores Treated by GLDA

Three different correlations were used to predict the permeability of the Berea sandstone cores treated by 0.6M GLDA at 300°F and 5 cm^3/min. Fifteen cores were selected and scanned dry, and saturated after treatment by GLDA using the CT scan tomography. The core porosity was determined after the treatment from the CT scan using **Eq. 62** (Izeg and Demiral 2005):

$$\phi = \frac{CT_{wr}-CT_{ar}}{CT_w-CT_a} \quad\dotfill (62)$$

where; CT_{wr} = CT number of water saturated rock, CT_{ar} = CT number of air saturated rock, CT_w = CT number of water, = 0, CT_a = CT number of air, = -1000.

After calculating the final porosity, the final core permeability can be predicted by one of the following correlations (Hill et al. 1993):

$$\text{Lambert correlation,}\quad \frac{k_{final}}{k_{initial}} = e^{45.7\ \phi_f-\phi_i} \quad\dotfill (63)$$

$$\text{Lund and Fogler,}\quad \frac{k_{final}}{k_{initial}} = e^{M\ \frac{\phi_f-\phi_i}{\Delta\phi_{max}}} \quad\dotfill (64)$$

$$\text{Labrid,}\quad \frac{k_{final}}{k_{initial}} = M\ \left(\frac{\phi_f}{\phi_i}\right)^n \quad\dotfill (65)$$

Where: k_f = permeability after the treatment, md, k_i = core initial permeability, md, ϕ_f = final porosity, fraction, ϕ_i = initial porosity, fraction, $\Delta\phi_{max}$ = 0.08, M= 1, and n = 3.

Table 26 shows the CT number calculation for the fifteen Berea sandstone cores including the actual final permeability and the predicted permeability from the CT number. **Fig. 110** shows the predicted permeability versus the actual measured permeability for Berea sandstone cores treated by 0.6M GLDA at pH 3.8 at a temperature of 300°F and injection rate of 5 cm^3/min. Lambert correlation, Eq. 63, gave the best results in predicting the core permeability after treatment by GLDA with an average error of 10% error. Labrid correlation gave 18% average error and Lund and Fogler correlation gave 70% average error in predicting the core permeability after the treatment.

Table 26—PERMEABILITY PREDICTION FOR BEREA SANDSTONE CORES AT 5 cm³/min AND 300°F USING 0.6M GLDA at pH 3.8

Core no.	ϕ_i	k_i, md	K_f, md	CT_{wr}	CT_{ar}	ϕ_f	k_f, Eq. 63	k_f, Eq. 64	k_f, Eq. 65
1	0.200	105	153	1760	1550	0.210	166	268	122
2	0.195	110	165	1786	1580	0.206	182	309	130
3	0.18	85	110	1790	1600	0.190	134	217	100
4	0.192	90	105	1768	1570	0.198	118	158	99
5	0.184	86	108	1756	1565	0.191	118	166	96
6	0.21	110	155	1772	1550	0.222	190	339	130
7	0.215	110	160	1856	1630	0.226	182	309	128
8	0.205	95	120	1859	1645	0.214	142	217	108
9	0.185	85	145	1710	1520	0.190	105	132	92
10	0.182	80	150	1737	1540	0.197	159	326	101
11	0.194	95	145	1769	1564	0.205	157	266	112
12	0.186	85	150	1708	1510	0.198	147	262	103
13	0.195	90	130	1811	1610	0.201	118	158	99
14	0.205	102	132	1863	1650	0.213	147	216	114
15	0.214	98	110	1848	1630	0.218	118	143	104
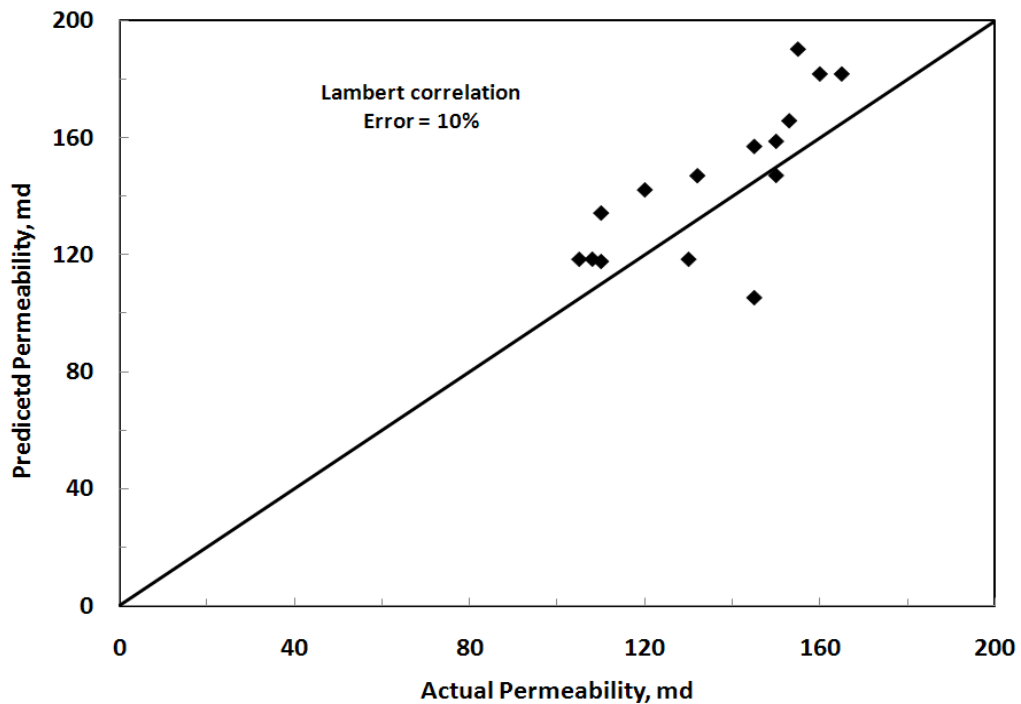
Fig. 110—Permeability prediction of Berea sandstone cores treated by 0.6M GLDA at pH 3.8, 300°F, and 5 cm³/min using Lambert correlation.

Conclusions

In this part of the study 0.6M GLDA chelating agent with different initial pH values (1.7, 3, 3.8, 11, and 13) was used to stimulate Berea sandstone cores at temperatures up to 300°F. The following are the conclusions that were drawn from this study:

1. GLDA initial pH value was found to have a strong effect on the permeability ration increase for Berea sandstone cores.

2. The lower the injection rate the more the contact time of GLDA with the rock, more cations were dissolved at low rates than at high injection rates.

3. Increasing temperature from 200 to 300°F enhanced the reaction rate and increased the core permeability.

4. CT scans showed decrease in the CT number for different pH values. The best conditions were obtained at pH 1.7.

5. Lambert correlation was found to be the best correlation to predict the core permeability after treating Berea cores by 0.6M GLDA at pH 3.8, 300°F, and 5 cm^{3}/min.

CHAPTER VIII

NOVEL ENVIRONMENTALLY FRIENDLY FLUIDS TO REMOVE CARBONATE MINERALS FROM DEEP SANDSTONE FORMATIONS

Introduction

Carbonate minerals are present in sandstone formations. These minerals are either introduced to the formation during drilling/completion operations or naturally present in the rock. There is a need to remove these carbonates to enhance the well performance. This especially true if there is a need to use HF-based fluids to prevent the precipitation of calcium fluorides and calcium fluosilicstes.

In this part of the study, GLDA (glutamicacid-N,N-diaceticacid) a new environmentally friendly chelate was used to remove carbonate minerals from sandstone formations. We also compared its performance with available chelates like EDTA (Ethylenediaminetetraacetic acid) and HEDTA (hydroxyethylenediaminetriacetic acid). Berea (8 wt% clays) and Bandera (14 wt% clays) sandstone cores were used in the coreflood experiments. The concentration of the chelates used was 0.6M at pH values of 11 and 4. The coreflood experiments were run at a flow rate of 5 cm^3/min and at a temperature of 300°F.

Coreflood experiments showed that at high pH values (pH =11) GLDA, HEDTA, and EDTA were almost the same in increasing the permeability of both Berea and Bandera sandstone cores. GLDA, HEDTA, and EDTA were compatible with Bandera sandstone cores. The weight loss from the core was the highest in the case of HEDTA and the lowest in the case of GLDA at pH 11. At pH 4 the 0.6M-GLDA performed better than 0.6M HEDTA in the coreflood experiments. The permeability ratio (final/initial) for Bandera sandstone cores was 2 in the case of GLDA and 1.2 in the case of HEDTA at pH of 4 and 300°F. At pH 11, HEDTA was the best chelating agent to stimulate Bandera sandstone cores and at pH 4, GLDA was the best one. For Berea sandstone cores EDTA at pH of 11 was the best in increasing the permeability of the core at 300°F.

The objective of this part of the study is to (1) determine the compatibility of EDTA, HEDTA, and GLDA with both Berea and Bandera sandstone cores at pH of 11, (2) Determine the compatibility of HEDTA and GLDA at pH of 4 with both Berea and Bandera cores, and (3) Indentify the best chelating agent that can be used to stimulate both Berea and Bandera sandstone core at pH values of 11, and 4.

Experimental Studies

Materials

Chelating agents used in this study were GLDA, HEDTA, and EDTA, and were supplied from AkzoNobel. The original concentration of the chemicals was 40 wt% at the different pH values. The concentration of different chelants that was used in the coreflood experiments was 0.6M. Core plugs were cut in a cylindrical form from sandstone blocks of dimensions 9 x 9 x 9 in. The XRD results for the different sandstone cores Berea, and Bandera are listed in **Table 27**. The Bandera sandstone cores contains 10 wt% Illite which may cause fines migration, 16 wt% dolomite, and 12 wt% Ca-feldspar which are big sources of calcium.

Table 27—MINERAL COMPOSITION FOR DIFFERENT SANDSTONE CORES		
Mineral	**Berea**	**Bandera**
Quartz	86	57
Dolomite	1	16
Calcite	2	--
Feldspar	3	--
Kaolinite	5	3
Illite	1	10
Chlorite	2	1
Plagioclase	--	12

Experimental Procedures

The coreflood set-up used in this part was completely explained in Chapter II, **Fig. 7**. In each coreflood experiment, the core was first loaded into a Hassler sleeve core holder at an overburden pressure of 2,500 psig and temperatures up to 300°F. The core was subjected to vacuum for an hour. Then, it was saturated with injection water until the brine permeability became constant. The brine used in the experiments was 5 wt% NaCl. A 1000 psi back pressure was applied in the coreflood experiments to achieve good saturation and displacement of the fluid and to keep CO_2 in solution. The pore volume of the core was determined after saturating the core by dividing the difference between the saturated core and dry core by the brine density (1.034 g/cm^3 at 22°C). The cores were CT-scanned dry, saturated with 5 wt% NaCl, and after

the treatment. Before flooding the cores by chelating agent solution, the core was heated-up to the test temperature for at least three hours to ensure the stabilization of the core and fluid temperatures. The effluent samples were collected in all the coreflood experiments to analyze for calcium, magnesium, and iron using the ICP. The final core permeability was measured in the reverse direction (flow back or production direction) 24 hrs after the experiment. The final core permeability was also measured using brine of 5 wt% NaCl by injecting at least 20 PV to ensure the pressure stabilization and good core saturation. The final permeability was measured at three different injection rates 2, 5, and 7 cm^3/min and then the average value was taken.

Results and Discussion

Stimulating Berea Sandstone Cores with High pH Fluids

In this part Berea sandstone cores were treated using 0.6M of EDTA, HEDTA, and GLDA at 300^oF. The compatibility of each chelant will be shown and the permeability increase also, will be investigated.

Coreflood experiments were performed on the Berea sandstone cores at 5 cm^3/min and 300^oF using 0.6M GLDA, 0.6M EDTA, and 0.6M HEDTA at pH 11. From the pressure drop performance across the core, the three fluids were compatible with the Berea sandstone cores. **Fig. 111** shows the normalized pressure drop across the core ($\Delta p/\Delta p_{initial}$) for EDTA, GLDA, and HEDTA. The three chelating agents are compatible with Berea sandstone, and the increase in the pressure drop across the core was due to the increase in viscosity of the fluid inside the core. The viscosity increase was due to the complexation of different cations from the sandstone core such as calcium, iron, magnesium, and aluminum. The normalized pressure drop across the core was almost the same for the three fluids until 2 PV. After 2 PV the normalized pressure drop for EDTA was greater than that for GLDA and HEDTA. This indicates after injecting 2 PV of EDTA inside the Berea sandstone core more calcium and magnesium were dissolved and that affected the cementing materials of the core and may start fines migration but it was small.

Fig. 112 shows the permeability ratio ($k_{final}/k_{initial}$) for the Berea sandstone core treated by 0.6M chelate at 300^oF and 5cm^3/min. At high pH value (11) the 0.6M-EDTA performed better as the increase in permeability was 1.2. GLDA and HEDTA almost performed the same at pH 11 in the coreflood experiment using Berea sandstone cores, the permeability ration was 1.16, and 1.14 for 0.6M GLDA , and 0.6M HEDTA respectively. We can conclude that at high pH values and at the conditions we did the coreflood experiments, EDTA is the best chelating agents that can be used to stimulate Berea sandstone cores at 300^oF.

Fig. 113 shows the amount of dissolved calcium, iron, and magnesium for the coreflood experiments performed using 0.6M of EDTA, HEDTA, and GLDA at 300^oF and at injection rate of

5 cm^3/min. EDTA at pH of 11 was the best chelating agent in chelating calcium, iron, and magnesium. At high pH (11), GLDA was the lowest chelating agent in chelating calcium, iron, and magnesium.

Fig. 111—Pressure drop across the core during the coreflood experiment for 0.6M GLDA, 0.6M HEDTA, and 0.6M EDTA at 300°F and 5 cm^3/min using Berea sandstone cores.
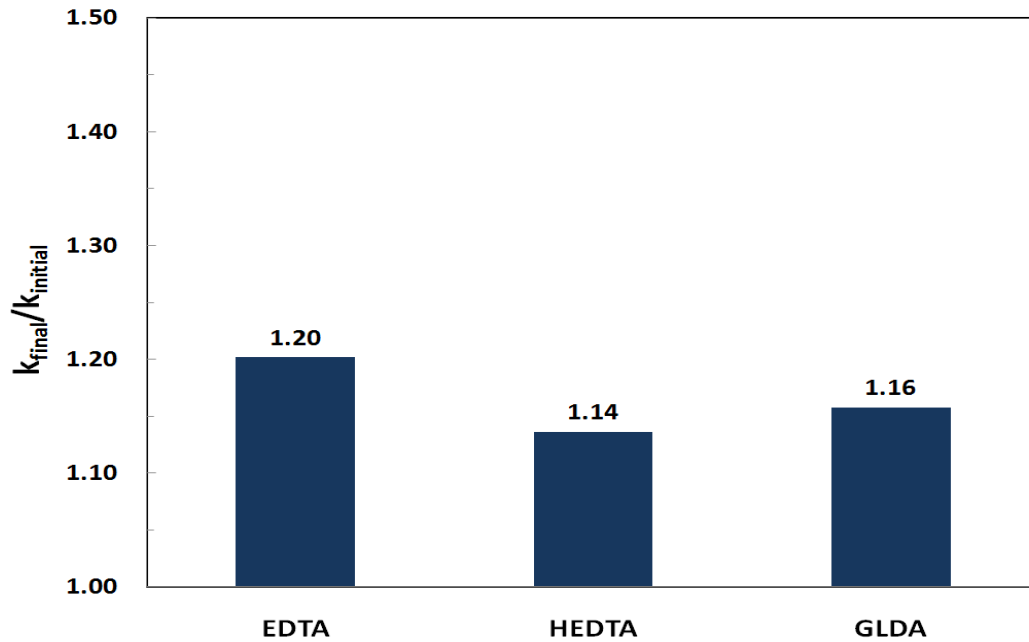
Fig. 112—Permeability ratio for the Berea sandstone cores treated by 0.6M chelate (pH =11) at 300°F and 5 cm³/min.

Fig. 113—Amount of different cations, calcium, iron, and magnesium, in the coreflood effluent for Berea cores treated by 0.6M chelate (pH =11) at 300°F and 5 cm³/min. EDTA was the most powerful chelants among the three chelants.

At high pH values, the three chelating agents have high thermal stability (Jim et al. 2010), therefore, the ability of chelating agent to chelate depends on the stability constant of the chelating agent with each cation. The stability constant for EDTA, HEDTA, and GLDA with calcium, iron, and magnesium are listed in **Table 28** (Martell and Smith 2003). The stability constants were the highest for EDTA, and then for HEDTA and was the least for GLDA. The experimental results of the analysis of the coreflood effluent samples confirmed that EDTA was the best chelating agent in chelating calcium, iron, and magnesium. The core weight loss shown in **Fig. 114** showed that the maximum weight loss of the core was attained in the case of 0.6M EDTA at pH 11. The weight loss of the core was 7.25, 5.25, and 4.25 g for EDTA, HEDTA, and GLDA respectively.

Table 28—STABILITY CONSTANT FOR EDTA, HEDTA, AND GLDA CHELATING AGENTS

Chelating Agent	**Log (stability constant)**		
	Ca^{2+}	Fe^{3+}	Mg^{2+}
EDTA	10.7	25.0	8.83
HEDTA	8.4	19.8	7.00
GLDA	5.9	11.7	5.20

.

Fig. 114—Weight loss of the core, Berea sandstone, after the coreflood experiments using 0.6M chelates (pH = 11) at 300°F and 5 cm³/min. The core weight loss was highest for the core treated by 0.6M EDTA.

Stimulating Bandera Sandstone Cores with High pH Fluids

Fig. 115 shows the normalized pressure drop across the core for Bandera sandstone cores treated by 0.6M of EDTA, HEDTA, and GLDA at 300°F and 5 cm³/min. The three chelants almost were compatible with the Bandera sandstone core which contains 10 wt% illite. EDTA and HEDTA were more compatible than GLDA with Bandera sandstone at pH of 11. The pressure drop across the core started to decrease after injecting 2 PV for the three chelants and continued decreasing until 7.5 PV. Although, the amount of dissolved cations was the highest in the case of EDTA, the normalized pressure drop across the core was the least showing a good compatibility of EDTA with illitic-sandstone cores at pH of 11.

Fig. 116 shows the pressure drop across the core for Bandera sandstone core treated by 15 wt% HCl at 300°F, and 5 cm³/min. The initial pressure drop across the core was 400 psi and the initial core permeability was 4.1 md. After injecting the 15 wt%-HCl, the pressure drop across the core started to increase gradually showing fines migration inside the core. Due to the high content of Illite in this core, HCl was incompatible with the Illite and caused fines migration. The core was left for 24 hrs and after that the permeability was measured using brine (5 wt% NaCl) in

the production direction, the pressure stabilized at 920 psi and the final core permeability was 0.85 md. The permeability ratio ($k_{final}/k_{initial}$) was 0.21 showing a bad compatibility between HCl and iliitic-sandstone. Comparing the performance of HCl with the chelating agents we can conclude that EDTA, HEDTA, and GLDA were compatible with the illitic-sandstone cores and increased the permeability by ratios of 1.41, 1.45, and 1.37 respectively as shown in **Fig. 117**.
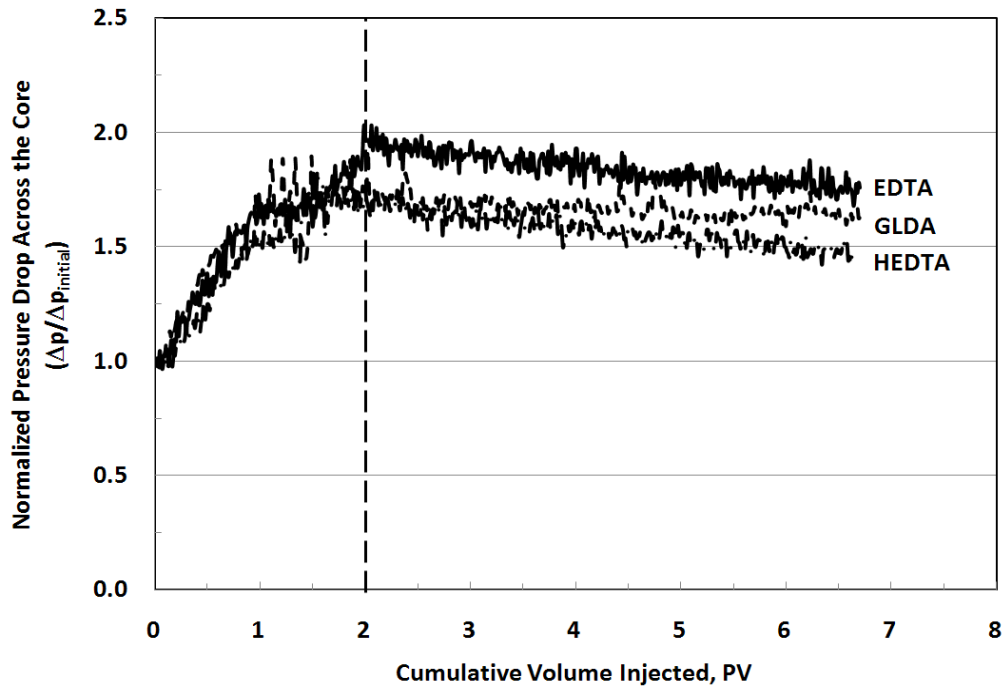

Fig. 115—Pressure drop across the core during the coreflood experiment for 0.6M GLDA, 0.6M HEDTA, and 0.6M EDTA at 300°F and 5 cm³/min using Bandera sandstone cores.
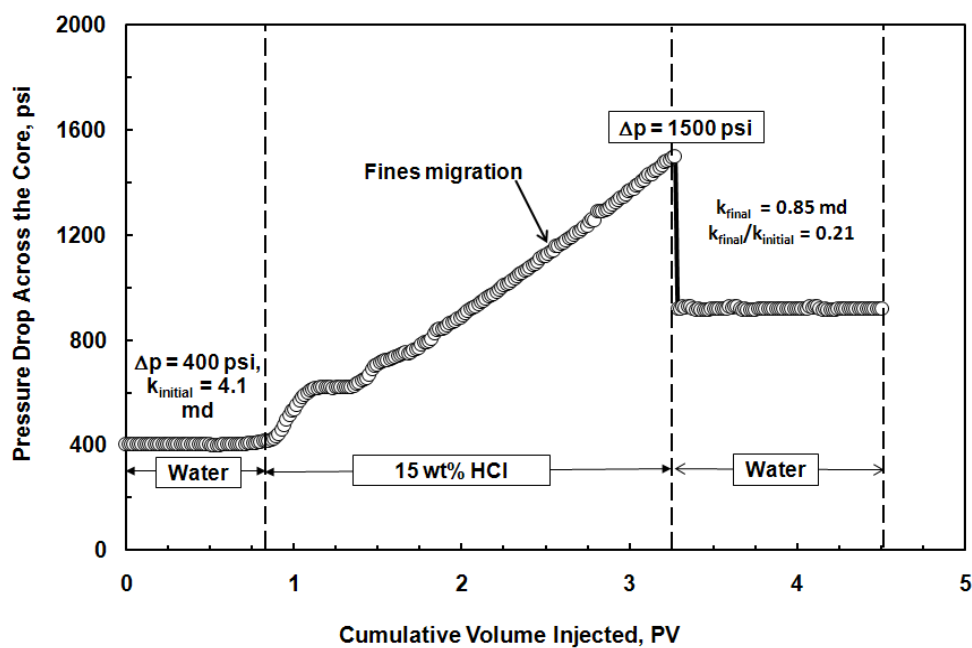
Fig. 116—Pressure drop across the core for 15 wt% HCl at 300°F and 5 cm³/min using Berea sandstone cores. The 15 wt% HCl was not compatible with the illite as it caused fines migration and damaged the core.

Fig. 117—Permeability ratio for the Bandera sandstone cores treated by 0.6M chelate (pH =11) at 300°F and 5 cm³/min.

Fig. 118 shows the amount of dissolved calcium, iron, and magnesium for the coreflood experiments performed using 0.6M of EDTA, HEDTA, and GLDA at 300°F and at injection rate of 5 cm^3/min for Bandera sandstone cores. Bandera sandstone contains 16 wt% dolomite, and 12 wt% calcium-feldspar, therefore, EDTA and HEDTA were able to chelate more calcium than that they chelated in the Berea sandstone cores. The amount of chelated iron was less than that chelated in the case of Berea sandstone cores for the three chelants because chlorite content for Berea core is greater than that for Bandera cores, Table 27. For Bandera illitic-sandstone cores the best chelating agent based on the coreflood experiments we performed was HEDTA. The total amount of chelated calcium, iron, and magnesium was the highest for HEDTA, and then EDTA and was the minimum for GLDA. Also, the weight loss of the core, Fig. 119, confirmed that HEDTA and EDTA were better than GLDA in chelating calcium, iron, and magnesium from illitic-sandstone cores at high pH values at 300°F.
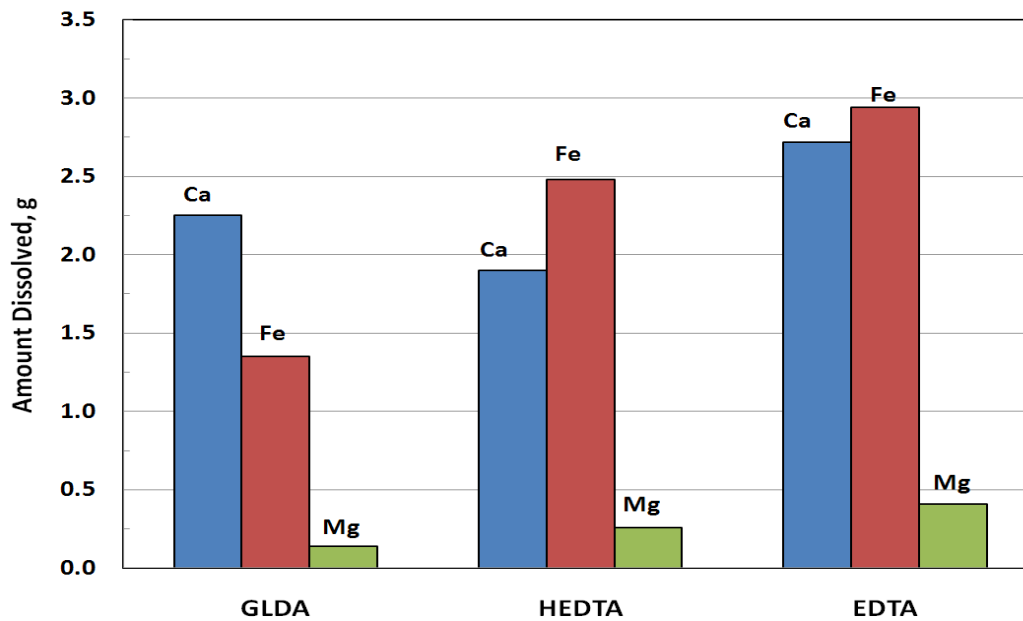

Fig. 118—Amount of different cations, calcium, iron, and magnesium, in the coreflood effluent for Bandera cores treated by 0.6M chelate (pH =11) at 300°F and 5 cm^3/min. HEDTA was the most powerful chelants among the three chelants.
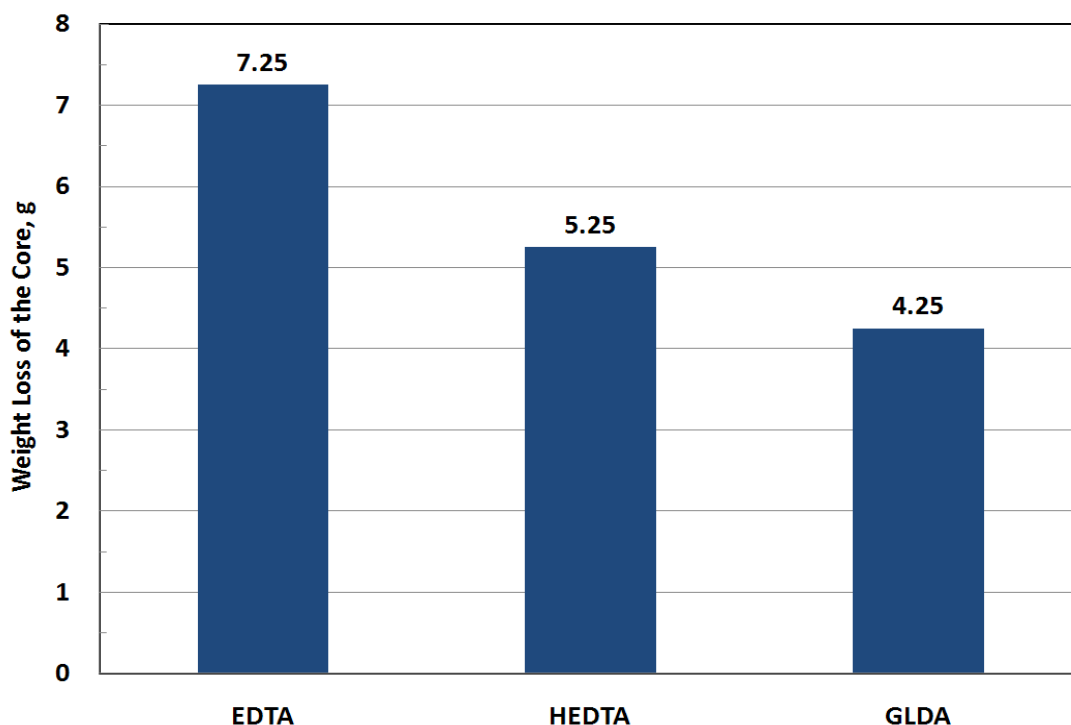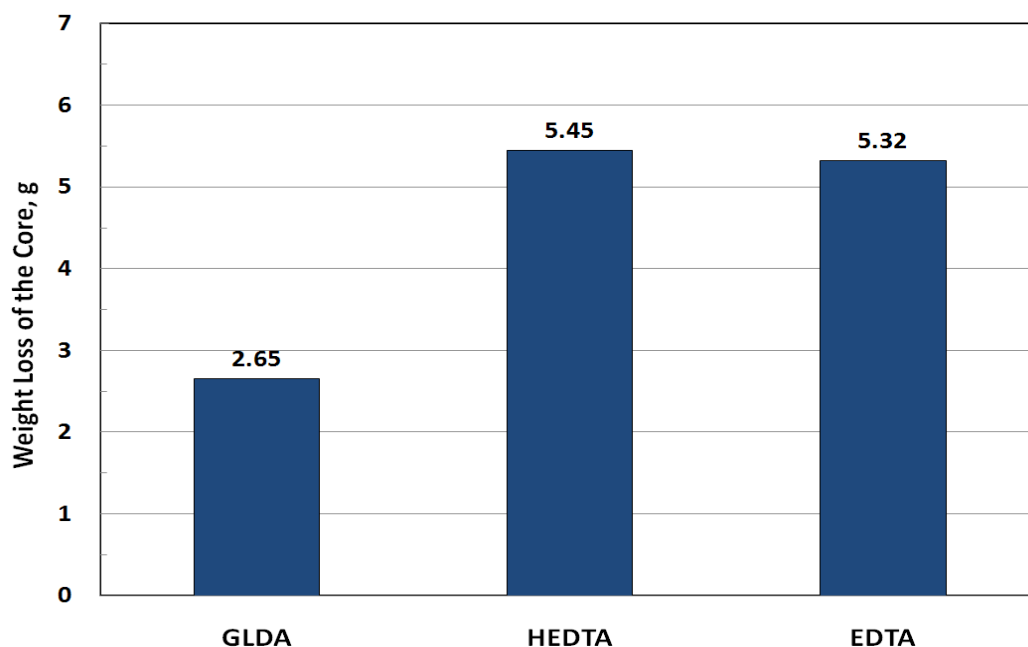
Fig. 119—Weight loss of the core, Bandera sandstone, after the coreflood experiments using 0.6M chelates (pH = 11) at 300°F and 5 cm³/min. The core weight loss was highest for the core treated by 0.6M EDTA.

Stimulating Berea Sandstone Cores with Low pH Fluids

The low pH of the same chelating agents that were used before at high pH (HEDTA, and GLDA) will be investigated on Berea sandstone core to determine the compatibility of those chelants with the Berea sandstone core at 300°F and 5 cm³/min.

Fig. 120 shows the normalized pressure drop across the core for 0.6M HEDTA (pH = 4), and 0.6M GLDA (pH = 4) at 300°F and 5 cm³/min using Berea sandstone cores. Both chelants almost have the same trend. After injecting 2 PV GLDA was more compatible than HEDTA, and after injecting 5 PV, the normalized pressure drop was the same for the two chelants. Based on these result we can conclude that both HEDTA and GLDA at pH 4 are compatible with the Berea sandstone core.

Fig. 121 shows the permeability ratio for both 0.6M HEDTA, and 0.6M GLDA at pH of 4. The permeability ratio was 1.74 for GLDA and 1.24 for GLDA showing a good ability of GLDA in stimulating Berea sandstone cores at low pH. The amount of dissolved calcium was 1.98 g for GLDA and was 1.5 g for HEDTA as shown in **Fig. 122**. GLDA at low pH was able to dissolve more weight of the core than HEDTA. The weight loss of the core was 4.95 g for GLDA and 4.71 g for HEDTA, **Fig. 123**.
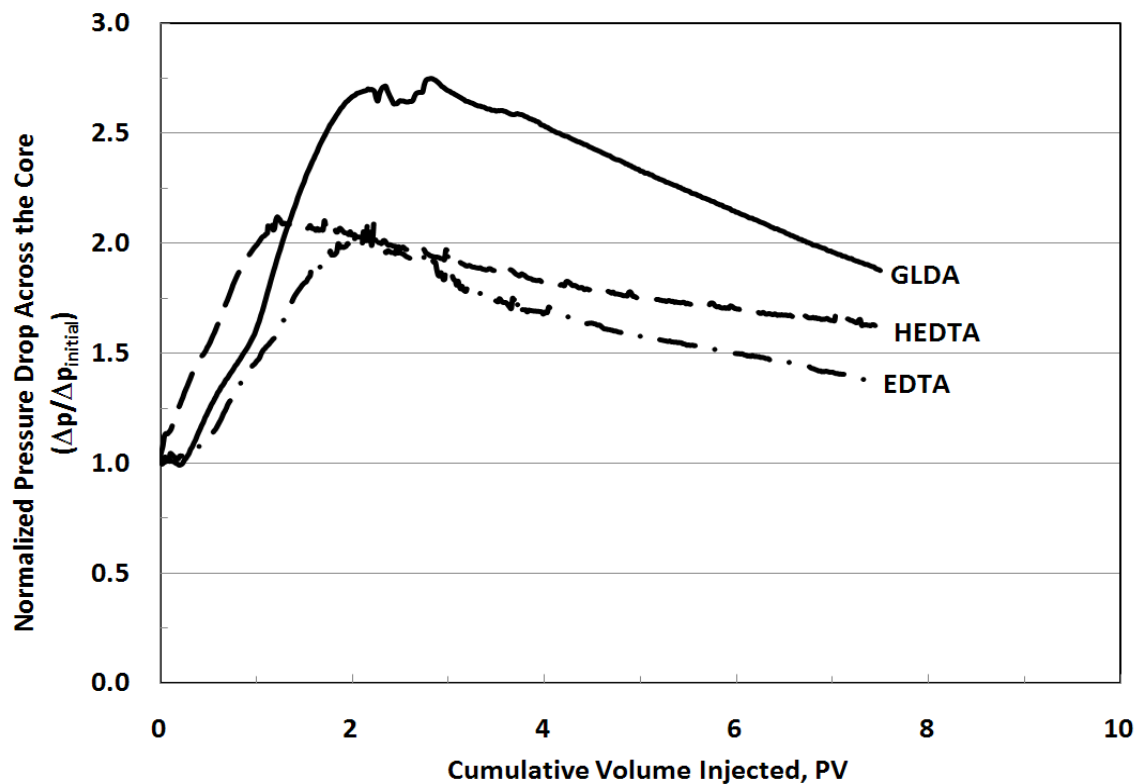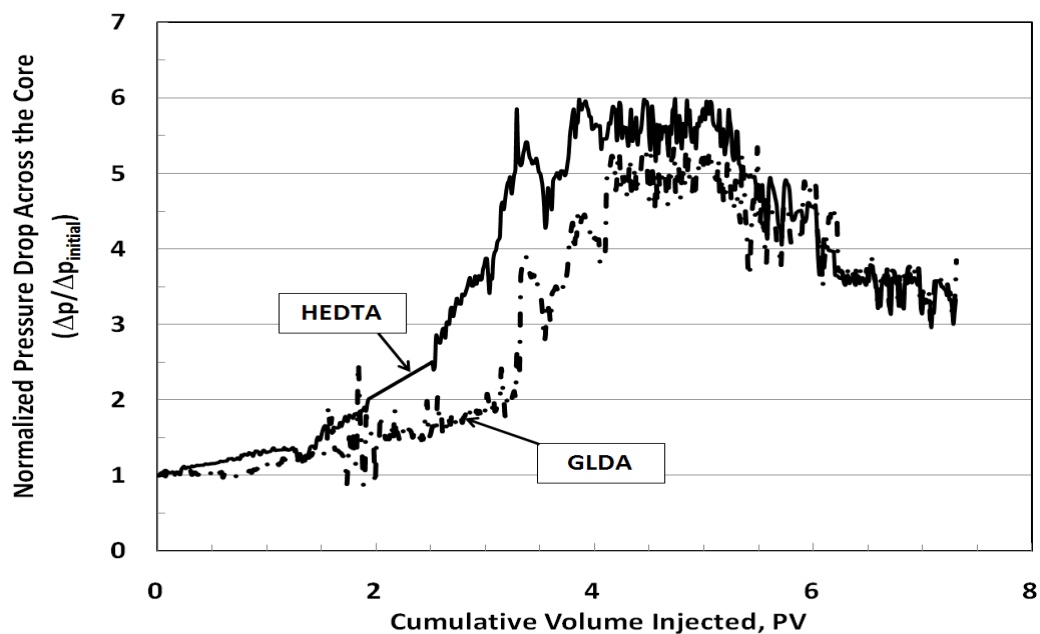
Fig. 120—Pressure drop across the core during the coreflood experiment for 0.6M GLDA (pH = 4), and 0.6M HEDTA (pH = 4), at 300°F and 5 cm³/min using Berea sandstone cores.
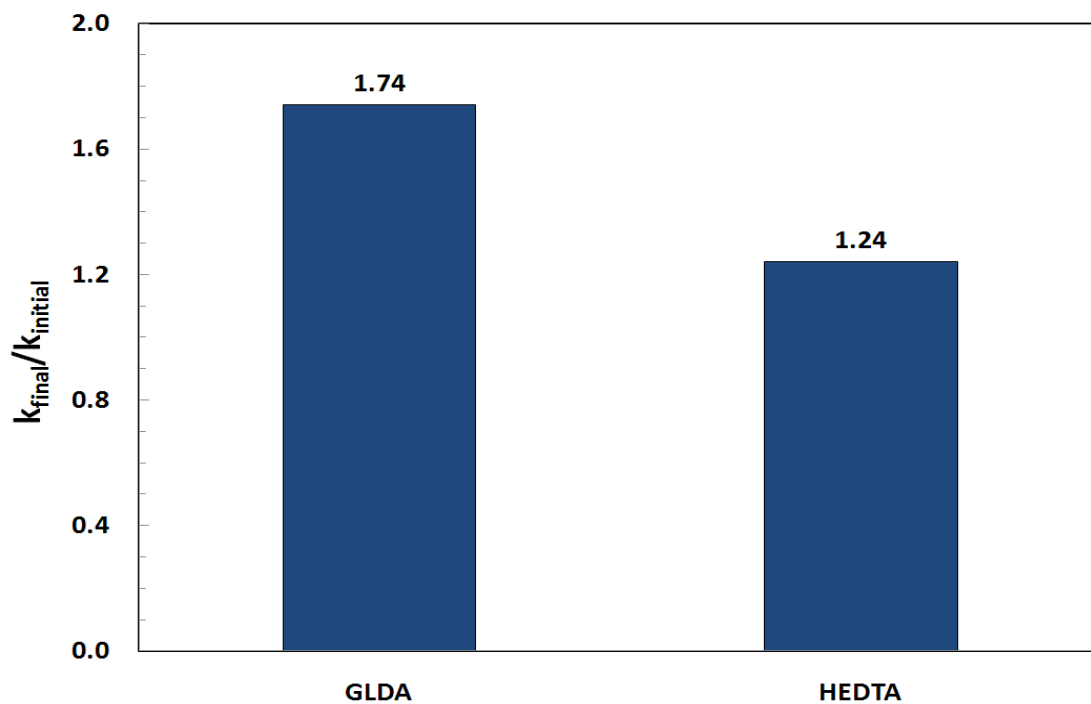
Fig. 121—Permeability ratio for the Berea sandstone cores treated by 0.6M chelate (pH =4) at 300°F and 5 cm³/min.
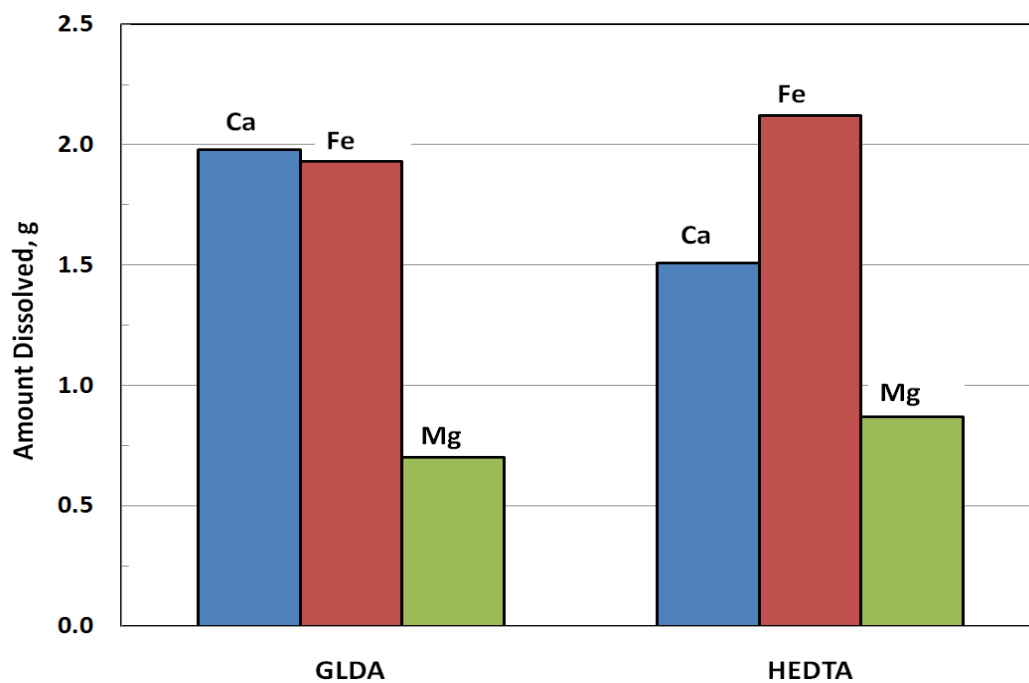
Fig. 122—Amount of different cations, calcium, iron, and magnesium, in the coreflood effluent for Berea cores treated by 0.6M chelate (pH = 4) at 300°F and 5 cm³/min.
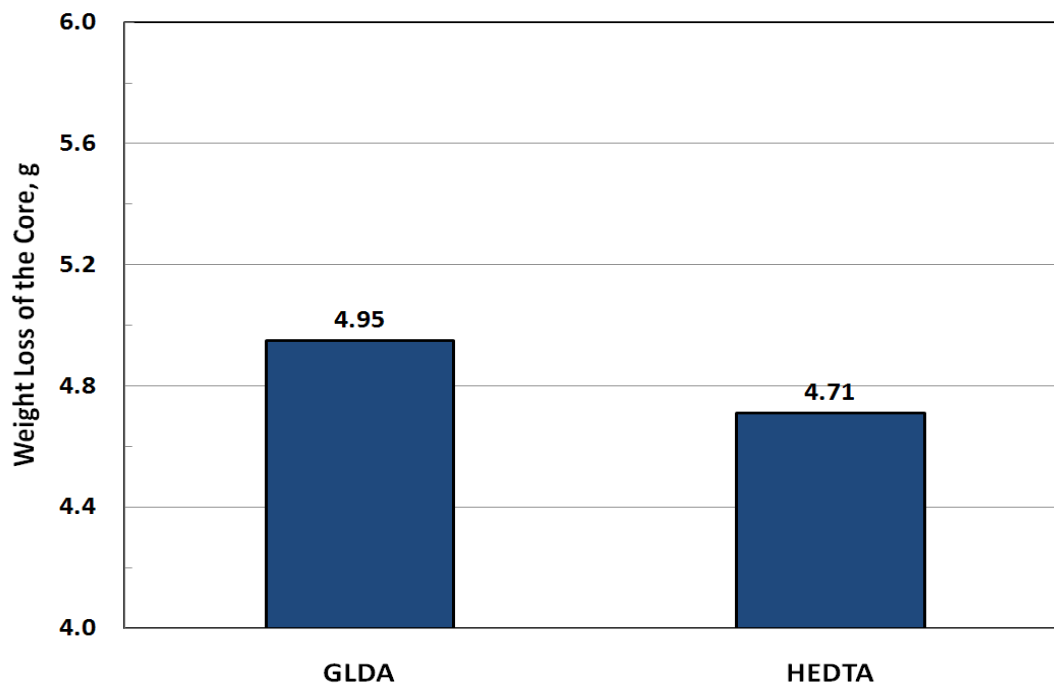
Fig. 123—Weight loss of the core, Berea sandstone, after the coreflood experiments using 0.6M chelates (pH = 4) at 300°F and 5 cm³/min. GLDA performed better than HEDTA at low pH.

Stimulating Bandera Sandstone Cores with Low pH Fluids

Fig. 124 shows the normalized pressure drop across the core for 0.6M HEDTA (pH = 4), and 0.6M GLDA (pH = 4) at 300°F and 5 cm^3/min using Bandera sandstone cores. Both HEDTA and GLDA were compatible with the illitic-sandstone Bandera core. The normalized pressure drop started to decrease after injecting 3PV of both fluids. Unlike HCl, both HEDTA and GLDA at pH 4 were found to be compatible with Bandera sandstone cores.

Fig. 125 shows the permeability ratio for HEDTA and GLDA. The permeability ratio for GLDA was 1.96, and it was 1.17 for HEDTA. GLDA dissolved more calcium than HEDTA at pH of 4 and enhanced the Bandera core permeability better than HEDTA. The amount of calcium was 2.1 g in case of GLDA, and it was 1.67 g for HEDTA ad shown in **Fig. 126**.

GLDA at low pH value (4) performed better than HEDTA in both Berea and Bandera sandstone cores at 300°F. GLDA at pH of 4 increased the core permeability 1.4 times that HEDTA did with Berea sandstone cores, and 1.7 times the permeability increase attained with HEDTA in the case of Bandera sandstone cores.
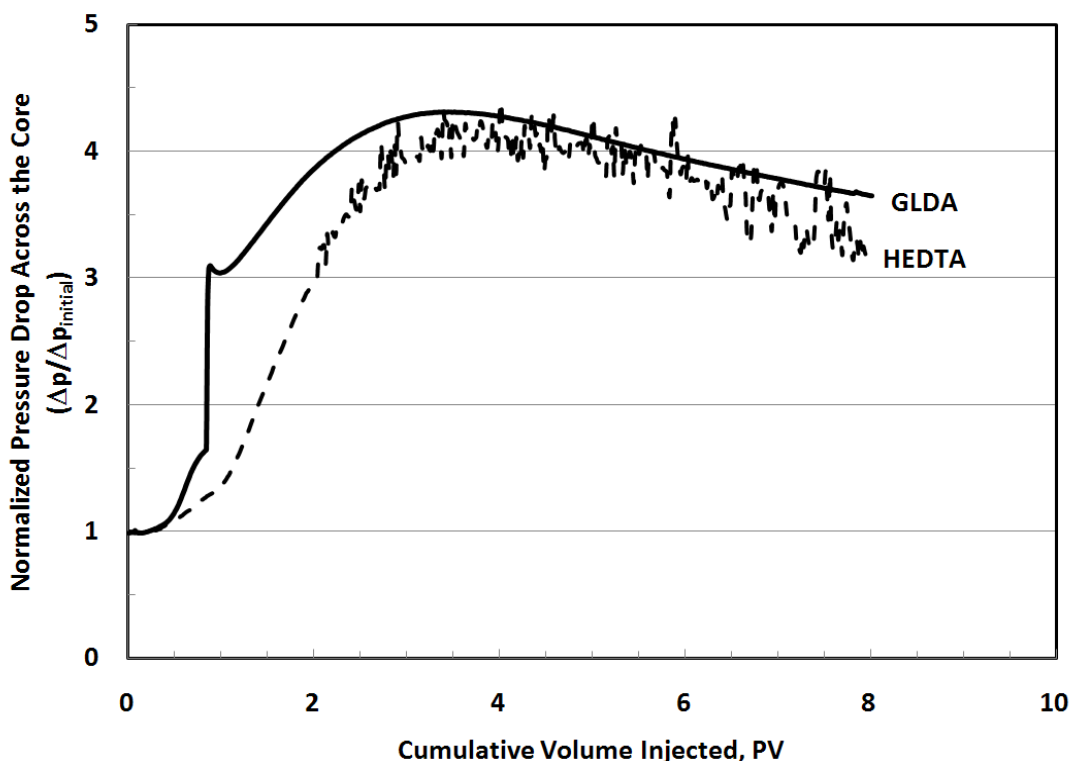
Fig. 124—Pressure drop across the core during the coreflood experiment for 0.6M GLDA (pH = 4), and 0.6M HEDTA (pH = 4), at 300°F and 5 cm^3/min using Bandera sandstone cores.
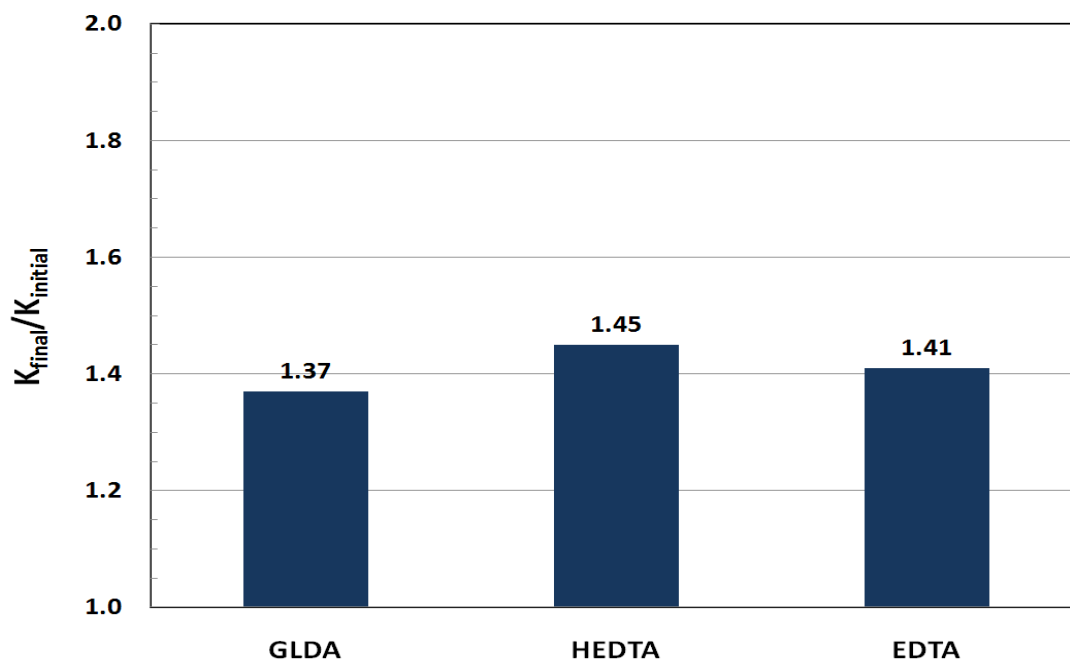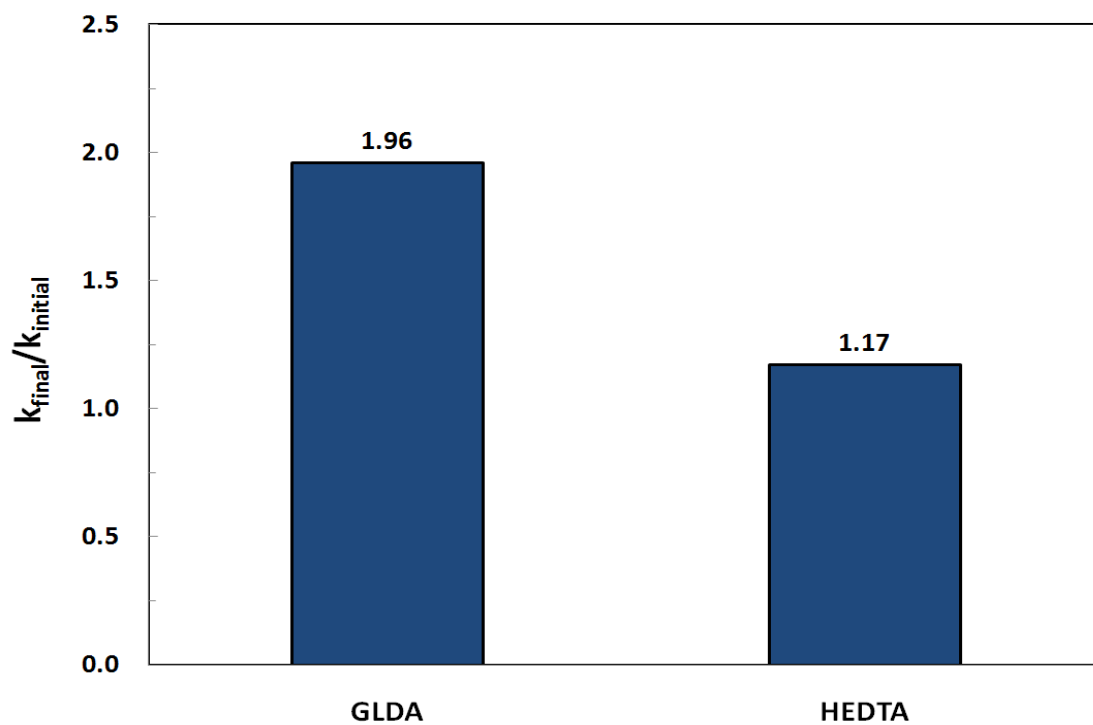
Fig. 125—Permeability ratio for the Bandera sandstone cores treated by 0.6M chelate (pH =4) at 300°F and 5 cm³/min.
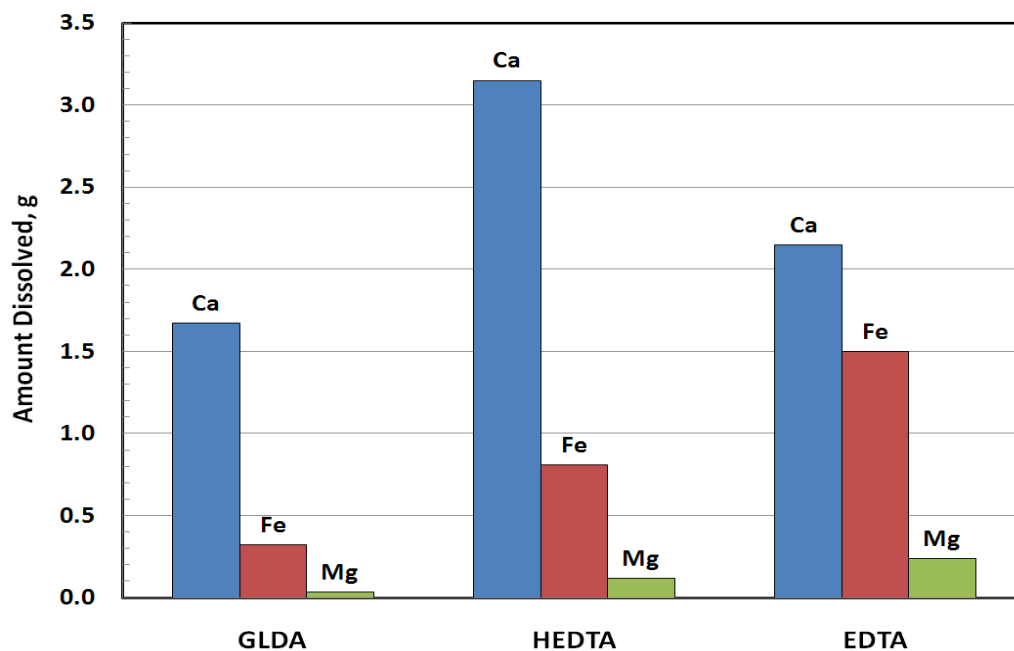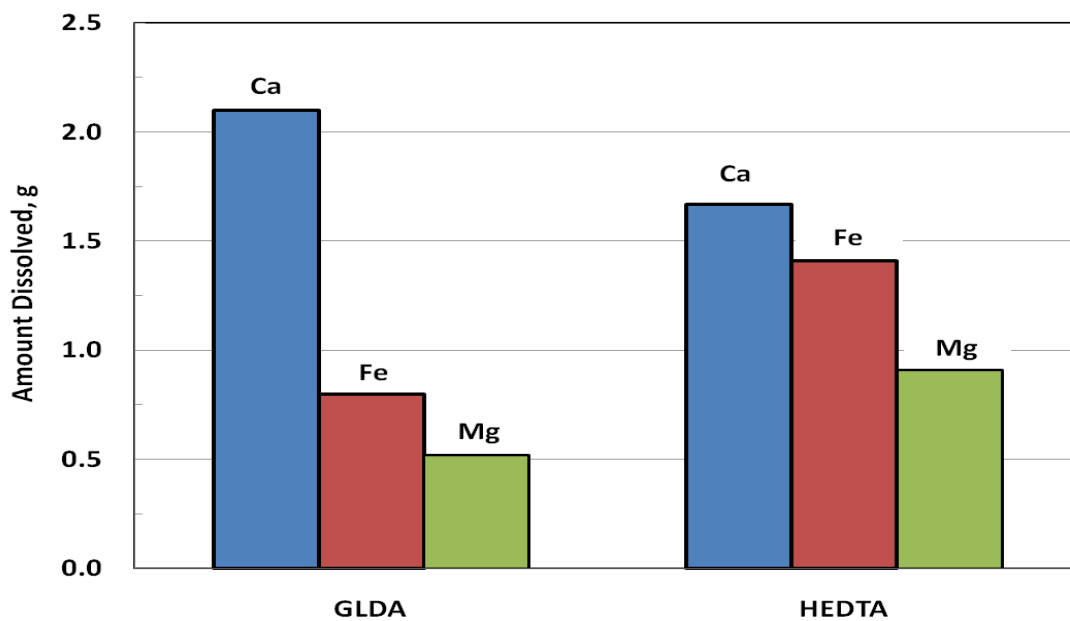

Fig. 126—Amount of different cations, calcium, iron, and magnesium, in the coreflood effluent for Bandera cores treated by 0.6M chelate (pH = 4) at 300°F and 5 cm³/min.

Conclusions

Different chelating agents were studied using the coreflood experiments at $300^{o}F$ and at a flow rate of 5 cm^3/min. The chelating agents that were tested in this part were EDTA, HEDTA, and GLDA at pH of 11, and HEDTA, and GLDA at pH of 4. A concentration of 0.6M was used in all the coreflood experiments using Berea and Bandera sandstone cores. The following are the conclusions that were drawn from this part:

1. EDTA, HEDTA, and GLDA were compatible with both Berea and Bandera illitic-sandstone cores at pH values of 11, and 4.

2. EDTA at pH 11 was the best chelating agent in enhancing the permeability of Berea sandstone cores.

3. HEDTA at pH 11 was the best chelating agent in increasing the permeability of Bandera illitic-sandstone cores.

4. GLDA at pH 4 outperformed HEDTA in stimulating both Berea and Bandera illitic-sandstone cores.

CHAPTER IX

REMOVING THE DAMAGE AND STIMULATION OF ILLITIC-SANDSTONE RESERVOIRS USING COMPATIBLE FLUIDS

Introduction

Illitic-sandstone reservoirs are very sensitive to HCl based fluids. When HCl touch illitic-sandstone it breaks down and causes fines migration and cause formation damage. The migration of fines through the porous media will block the pores, reduce permeability and decrease the production rate of oil and gas wells.

Alternative fluids to HCl/HF mud acids were introduced to stimulate and remove the damage from illitic-sandstone reservoirs. Those fluids are based on chelating agents such as EDTA (ethylenediamine tetra acetic acid), HEDTA (hydroxyl ethylenediamine tri acetic acid), and GLDA (glutamic acid-N,N-diacetic acid). In this study sandstone cores with different illite content were examined. Illite content of 1, 10, 14, and 18 wt% of the sandstone cores were used in the coreflood experiment at 300^oF. Different combinations of GLDA/HF were tested to get the optimum ratio of GLDA/HF to be used in removing the damage from the sandstone cores. The core permeability was measured before and after the treatment to determine the effectiveness of each fluid in removing the damage and stimulation of sandstone cores. CT scan was used to scan the cores before and after the treatment to locate the damage caused by HCl/HF acids in the illitic cores. Different stages of preflush and postflush were used to determine the optimum volume for each stage to yield the maximum core permeability after the treatment.

Our results showed that 15 wt% HCl caused severe damage to sandstone cores with different illite content. GLDA, HEDTA, and EDTA showed a good compatibility with the illitic-sandstone cores at 300^oF. Permeability measurements showed that GLDA performed better than HEDTA and EDTA at pH of 4. The optimum ratio of GLDA/HF concentration was found to be 20wt% GLDA/1wt% HF which gives the maximum increase in core permeability. The three fluids tested in this study showed good compatibility with illite so they can be used to stimulate or remove the damage from illitic-sandstone reservoirs alone or in combination with HF acid.

The objectives of this part of the study are to: (1) stimulate different illite content sandstone cores with EDTA, HEDTA, and GLDA chelating agents, (2) removing the damage caused by calcium carbonate weighted drilling fluid using HEDTA and GLDA chelating agents, (3) determine the optimum GLDA/HF ratio to obtain the maximum possible enhancement in

permeability, and (4) identify the volume of required preflush of GLDA to prevent the precipitation during injecting the main flush.

Experimental Studies

Materials

Chelating agents used in this part of the study were GLDA, HEDTA, and EDTA, and were supplied from AkzoNobel. The original concentration of the chemicals was 40 wt% at the different pH values. The concentration of different chelants that was used in the coreflood experiments was 0.6M. Core plugs were cut in a cylindrical form from sandstone blocks of dimensions 9 x 9 x 9 in. The XRD results for the different sandstone cores Berea, Bandera, Socito, and Kentucky are listed in **Table 29**. The drilling fluid that was used to damage the sandstone cores has a composition that was listed in **Table 30**.

Table 29—MINERAL COMPOSITION FOR DIFFERENT SANDSTONE CORES				
Mineral	**Berea**	**Bandera**	**Kentucky**	**Scioto**
Quartz	87	57	66	70
Dolomite	1	16	--	--
Calcite	2	--	--	--
Feldspar	3	--	2	2
Kaolinite	5	3	Tr	Tr
Illite	1	10	14	18
Chlorite	1	1	--	4
Plagioclase	--	12	17	5

Table 30—DRILLING FLUID COMPOSITION ON LAB SCALE		
Material	**Quantity**	**Units**
Distilled Water	308	cc
Defoamer	0.33	cc
XC-polymer	1.20	g
Biocide	0.17	cc
Starch	2.00	g
KCl	97.6	g
KOH	0.50	cc
Sodium sulfite	0.25	g
$CaCO_3$ (Coarser)	7.99	g
Lubricant	7.00	cc

Results and Discussion

Stimulation of Berea Sandstone Using GLDA/HF Solutions

Berea and Bandera sandstone cores of 6 in. length and 1.5 in. diameter were used in the coreflood experiments using the set up shown in **Fig. 7**. The first coreflood experiment was run using Berea sandstone core at 300°F and 5 cm^3/min using 20 wt% GLDA at pH 3.8. The initial permeability of the treated core was 95 md and the final permeability after the treatment was 155 with 1.63 improvement factor ($k_{final}/k_{initial}$). The core permeability was increased from 95 to 155 md after injecting 8.7 PV of GLDA into the Berea sandstone core and the average calcium concentration was 7,000 ppm. The same conditions were repeated using Berea sandstone and mixture of 20 wt% GLDA + 3 wt% HF at the same temperature and flow rate. **Fig. 127** shows the total calcium concentration in the coreflood effluent samples, the calcium concentration dropped to an average value of 4,000 ppm when GLDA+HF was used without preflushing the core. The source of calcium in Berea sandstone core is calcite and dolomite, and the fluosilic acid from the secondary reaction of HF with quartz with the calcium will precipitate calcium fluosilicates ($CaSiF_6$) inside the core and cause formation damage. The precipitation of $CaSiF_6$ reduced the total calcium concentration in the coreflood effluent samples. The decreased average calcium concentration in the effluent samples also, can be attributed to the precipitation of calcium fluoride (CaF_2). The core permeability was 85 md and dropped to 40 md after the treatment by GLDA + HF. There many scenarios could be contributing to this damage besides the calcium fluosilicates and calcium fluorides such as sodium fluosilicates (Na_2SiF_6) and potassium

fluosilicates (K_2SiF_6). The sources of sodium and potassium in the Berea sandstone core are the feldspars present in the core. These results confirmed the necessity of preflushing the core before HF treatment even if the amount of calcium in the core was low (3 wt% calcite and dolomite).
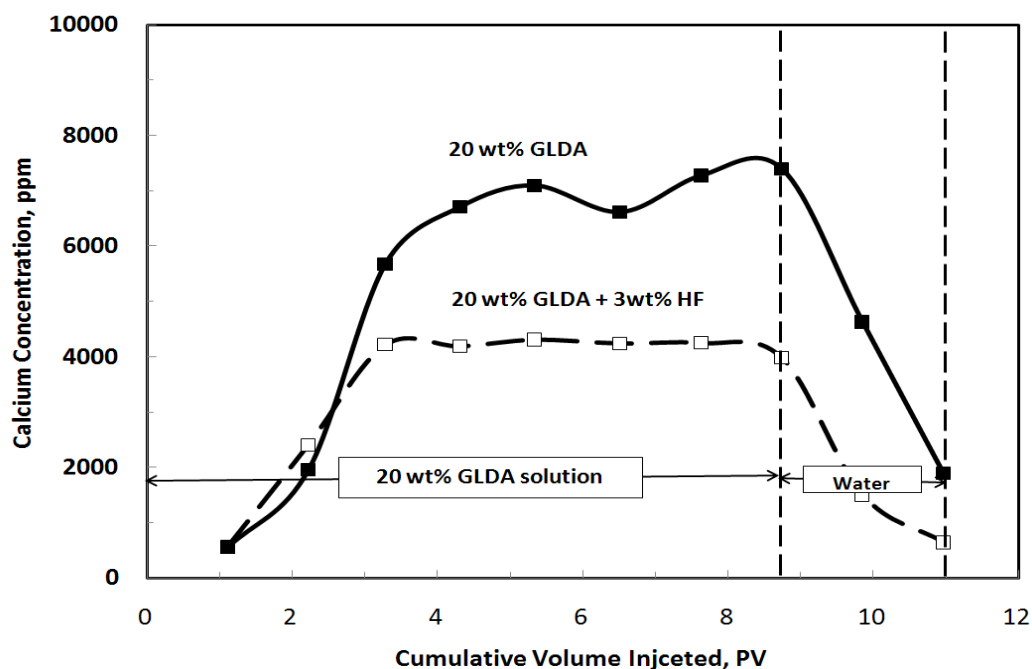
Fig. 127—Total calcium concentration in the coreflood effluent samples showing the damage caused by HF. The decreased calcium concentration means the precipitation of $CaSiF_6$ or CaF_2.

CT scan was used to scan the core before and after the treatment to check for the core porosity. **Fig. 128** showed the 2D CT scan for the first coreflood experiment (Berea sandstone cores treated by 20 wt% GLDA at pH 3.8, 300°F and 5 cm³/min). The CT number for the core before the treatment had an average value of 1720 and after the treatment it was 1600. The decrease in the CT number indicated an increase in the core porosity after the treatment. **Fig. 129** shows the 2D CT scans for the Berea sandstone cores treated by 20 wt% GLDA at pH 3.8 + 3 wt% HF at 300°F and 5 cm³/min. The images showed an increase in the CT number from 1750 to 2000 indicating decrease in the core porosity due to precipitations.
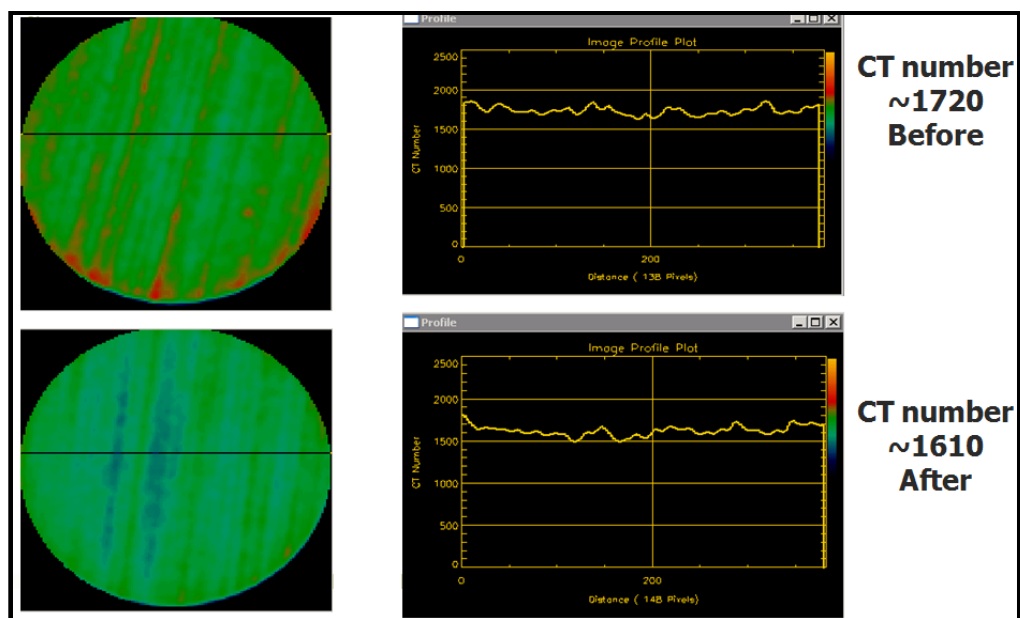
Fig. 128—2D CT scans showing decrease in the CT number after the treatment from 1720 to 1610. The reduction in CT number indicated increase in the core porosity. Berea sandstone core treated by 20 wt% GLDA at pH 3.8, T = 300°F, and 5 cm³/min.
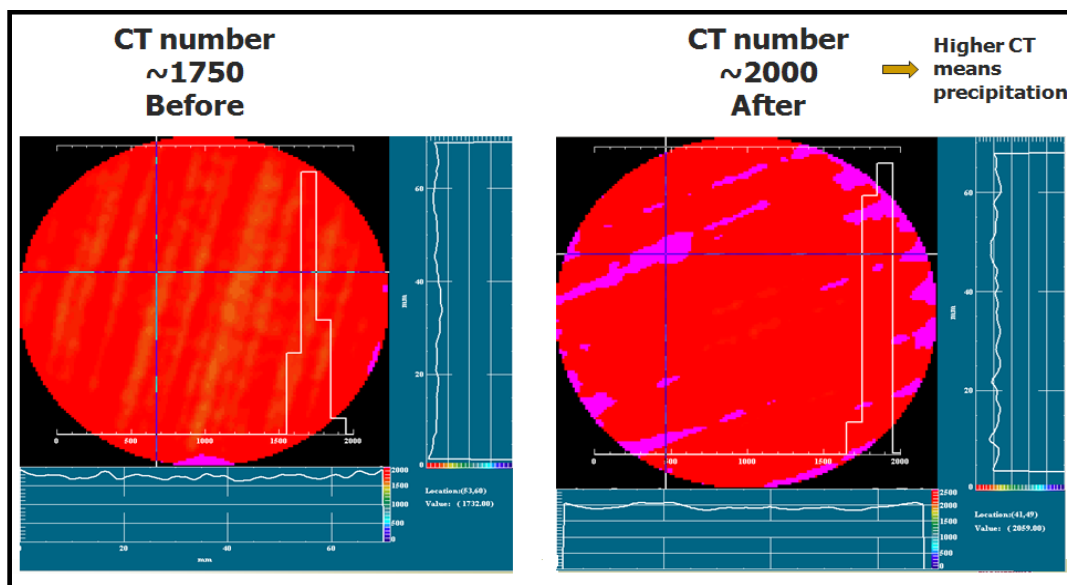
Fig. 129—2D CT scans showing increase in the CT number after the treatment from 1750 to 2000. The increase in CT number indicated decrease in the core porosity. Berea sandstone core treated by 20 wt% GLDA + 3 wt% HF at pH 3.8, T = 300°F, and 5 cm³/min.

Effect of HF Concentration on the Stimulation of Berea Sandstone Cores Using GLDA/HF

Different coreflood experiments were run using Berea sandstone cores to determine the optimum GLDA/HF ratio to give the maximum increase in the core permeability after the treatment. The coreflood experiments were run at $300^{o}F$ and 5 cm^{3}/min and all the cores were flushed by 10 PV 20 wt% GLDA at pH 3.8 (preflush). **Fig. 130** shows the relationship between the permeability ratio ($k_{final}/k_{initial}$) and the GLDA/HF concentration. The permeability increase was the maximum when 20 wt% GLDA injected alone without HF acid because there was no precipitations. Adding HF produced fluosilic acid and precipitated calcium, sodium, and potassium fluosilicate or calcium fluoride. The lower the HF concentration, the lower the fluosilic acid and the lower the precipitation. The maximum permeability increase was obtained at HF concentration of 1 wt% and it was 1.65. Decreasing the HF concentration to 1 wt% yielded permeability ratio increase less than the GLDA alone. From these results we can conclude that if the damage in the sandstone reservoir was due to carbonates it is better to use GLDA without HF , but if there was silicates among the damaging materials we can use 20 wt% GLDA+ 1 wt% HF. In all experiments the main flush was 4 PV of GLDA + HF.
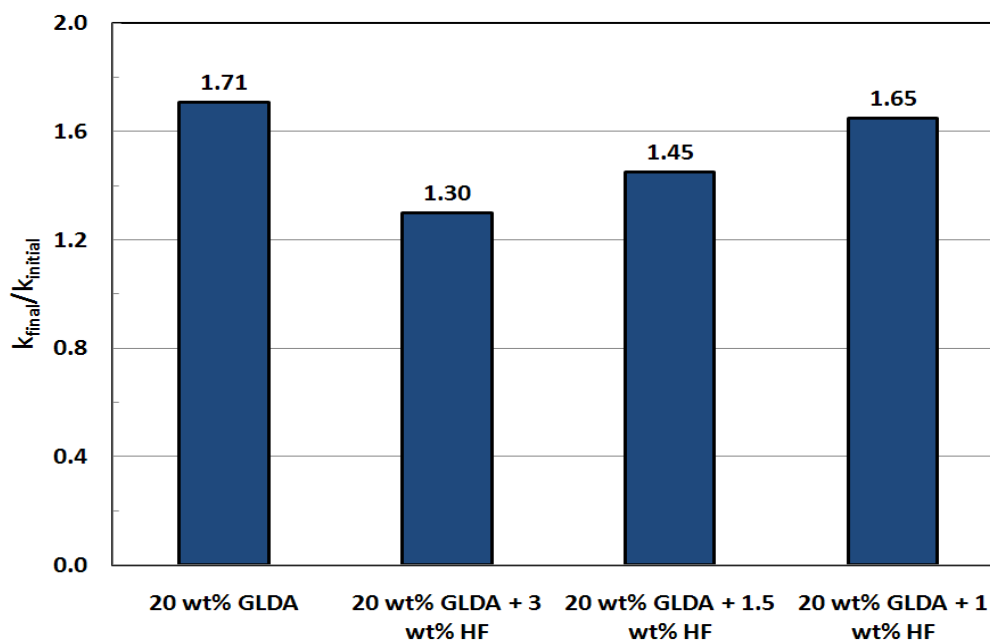
Fig. 130—Relationship between GLDA/HF concentration and the permeability ratio of Berea sandstone core at 5 cm^{3}/min and $300^{o}F$. GLDA pH = 3.8.

Effect of Preflush on the Stimulation of Berea and Bandera Sandstone Using GLDA/HF

The presence of carbonate minerals in the sandstone cores required flushing the core to remove these minerals to minimize the calcium fluosilicates or fluorides precipitations inside the core. **Fig. 131** shows the effect of flushing the Berea sandstone core by 10 PV 20 wt% GLDA at pH 3.8. The calcium concentration before in the preflush just before switching to 20 wt% GLDA + 3 wt% HF was 5,000 ppm, it dropped to 3,500 ppm after switching to the main flush (20 wt% GLDA + 3 wt% HF). Comparing this to fig. 127 at which the calcium concentration dropped from 7,000 to 4,000 ppm indicating high precipitation of calcium. In this case it is still there is precipitation but lower than before in the case where there was no preflush. The coreflood experiment was run at 300°F and 5 cm^3/min and the core permeability was increased from an initial value of 85 md to 110 md (k_{final}/$k_{initial}$ = 1.3). The permeability ratio when there was no preflush was 0.47 compared to 1.3 in the case of 10 PV GLDA preflush. Flushing the core by 10 PV GLDA at pH 3.8 during the treatment of Berea sandstone core by GLDA+HF increased the permeability ratio from 0.47 (damage) to 1.3. The calcium concentration decreased after switching to the main flush due to the precipitations and the magnesium and iron concentration started to increase due to the reaction of HF with clays and chlorite. HF was able to produce 18,000 ppm iron and 8,000 ppm magnesium from clays and chlorite.

    Fig. 132 shows the stimulation of Bandera (illitic-sandstone) core by 20 wt% GLLDA at pH 3.8 + 3 wt% HF at 300°F and 5 cm^3/min. The core was flushed first by 5.2 PV 20 wt% GLDA at pH 3.8. In the preflush stage the calcium concentration was 23,000 ppm, this is high calcium concentration because of this core has 16 wt% dolomite and 12 wt% calcium feldspar. The calcium concentration dropped to 14,000 ppm after switching to GLDA+HF due to precipitation. The iron concentration increased from 17,000 to 35,000 ppm after switching to the main flush due to the reaction of HF with chlorite and clays. The amount of illite in this core was 10 wt%, therefore, the amount of produced iron was greater in this core compared to Berea sandstone (1 wt% illite). The core permeability after the treatment was increased from 3.2 to 3.5 md.
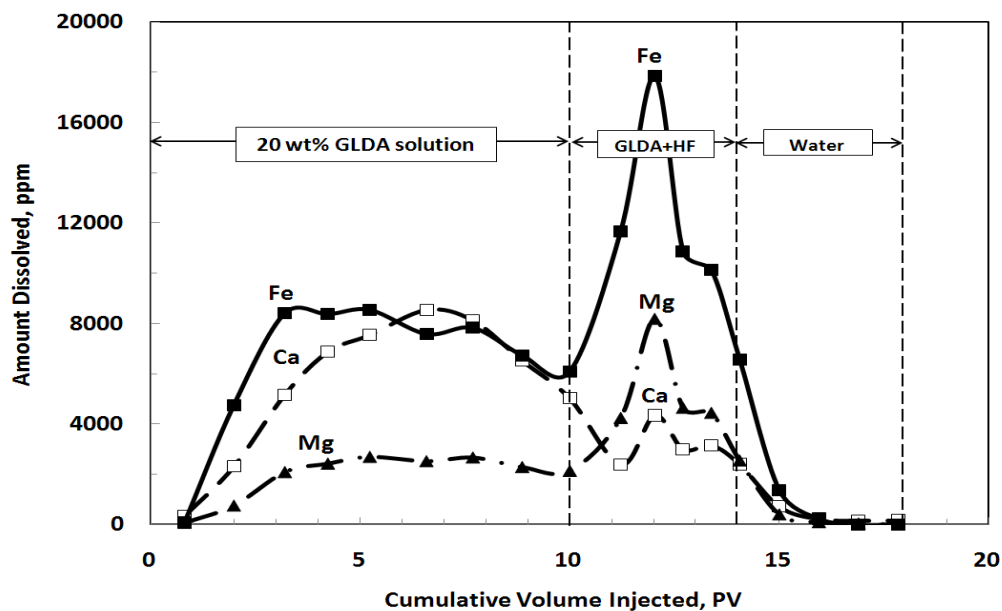
Fig. 131—Different stages of GLDA/HF treatment for Berea sandstone core at 300°F and 5 cm³/min.
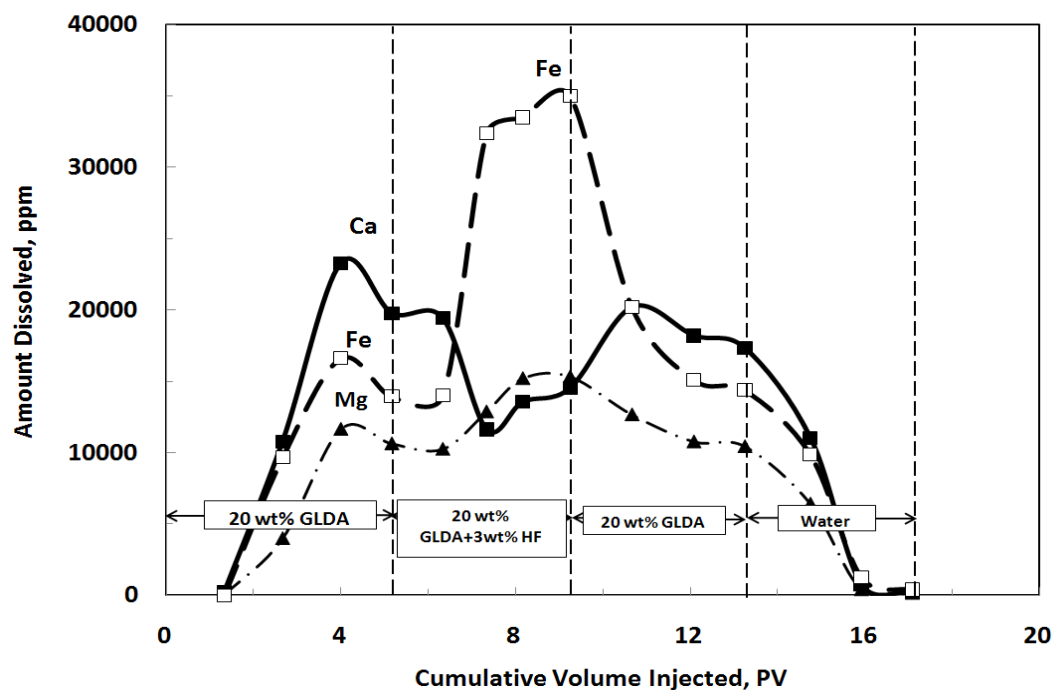
Fig. 132—Effect of preflush, main flush, and post flush on the stimulation of Bandera (illitic-sandstone) by 20 wt% GLDA + 3 wt% HF. T = 300°F and q = 5 cm³/min.

Several coreflood experiments were run using Bandera sandstone cores and 20 wt% GLDA (pH 3.8) + 3 wt% HF at 300^oF and 5 cm^3/min at a constant post flush volume of 10 PV 20 wt% GLDA at pH 3.8 and constant main flush volume of 4 PV. **Fig. 133** shows the effect of preflush volume of GLDA on the permeability ratio of Bandera sandstone cores. The greater the volume of the preflush the higher the permeability increase of the core. When no preflush was used the permeability ratio was 0.4 (damage) increasing the preflush volume increased the permeability ratio up to 1.68 when 10 PV preflush was used. Bnadera sandstone has abundance sources of calcium (16 wt% dolomite and 12 wt% calcium feldspar), therefore it is necessary to remove the calcium as much as we can from the core to avoid t precipitations and damaging the core.
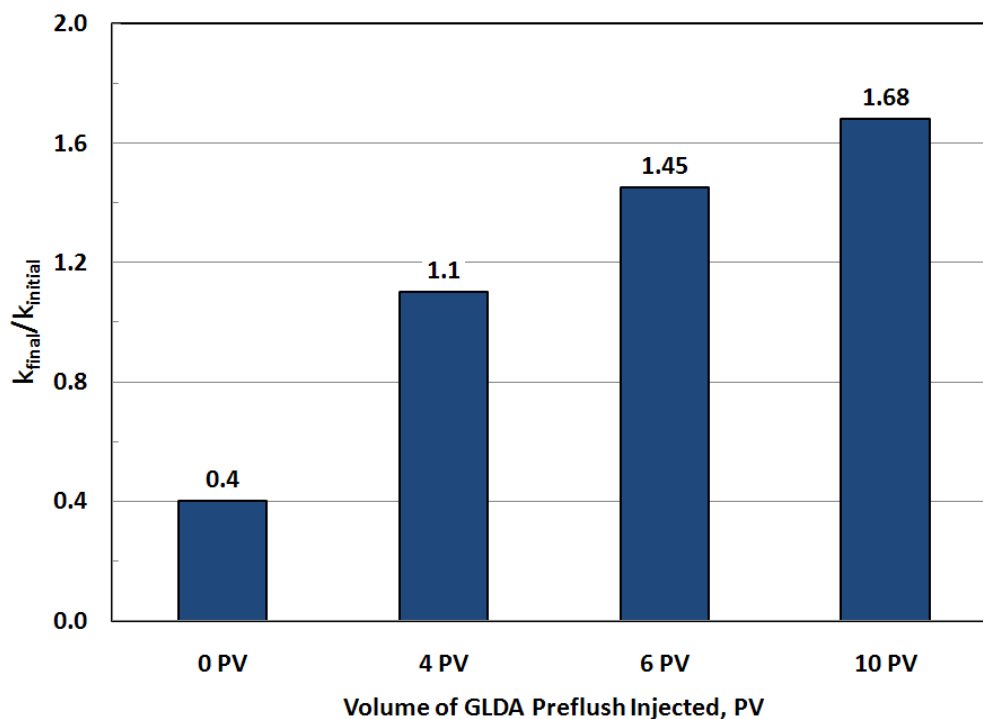
Fig. 133—Effect of GLDA preflush volume on the permeability ratio of Bandera sandstone core at 300^oF and 5 cm^3/min.

Fines Migration by HCl

A coreflood experiment was run using illitic sandstone Bandera core and 15 wt% HCl at 80^oF and 5 cm^3/min. The initial core permeability was 4.1 md after flowing the 15 wt% HCl in the illitic core it caused fines migration and damaged the core. The pressure drop increased from an initial value of 400 psi during flowing 5 wt% NaCl brine solution to 1500 psi after flowing HCl,

Fig. 134 The pressure drop increased gradually with the pore volume with a gradient of 440 psi/PV indicating fines migration and blocking the pore throats and permeability throughout the core. After injecting HCl the core was flowed back using 5 wt% NaCl brine solution until the pressure drop across the core stabilized. The core permeability after the flowing back was 0.85 md showing the damage caused by HCl.
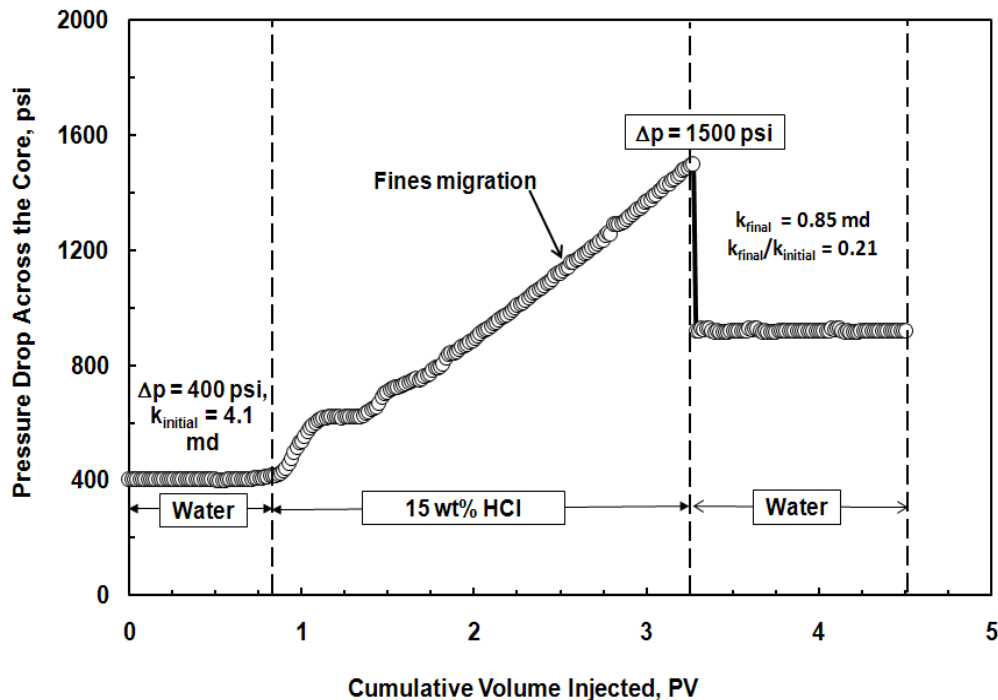
Fig. 134—Pressure drop across the core for 15 wt% HCl at 80°F and 5 cm³/min using Berea sandstone cores. The 15 wt% HCl was not compatible with the Illite as it caused fines migration and damaged the core.

Fig. 135 shows the 2D CT scan for a slice from the Bandera illitic-sandstone cores before and after flowing HCl inside the core. The CT number after saturating the core by brine was around 1800, after flowing HCl inside the core we observed fluctuation in the CT number between 1700 and 1850 and there was a change in the color of the slice. The core was saturated after flowing HCl for 24 hours under vacuum and then the Hassler core holder was used to saturate the core with a back pressure of 1000 psi to insure good core saturation. The scan after saturation for the treated core showed difference in CT number in the all slices taken along the core length showing blocking or redistribution of the clays inside the core.

CT no fluctuating between 1700 and 1850 and the distribution of clays changed after injecting 15 wt% HCl	CT no. = 1800 before fines migration
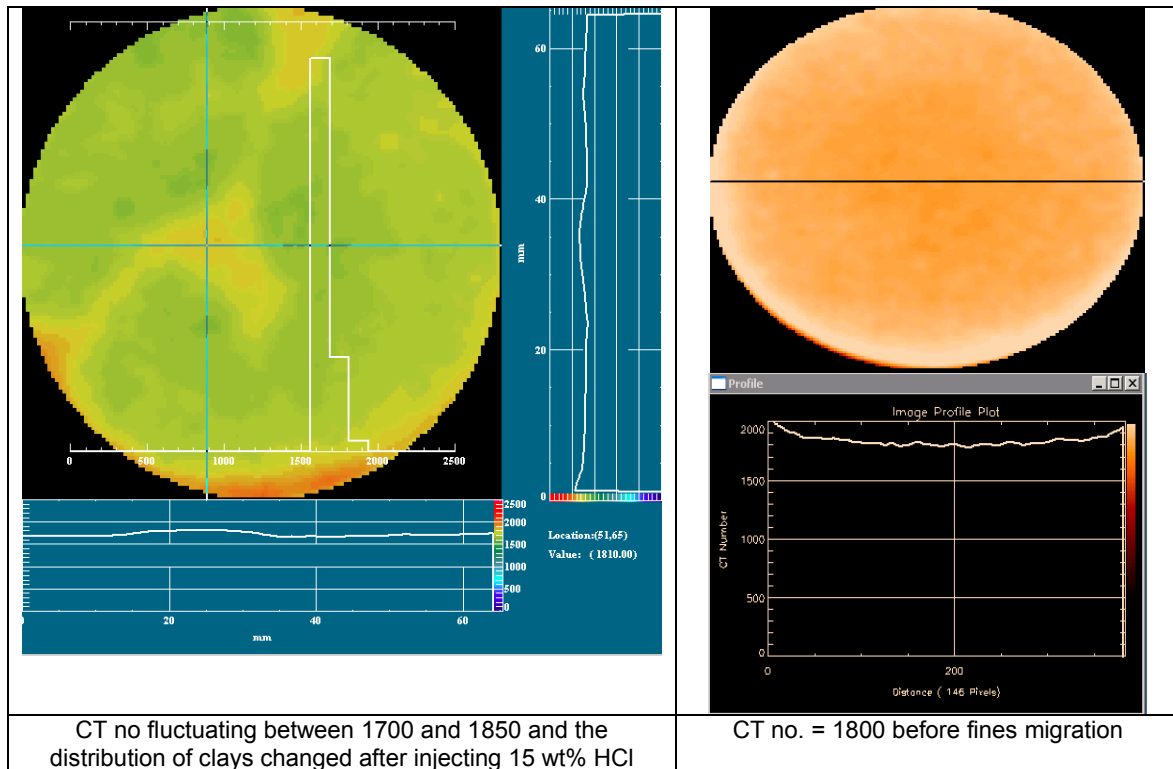
Fig. 135—2D CT scans showing the effect of injecting 15 wt% into the illitic sandstone core, showing fines migration through the color difference in the slice.

Removing the Damage Caused by Drilling Fluid

The drilling fluid showed in **Table 30** was used to damage Berea sandstone cores. The cores were saturated by 5 wt% NaCl brine and then the drilling fluid was injected through the core. Two coreflood experiments were performed to compare GLDA and HEDTA in removing the damage from the sandstone core. The first coreflood was run using Berea sandstone core of an initial permeability of 102 md, the core was damaged by the drilling fluid and then the core was flowed back using brine and the flow back permeability after damage was 25 md. HEDTA solution of 0.6M concentration at pH 4 was used to remove the damage from the core at 300°F and 5 cm^3/min. The pore volume of the injected HEDTA was 6.2 PV after that the core was left to cool down and after 24 hours the core permeability was measured in the production direction (flow back) and it was 84 md, **Fig. 136**. The amount of cations that were removed by HEDTA was 1.68 g calcium, 1.7 g iron, and 0.8 g magnesium.
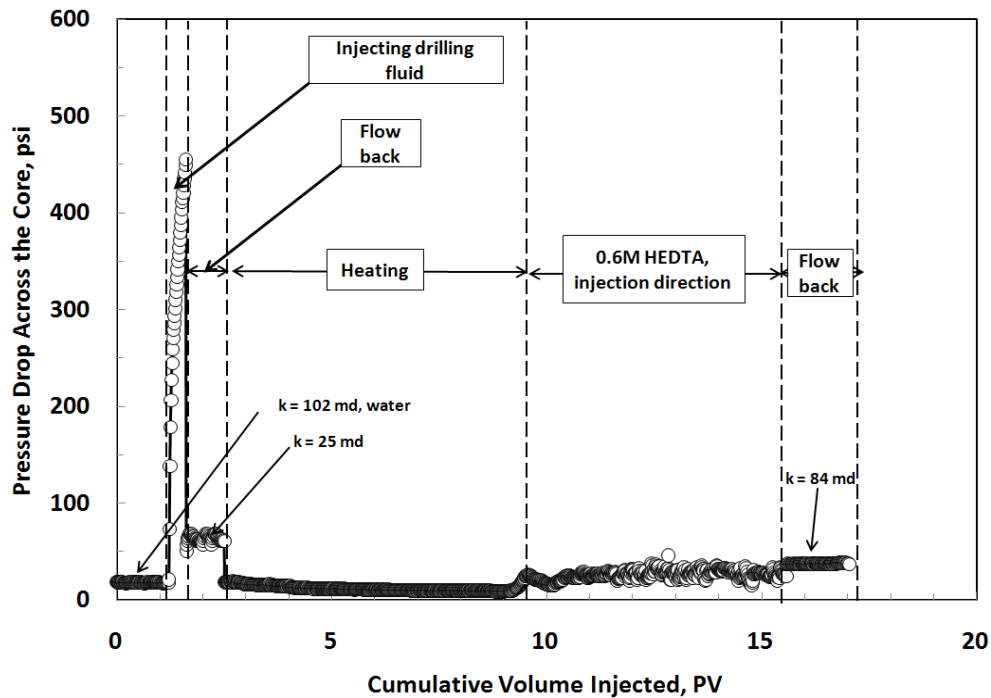
Fig. 136—Different stages of the coreflood for removing the damage of the Berea sandstone core using 0.6M HEDTA at pH 4, T = 300°F and flow rate = 5 cm³/min.

The second coreflood experiment was conducted at the same conditions using 0.6M GLDA at pH 4. This experiment was run at the same conditions of temperature and flow rate as the previous experiment. The damaged core permeability after the flow back was 10 md, in this case we got more damage than the previous case. After heating the core the 0.6M GLDA at pH 4 was injected into the core to remove the damage caused by the drilling fluid. The core permeability after flowing back the core after 24 hours was 86 md, **Fig 137**. The amount of dissolved calcium was 1.55 g, the iron was 1.1 g, and the magnesium was 0.55 g after injecting 6.5 PV GLDA into the core.
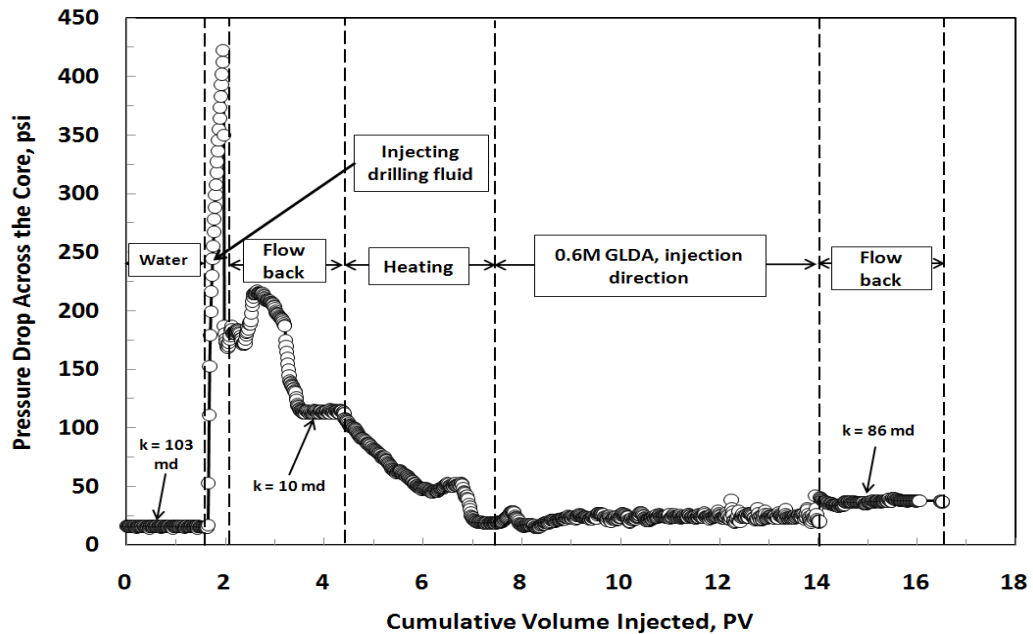
Fig. 137—Different stages of the coreflood for removing the damage of the Berea sandstone core using 0.6M GLDA at pH 4, T = 300°F and flow rate = 5 cm³/min.

Figs. 138 and 139 show the ability of HEDTA and GLDA to remove the damage from the Berea sandstone cores damaged by calcium carbonate-weighted drilling fluid. GLDA and HEDTA retained the damaged core permeability to its original permeability after injecting almost the same concentration (0.6M), the same pH (4) and the same pore volume (~6). The retained permeability almost was 0.83 in the two cases (GLDA and HEDTA), but GLDA increased the damaged core permeability from 10 to 86 md (8.6 times), and HEDTA increased the damaged core permeability from 25 to 85 md (3.6 times). GLDA performed better than HEDTA at the same conditions in removing the damage of Berea sandstone cores.
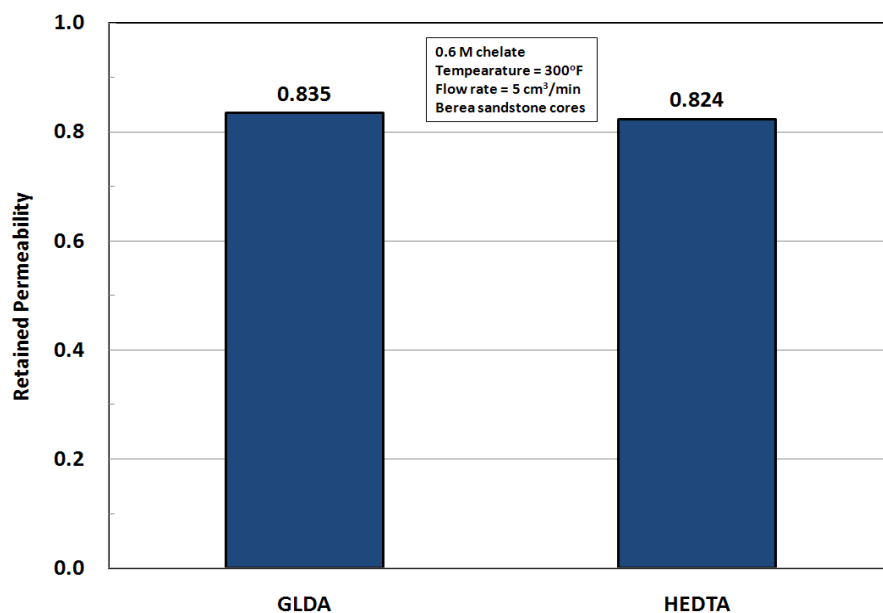
Fig. 138—Retained permeability ($k_{retained}/k_{initial}$) for the Berea sandstone cores using GLDA and HEDTA. Almost the two chelants did the same in retaining the core permeability.
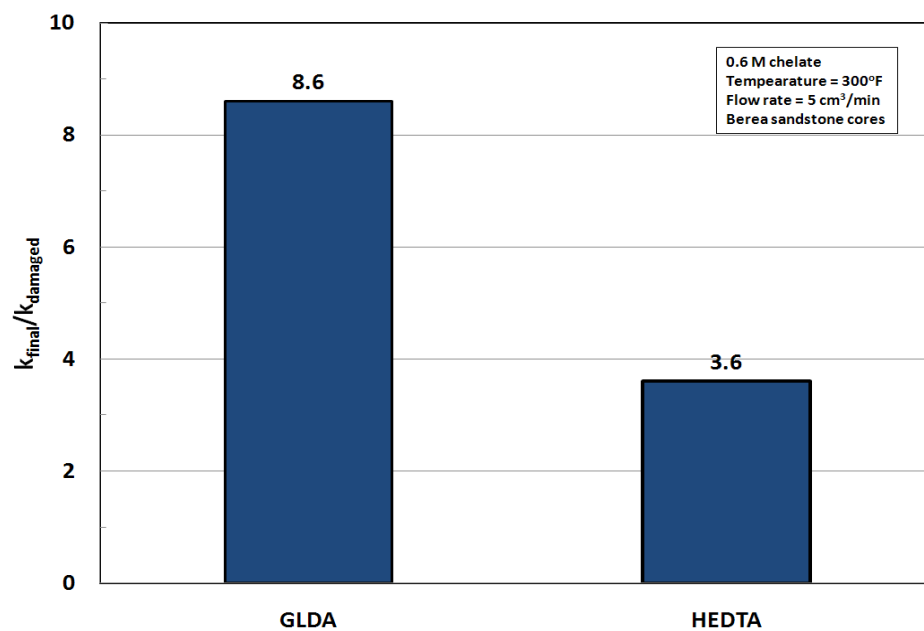
Fig. 139—Ability of GLDA and HEDTA in increasing the core permeability from the damaged permeability by the drilling fluid to the final core permeability. GLDA enhanced the permeability of the core better than HEDTA.

Stimulation of Scioto Cores and Kentucky Cores

In this part we tested sandstone cores with higher illite content, Scioto sandstone with 18 wt% illite and Kentucky sandstone with 14 wt% illite. GLDA of 0.6M and pH 3.8 was used in the coreflood experiment at 300°F. Scioto sandstone core was used in the coreflood experiment at injection rate of 1 cm^3/min the core had an initial permeability of 0.2 md and initial porosity of 0.13. Injecting 4 PV GLDA into the core yielded the following amounts of cations: 1.44 g iron, 0.06 magnesium, and 0.015 g calcium. The amount of dissolved iron was high because of the chlorite content in this core was 4 wt%. In this core there was no much sources of calcium, there was no calcite or dolomite, but there was small amount of calcium feldspar. The GLDA at pH 3.8 was compatible with the illitic-sandstone core and increased the core permeability from 0.2 to 0.35 md. **Fig. 140** shows the pressure drop across the core and it is obvious that there was no fines migration as injecting more than 4 PV did not cause appreciable increase in the pressure drop like HCl did in Bandera core just with 10 wt% illite. GLDA was compatible with illite content up to 18 wt%.
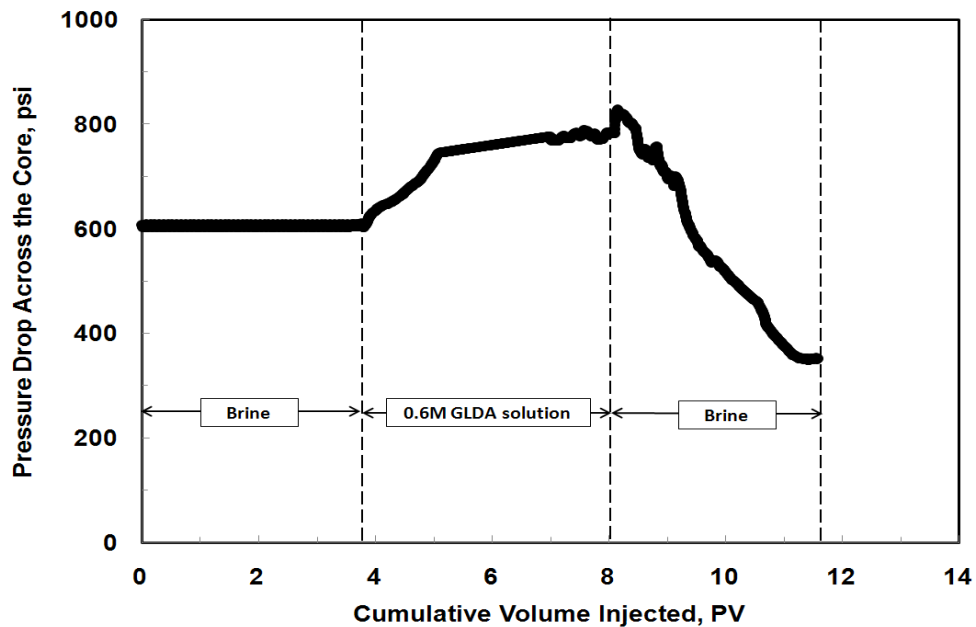
Fig. 140—Pressure drop across the Scioto sandstone core treated by 0.6M GLDA of pH 3.8 at 300°F and 1 cm^3/min. There was compatibility between the GLDA and the core as the increase in the pressure drop just was due to the difference in viscosity of GLDA and brine.

Another coreflood experiment was performed using Kentucky core with 14 wt% illite content. GLDA (0.6M) was injected into the core at 0.5 cm^3/min at 300°F, the initial core permeability was 0.1 md and the initial porosity was 0.08. Four pore volumes were injected into the core, the core permeability increased from 0.1 to 0.16 md and the GLDA at pH 3.8 was compatible with the illitic-sandstone Kentucky core at 300°F. The amounts of cations in the coreflood effluent were as follows: 0.3 g calcium, 0.05 g iron, and 0.04 g magnesium. There was more calcium than in the case of Scioto core because the amount of calcium feldspar in the Kentucky core was 17 wt%.

Conclusions

Different sandstone cores with different illite content were used in the coreflood experiment to show the computability of GLDA with the illite mineral inside those cores. GLDA and HEDTA were compared in terms of removing the damage from the sandstone cores. The following are the conclusions that were drawn from this study:

1. GLDA stimulated the Berea sandstone cores better than GLDA/HF mixture.
2. Preflushing the core by GLDA minimized the damage caused by HF acid in the main flush.
3. GLDA was compatible with the sandstone cores with different illite content up to 18 wt% illite.
4. GLDA removed the damage from the sandstone core better than HEDTA.
5. HCl acid was not compatible with the illitic sandstone Bandera core and damaged the core.

CHAPTER X
CONCLUSIONS AND RECOMMENDATIONS

The objective of this work was to evaluate the use of a newly developed environmentally friendly fluid, L-glutamic-N,N-diacetic acid (GLDA), as a stand-alone stimulation fluid for carbonate and sandstone reservoirs. In Chapter I we showed the problems associated with HCl and other stimulation fluids such as corrosion of well tubular at high temperatures. Numerous additives were required to reduce the corrosion problems at high temperatures. There are some reservoirs have low fracture pressure, and to avoid formation fracture during the acidizing treatments HCl should be injected at low injection rates. Injecting HCl at low injection rates caused face dissolution and washout problems and did not bypass the damaged zone. In turn, after the treatment there will be still a positive skin which means no increase in the production rate. Using HCl/HF mud acid in high calcite content sandstone reservoirs caused damage and precipitations of fluorides and fluosilicates. Mud acid also can cause problems in illitic-sandstone reservoirs due to the fines migration.

In Chapter II, we studied the ability of GLDA to dissolved calcite over a wide range of pH (1.7 to 13). We found that GLDA was effective at low pH values because of the presence of hydrogen ions increased the reaction rate of GLDA with calcite. At high pH there was no hydrogen, therefore, the reaction was low and was due to complexation mechanism only. Rotating disk was used to compare the rate of dissolution of GLDA at different pH values. GLDA at pH 1.7 had higher dissolution rate than pH 13. Thermal stability tests were performed at high temperatures for long time, and GLDA was found to be thermally stable up to 400^oF and 24 hours. GLDA was found to be thermally stable in high ionic strength solutions such as sea water and sodium chloride solutions. In this part the coreflood experiments showed that GLDA was effective in creating wormholes at pH 1.7.

In Chapter III, several coreflood experiments were performed at different pH values, injection rates, and temperatures. GLDA at pH of 1.7 and 3 was more effective than that at pH of 13 in creating wormholes at different temperatures and injection rates. The optimum GLDA concentration in the coreflood experiments was found to be 20 wt%. GLDA was compared to HEDAT, acetic acid, and LCA, GLDA outperformed all those fluids in terms of volume required to create wormholes at high temperatures.

In Chapter IV, the optimum conditions of wormhole formation in calcite cores using GLDA were studied. Optimum injection rate existed at different pH values and at different temperatures in the coreflood experiments. Different factors affected the wormhole formation such as: rock permeability, injection rate, pH value, and temperature. The higher the rock permeability, the

higher the surface area and the higher the dissolved calcite. GLDA performed better at low injection rates because of the increased contact time with the rock which allowed for more time of reaction between GLDA and calcite cores. GLDA at low pH created bigger wormholes than at higher pH. At low injection rates there was no face dissolution observed in the core in the case of GLDA compared to 15 wt% HCl. Adding sodium chloride to GLDA enhanced its performance in the coreflood experiment due to the enhanced of thermal stability at high temperature. GLDA was able to stimulate low permeability contrast parallel cores due to the build in viscosity and low reactive nature of GLDA.

The effect of reservoir fluid type water, oil, or gas on the stimulation of calcite cores by GLDA was studied in Chapter V. The results showed that GLDA performed better in the oil-saturated cores due to the reduced diffusion. GLDA at pH of 4 stimulated calcite cores better than HEDTA at 300^oF and at different injection rates. The results obtained with carbonate cores saturated with nitrogen gas were almost similar to those obtained when the cores were saturated with water. In this part analytical model was developed to predict the performance of GLDA in calcite cores. This model can be used to predict the pressure drop across the core, the only factor that was found to control the pressure drop was the viscosity. GLDA viscosity was measured at different temperatures and calcium concentrations, and the correlations from the measurements were used in the prediction of the pressure drop. Coreflood experiments showed that at low pH values, GLDA was the best chelating agent to stimulate calcite cores compared to HEDAT and EDTA.

GLDA was very effective in stimulating dolomite cores at different pH over a wide range of temperatures (180, 250 and 300^oF), Chapter VI. There was an optimum injection rate at which the amount of GLDA needed to create wormholes was minimum. Also, GLDA effectively chelated magnesium and calcium from dolomite cores. GLDA was stable up to temperatures of 300^oF and the concentration of GLDA after the treatment was the same as that before the treatment, further confirming thermal stability of GLDA at this temperature.

In Chapter VII, GLDA showed a strong ability in chelating calcium, magnesium, iron, and aluminum ions from the sandstone cores. At 300^oF GLDA at different pH values was able to enhance the core permeability. Decreasing the injection rate from 5 to 2 cm^3/min increased the contact time between the fluid and the rock and increased the amount of dissolved ions. X-ray CT scan showed a porosity increase after the treatments. The concentration of GLDA after the coreflood experiment was almost the same before the treatment showing a high thermal stability up to 300^oF in the coreflood experiment. Lambert correlation was found to be the best correlation to predict for the core permeability after treating Berea sandstone cores by 20 wt% GLDA solutions. GLDA was compatible with all clay types found in Berea sandstone cores.

In Chapter VIII, Coreflood experiments showed that at high pH values (pH =11) GLDA, HEDTA, and EDTA were almost the same in increasing the permeability of both Berea and Bandera sandstone cores. GLDA, HEDTA, and EDTA were compatible with Bandera sandstone cores. The weight loss from the core was highest in case of HEDTA and lowest in case of GLDA at pH 11. At pH 4 the 0.6M-GLDA performed better than 0.6M HEDTA in the coreflood experiments. The permeability ratio (final/initial) for Bandera sandstone cores was 2 in the case of GLDA and 1.2 in the case of HEDTA at pH of 4 and 300°F. At pH 11, HEDTA was the best chelating agent to stimulate Bandera sandstone cores and at pH 4, GLDA was the best one. For Berea sandstone cores EDTA at pH of 11 was the best in increasing the permeability of the core at 300°F.

In the last part of this study, Chapter IX, alternative fluids to HCl/HF mud acids were introduced to stimulate and remove the damage from illitic-sandstone reservoirs. Those fluids are EDTA (ethylenediamine tetra acetic acid), HEDTA (hydroxyl ethylenediamine tri acetic acid), and GLDA (glutamic acid-N,N-diacetic acid). In this Chapter, sandstone cores with different illite content were examined. Illite content of 1, 10, 14, and 18 wt% of the sandstone cores were used in the coreflood experiment at 300°F. Different combinations of GLDA/HF were tested to get the optimum ratio of GLDA/HF to be used in removing the damage from the sandstone cores to reduce the precipitates by HF acid. The core permeability was measured before and after the treatment to determine the effectiveness of each fluid in removing the damage and stimulation of sandstone cores. CT scan was used to scan the cores before and after the treatment to locate the damage caused by HCl/HF acids in the illitic cores. Different stages of preflush and postflush were used to determine the optimum volume for each stage to yield the maximum core permeability after the treatment.

Our results showed that 15 wt% HCl caused severe damage to sandstone cores with different illite content. GLDA, HEDTA, and EDTA showed a good compatibility with the illitic-sandstone cores at 300°F. Permeability measurements showed that GLDA performed better than HEDTA and EDTA at pH of 4. The optimum ratio of GLDA/HF concentration was found to be 20wt% GLDA/1wt% HF which gives the maximum increase in core permeability compared with the 20 wt% GLDA. The three fluids tested in this study showed good compatibility with illite so they can be used to stimulate or remove the damage from illitic-sandstone reservoirs alone or in combination with HF acid.

Having studied GLDA as a stand-alone stimulation fluid, we recommend the following:

i. GLDA should be used to stimulate carbonate reservoirs in wells completed with cr-13 tubing because the use of HCl will cause severe damage to the well completion.

ii. For high temperature reservoirs (> 300°F) HCl if used will cause severe damage to the well completion (casing, and production tubing), therefore low corrosive fluids should be used such as GLDA.

iii. GLDA is an effective stimulation fluid for carbonate reservoirs and should be used in the case of environmental issues because it is biodegradable and environmental friendly, and can be considered as a hot, green fluid.

iv. In the case of face dissolution or washout problems where HCl had to be injected at low injection rates because of the fracture issues, GLDA can be used effectively in those reservoirs at very low injection rates.

v. GLDA is a very good solution to stimulate illitic-sandstone reservoirs, because it was compatible with illite in the sandstone core.

vi. If the calcite content in the sandstone reservoir is high, GLDA should be used and GLDA can be used to remove the damage caused by calcium carbonate filter cake.

The following list provides some topics for future research:

i. Reaction kinetics of GLDA with calcite should be examined deeply to determine the type of reaction and the diffusion coefficient at different pH values. The effect of salts, corrosion inhibitors, etc., on the dissolution rate should be investigated.

ii. Corrosion rates at different pH values and temperatures should be studied and selecting the suitable type and concentration of the corrosion inhibitors.

iii. Stability and compatibility of GLDA with different salts and surfactant should be investigated.

REFERENCES

Abrams, A., Scheuerman, R.F., Templeton, C.C., and Richardson, E.A.1983. Higher-pH Acid Stimulation System. *SPE Journal of Petroleum Technology* **35** (12): 2175-2184. SPE-7892-PA. doi: 10.2118/7892-PA.

Al-Anazi, H.A., Nasr-El-Din, H.A., Hashem, M.K., and Hopkins, J.K. 2000. Matrix Acidizing of Water Injectors in a Sandstone Field in Saudi Arabia: A Case Study. Paper SPE 62825 presented at the SPE/AAPG Western Regional Meeting, Long Beach, California, 19-23 June. doi: 10.2118/62825-MS.

Al-Ghamdi, A.H., Mahmoud, M.A., Hill, A.D., and Nasr-El-Din, H.A. 2009. Diversion and Propagation of Viscoelastic Surfactant Based Acid in Carbonate Cores. Paper SPE 121713 presented at the SPE International Symposium on Oilfield Chemistry, The Woodlands, Texas, 20-22 April. doi: 10.2118/121713-MS.

Al-Ghamdi, A.H., Mahmoud, M.A., Hill, A.D., and Nasr-El-Din, H.A. 2010. When Do Surfactant-Based Acids Work as Diverting Agents? Paper SPE 128074 presented at the SPE International Symposium and Exhibition on Formation Damage Control, Lafayette, Louisiana, 10–12 February. doi: 10.2118/128074-MS.

Ali, A.H.A., Frenier, W.W., Xiao, Z., and Ziauddin, M. 2002. Chelating Agent-Based Fluids for Optimal Stimulation of High-Temperature Wells. Paper SPE 77366 presented at the SPE Annual Technical Conference and Exhibition, San Antonio, Texas, 29 September–2 October. doi: 10.2118/77366-MS.

Ali, S.A., Ermel, E., Clarke, Fuller, M.J., Xiao, Z., and Malone, B. 2008. Stimulation of High-Temperature Sandstone Formations from West Africa with Chelating Agent-Based Fluids. *SPE Production & Operations* **23** (1): 32-38. SPE-93805-PA. doi: 10.2118/93805-PA.

Allen, O.T., and Roberts, A.P.1993. *Production Operation: Well Completions, Workover, and Stimulation*. Vol. 2, 4th Edition, Tulsa, Oklahoma: Oil and Gas Consultants International.

Amaefule, J.O., Kersey, D.G., Norman, D.L., and Shannon, P.M. 1988. Advances in Formation Damage Assessment and Control Strategies. CIM Paper 88-39-65 presented at the 39th Annual Technical Meeting of Petroleum Society of CIM and Canadian Gas Processors Association, Calgary, Alberta, June 12-16. doi: 10.2118/88-39-65.

Anderson, M.S. 1991. Reactivity of San Andres Dolomite. *SPE Production Engineering* **6** (2): 227-232. SPE-20115-PA. doi: 10.2118/20115-PA.

Bernadiner, M.G., Thompson, K.E., and Fogler, H.S. 1992. Effect of Foams Used During Carbonate Acidizing. *SPE Production Engineering* **7** (4): 350-356. SPE-21035-PA. doi: 10.2118/21035-PA.

Binder, M.S. and Vampa, V.C. 1989. A General Model for Convection-Dispersion-Dynamic Adsorption in Porous Media with Stagnant Volume. *Journal of Petroleum Science & Engineering* **3** (3): 267-281. doi: 10.1016/0920-4105(89)90023-5.

Bryant, S.L. and Buller, D.C. 1990. Formation Damage From Acid Treatments. *SPE Production Engineering* **5** (4): 455-460. SPE-17597-PA. doi: 10.2118/17597-PA.

Buijse, M. and Glasbern, G. 2005. A Semiempirical Model to Calculate Wormhole Growth in Carbonate Acidizing. Paper SPE 96892 presented at the SPE Annual Technical Conference and Exhibition, Dallas, TX, 9-12 October. doi: 10.2118/96892-MS.

Chang, F., Qu, Q., and Frenier, W.W. 2001. A Novel Self-Diverting-Acid Developed for Matrix Stimulation of Carbonate Reservoirs. Paper SPE 65033 presented at the SPE International Symposium on Oilfield Chemistry, Houston, Texas, 13–16 February. doi: 10.2118/65033-MS.

Civan, F. 2000. *Reservoir Formation Damage: Fundamentals, Modeling, Assessment, and Mitigation*. Houston, Texas: Gulf Publishing Company.

Conway, M.W., Asadi, M., Penny, G.S., and Chang, F. 1999. A Comparative Study of Straight/Gelled/Emulsified Hydrochloric Acid Diffusivity Coefficient Using Diaphragm Cell and Rotating Disk. Paper SPE 56532 presented at the Annual Technical Conference and Exhibition, Houston, Texas, 3-6 October. doi: 10.2118/56532-MS.

Economides, M.J. and Kenneth, G.N. 2000. *Reservoir Stimulation*. 2nd edition. Houston, Texas: Gulf Publishing Company.

Ezzat, A.M. 1990. Completion Fluids Design Criteria and Current Technology Weaknesses.Paper SPE 19434 presented at the SPE Formation Damage Control Symposium, Lafayette, Louisiana, February 22-23. doi: 10.2118/19434-MS.

Fredd, C.N. 1998. The Influence of Transport and Reaction on Wormhole Formation in Carbonate Porous Media: A Study of Alternative Stimulation Fluids. Ph.D. Dissertation, University of Michigan, Ann Arbor, MI.

Fredd, C.N. 2000a. *Reservoir Stimulation: Advances in Understanding and Predicting Wormhole Formation*. 3rd edition, Englewood Cliffs, New Jersey: Prentice Hall.

Fredd, C.N. 2000b. Dynamic Model for Wormhole Formation Demonstrates Conditions for Effective Skin Reduction During Carbonate Matrix Acidizing. Paper SPE 59537 presented at the SPE Permian Basin Oil and Gas Recovery Conference, Midland, Texas, 21-23 March. doi: 10.2118/59537-MS.

Fredd, C.N. and Fogler, H.S. 1997. Chelating Agents as Effective Matrix Stimulation Fluid for Carbonate Formations. Paper SPE 37212 presented at the SPE International Symposium on Oilfield Chemistry, Houston, Texas, 18-21 February. doi: 10.2118/37212-MS.

Fredd, C.N. and Fogler, H.S. 1998a. Alternative Stimulation Fluids and Their Impact on Carbonate Acidizing. *SPE Journal*, **3** (1): 34-41. SPE-31074-PA. doi: 10.2118/31074-PA.

Fredd, C.N. and Fogler, H.S. 1998b. Influence of Transport and Reaction on Wormhole Formation in Porous Media. *American Institute of Chemical Engineers Journal*, **44** (9): 1933-1949. doi: 10.1002/aic.690440902.

Fredd, C.N. and Fogler, H.S. 1998c. The Influence of Chelating Agents on the Kinetics of Calcite Dissolution. *Journal of Colloid and Interface Science*, **204** (1): 187-197. doi**:**10.1289/ehp.

Fredd, C.N. and Fogler, H.S. 1999. Optimum Conditions for Wormhole Formation in Carbonate Porous Media: Influence of Transport and Reaction. *SPE Journal*, **4** (3): 196-205. SPE-56995-PA. doi: 10.2118/56995-PA.

Frenier, W.W., Brady, M., Al-Harthy, S., Arangath, R., Chan, K.S., et al. 2004. Hot Oil and Gas Wells Can Be Stimulated without Acids. *SPE Production & Facilities* **19** (4): 189-199. SPE-86552-PA. doi: 10.2118/86522-PA.

Frenier, W.W. 2001. Novel Scale Removers are Developed for Dissolving Alkaline Earth Deposits. Paper SPE 65027 presented at the SPE International Symposium on Oilfield Chemistry, Houston, Texas, 13-16 February. doi: 10.2118/65027-MS.

Frenier, W.W., Fredd, C.N., and Chang, F. 2001. Hydroxyaminocarboxylic Acids Produce Superior Formulations for Matrix Stimulation of Carbonates at High Temperatures. Paper SPE 71696 presented at the SPE Annual Technical Conference and Exhibition, New Orleans, Louisiana, 30 September-3 October. doi: 10.2118/71696-MS.

Frenier, W.W., Wilson, D., Crump, D., and Jones, L. 2000. Use of Highly Acid-Soluble Chelating Agents in Well Stimulation Services. Paper SPE 63242 presented at the SPE Annual Technical Conference and Exhibition, Dallas, Texas, 1-4 October. doi: 10.2118/63242-MS.

Frenier, W.W., Rainey, M., Wilson, D., Crump, D., and Jones, L. 2003. A Biodegradable Chelating Agent is Developed for Stimulation of Oil and Gas Formations. Paper SPE 80597 presented at the SPE/EPA/DOE Exportation and Production Environmental Conference, San Antonio, Texas, 10-12 March. doi: 10.2118/80597-MS.

Frick, T.P., Mostofizadeh, B., and Economides, M.J. 1994. Analysis of Radial Core Experiments for Hydrochloric Acid Interaction with Limestone. Paper SPE 27402 presented at the SPE International Symposium on Formation Damage Control, Lafayette, Louisiana, 7–10 February. doi: 10.2118/27402-MS.

Furui, K., Burton, R.C., Burkhead, D.W., Abdelmalek, N.A., Hill, A.D., Zhu, D., and Nozaki, M. 2010. A Comprehensive Model of High-Rate Matrix Acid Stimulation for Long Horizontal Wells in Carbonate Reservoirs. Paper SPE 134265 presented at the Annual Technical Conference and Exhibition, Florence, Italy, 19-22 September. doi: 10.2118/134265-MS.

Gdanski, R.D. 2005. Recent Advances in Carbonate Stimulation. IPTC 10693 presented at the International Petroleum Technology Conference, Doha, Qatar, 21-23 November. doi: 10. 2118/10693-MS.

Gdanski, R.D. and Shuchart, C.E. 1998. Advanced Sandstone-Acidizing Designs with Improved Radial Models. *SPE Production & Facilities* **13** (4): 272-278. doi: 10. 2118/52397-PA.

Gidley, J.L., Brezovec, E.J., and King, G.E. 1996. An Improved Method for Acidizing Oil Wells in Sandstone Formations. *SPE Production & Facilities* **11** (1): 4-10. SPE-26580-PA. doi: 10. 2118/26580-PA.

Glasbern, G., Kalia, N., and Talbot, M. 2009. The Optimum Injection Rate for Wormhole Propagation: Myth or Reality? Paper SPE 121464 presented at the European Formation Damage Conference, Scheveningen, The Netherlands, 27-29 May. doi: 10. 2118/121464-MS.

Gomaa, A.M., Mahmoud, M.A., and Nasr-El-Din, H.A. 2009. When Polymer-Based Acids Can Be Used? A Coreflood Study. Paper IPTC 13739 presented at the International Petroleum Technology Conference, Doha, Qatar, 7–9 December. doi: 10. 2118/13739-MS.

Hartman, R.L., Lecerf, B., Ziauddin, M., and Fogler, H.S. 2006 Acid-Sensitive Aluminosilicates: Dissolution Kinetics and Fluid Selection for Matrix-Stimulation Treatments. *SPE Production & Operation* **21** (2): 194-204. SPE-82267-PA. doi: 10. 2118/82267-PA.

Haung, T., Hill, A.D., and Schechter, R.S. 1997. Reaction Rate and Fluid Loss: The Keys to Wormhole Initiation and Propagation in Carbonate Acidizing. Paper SPE 37312 presented at the SPE International Symposium on Oilfield Chemistry, Houston, Texas, 18-21 February. doi: 10. 2118/37312-MS.

Haung, T., Ostensen, L., and Hill, A.D. 2000. Carbonate Matrix Acidizing with Acetic Acid. Paper SPE 58715 presented at the SPE International Symposium on Formation Damage Control held in Lafayette, Louisiana, 23-24 February. doi: 10. 2118/58715-MS.

Hill, A.D. and Schechter, R. S. 2000. *Reservoir Stimulation: Fundamentals of Acid Stimulation*. 3rd edition, Englewood Cliffs, New Jersey: Prentice Hall PTR.

Hill, A.D., Economides, M.J., and Economides, C.E. 1993. *Petroleum Production System: Sandstone Acidizing*. Englewood Cliffs, New Jersey: Prentice Hall PTR.

Hill, A.D., Zhu, D., and Wang, Y. 1995. The Effect of Wormholing on the Fluid-Loss Coefficient in Acid Fracturing. *SPE Production & Facilities* **10** (4): 257-263. SPE-27403-PA. doi: 10. 2118/27403-PA.

Hoefiner, M.L. and Fogler, H.S. 1985. Effective Matrix Acidizing in Carbonates Using Micro emulsions. *Chemical Engineering Progress* (May), **81**: 40-44. doi: 10.1016/ j.petrol.2006. 08. 005.

Huang, T., McElfresh, M.P., and Gabrysch, A.D. 2002. Acid Removal of Scale and Fines at High Temperatures. Paper SPE 74678 presented at the SPE Oilfield Scale Symposium, Aberdeen, UK, 30-31 January. doi: 10. 2118/74687-MS.

Huang, T., McElfresh, M.P., and Gabrysch, A.D. 2003. Carbonate Acidizing Fluids at High Temperatures: Acetic Acid, Chelating Agents or Long-Chained Carboxylic Acids? Paper SPE 82268 presented at the SPE European Formation Damage Conference, The Hague, The Netherlands, 13-14 May. doi: 10. 2118/82268-MS.

Huang, T., Ostensen, L., and Hill, A.D. 2000. Carbonate Matrix Acidizing with Acetic Acid. Paper SPE 58715 presented at the SPE International Symposium on Formation Damage Control, Lafayette, Louisiana, 23-24 February. doi: 10. 2118/58715-MS.

Hung, K.M., Hill, A.D., and Sepehrnoori, K. 1989. A Mechanistic Model of Wormhole Growth in Carbonate Matrix Acidizing and Acid Fracturing. *SPE Journal of Petroleum Technology* **41** (1): 59-66. SPE-16886-PA. doi: 10.2523/16886-PA.

Izeg, O. and Demiral, B. 2005. CO_2 Injection in Carbonates. Paper SPE 93773 presented at the SPE Western Regional Meeting, Irvine, CA, 30 March-1 April. doi: 10. 2118/93773-MS.

Kline, W.E. and Fogler, H.S. 1981. Dissolution Kinetics: Catalysis by Strong Acids. *Journal of Colloid and Interface Science* **82** (1): 93-102. doi: 10.1016/0021-9797(81)90127-2.

LePage, J.N., De Wolf, C.A., Bemelaar, J.H., and Nasr-El-Din, H.A. 2010. An Environmentally Friendly Stimulation Fluid for High Temperature Applications. Accepted, *SPE Journal.* SPE-121709-PA. doi: 10. 2118/121709-PA.

Levich, V.G. 1962. *Physicochemical Hydrodynamics*. Englewood Cliffs, New Jersey: Prentice-Hall.

Li, Y.H., Fambrough, J.D., and Montgomery, C.T. 1998. Mathematical Modeling of Secondary Precipitation from Sandstone Acidizing. *SPE Journal* **3** (4): 393-401. SPE-53001-PA. doi: 10. 2118/53001-PA.

Lund, K., Fogler, H.S., McCune, C.C., and Ault, J.W. 1973. Acidization I. The Dissolution of Dolomite in Hydrochloric Acid. *Chemical Engineering Science* **28** (3): 691-700.

Lund, K., Fogler, H.S., McCune, C.C., and Ault, J.W. 1975. Acidization II. The Dissolution of Calcite in Hydrochloric Acid. *Chemical Engineering Science* **30** (8): 825-835.

Mahmoud, M.A., Nasr-El-din, H.A., De Wolf, C.A., and LePage, J.N. 2010a. An Effective Stimulation Fluid for Deep Carbonate Reservoirs: A Coreflood Study. Paper SPE 131626 presented at the 2010 International Oil and Gas Conference, Beijing, China, 8-10 June. doi: 10. 2118/131626-MS.

Mahmoud, M.A., Nasr-El-din, H.A., De Wolf, C.A., and LePage, J.N. 2010b. Stimulation of Carbonate Reservoirs Using GLDA (Chelating Agent) Solutions. SPE 132286 presented at

the SPE Trinidad and Tobago Energy/Resources Conference, Port of Spain, Trinidad, 27-30 June. doi: 10. 2118/132286-MS.

Mahmoud, M.A., Nasr-El-Din, H.A., De Wolf, C.A., and LePage, J.N. 2010c. Optimum Injection Rate of a New Chelate that Can Be Used to Stimulate Deep Carbonate Reservoirs. Paper SPE 133497 presented at the Annual Technical Conference and Exhibition, Florence, Italy, 19-22 September. doi: 10. 2118/133497-MS.

Mahmoud, M.A., Nasr-El-din, H.A., De Wolf, C.A., LePage, J.N., and Bemelaar, J.H. 2010d. Evaluation of a New Environmentally Friendly Chelating Agent for High Temperature Applications. Paper SPE 127923 presented at the International Symposium on Formation Damage Control, Lafayette, Louisiana, 10 –12 February. doi: 10. 2118/127923-MS.

Martell, A.E. and Calvin, M. 1952. *Chemistry of the Metal Chelate Compounds*. Englewood Cliffs, New Jersey: Prentice-Hall Inc.

Martell, A.E. and Smith, R.M., 2003. *Critically Selected Stability Constants of Metal Complexes*. New York: Plenum Press.

Martin, A.N. 2004. Stimulating Sandstone Formations with non-HF Treatment System. Paper SPE 90774 presented at the SPE Annual Technical Conference and Exhibition, Houston, Texas, 26-29 September. doi: 10. 2118/90774-MS.

Mostofizadeh, B. and Economides, M.J. 1994. Optimum Injection Rate from Radial Acidizing Experiments. Paper SPE 28547 presented at the SPE Annual Technical Conference and Exhibition, New Orleans, Louisiana, 25-28 September. doi: 10. 2118/28547-MS.

Nasr-El-Din, H.A., Solares, J.R., Al-Mutairi, S.H., and Mahoney, M.D. 2001. Field Application of Emulsified Acid-Based System to Stimulate Deep, Sour Gas Reservoirs in Saudi Arabia. SPE 71693 presented at the 2001 SPE Annual Conference and Exhibition, New Orleans, Louisiana, 30 September–3 October. doi: 10. 2118/71693-MS.

Parkinson, M., Munk, T., Brookley, J., Caetano, A., Albuquerque, M., Cohen, D., and Reekie, M. 2010. Stimulation of Multilayered-Carbonate-Content Sandstone Formations in West Africa Using Chelant-Based Fluids and Mechanical Diversion. Paper SPE 128043 presented at the SPE International Symposium and Exhibition on Formation Damage, Lafayette, Louisiana, 10-12 February. doi: 10. 2118/128043-MS.

Permadi, P. and Susilo, A. 2009. Permeability Prediction and Characteristics of Pore Structure and Geometry as Inferred from Core Data. Paper SPE 125350 presented at the SPE/EAGE Reservoir Characterization and Simulation Conference, Abu Dhabi, UAE, 19-21 October. doi: 10. 2118/125350-MS.

Quinn, M.A., Lake, L.W., and Schechter, R.S. 2000. Designing Effective Sandstone Acidizing Treatments through Geochemical Modeling. *SPE Production & Operations* **15** (1): 33-41. SPE-60846-PA. doi: 10. 2118/60846-PA.

Robert, J.A. and Crowe, C.W. 2000. *Reservoir Stimulation: Carbonate Acidizing Design*. 3rd edition, Englewood Cliffs, New Jersey: Prentice Hall.

Schechter, R.S. 1992. *Oil Well Stimulation*. New York: Prentice Hall.

Shaughnessy, C.M. and Kline, W.E. 1982. EDTA Removes Formation Damage at Prudhoe Bay. Paper SPE 11188 presented at the Annual Technical Conference and Exhibition of SPE, New Orleans, Louisiana, 25-27 September. doi: 10. 2118/11188-MS.

Shukla, S., Zhu, D., and Hill, A.D. 2003. Gas Assisted Acidizing of Carbonate Formations. Paper SPE 82273 presented at the SPE European Formation Damage Conference, The Hague, The Netherlands 13-14 May 2003. doi: 10. 2118/82273-MS.

Shukla, S., Zhu, D., and Hill, A.D. 2006. The Effect of Phase Saturation Conditions on Wormhole Propagation in Carbonate Acidizing. *SPE Journal* **11** (3): 273-281. SPE-82273-PA. doi: 10. 2118/82273-PA.

Taylor, K.C. and Nasr-El-Din, H.A. 2002. Coreflood Evaluation of In-Situ Gelled Acids. Paper SPE 73707 presented at the SPE International Symposium and Exhibition of Formation Damage Control, Lafayette, Louisiana, 20-21 Feb. doi: 10. 2118/73707-MS.

Taylor, K.C., Al-Ghamdi, A.H., and Nasr-El-Din, H.A. 2003. Measurement of Acid Reaction Rates of a Deep Dolomitic Gas Reservoir. PETSOC 2003-068 presented at the Petroleum Society's Canadian International Petroleum Conference, Calgary, Alberta, Canada, June 10–12. doi: 10. 2118/ 2003-068.

Taylor, D., Kumar, P.S., Fu, D., Jemmali, M., Helou, H., et al. 2003. Viscoelastic Surfactant Based Self-Diverting Acid for Enhanced Stimulation in Carbonate Reservoirs. Paper SPE 82263 presented at the SPE European Formation Damage Conference, The Hague, The Netherlands, 13–14 May. doi: 10. 2118/82263-MS.

Thomas, R.L., Nasr-El-Din, H.A., Lynn, J.D., Mehta, S., and Zaidi, S.R. 2001. Precipitation During the Acidizing of a HT/HP Illitic Sandstone Reservoir in Eastern Saudi Arabia: A Laboratory Study. Paper SPE 71690 presented at the SPE Annual Technical Conference and Exhibition, New Orleans, Louisiana, 30 September-3 October. doi: 10. 2118/71690-MS.

Tyler, T.N., Metzger, R.R., and Twyford, L.R. 1985. Analysis and Treatment of Formation Damage at Prudhoe Bay, Alaska. *SPE Journal of Petroleum Technology* **37** (6): 1010-1018. SPE-12471-PA. doi: 10. 2118/12471-PA.

Van Ginkel, G.G., Geets, R., and Nguyen, P.D. 2005. *Biodegradation of L-Glutamatediacetic acid by Mixed Cultures and an Isolate. Biodegrability of Chelating Agents*. New York: American Chemical Society.

Wang, Y., Hill, A.D., and Schechter, R.S. 1993. The Optimum Injection Rate for Matrix Acidizing of Carbonate Formations. Paper SPE 26578 presented at the Annual Technical Conference and Exhibition, Houston, Texas, 3-6 October. doi: 10. 2118/26578-MS.

Wang, X., Qu, Q., Cutler, J.L., and Boles, J.L. 2009. Nonaggressive Matrix Stimulation Fluids for Simultaneous Stimulation of Heterogeneous Carbonate Formations. Paper SPE 121712 presented at the SPE International Symposium on Oilfield Chemistry, The Woodlands, Texas, 20-22 April. doi: 10. 2118/121712-MS.

Welton, J. E. 1984. *SEM Petrology Atlas*. Tulsa, Oklahoma: American Association of Petroleum Geologists.

Willey, J.D. 2004. The Effect of Ionic Strength on the Solubility of an Electrolyte. *Journal of Chemical Education*, **81** (11): 1644-1646.

Williams, B.B., Gidley, J.L., and Schechter, R.S. 1979. *Acidizing Fundamentals.* New York: Society of Petroleum Engineers of AIME.

Yu, M., Mahmoud, M.A, and Nasr-El-Din, H.A. 2009. Quantitative Analysis of Viscoelastic Surfactants. Paper SPE 121715 presented at the SPE International Symposium on Oilfield Chemistry, The Woodlands, Texas, 20-22 April. doi: 10. 2118/121715-MS.

Yu, M., Mahmoud, M.A., and Nasr-El-Din, H.A. 2010. Propagation and Retention of Viscoelastic Surfactants Following Matrix Acidizing Treatments in Carbonate Cores. Paper SPE 128074 presented at the SPE International Symposium and Exhibition on Formation Damage Control, Lafayette, Louisiana, 10–12 February. doi: 10. 2118/128074-MS.

Zeiler, C., Alleman, D., and Qu, Q. 2006. Use of Viscoelastic-Surfactant-Based Diverting Agents for Acid Stimulation: Case Histories in GOM. *SPE Production & Opertaion* **21** (4): 448-454. SPE-90062-PA. doi: 10. 2118/90062-PA.

Zerhboub, M., Touboul, E., Ben-Naceur, K., and Thomas, R.L. 1994. Matrix Acidizing: A Novel Approach to Foam Diversion. *SPE Production& Operations* **9** (2): 121-126. SPE-22854-PA. doi: 10. 2118/22854-PA.

VITA

Name:	Mohamed Ahmed Nasr Eldin Mahmoud
Address:	P.O. BOX 43721, Faculty of Petroleum Engineering
	Suez
	Egypt
E-mail address:	mohnasreldin79@yahoo.com
Education:	B.S., Petroleum Engineering, Suez Canal University, Egypt, 2001
	M.S., Petroleum Engineering, Suez Canal University, Egypt, 2006
	Ph.D., Petroleum Engineering, Texas A&M University, 2011